

# EVALUATION OF THE VULNERABILITY OF SELECTED AQUIFER SYSTEMS IN THE EASTERN DAHOMEY BASIN, SOUTH WESTERN NIGERIA

**Saheed Adeyinka Oke**

A thesis submitted in fulfilment of the requirement for the degree of

**Doctor of Philosophy**

in the Faculty of Natural and Agricultural Sciences  
(Institute for Groundwater Studies)  
at the University of the Free State

Promoter: Prof Danie Vermeulen

Co-promoter: Dr Modreck Gomo

BLOEMFONTEIN

January 2015



## DECLARATION

I, Saheed Adeyinka Oke, declare that the thesis that I herewith submit for the Doctoral Degree in Geohydrology at the Institute for Groundwater Studies, Faculty of Natural and Agricultural Sciences, University of the Free State, is my independent work, and that I have not previously submitted it for a qualification at another institution of higher education.

I, Saheed Adeyinka Oke, hereby declare that I am aware that the copyright is vested in the University of the Free State.

I, Saheed Adeyinka Oke, declare that all royalties as regards intellectual property that was developed during the course of and/or in connection with the study at the University of the Free State will accrue to the University.

I, Saheed Adeyinka Oke, hereby declare that I am aware that the research may only be published with the promoters' approval.

-----  
Oke Saheed Adeyinka  
30 January, 2015

## ACKNOWLEDGEMENTS

In the name of Allah the Most Glorious, Most Merciful. All adorations, praises and glorifications are due to Him who made this research work possible. I acknowledge that all the effort involved in the completion of this degree was by His will. Whatever He makes difficult, no one can make easy, and whatever He makes easy no one can make difficult. He chose whomever He likes for a purpose and I am very grateful to Him for choosing me to accomplish this feat.

The foundation for this degree was laid by my parents, particularly my mother Jadesola Adunni Ayisat Okeowo. You tricked me into doing my Masters at a certain time when I felt otherwise, although knowing fully well my love for academic excellence and research. Your moral, financial and motherly support can only come from a woman of your status. You are indeed a mother. The role you and Dad played in making sure I have a stable and meaningful life is much appreciated.

Behind the success of this work is Ifedolapo Aduke Mariam Oke. Your cooperation, perseverance and understanding are much appreciated. You kept the home front running in spite of all the denials. I will always wish to have you in another world. To the special gift given to me by Allah during the dawn of this programme, you added to my joy. Hameedat, Hassan and Husseinat, I couldn't have wished and asked for something as special as you all. You always make me happy.

I started my studies at UFS with Prof Gerrit van Tonder as promoter, but the cold hand of death decided that we couldn't finish it together. His friendship, simplicity and frankness will not be forgotten.

To Prof Danie Vermeulen, you are indeed a worthy promoter. You gave me a chance and an opportunity when I was in need. I have always knocked and you have never closed the door on me. I couldn't have wished for a better guide. Likewise, Dr Modreck Gomo, the decision to add you as a co-promoter is like putting a round peg in a round hole. Your advice, encouragement and criticism have never been wished away.

To my colleagues at IGS, I want to say a big thank you. Special thanks to Elco Lukas for assisting with the spread sheets. Vanessa Aphane, thank you for editing this write up. Shakhane (Shakes) and Dakalo, you are worthy friends, and finally to Dora du Plessis and Lorinda Rust, I will always be grateful to you.

This research work was possible due to the funding provided by the Institute For Groundwater Studies (IGS), Erasmus Mundus Intra African Caribbean Pacific (Intra-ACP) mobility scholarship and academic conference sponsorship by the Academic Society of South Africa (ASSAf) and the South Africa Geophysical Association (SAGA).

# Table of Contents

DECLARATION .....	iii
ACKNOWLEDGEMENTS .....	iv
Table of Contents.....	v
List of Figures .....	x
List of Tables .....	xiv
List of Acronyms and Abbreviations .....	xvi
List of Symbols.....	xviii
CHAPTER 1 INTRODUCTION.....	1
1.1 Background Information .....	1
1.2 Study Rationale .....	3
1.3 Research Aims and Objectives .....	5
1.4 Definition of Vulnerability Terms.....	5
1.5 Structure of the Thesis.....	7
CHAPTER 2 OVERVIEW ON GROUNDWATER VULNERABILITY.....	9
2.1 The General Concepts.....	9
2.1.1 Intrinsic Vulnerability .....	10
2.1.2 The Common Approach.....	11
2.2 General Approaches of Mapping Groundwater Vulnerability .....	12
2.2.1 Hydrogeological Complex and Setting Method.....	12
2.2.2 Mathematical Methods.....	12
2.2.3 Statistical Methods.....	13
2.2.4 Parametric System Method.....	13
2.2.5 Index Methods .....	14
2.3 Description of Some Basic Methods .....	14
2.3.1 The PCOK Method.....	14
2.3.2 The COP Method .....	16
2.3.3 The PI Method .....	18
2.3.4 The EPIK Method .....	22
2.3.5 The Slovene Approach .....	23
2.3.6 The DRASTIC Method .....	26
2.3.7 The AVI Method.....	29

2.3.8	The SINTACS Method .....	29
2.3.9	The GOD Method .....	30
2.3.10	The PaPRIKA Method.....	30
2.4	Travel Time in Vulnerability Pathways.....	31
2.4.1	Travel Time Formulas .....	33
2.5	Validation of Vulnerability Methods .....	39
2.6	Challenges and Expected Contributions to Vulnerability Assessments .....	40
2.7	Characterisations of Study Sites for Vulnerability Assessment.....	43
2.8	Conclusion .....	44
CHAPTER 3 PHYSIOGRAPHY AND GEOLOGY OF THE DAHOMEY BASIN .....		45
3.1	Introduction .....	45
3.2	Description of the Study Area .....	45
3.2.1	Location, Climate and Geology of Nigeria .....	45
3.2.2	Location, Climate and Geology of Southwestern Nigeria .....	47
3.2.3	Location, Climate and Geology of the Dahomey Basin .....	49
3.3	Stratigraphy Succession of the Eastern Dahomey Basin.....	51
3.3.1	Abeokuta Formation.....	51
3.3.2	Ewekoro Formation.....	53
3.3.3	Akinbo Formation.....	54
3.3.4	Oshosun Formation .....	55
3.3.5	Ilaro Formation.....	56
3.3.6	Coastal Plain Sand/ Benin Formation .....	57
3.4	Conclusion .....	58
CHAPTER 4 HYDROGEOLOGICAL CHARACTERISATION OF THE EASTERN DAHOMEY BASIN.....		59
4.1	General Introduction .....	59
4.2	Geophysical Characterisation of the Dahomey Basin Vadose Zones.....	60
4.2.1	Surface Geophysics.....	60
4.2.2	Schlumberger Array .....	61
4.2.3	Resistivity Data Evaluation.....	63
4.2.4	1D Inversion of Field Resistivity Data.....	64
4.2.5	Geo-electrical Sections .....	67
4.2.6	Lithological Characteristics .....	69
4.2.7	Water Table Delineation and Vadose Zone Estimation .....	72

4.2.8	Limitations .....	72
4.2.9	Conclusion .....	72
4.3	Vadose Zone Characterisations of the Dahomey Basin .....	75
4.3.1	Introduction.....	75
4.3.2	Procedure .....	75
4.3.3	Grain Size Analysis.....	81
4.3.4	Textural Characteristics .....	86
4.3.5	Hydraulic Conductivity Estimation from Grain Size Analysis and Permeameter . .....	87
4.3.6	Porosity and Shape Estimation .....	95
4.3.7	Conclusion .....	98
4.4	Lithochemical Characterisations of the Dahomey Basin Sediments .....	98
4.4.1	Introduction.....	98
4.4.2	Geochemical Analysis.....	99
4.4.3	Clay Type and Implication for Groundwater Vulnerability .....	100
4.4.4	Conclusion .....	104
4.5	Characterisations of the Groundwater Bearing Unit of the Dahomey Basin.....	104
4.5.1	Rainfall Pattern .....	104
4.5.2	Groundwater Level and Monitoring .....	106
4.5.3	Aquifer Abstraction Rate .....	108
4.5.4	Conclusion .....	109
4.6	Hydrogeochemical Characterisations of the Dahomey Basin Aquifer .....	110
4.6.1	Introduction.....	110
4.6.2	Sampling and Experimental Analysis .....	110
4.6.3	Hydrochemical Data Evaluation .....	111
4.6.4	Ionic Ratio.....	112
4.6.5	Hydrogeochemical Facies and Evolving Water Quality .....	114
4.6.6	Source of Chloride in Groundwater .....	119
4.6.7	Microbiological Load in Groundwater of the Dahomey Basin .....	121
4.6.8	Aqueous Geochemical Characteristics.....	122
4.6.9	Conclusion .....	127
CHAPTER 5 PROPOSED SIMPLIFIED VULNERABILITY APPROACH FOR DATA SCARCE AREAS .....		128
5.1	Introduction .....	128

5.2	The Concept of the Rainfall–Travel Time Method .....	128
5.3	The Rainfall Factor.....	130
5.3.1	Rating and Assumption of the Rainfall Factor .....	131
5.3.2	Conditions Influencing Percolation .....	133
5.4	The Travel Time Factor.....	134
5.4.1	Travel Time Factor Assumptions.....	134
5.4.2	Rating of Rainfall–Travel Time Parameters.....	138
5.4.3	Hydraulic Conductivity Rating .....	139
5.4.4	Soil Rating .....	140
5.4.5	Rock Type Rating .....	141
5.4.6	Textural Property Rating .....	142
5.4.7	Porosity.....	142
5.4.8	Depth-to-Water Rating .....	143
5.4.9	Slope Rating .....	144
5.5	Rainfall–Travel Time Vulnerability Index .....	144
5.6	Rainfall–Travel-Time Vulnerability Method Limitations .....	145
5.7	Conclusion.....	146
CHAPTER 6.....		148
APPLICATION OF THE RAINFALL–TRAVEL TIME VULNERABILITY METHOD TO THE SHALLOW AQUIFERS OF THE DAHOMEY BASIN .....		148
6.1	Introduction .....	148
6.2	Geology and Soils of the Dahomey Basin .....	148
6.3	Preparation of Vulnerability Maps .....	149
6.4	Data Collection .....	150
6.4.1	Rainfall Rating .....	152
6.4.2	Travel Time Rating.....	152
6.5	The Dahomey Basin Rainfall–Travel Time Vulnerability Map .....	155
6.6	Conclusion .....	157
CHAPTER 7 ASESSMENT OF THE DAHOMEY BASIN VULNERABILITY WITH CONVENTIONAL METHODS .....		158
7.1	Introduction .....	158
7.2	Application of the DRASTIC Method .....	158
7.2.1	DRASTIC Data Collection and Management .....	159
7.2.2	DRASTIC Vulnerability Map.....	167

7.2.3	Comparison of Rainfall–Travel Time and DRASTIC Map .....	168
7.3	Application of the AVI Method .....	168
7.3.1	Comparison of Rainfall–Travel Time and AVI Map .....	170
7.4	Application of the PI Method .....	171
7.4.1	The P-Map .....	172
7.4.2	The I-Map .....	174
7.4.3	PI-Map .....	175
7.5	Conclusion .....	176
CHAPTER 8 VALIDATION OF THE RAINFALL–TRAVEL TIME METHOD .....		177
8.1	Validation Techniques of the Rainfall–Travel Time Method .....	177
8.1.1	Validation with Chloride .....	177
8.1.2	Validation with Dissolved Oxygen .....	181
8.1.3	Validation with Bacteriological Counts .....	184
8.2	Comparison between the Rainfall–Travel Time and Common Existing Methods ..	187
8.3	Comparison of the Vulnerability Methods and Maps .....	189
8.4	Significance of the Rainfall–Travel Time and other Vulnerability Methods on the Dahomey Basin Evaluations .....	192
8.5	Strengths and Weaknesses of the Rainfall–Travel Time Vulnerability Method ....	194
8.6	The Significance of Groundwater Assessment .....	195
8.7	Rainfall–Travel Time Vulnerability Method and Future Evaluation .....	195
CHAPTER 9 CONCLUSIONS AND RECOMMENDATIONS .....		198
9.1	Conclusions .....	198
9.1.1	Geological and Geohydrological Site Characterisations of the Dahomey Basin. ....	198
9.1.2	Development of Groundwater Vulnerability Maps for the Dahomey Basin Using Selected Existing Methods .....	199
9.1.3	Development of a New Simplified Vulnerability Assessment Method and Test its Application in the Dahomey Basin. ....	199
9.2	Recommendations .....	201
9.2.1	Recommendations on Further Studies .....	201
9.2.2	Recommendations to Governments, Communities and the General Populace of the Dahomey Basin .....	202
REFERENCES .....		204
APPENDIX A .....		226
SUMMARY .....		227



# List of Figures

Figure 1.1 Geological map of the Dahomey Basin showing the capital cities .....	3
Figure 2.1: Illustration of the origin–pathway–target model for groundwater vulnerability mapping and the concept of resource and source protection .....	11
Figure 2.2: Diagrammatic cross section showing the PCOK method distribution of factors for intrinsic vulnerability maps .....	15
Figure 2.3: Diagram of the COP method, containing numeric evaluation and index.....	17
Figure 2.4: Determination of P-factor in the PI method .....	19
Figure 2.5: Slovene Approach source and resources intrinsic vulnerability evaluation.....	24
Figure 2.6: Ranking factors of selected hazards used in the Slovene Approach .....	25
Figure 2.7: The VULK model source and resource vulnerability idea.....	35
Figure 2.8: Scheme of the Major Groundwater Basins vulnerability assessment .....	37
Figure 2.9: Scheme of the Major Groundwater Basins vulnerability assessment .....	38
Figure 2.10: Basic concepts defining the intrinsic vulnerability in relation to Work Packages (WP) of the GENESIS project .....	43
Figure 3.1: Location of Nigerian Basement and sedimentary rocks .....	47
Figure 3.2: Map of Nigeria showing the Basement and sedimentary rocks distribution .....	48
Figure 3.3: Generalised geological map of the Dahomey Basin.....	50
Figure 3.4: Ferruginised Ise (Abeokuta) Formation resting conformably on weathered granite gneiss in Abeokuta town .....	52
Figure 3.5: Afowo Formation of the Dahomey basin .....	52
Figure 3.6: Ferruginised Araromi Formation sand quarry.....	53
Figure 3.7: Colour banded limestone rock and calcareous fossils from the Ewekoro limestone, showing the well-preserved cylindrical shape of Gastropods .....	54
Figure 3.8: Thickly laminated and very rich fossiliferous shale.....	55
Figure 3.9: Shale showing the preferential path for groundwater flow .....	55
Figure 3.10: Unconsolidated sand grit and clay of Oshosun Formation .....	56
Figure 3.11: (a) Whitish alluvial sand dug during well construction in Ilaro Formation; and (b) red mottling and friable grit of the Oshosun Formation.....	56
Figure 3.12: Cross stratification of Coastal Plain Sand (CPS).....	57
Figure 3.13: Generalised stratigraphy of the Dahomey Basin .....	58
Figure 4.1: Sketch of the field setup for a VES in Schlumberger configuration.....	61
Figure 4.2: Resistivity sounding points showing VES traverses superimposed on the geological map of the Dahomey Basin .....	62
Figure 4.3: Methodology framework used in the interpretation of this section .....	63

Figure 4.4: Diagram of resistivity curve types in layered structures .....	65
Figure 4.5: Representative resistivity curve types in the Dahomey Basin .....	67
Figure 4.6: Interpreted geo-electric sections of the study area .....	68
Figure 4.7: Interpreted geo-electric sections of the study area.....	68
Figure 4.8: Grain size distribution of geological formations .....	70
Figure 4.9: Pseudo-sections of geological formations .....	71
Figure 4.10: Selected sampling sites across the Dahomey Basin .....	76
Figure 4.11: (a) Schematic diagram of permeameter experimental set-up; (b) length of core sample L; (c) Cross sectional area A.....	80
Figure 4.12: Grain size distribution and sediment textural characteristics of the Abeokuta Formation	81
Figure 4.13: Grain size distribution and sediment textural characteristics of the Ilaro Formation .....	82
Figure 4.14: Grain size distribution and sediment textural characteristics of the Oshosun Formation.	82
Figure 4.15: Grain size distribution of the Coastal Plain Sand .....	83
Figure 4.16: Grain size distribution and sediment textural characteristics of the Ewekoro Formation .	84
Figure 4.17: Textural percentage classification from lithology of the Dahomey Basin .....	84
Figure 4.18: Textural classification of sediment from the Dahomey Basin .....	87
Figure 4.19: Empirical hydraulic conductivities derived from GSA for vadose lithology .....	88
Figure 4.20: Lithological borehole profile cutting through the CPS and ILA Formation.....	91
Figure 4.21: Lithological log of Ewekoro, Abeokuta and Oshosun Formations .....	92
Figure 4.22: A comparison between permeameter hydraulic conductivity ( $K_p$ ) and empirical hydraulic conductivity.....	93
Figure 4.23: Common shapes present in sediments (a) and the irregular shape of OSH (b) .....	97
Figure 4.24: Grain shape of ABK (a&b) and ILA (c&d) .....	97
Figure 4.25: Shapes of EWE (a&b) and CPS (c&d). .....	98
Figure 4.26: XRD diagram for CPS B lithology in the Dahomey Basin .....	103
Figure 4.27: XRD diagram for ILA B sediment in the Dahomey Basin .....	103
Figure 4.28: Twenty years' annual rainfall pattern of three prominent cities in the Dahomey Basin ..	105
Figure 4.29: Schematic hydrogeology cross section along the coastal areas of the Dahomey Basin	107
Figure 4.30: Groundwater monitoring borehole hydrograph of the Coastal Plain Sand at the Epe and Ikeja stations from June 2010 to October 2011 .....	107
Figure 4.31: Representative groundwater abstraction rate distribution of the Dahomey Basin .....	109
Figure 4.32: Ionic ratio of groundwater samples .....	113
Figure 4.33: Seasonal variation of Si and Cl for the Dahomey Basin.....	114
Figure 4.34: Expanded Durov diagram .....	115
Figure 4.35: Piper diagram showing the interpretation of water chemistry.....	115

Figure 4.36: Gibbs' plots of groundwater samples from the Dahomey Basin.....	117
Figure 4.37: (a) Plot of Ca+Mg/Cl vs Na/Cl ratio; (b) Plot of Ca/(SO <sub>4</sub> +HCO <sub>3</sub> ).....	117
Figure 4.38: (a) Dominant anion ratio plots and (b) plots of Ca <sup>2+</sup> /Mg <sup>2+</sup> ratio .....	120
Figure 4.39: Saturated indices of calcite dissolution and precipitation .....	124
Figure 5.1: Idealised illustration of the RTt model derived from the Source–Pathway–Receptor concept of the European Vulnerability Approach.....	129
Figure 5.2: Conceptualised flow of contaminated water in the RTt vulnerability method .....	130
Figure 5.3: Diffusive flow model illustration for groundwater movement .....	135
Figure 5.4: Dominant flow process as a function of saturated hydraulic conductivity and depth to lower permeability lithology.....	140
Figure 5.5: Objective and subjective criteria used in the RTt vulnerability method .....	147
Figure 6.1: Sedimentary formation, soil and rock types in the Dahomey Basin .....	149
Figure 6.2 (a) and (b): Shallow groundwater systems at varying depths .....	149
Figure 6.3: Rainfall map of the rainfall–travel time vulnerability method .....	154
Figure 6.4: Travel time map of the rainfall–travel time vulnerability method .....	155
Figure 6.5: Rainfall–travel time vulnerability map of the Dahomey Basin .....	156
Figure 7.1: Depth-to-water map of the Dahomey Basin .....	160
Figure 7.2: Net recharge map of the Dahomey Basin .....	162
Figure 7.3: Aquifer media map of the Dahomey Basin .....	163
Figure 7.4: Soil map of the Dahomey Basin .....	164
Figure 7.5: Processed topography Landsat imagery of the Dahomey Basin .....	165
Figure 7.6: Slopes map of the Dahomey Basin .....	165
Figure 7.7: Map of the Dahomey Basin vadose zone material .....	166
Figure 7.8: Hydraulic conductivity map of the Dahomey Basin .....	167
Figure 7.9: DRASTIC map of the Dahomey Basin .....	168
Figure 7.10: AVI travel time vulnerability map .....	171
Figure 7.11: Protective cover map of the Dahomey Basin .....	174
Figure 7.12: The I-Map of the Dahomey Basin .....	175
Figure 7.13: PI vulnerability map of the Dahomey Basin.....	176
Figure 8.1: (a) RTt vulnerability map cross-section; (b) Cross-section over chloride concentration map, (c) Plot of RTt index and Cl along the cross-section.....	180
Figure 8.2: Chloride plots against the rainfall–travel time index .....	181
Figure 8.3: (a) Section A–AA plots of RTt vulnerability index; (b) Cross-section plot A–AA on DO contour map; (c) Plot of cross-section of RT index with DO.....	182
Figure 8.4: (a) Cross plot of DO and RTt index vulnerability; (b) DO correlation plots with RTt vulnerability .....	183

Figure 8.5: (a) Cross-section plot of A–AA on the RTt index map; (b) THBC cross–section map; (c) Correlation plot between THBC and RTt index.....	185
Figure 8.6: (a) Bacteriology plots against the RTt index rating; (b) relationship between THBC and RTt groundwater vulnerability .....	186
Figure 8.7: Discrepancy plot of RTt with other vulnerability methods.....	188
Figure 8.8: Normalised plot of the Dahomey Basin vulnerability index .....	191
Figure 8.9: Comparison of percentages of vulnerability classes obtained by the application of the four different methods on the Dahomey Basin aquifers .....	191
Figure 8.10: Correlation plots of the RTt vulnerability method with other methods .....	193
Figure 8.11: Conceptual tree for the study of the RTt groundwater vulnerability method .....	197

## List of Tables

Table 2.1: Step determination of dominant I flow .....	20
Table 2.2: Step determination of I factor.....	20
Table 2.3: Index of vulnerability map derived from P-factor and I-factor .....	20
Table 2.4: Rating used to calculate EPIK protection index.....	23
Table 2.5: EPIK vulnerability and protection index .....	23
Table 2.6: Factors and data required for the four selected vulnerability methods in mapping Slovene karst catchment.....	26
Table 2.7: Assigned weights for DRASTIC hydrogeologic factors .....	28
Table 4.1: Apparent resistivity values of formation from the Dahomey Basin .....	65
Table 4.2: Apparent resistivity values of formation from the Dahomey Basin .....	66
Table 4.3: Apparent resistivity interpretation showing geo-electric parameters in $\Omega\text{m}$ .....	69
Table 4.4: Interpreted resistivity results of sounding points and closed water samples .....	69
Table 4.5: Interpreted apparent resistivity, lithological unit and hydrogeological implications .....	73
Table 4.6: Range of uniformity and coefficient value .....	78
Table 4.7: Grain size classification of the Dahomey Basin vadose sediment .....	85
Table 4.8: Hydraulic conductivity of selected sediments .....	88
Table 4.9: Average hydraulic conductivity values of the formations .....	89
Table 4.10: Percentile values of lithology of the Dahomey Basin sediment .....	90
Table 4.11: Hydraulic conductivity values of the permeameter experiment and a comparison to empirical methods .....	91
Table 4.12: Permeameter hydraulic conductivity ( $K_p$ ) correlation with empirical methods .....	92
Table 4.13: Selected hydraulic conductivity and porosity values of the Dahomey Basin soils and expected range of porosity.....	96
Table 4.14: Major metals of soils from the Dahomey Basin .....	100
Table 4.15: Representative mineralogical composition from lithology in the Dahomey Basin .....	101
Table 4.16: Cation Exchange Capacity of sediment.....	102
Table 4.17: Twenty years' rainfall data of three major cities in the Dahomey Basin .....	105
Table 4.18: Current abstraction rate of selected locations in the Dahomey Basin .....	108
Table 4.19: Physical and chemical parameters of the Dahomey Basin groundwater presented in mg/l .....	112
Table 4.20: Water quality and hydrochemical facies of the Dahomey Basin.....	118
Table 4.21: Rainwater chemistry in (meq/l) .....	120
Table 4.22: Total Plate Count on general and differential media counts (Total Viable CFU/mL $\times 10^3$ )122	122

Table 4.23: SI indices values of the Dahomey Basin groundwater .....	125
Table 5.1: Rainfall rating of the RTt method .....	132
Table 5.2.: Recharge rating of the RTt method.....	132
Table 5.3: Hydraulic conductivity range and weight used in calculating travel time .....	139
Table 5.4: Grouping of soil type base on hydraulic conductivity.....	141
Table 5.5: Rock type, hydraulic conductivity with assigned weight .....	141
Table 5.6.: Soil textural property, hydraulic conductivity and clay percentage .....	142
Table 5.7: Porosity rating based on Soil .....	143
Table 5.8: Porosity rating based on rock type.....	143
Table 5.9: Depth-to-water range and assigned weight used in travel time calculation .....	144
Table 5.10: Slope range and assigned weight.....	144
Table 5.11: RTt vulnerability class and index .....	145
Table 6.1: Depth-to-water level, rainfall and topography data .....	151
Table 6.2: Rainfall rating and weight of the Dahomey Basin .....	152
Table 6.3: Saturated hydraulic conductivity range in the Dahomey Basin .....	153
Table 6.4: Porosity ratings of the Dahomey Basin.....	153
Table 6.5: Rainfall–travel time source data and description .....	154
Table 6.6: Rating for rainfall–travel time vulnerability index .....	157
Table 6.7: Shallow aquifer formations in the Dahomey Basin and their generalised vulnerability classes .....	157
Table 7.1: Sources of data employed in the DRASTIC computation.....	159
Table 7.2: Depth-to-water range of the Dahomey Basin .....	160
Table 7.3: Net recharges estimation from precipitation and run off.....	161
Table 7.4: Rating of net recharge of the Dahomey Basin.....	161
Table 7.5: Rating of aquifer media of the Dahomey Basin .....	162
Table 7.6: Soil media range present in the Dahomey Basin.....	163
Table 7.7: Vadose zone impact and rating .....	166
Table 7.8: Vertical travel time estimate of vadose zone material in the Dahomey Basin.....	170
Table 7.9: Values of the factors T, R, S, L and F.....	173
Table 8.1: Parameters considered under the four vulnerability methods in this research.....	189
Table 8.2: Vulnerability classification and range.....	190

## List of Acronyms and Abbreviations

ABK	Abeokuta Formation
AVI	Aquifer Vulnerability Index
CIS	Common Implementation Strategy
COP	Concentration of flow–Overlying soils–Precipitation
CPS	Coastal Plain Sand
Cu	Coefficient Uniformity
DC	Direct Current
DEM	Digital Elevation Model
DO	Dissolved Oxygen
eFC	Effective Field Capacity
ETR	Evapo-transpiration
EWE	Ewekoro Formation
FOS	Federal Office of Statistics
GIS	Geographic Information System
GLA	Geologische Landesämter (German States Geological Surveys)
GLS	Global Land Survey
GSA	Grain Size Analysis
GSD	Grain Size Distribution
GSI	Geological Survey of Ireland
HPA	High Protection Areas
ILA	Ilaro Formation
ITCZ	Inter-tropical Convergence Zone
Khazen	Hazen Empirical Hydraulic Conductivity
Km&U	Matthes & Ubell Hydraulic Conductivity
Kp	Permeameter Hydraulic Conductivity
MGWB	Major Groundwater Basins
MPA	Maximum Protection Areas
NAFDAC	National Agency for Food and Drug Administration and Control
NASA	National Aeronautics and Space Administration
NERC	Natural Environment Research Council

NIHSA	Nigeria Hydrological Service Agency
NPC	National Population Commission
NRC	National Research Council
OSH	Oshosun Formation
PCSM	Point Count System Model
Redox	Oxidation–reduction
RTt	Rainfall Travel-time Method
SEM	Scanning Electron Microscope
TECC	Total Escherichia Coli Counts
THBC	Total Heterotrophic Bacteria Counts
TSSC	Total Salmonella/Shigella Counts
USA	United States of America
USGS	United States Geological Survey (USGS)
USEPA	United States Environmental Protection Agency
UTM	Universal Transverse Mercator
VES	Vertical Electrical Sounding
WAPCO	West African Portland Cement Company
WFD	Water Framework Directive
WISH	Windows Interpretation System for Hydrogeologist Software
WHO	World Health Organization
XRF	X-Ray Fluorescence Technology



## List of Symbols

Ca(Mg)Cl	Calcium Magnesium Chloride Water Type
Cl	Chloride
CFU/mL	Colony-Forming Units per Milliliter
ha	Hectare (10 000 square metres)
Hg	Inches of Mercury
$k$	Intrinsic Permeability
$K$	Hydraulic Conductivity
$K_{sat}$	Saturated Hydraulic Conductivity
kPa	KiloPascal
l/s	Litre per second
m	metre
meq/l	Milliequivalent per litre
mg/l	Milligram/litre
MI	Mega litre (10 <sup>6</sup> litre)
Mm <sup>3</sup>	Mega cubic metre (10 <sup>6</sup> cubic metre)
mm	Millimetre
m <sup>2</sup> /d	Square metres per day
m <sup>3</sup> /d	Cubic metres per day
Na	Sodium
Na(K)Cl	Sodium Potassium Chloride Water Type
$\Omega$ m	Ohmmetre
$\rho$	Electrical Resistivity
$\theta$	Porosity

# CHAPTER 1

## INTRODUCTION

### 1.1 Background Information

Groundwater vulnerability evaluations are means to synthesise complex geohydrological information into a form useable to planners, decision- and policy-makers, geoscientists and the public (Liggett and Talwar, 2009). The vulnerability method as a means of groundwater protection and management has been continuously modified and validated since its first usage by Margat (1968). A common methodology used in groundwater vulnerability investigations includes DRASTIC (Aller *et al.*, 1987), COP (Vias *et al.*, 2006), EPIK (Doerfliger *et al.*, 1999), AVI (Van Stempvoort *et al.*, 1993), SINTACS (Civita, 2000), GOD (Foster, 1987), PI (Goldscheider *et al.*, 2000), VULK (Sinreich *et al.*, 2007), and many more. Some of these vulnerability methods are designed for particular aquifers, such as karst groundwater vulnerability, while others are addressed to general water resources protection or a singular source protection such as water wells.

To successfully exploit and protect groundwater from deterioration from its pristine status, a proper understanding of the geohydrological characteristics of the aquifer units in relation to its environmental susceptibility is important. Aquifers are not only characterised by hydraulic conductivity, but also by transmissivity (product of hydraulic conductivity and aquifer thickness) and diffusivity (ratio of transmissivity and storage coefficient). Others are soil/rock composition, prevailing climatic condition, pH, the resident time of water within the formation, topography, mode and source of recharge, the drainage area and permeability of the soil cover (Davis and De Wiest, 1966). These comprehensive data are limited in many developing countries.

The consequence of uncontrolled urbanisation and industrialisation (as witnessed in most developing countries) threaten the quality of many urban groundwater resources. By evaluating the degree of aquifer vulnerability and its protection from contamination, it is necessary to understand the intrinsic property of the aquifer to contamination and its geohydrological characteristics. These above properties depend on the sensitivity of the aquifer system to human or natural impacts (Vrba and Zaporozec, 1994). Sensitivity can also be defined as aquifer protective capacity particularly for porous mediums (Olorunfemi *et al.*, 1999). Classification of the aquifer systems according to risk is highlighted in Article 4 of the Water Framework Directive of the European Union (WFD, 2010), which sets out five objectives for groundwater protection:

- Prevent or limit the input of pollutants.
- Prevent the deterioration of good status of groundwater bodies.
- Achieve good groundwater status (both chemical and quantitative).
- Implement measures to reverse any significant and sustained upward trend.
- Meet the requirements of protected areas.

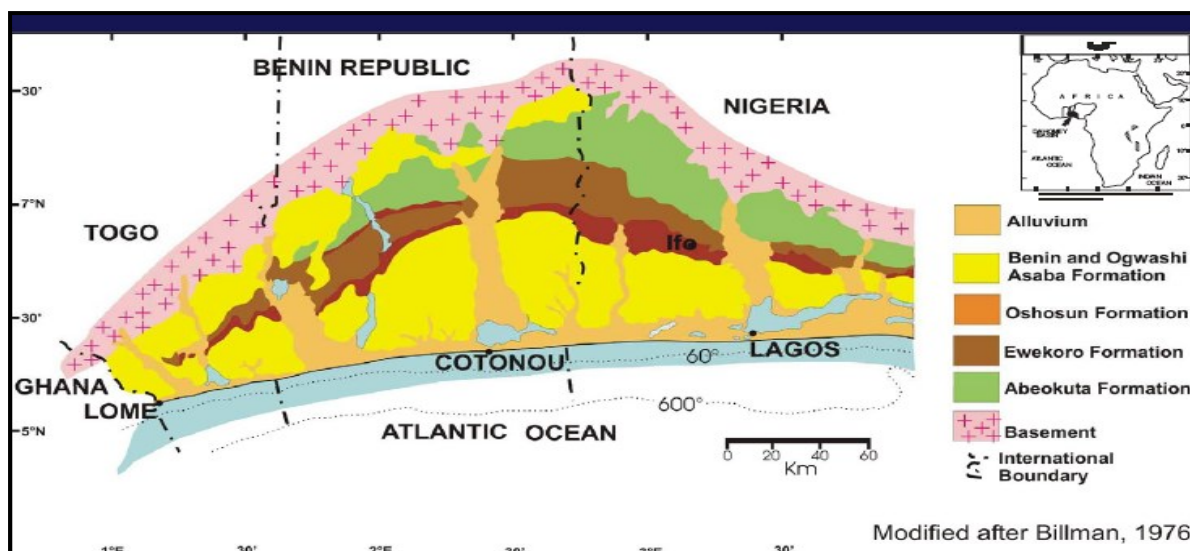
Groundwater protection requires information on groundwater vulnerability, namely mapping the intrinsic properties of aquifers to contamination. In most cases a comprehensive vulnerability assessment of the actual quantitative and qualitative status of a particular groundwater body is not feasible. This is due to insufficient monitoring data and/or the complexity of groundwater systems (CIS Groundwater risk assessment report, 2004). As an alternative, groundwater vulnerability indices are identified and mapped in order to reflect the actual, or to predict the potential severity of human induced deterioration in groundwater quantity and quality.

The problem of insufficient monitoring data is more compounded in data limited areas. Data limited areas are major regions with little documented scientific information for research applications. Major areas in African countries lack comprehensive hydrogeological research data due to reduced government spending on data acquisition and information management (Xu and Braune, 2010). It is perceived that most groundwater vulnerability methods sometimes are inapplicable to many areas of the African continent. This is not due to the scientific basis of the method, but largely because of unavailability of data.

The Dahomey Basin in southwestern Nigeria, one of the transboundary sedimentary basins of West Africa (Figure 1.1) is affected by the challenges of limited comprehensive geohydrological data. The basin is a marginally sag basin formed by continental rifting, thinning and faulting (Adegoke, 1969). Groundwater occurrence in the Dahomey Basin is found in confined and unconfined state, depending on the sedimentary rock depositions that serve as the aquifer (Jones and Hockey, 1964). The basin has also been tagged risky to contamination by Xu and Braune (2010), which is due to its fast growing rate, provincial densely populated towns and future megacities, including the national capitals of Lome, Cotonou, Port-Novo and Lagos, situated along its coast. Assessing the aquifer vulnerability in the Dahomey Basin, particularly the unconfined aquifers, would require evaluating the factors responsible for the groundwater protection.

Numerous methods have been proposed to assess groundwater vulnerability as stated earlier and can also be useful in assessing the vulnerability of the Dahomey Basin. However, due to the heterogeneity and localised and complex nature of the aquifers and its protective cover, and limited geohydrology data, there is a need of proposing other simplified methods with less data needs. The simplified methods will be targeting the intrinsic properties of the aquifer protective cover and depicted with vulnerability maps.

Vulnerability maps assist in land-use planning, regulation and protection. Vulnerability maps allow for delimitation of areas with different degrees of natural protection of groundwater against pollution (Orehova *et al.*, 2009). Maps showing the lateral distribution of well-protected and poorly protected aquifers are therefore essential for spatial development, regulation and provision of good water resources, particularly for the uncontrolled growing population of the Dahomey Basin. In view of the above background, unconfined aquifers in the Dahomey Basin of southwestern Nigeria are therefore targeted for its vulnerability studies.



Source: Billman (1976)

Figure 1.1 Geological map of the Dahomey Basin showing the capital cities

## 1.2 Study Rationale

The challenges of groundwater contamination and vulnerability assessments vary across regions of the world. Groundwater vulnerability investigations require a pool of geohydrological data for assessment, which is a challenge in African countries. African countries are not as economically developed as their European and American counterparts and scientific funding is hampering the availability of data pool to conduct geohydrological and groundwater vulnerability research. Established vulnerability methods can be employed to assess the Dahomey Basin groundwater vulnerability to contamination, but due to a lack of comprehensive geohydrological data in most African countries and the Dahomey Basin inclusive (Adelana and MacDonald, 2008); it is pertinent to develop a simplified vulnerability method suitable for assessing the Dahomey Basin and other data limited areas. The developed vulnerability method must address the peculiarity of these challenges confronting African countries.

In developing a new vulnerability methodology for assessing the Dahomey Basin, it is important to investigate the protective cover over the aquifer. Investigations of the natural protection above the aquifer is necessarily required to promote laws and land-use practises aimed at preventing groundwater contamination. These protective covers are defined by groundwater vulnerability maps. Therefore, the major significance of this research will be to formulate a simplified way of assessing groundwater vulnerability for data scarce areas.

Groundwater resources are identified as an important source of water supply in many parts of Africa, including the Dahomey Basin (Giordano, 2009; Xu and Braune, 2010). This is largely because groundwater requires little or no treatment except in areas with elevated metal and non-metal concentrations (Edmunds and Smedley, 2005), and can be cheaply developed when compared to municipal water sources. The relative qualities of most African groundwater result from their natural attenuation capacity and related hydrogeochemical processes (Xu and Braune, 2010). However, so many factors can lead to aquifer

contamination in the Dahomey Basin, some of which includes poor urban planning, indiscriminate refuse dumping, improper land use and unregulated chemical applications in agricultural activities.

Demographic change is another contributing factor. In contrast to the lack of extensive geohydrological knowledge, the prospects of demographic change in Africa in the twenty-first century are known with some certainty. The population of sub-Saharan Africa increased from 478 million in 1980, to 700 million in 2007, 1 100 million in 2013 and 1 500 million in 2050, and it will become increasingly urban (MacDonald *et al.*, 2005; United Nations, 2013). The overall water demand, is therefore, expected to be more than double in the first half of the twenty-first century, without considering rises in *per capita* food and water consumption (MacDonald *et al.*, 2005).

The demographic change is alarming in Nigeria, the most populous country on the continent and seventh most populous in the world. Census figures put the country at 55.7 million in 1963, 88.9 million in 1991, 140.4 million in 2006 and 160 million in 2012 (National Population Commission [NPC], 2014; United Nations, 2013). A double in population means double land usage and more demand on the available water resources. The above scenario is further disturbing in the Dahomey Basin, including Lagos which forms part of the basin. Lagos is the world's sixth largest city and the most populous city in Africa, with 2 607 person per square kilometre in 2006 (NPC, 2014), and estimated density of 5 032 person per square kilometre in 2025 (Ojuri and Bankole, 2013). The population of Lagos was put at 18 million by the United Nations and is expected to be 24.6 million by the year 2025, which makes it the third most populous megacity in the world (Robins *et al.*, 2007).

It was estimated that 40.1% of Nigerians derive their sources of water from groundwater (Federal Office of Statistics [FOS], 2001; Ahianba *et al.*, 2008) which increases to 65.7% accessing improved drinking water by 2013 (NPC, 2014). A breakdown of this study show that 36.3% of Nigerians use water from boreholes or tube wells and 29.4% access water from large diameter hand-dug wells (NPC, 2014). This means one-third of the inhabitants of the Dahomey Basin rely on hand-dug wells and more than half of the basins inhabitants rely solely on groundwater. Therefore, as the population relying on groundwater increases and the requirements of the Millennium Development Goals of providing water in the right quantity and quality by 2015 (United Nations Millennium Project, 2005) seems challenging, the role of groundwater in supplying quality water cannot be ignored. It is therefore important to assess the vulnerability of the Dahomey Basin aquifer in order to protect it from potential pollution.

### 1.3 Research Aims and Objectives

The main aim of the research thesis is to evaluate the vulnerability of selected aquifer systems in the Eastern Dahomey Basin, South West of Nigeria. The sub-aims and corresponding objectives are given as follows:

**Sub-aim 1:** Geological and geohydrological site characterisation of the Dahomey Basin.

Objectives:

- Use of geophysics to delineate the depth-to-water table, vadose zone estimation and lithology characteristics of the Dahomey Basin.
- To determine the textural and hydraulic property of vadose and aquifer materials in the laboratory and their relation to groundwater vulnerability.
- Examining the litho geochemical characteristics of the vadose material for possible sorption or cation exchange.
- Characterising the hydrogeochemical properties of the groundwater systems.

**Sub-aim 2:** Development of groundwater vulnerability maps for the Dahomey Basin using selected existing methods.

Objectives:

- Justification of the selected existing vulnerability methods.
- Assessing the degree of vulnerability of the Dahomey Basin with the selected existing methods.
- Major significance of the assessment with the existing vulnerability methods and implication for the Dahomey Basin.

**Sub-aim 3:** Develop a new simplified vulnerability assessment method and test its application in the Dahomey Basin.

Objectives:

- Proposing the rationale and governing principles for the new method.
- Developing of the methodology for the proposed vulnerability assessment approach.
- Testing the application of the method.
- Validation of the new method.

### 1.4 Definition of Vulnerability Terms

The definition of groundwater vulnerability is important because the term vulnerability means different things to different people. The groundwater vulnerability definition will also differentiate vulnerability from similar terms such as susceptibility, pollution risk and contamination risk. The term vulnerability was first used in Europe in the 1960s and researchers have given different definitions to groundwater vulnerability, namely:

“**Aquifer vulnerability** is the possibility of percolation and diffusion of contamination from the ground surface into natural water table reservoirs, under natural conditions” (Margat, 1968, quoted from Vrba and Zoporozec, 1994).

“Vulnerability is the degree of endangerment, determined by natural conditions and independent of present source of pollution” (Olmer and Rezac, 1974, quoted from Vrba and Zoporozec, 1994).

“Vulnerability is the risk of chemical substances used or disposed of on or near the ground surface to influence groundwater quality” (Villumsen *et al.*, 1983, quoted from Vrba and Zoporozec, 1994).

“**Groundwater vulnerability** is the sensitivity of groundwater quality to anthropogenic activities which may prove detrimental to the present and/ or intended usage-value of the resources” (Bachmat and Collin, 1987, quoted from Vrba and Zoporozec, 1994).

“Vulnerability of a hydrogeological system is the ability of this system to cope with external, natural and anthropogenic impacts that affect its state and character in time and space” (Sotornikova and Vrba, 1987, quoted from Vrba and Zoporozec, 1994).

“Groundwater vulnerability is a measure of the risk placed upon the groundwater by human activities and the presence of contaminants ... without the presence of contaminants, even the most susceptible groundwater is not at risk, and thus, is not vulnerable” (Palmquist, 1991, quoted from Vrba and Zoporozec 1994).

“Groundwater vulnerability is the tendency of, or likelihood for, contaminants to reach a specified position in the groundwater system after introduction at some location above the uppermost aquifer” (US National Research Council, 1993, quoted from Vrba and Zoporozec, 1994).

“Vulnerability is an intrinsic property of a groundwater system that depends on the sensitivity of that system to human and/ or natural impacts” (International Association of Hydrogeologists, quoted from Vrba and Zoporozec, 1994).

“Vulnerability is a combination of (a) the inaccessibility of saturated zone, in a hydraulic sense, to the penetration of pollutants; and (b) the attenuation capacity of the strata overlying the saturated zone as a result of physiochemical retention or reaction of pollutant... It is ... a statement about the intrinsic characteristics of the strata (unsaturated zone or confining beds) separating the saturated aquifer from the land surface, thus providing an indication of the impact of land-use decisions at that point on the immediately underlying groundwater” (Foster, 1998; in Robins *et al.*, 1998).

Due to an abundance of available definitions of groundwater vulnerability, the concept is perceived as ambiguous and lacking clear definition (Daly *et al.*, 2002; Frind *et al.*, 2006, Stigter *et al.*, 2006, Sorichetta, 2010). The definition proposed by Liggett and Talwar (2009) that groundwater vulnerability assessments are means to synthesis complex hydrogeologic

information into a useable form by planners, decision- and policy-makers, geoscientists and the public is good, but too wide and unclear.

This study therefore suggests that to understand how vulnerability is defined in an area, it is important to be aware of the parameters used to assess vulnerability in the area. In this case, vulnerability is an intrinsic characteristic of the natural environment, which is independent of contaminant type and source, as well as specific land use and management practices. It is very close to the definition of **aquifer sensitivity** developed by the United States Environmental Protection Agency (USEPA, 1993). A further definition and concept of vulnerability in relation to protection of groundwater can be found in Vrba and Zaporozec (1994), Frind *et al.* (2006), Popescu *et al.* (2008) and Sorichetta (2010). These vulnerability definitions vary in approach, but they are all risk assessments from a source through the pathway to a receptor which is the groundwater system.

**Groundwater risk** is defined as a threat posed by a hazard to human health due to pollution of a specific natural aquifer discharge. Aquifer risk is different to aquifer vulnerability because aquifer risk involves assessing the presence and level of a particular substance such as chemicals in groundwater systems, while aquifer vulnerability is predicting the extent of the aquifer to contamination.

**Intrinsic vulnerability** is the term used to define the vulnerability of groundwater to contaminants generated by human activities (Daly *et al.*, 2002). It takes account of the inherent geological, hydrological, and geohydrological characteristics of an area, but is independent of the nature of the contaminants. Intrinsic vulnerability differs from **specific vulnerability**, the latter being used to define the vulnerability of groundwater to a particular contaminant or group of contaminants. It takes account of the properties of the contaminants and their relationships with the various components of intrinsic vulnerability (Daly *et al.*, 2002).

## 1.5 Structure of the Thesis

This thesis is divided into nine chapters.

**Chapter 1** presents the introduction of the research, the research rationalisation, the research objectives, definition of important terms and general structures of the thesis.

**Chapter 2** entails a comprehensive literature overview on aquifer vulnerability, including common methods of assessment, travel time concept and validation of vulnerability methods.

**Chapter 3** reviews the previous works on the Dahomey Basin, including its geology, stratigraphy and hydrogeological conditions, topography, formations, and soil types.

**Chapter 4** investigates and characterises the hydrogeological properties of the Dahomey Basin. A multidimensional approach is applied. This approach includes:



- The application of a geo-electric method in the characterisation of the lithology and estimation of bed thickness and overall depth of groundwater depth.
- Litho-geochemical characterisation of the vadose zone.
- Hydrochemical evaluation of dominant chemical processes within the groundwater system, including geochemical processes and water quality evaluation.
- Hydraulic characterisation of the vadose material, including laboratory estimation of hydraulic conductivity, shape sediments and sediment distribution.

**Chapter 5** presents the development of the concept of the rainfall–travel time (RTt) vulnerability method. Its methodology, data acquisition, application and weaknesses are shown. RTt vulnerability parameters weighting and rating are explained.

**Chapter 6** presents the applications of the RTt vulnerability concept to the shallow aquifers of the Dahomey Basin. Maps of rainfall and travel time are presented. A final vulnerability map is derived from the rainfall and travel time map.

In **Chapter 7** established methods of estimating aquifer vulnerability are used. These include DRASTIC, PI and AVI. The DRASTIC methodology uses parameters rating to estimate groundwater vulnerability. Based on these ratings, maps showing different parameters ratings are used to produce a comprehensive vulnerability map of the Dahomey Basin. Furthermore, a PI map and an AVI map are presented and compared with the RTt vulnerability maps.

Validation of the RTt index map with chloride, dissolved oxygen, and microorganisms are presented in **Chapter 8**. Similarities, differences and the likely reasons for the different vulnerability classes are presented. In addition, the strengths and limitations of the RTt index map to other vulnerability maps are shown. Evaluation comparisons between the four vulnerability plots are evaluated based on the normalised values and reasons for the differences and similarities are stated.

**Chapter 9** summarises and concludes the overall findings of this research. The future outlook, recommendations and significance of the research are presented. The chapter concludes by highlighting the gap filled by the research.

# CHAPTER 2

## OVERVIEW ON GROUNDWATER VULNERABILITY

### 2.1 The General Concepts

Aquifer vulnerability investigations of porous aquifers have been developed since the late sixties and early seventies (Margat, 1968; Albinet and Margat, 1970). Groundwater vulnerability definitions and classifications are broad and different methods were developed for specific aims. Gogu and Dessargues (2000), Magiera (2000) and Goldscheider (2002) reviewed the various existing vulnerability methods. Statistical, Point Count System Models (PCSM), mathematical models, index and the analogical model are some of the methods developed and used in vulnerability investigations. It is also noted that vulnerability classifications can be done according to the scale (site, local, regional) or purpose (e.g. risk management, protection zoning) and also to distinguish between source and resource vulnerability maps, on the one hand, and specific and intrinsic vulnerability maps, on the other.

Based on the availability of input data of the geohydrological system under consideration, three basic vulnerability methods can be adopted:

- Subjective methods.
- Physically based methods.
- Statistical methods.

The most popular of these methods is the subjective method. This is based on the rating of individual hydrogeological factors. The physically based method is an objective or process based method widely used next to the subjective method. The physically based method relies on the physical processes that take place in the hydrogeological systems. The third approach of statistical methods attempt at predicting contaminant concentrations or probabilities of contamination based on the correlations between aquifer properties and contaminant source and occurrence (Focazio *et al.*, 2001; Hojberg *et al.*, 2006; Sorichetta, 2010).

Two important issues that must be addressed before assessing groundwater vulnerability are:

- The assessment for addressing groundwater intrinsic or specific vulnerability.
- The selection of the target to be assessed.

Intrinsic vulnerability is the susceptibility of groundwater to contaminants generated by human activities (Vias *et al.*, 2006). The intrinsic vulnerability takes into account the hydrogeological characteristics of an area, but is independent of the nature of the contaminant and the contamination scenario (Daly *et al.*, 2002; Vias *et al.*, 2006). Specific vulnerability takes into account the physical–chemical properties of contaminants and their relationship to the physical–chemical properties of the hydrogeological system. Specific vulnerability is useful when considering the aspect of land-use practises.

The target of groundwater vulnerability assessment can be set either at the groundwater table (top of the aquifer in unconfined, confined or leaky-confined conditions) or at the particular location in the saturated zone (Brouyère *et al.*, 2001; Daly *et al.*, 2002; Voigt *et al.* 2004). Based on the target, groundwater vulnerability can further be grouped into two:

- The resources protection vulnerability methods.
- The source protection vulnerability methods.

For resource protection, groundwater surface is the target and the pathway to the surface consists of vertical movement through the layers above the groundwater surface (Figure 2.1). For source protection, the water in the well or spring is the target and the pathway includes mostly horizontal movement in the aquifer (Goldscheider *et al.*, 2000). Although both are closely related to one another, it is however possible to protect source without protecting the resources.

### 2.1.1 Intrinsic Vulnerability

Conventional methods that use intrinsic vulnerability (DRASTIC, AVI, SINTACS) are able to distinguish degrees of vulnerability at regional scales where different lithologies exist (Vias *et al.*, 2005). However, the above mentioned methods' weaknesses are that they are much less effective in assessing vulnerability in carbonate aquifers as they do not take into account the peculiarities of karst. Vulnerability methods developed for addressing the karst environment are termed the European approach. Examples of European vulnerability approaches include EPIK (Doerfliger *et al.*, 1999); Irish approach (Daly and Drew, 1999); GOD (Foster, 1987; Robbins *et al.*, 1998); COP (Vias *et al.*, 2006); and PI (Goldscheider *et al.*, 2000). Some of the European vulnerability approaches can also be applicable to non karst environments (e.g. PI, GOD and SINTAC).

To evaluate intrinsic vulnerability, three basic points were noted by Daly *et al.* (2002). These basic points are:

- The advective travel time.
- The relative quantity of contaminants that reach the target because not all contaminants that leave the surface catchment infiltrate into aquifer, some leaves as surface run-off.
- The physical attenuation (dispersion, dilution, dual porosity effect).

These points were highlighted in the European vulnerability approach (European Commission COST Action 620, 2003). Assessing intrinsic vulnerability is like evaluating the protective capacity of cover layers to the introduction and transport of contaminants into the groundwater. Common intrinsic vulnerability methods are subjective (overlay or index) methods. The most common ones, as reviewed by Gogu *et al.* (2000), are the following: Albinet and Margat (1970), Goossens and Van Damme (1987), Carter and Palmer (1987), GOD (Foster, 1987), DRASTIC (Aller *et al.*, 1987), SINTACS (Civita, 1994), SEEPAGE (Moore and John, 1990), AVI (Van Stempvoort *et al.*, 1993), ISIS (Civita and De Regibus, 1995), EPIK (Doerfliger and Zwahlen, 1998) and the German method (Von Hoyer and Söfner, 1998).

## 2.1.2 The Common Approach

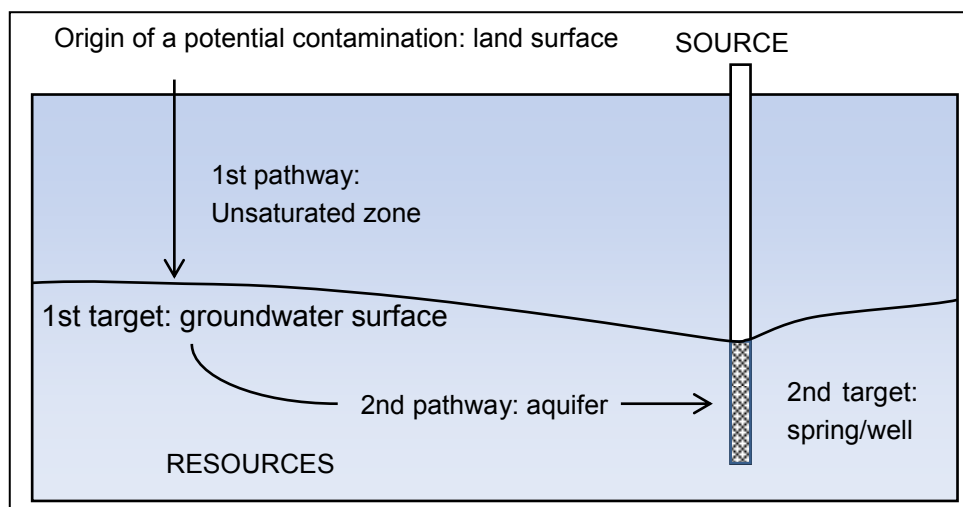
The European approach to groundwater vulnerability frameworks for protection of groundwater resources was based on two concepts:

- The protection of groundwater resources (target regional vulnerability assessment of overlying layers down to groundwater surface).
- The protection of groundwater sources (target well or spring including karst network) (Daly *et al.*, 2002).

As contained in the COST Action 620 (2003), the concept of the European approach should be broad-based and encompass all European conditions, but be sufficiently flexible to address the individual karstic regions it was designed for. The approach also suggests that the vulnerability methodologies should provide allowances for local conditions, information availability, time and resources.

### 2.1.2.1 The Origin–Pathway–Target Model

COST Action 620 (2003) suggests that the concept of vulnerability mapping should be based on the origin–pathway–target model of environmental management (Daly *et al.*, 2002). Origin is the term used to describe the location of a potential contaminant release. COST Action 620 suggests taking the land surface as the origin. This refers to land-use practices like cattle pasture and the spreading of pesticides. However, some contaminants are released below the ground surface, for example via leakages in sewerage systems and underground petrochemical tanks. The target (receptor) is the water which has to be protected. For resource protection, the target is the groundwater surface and for source protection it is the water in the well or spring. The pathway includes everything in between the origin and the target. For resource protection, the pathway consists of the vertical passage within the protective cover and for source protection it also includes horizontal flow in the aquifer (Figure 2.1). Different existing groundwater methodologies that use the European approach will be discussed later.



Source: Goldscheider *et al.* (2000).

Figure 2.1: Illustration of the origin–pathway–target model for groundwater vulnerability mapping and the concept of resource and source protection

## 2.2 General Approaches of Mapping Groundwater Vulnerability

Different methods have been applied to mapping of groundwater vulnerability. These methods, as discussed earlier, can be found in Vrba and Zaporozec, (1994), COST Action 620 (2003), Gogu and Dassargues (2000). Five broad methods were deduced by Goldscheider (2002) from the 69 vulnerability methods discussed by Magiera (2000) for mapping groundwater vulnerability:

- Hydrogeological complex and setting methods.
- Index models and analogical relations.
- Parametric system models.
- Mathematical models.
- Statistical methods.

### 2.2.1 Hydrogeological Complex and Setting Method

The hydrogeological complex and setting (HCS) method was first used by Margat (1968) and Albinet and Margat (1970). This method is based on the assumption that two areas with comparable hydrogeological properties are characterised by similar groundwater vulnerability (Vrba and Zaporozec, 1994). The method is applicable to small-scale mapping (1:1 million). The HCS method takes into account the geological, hydrogeological and topographical maps above the lithology (Goldscheider, 2002). The method was applied by Albinet and Margat (1970) to produce a vulnerability of France. The German vulnerability map was prepared with the same HCS by Vierhuf *et al.* (1981), using the same scale. The vulnerability was determined on the basis of the properties of the overlying layers and the depth of the groundwater table.

The major disadvantage of the HCS method is that validation is not possible, but HCS advantages include identifying different areas with significant different geological formations such as karst environment. Aller *et al.* (1987) further used the HCS concept to develop DRASTIC. However, the point count system model (PCSM) was used in assigning values to the DRASTIC-index.

### 2.2.2 Mathematical Methods

There are a few examples of numerical methods used to assess groundwater vulnerability. Numerical methods are mostly applied separately to saturated and unsaturated zones and are frequently used in contaminant migration predictions. This makes the numerical methods relevant in operation and water management protection zones (Goldscheider, 2002). Mageira (2000) describes nine examples for the application of mathematical methods for specific vulnerability mapping on a large to medium scale. These models take into account both the properties of the contaminant (mostly nitrates and pesticides) and the properties of the overlying layers and are often verified. Numerical methods are rarely used in groundwater vulnerability assessment even though it allows assessing and validating the consistency of other methods to vulnerability mapping (Daly *et al.*, 2002).

The advantage of the mathematical methods is that it is easy to verify since they are used in contaminant mapping. Neukum *et al.* (2008) presented a validation method based on simple numerical modelling and field investigations to validate qualitative vulnerability methods. Voigt *et al.* (2004) used mean travel time as a vulnerability indicator. Frind *et al.* (2006) applied a standard numerical flow and transport code to provide relative measures of intrinsic well vulnerability based on solute breakthrough curves. Neukum and Azzam (2009) presented a methodology which comprised four indicators to estimate vulnerability based on properties of solute breakthrough curves at the groundwater table. An index rating system was added to Neukum and Azzam (2009) effort by Yu *et al.* (2010).

### **2.2.3 Statistical Methods**

Due to the selective parameters evaluated out of the complex variables that should actually be assessed in most other vulnerability evaluations, the statistical and geostatistical methods provide alternative ways of evaluating large parameters in the vulnerability approach. This has successfully been applied on small to medium scale mapping (Mageira, 2000; Panagopoulos *et al.*, 2006; Sorichetta *et al.*, 2010). The first step in a geostatistical vulnerability analysis is to map a selected number of influencing factors, such as depth-to-groundwater table, soil type, permeability and recharge. The second step is to map the spatial distribution of the concentration of a certain contaminant in the groundwater. The third step is to establish a correlation between the influencing factors and the contaminant concentration. This correlation can be used to map the specific vulnerability of groundwater to the selected contaminant (e.g. Teso *et al.*, 1996). The major disadvantage of the geostatistical method is the difficulty in finding a correlation between contaminant concentrations and influencing factors responsible. It is also difficult to develop, and once established, can only be applied to regions that have similar environmental conditions to the region in which the statistical model was developed.

### **2.2.4 Parametric System Method**

This is the most common approach in groundwater vulnerability mapping. Due to the wide usage of parametric methods, it has been subdivided into different approaches. Common among these approaches are the Point Count System Models (PCSMs) that weight critical factors affecting vulnerability, matrix factors (MS), rating system (RS) and sophisticated models of the processes occurring in the vadose zone (Lasserre *et al.*, 1999; Connell and Daele, 2003; Babiker *et al.*, 2005; Vías *et al.*, 2005; Panagopoulos *et al.*, 2006; Mende *et al.*, 2007; Rahman, 2008; Saidi *et al.*, 2011). All these approaches of parametric methods are the same. The parametric system method procedure involves the selection of factors (parameters) assumed to be significant for vulnerability. Each factor has a natural range which is subdivided into discrete intervals, and each interval is assigned a value reflecting the relative degree of sensitivity to contamination. The vulnerability of an area is determined by putting together the values of the different factors using a matrix (MS), a rating system (RS) or a point count system model (PCSM).

Examples of the different parametric methods that are usually named with an acronym formed from first letters of the factors that are taken into account are DRASTIC (Aller *et al.*,

1987), EPIK (Doerfliger and Zwahlen, 1998), SINTACS (Civital and De Maio, 2000), PI (Goldscheider *et al.*, 2000) from the point count system and GOD (Foster, 1987) from the rating system. DRASTIC means **D**epth-to-groundwater, net **R**echarge, **A**quifer media, **S**oil media, **T**opography, **I**mpact of vadose zone and hydraulic **C**onductivity. GOD means **G**roundwater occurrence (e.g. none, confined, unconfined), **O**verlying lithology (e.g alluvial, gravel, sandstone, limestone) and the **D**epth-to-groundwater table. PI stands for **P**rotective cover of the lithology above the water table and **I**nfiltration condition at which the protective cover is bypassed. Full descriptions of some of these methods will subsequently be presented.

### 2.2.5 Index Methods

Index methods and analogical relations follow the standard descriptions of hydrological and geohydrological investigations based on mathematical standard, for example transport equations (Magiera, 2000; Goldscheider, 2002). Most index methods are for the evaluations of specific vulnerability of groundwater to pesticides on a large to medium scale. The index method takes into consideration the overlying lithology and the contaminant. The attenuation factor introduced by Rao *et al.* (1985) is one of the earliest index methods used to map pesticides. Further work based on Rao *et al.* (1985) was the processed based indexed method used by Lowe *et al.* (2005) and incorporates physical and chemical processes through mathematical equations addressing the behaviour of certain chemicals in the subsurface.

## 2.3 Description of Some Basic Methods

For ease of understanding, a brief detail description of some major and common vulnerability methodologies will be attempted. The methods will include intrinsic, European approach, source and resource vulnerability methods.

### 2.3.1 The PCOK Method

The PCOK conceptualised vulnerability method is based on the hazard–pathway–target model. The PCOK was designed by Daly *et al.* (2002) for the European Commission. The **P** represents precipitation. This is simply the total quantity, duration and intensity of precipitation that can influence the quantity and rate of infiltration. The four scenarios considered under the P-factor are:

- Humid climate with extreme events.
- Humid climate without extreme events.
- Dry climate with extreme events.
- Dry climate without extreme events.

The **C** represents the flow–concentration factor. This is the degree to which infiltration occurs. The C-factor is dependent on many parameters which include:

- Presence of karst features or other places which concentrate infiltration flow.
- The parameters which controls run-off, including slope, vegetation and physical soil properties.

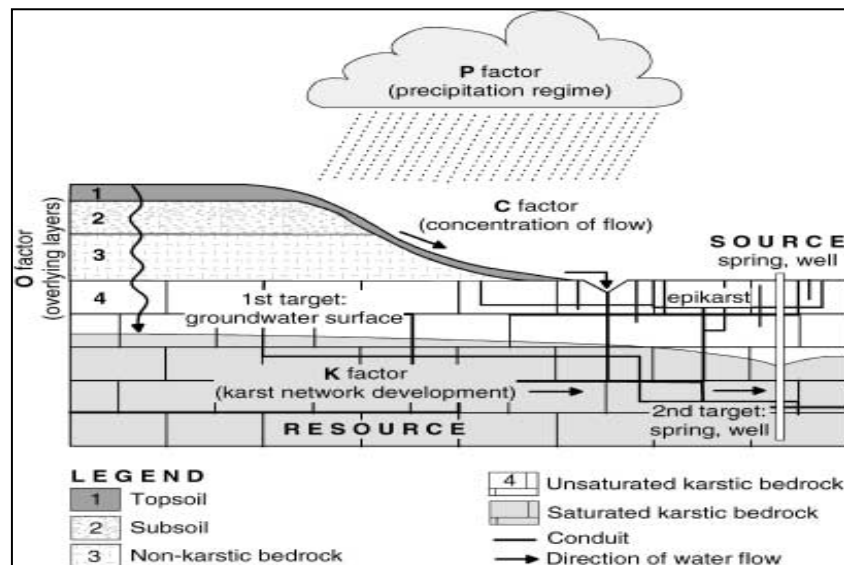
The **O**-factor is the overlying layers between the land surface and the groundwater. Daly *et al.* (2002) identified four possible layer types according to previous work of Holting *et al.* (1996) and Goldscheider *et al.* (2000) for the O-factor:

- **Topsoil**, which are weathering zones composed of minerals, organics substances, water, air, living matter and roots.
- **Subsoil**, sediment of granular, unconsolidated material such as sand, clay and gravel are grouped here.
- **Non-karst bedrock**, consisting of non-karstic rock like sandstone, schist, shale and basalt.
- **Unsaturated karstic bedrock**, which includes epikarst.

Further parameters considered in the O-factor reflecting the protective capacity of the overlying layers are:

- Important key data collected including layer thickness, hydraulic conductivity values, effective porosity values, macro-porosity or fissuring, fracturing or karstification.
- Other data that the main data can assess including grain-size distribution, lithological content, soil type, vegetation indicators and drainage density.

The **K**-factor is the main factor considering the karstic network of the saturated aquifer. The karstic source considered in these methods was both for the well and the spring (Figure 2.2). This means that the vertical and horizontal pathways through the saturated karstic bedrock must be considered. The K-factor was lastly based on the COST Action 620 classification which in turn was based on a general description of the bedrock, giving a range of possibilities from porous carbonate-rock aquifers to highly karstified networks.



Source: Modified after Goldscheider *et al.* (2000).

Figure 2.2: Diagrammatic cross section showing the PCOK method distribution of factors for intrinsic vulnerability maps



### 2.3.2 The COP Method

The need to act on the recommendations of Daly *et al.* (2002), which failed to give guidelines, tables or formulae for vulnerability assessment, propelled Vias *et al.* (2006) to propose the COP method following the European approach and the factors highlighted in Daly *et al.* (2002). The COP acronym stands for **C**oncentration of flow–**O**verlying soils–**P**recipitation, respectively. The COP method uses quantification and categorisation of parameters with the weighting of variables for the vulnerability index. This method is based on the concept of assessing the natural protection of groundwater.

The COP method follows the factor classifications of the PCOK parameters (Daly *et al.*, 2002) with little modifications (Figure 2.3). The overlying layers are divided into the soil sub-factor [ $O_S$ ] and lithology sub-factor [ $O_L$ ]. The COP method further subdivides the properties of rock responsible for its hydrogeological characteristics, including effective porosity and hydraulic conductivity, degree of fracturing [ $I_y$ ], thickness of each layer [ $m$ ] and confining conditions [ $cn$ ]. An index similar to vertical protection (layer index) derived from the product of multiplication of thickness and lithology of each layer, is proposed. This concept is based on the AVI and PI method by Van Stempvoort *et al.* (1993) and Goldscheider *et al.* (2000).

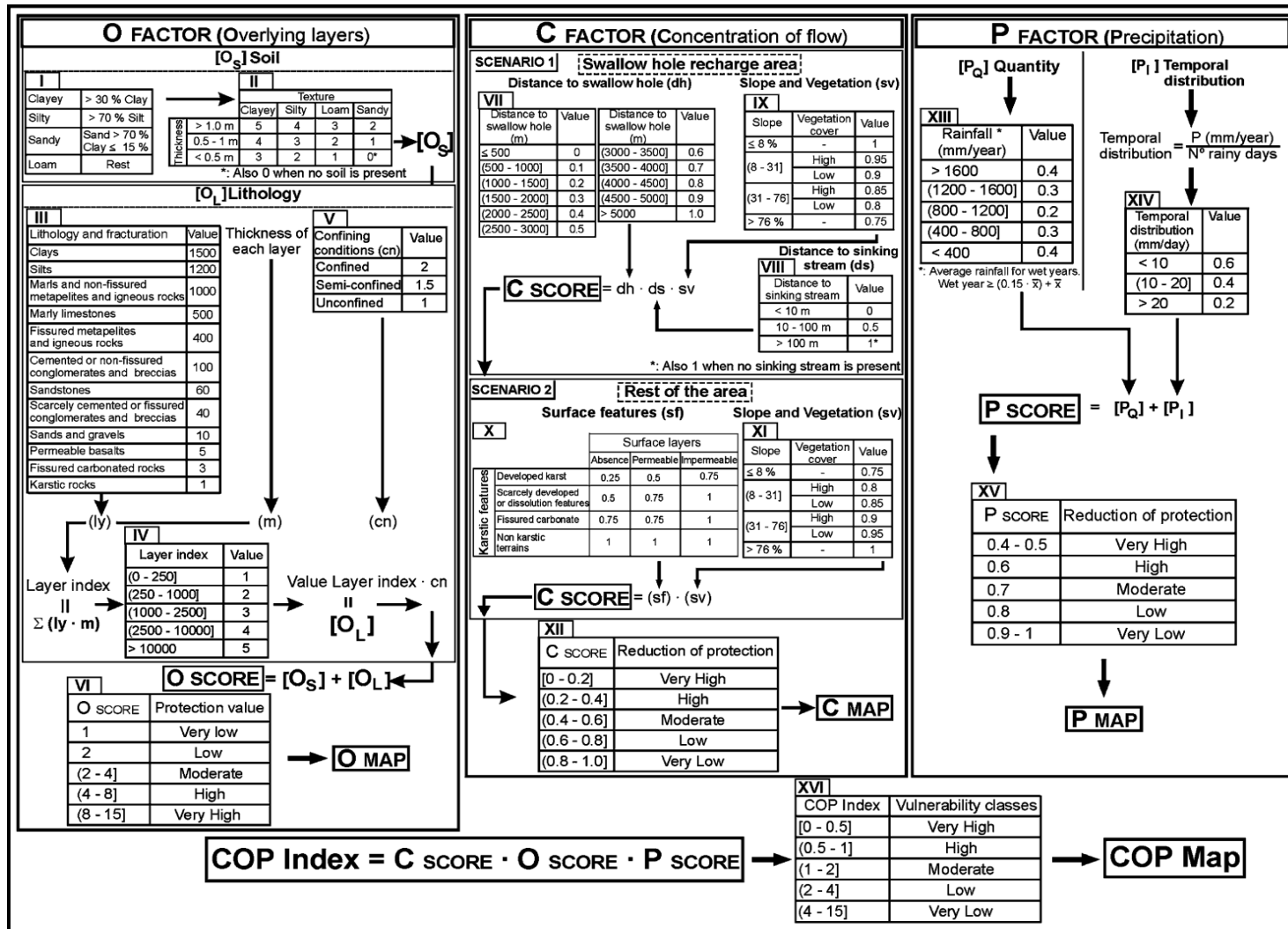
The C-factor is a modifier of the Overlying factors [ $O$ ]. The C-factor is the degree to which precipitation at or near an aquifer outcrop is concentrated into the swallow hole, bypassing the unsaturated zone. The C-factor concept in the COP method is based on the PI method of Goldscheider *et al.* (2000), and the EPIK method of Doerfliger and Zwahlen (1998). The C-factor is further subdivided into two scenarios. Scenario 1 includes swallowed holes recharge areas considered under four variables:

- Distance to a swallow hole [ $dh$ ].
- Slope and vegetation [ $sv$ ].
- Distance to sinking stream [ $ds$ ].
- No sinking stream is present.

Scenario 2 includes the rest of the area. This is also under two variables:

- Surface features [ $sf$ ].
- Slope and vegetation [ $sv$ ].

Precipitation represents the P-factor in the COP method. Precipitation as used in COP is the quantity of precipitation and the factors which influence the rate of infiltration such as temporal distribution, duration and intensity of extreme rainfall events and frequency. Two sub-factors- [ $PQ$ ] quantity of precipitation and [ $PI$ ] - temporal distribution of precipitation are used. COP precipitation based on the assumptions that increase in precipitation up to 800-1 200 mm increases vulnerability, because transit time of contaminants infiltrating from the surface into groundwater is likely to be more important than the dilution process. The COP index range include 0–0.5 as very high vulnerability, 0.5–1 as high vulnerability, 1–2 as moderate vulnerability, 2–4 as low vulnerability and 4–5 as very low vulnerability (Figure 2.3).



Source: Vias et al. (2006).

Figure 2.3: Diagram of the COP method, containing numeric evaluation and index

The COP method was used to map the intrinsic vulnerability of two carbonate aquifers in southern Spain with a differing climate, hydrogeology and geology (Vias *et al.*, 2006). Other areas where it was used, are mapping the karst terrains of South Africa (Leyland, 2008) and the application of modified COP+K in the Herrerias cave of Asturias, Spain (Marin *et al.*, 2012; Andreo *et al.*, 2009). The K-factor is based on the transit time, the information of the karst network, and the degree of connection of it to the spring or well (Andreo *et al.*, 2006).

### **Strengths of the COP Method**

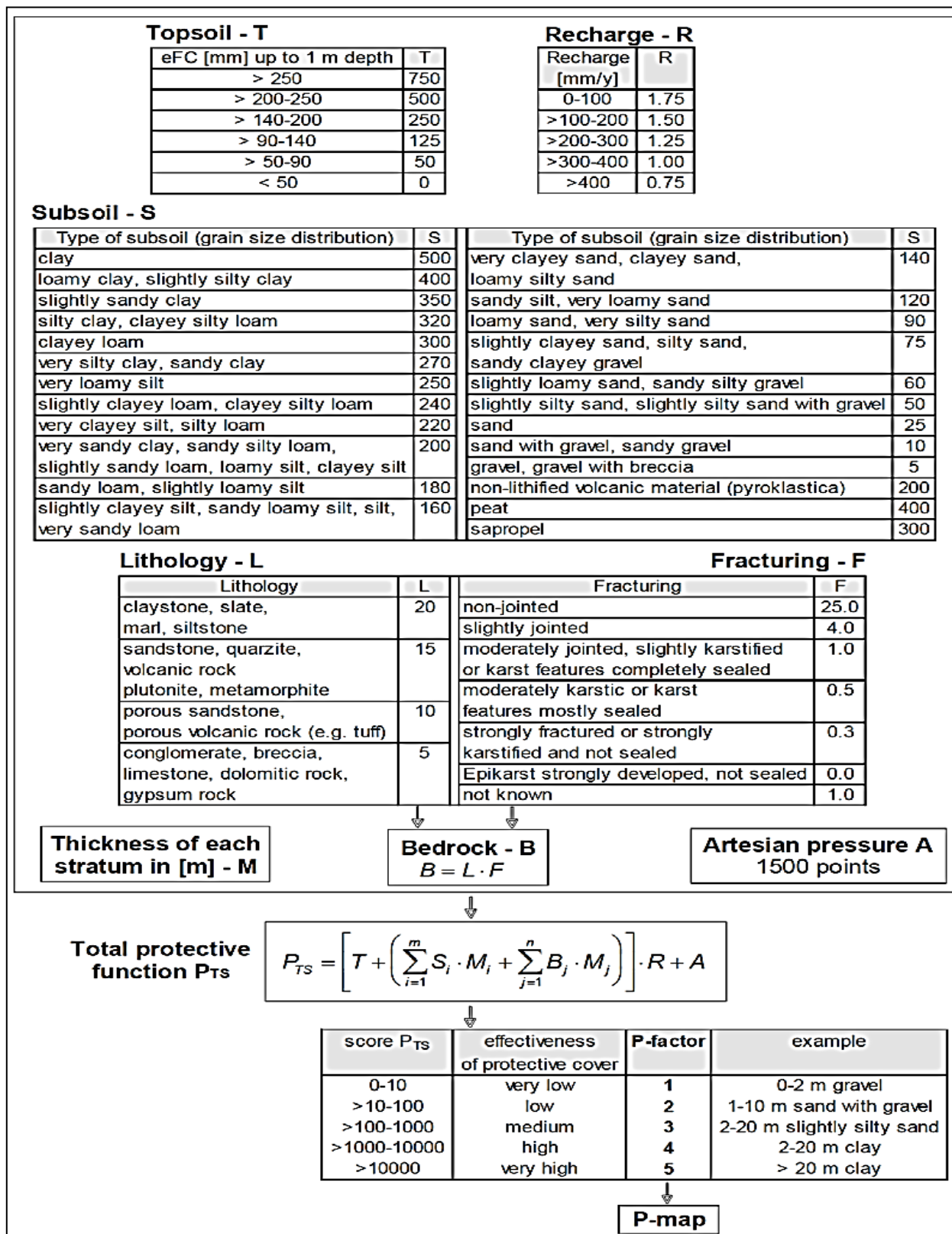
Advantages of the COP method is that it can be applied using available geo-environmental data, but with some fieldwork. COP can also be used without the extensive input of a Geographic Information System (GIS) common to most vulnerability methodologies. In summary, the overlying layers [O] of the COP method were basically derived by multiplying the thickness and the lithology of each layer. This is the same as the simplified AVI method by Van Stempvoort *et al.* (1993). If a simpler method could effectively summarise the overlying lithology of COP and PCOK, there is no need going through the longer route.

### **2.3.3 The PI Method**

The PI method developed by Goldscheider *et al.* (2000) marked a further advance in assessing the degree of vulnerability of karst aquifers. The PI method applies the concept of pollutant transport from an origin on the surface (i.e. above the soil) through the pathway of the unsaturated zone to the groundwater surface. The P-factor is applicable to all types of aquifers and is based on an assessment scheme initially proposed by Hölting *et al.* (1995), while the I factor accounts for the karst specific recharge and infiltration processes.

The P-factor describes the effectiveness of the protective cover resulting mainly from the thickness and hydraulic properties of all the strata between the ground surface and the groundwater table (Figure 2.4), the soil, the subsoil, the non-karstic bedrock and the unsaturated zone of the karstic bedrock (Goldscheider, 2002). The I factor describes the infiltration conditions, particularly the degree to which the protective cover is bypassed as a result of lateral surface and subsurface flow (Table 2.1 and Table 2.2). Therefore, the I factor distinguishes between the dominant flow processes (infiltration, subsurface flow or surface flow).

The final protection factor  $\pi$  is the product of P and I. It is subdivided into five classes (Table 2.3). A protective factor of  $\pi \leq 1$  indicates a very low degree of protection and an extreme vulnerability to contamination;  $\pi = 5$  indicates a high degree of protection and a very low vulnerability.



Source: Goldscheider *et al.*, 2000.

Figure 2.4: Determination of P-factor in the PI method

Table 2.1: Step determination of dominant I flow

<b>First step: Determination of the dominant process</b>				
		Depth to low permeability layer		
		<30 cm	30–100 cm	>100 cm
Saturated hydraulic conductivity (m/s)	>10 <sup>-4</sup>	Type D	Type C	Type A
	>10 <sup>-5</sup> –10 <sup>-4</sup>		Type B	
	>10 <sup>-6</sup> –10 <sup>-5</sup>	Type E		
	<10 <sup>-6</sup>	Type F		
<b>Second step: Determination of I factor</b>				
Forest				
Dominant flow process		<3.5%	3.5–27%	>27%
Infiltration	Type A	1.0	1.0	1.0
	Type B	1.0	0.8	0.6
Subsurface flow	Type C	1.0	0.6	0.6
	Type D	0.8	0.6	0.4
Surface flow	Type E	1.0	0.6	0.4
	Type F	0.8	0.4	0.2
<b>Field/Meadow/Pature</b>				
Dominant flow process		<3.5%	3.5–27%	>27%
Infiltration	Type A	1.0	1.0	0.8
	Type B	1.0	0.6	0.4
Subsurface flow	Type C	1.0	0.4	0.2
	Type D	0.6	0.4	0.2
Surface flow	Type E	0.8	0.4	0.2
	Type F	0.6	0.2	0.0

Table 2.2: Step determination of I factor

<b>Third step: Determination of the I factor</b>							
Surface Catchment map		I factor					
		0.0	0.2	0.4	0.6	0.8	1.0
A	Swallow hole, sinking and 10 m buffer	0.0	0.0	0.0	0.0	0.0	0.0
B	100 m buffer on both sides of sinking stream	0.0	0.2	0.4	0.6	0.8	1.0
C	Catchment of sinking stream	0.2	0.4	0.6	0.8	1.0	1.0
D	Area discharging inside karst area	0.4	0.6	0.8	1.0	1.0	1.0
E	Area discharge out of the karst area	1.0	1.0	1.0	1.0	1.0	1.0

Table 2.3: Index of vulnerability map derived from P-factor and I-factor

Vulnerability map Vulnerability of groundwater		P-map Protection function of overlying layers		I-map Degree of bypassing		
Description	Π-factor	Description	P-factor	Description	I-factor	
Extreme	>0–1	Very low	1	Very high	0-0.2	Red
High	>1–2	Low	2	High	0.4	Orange
Moderate	>2–3	Moderate	3	Moderate	0.6	Yellow
Low	>3–4	High	4	Low	0.8	Green
Very low	>4–5	Very high	5	Very low	1.0	Blue

The following characteristics of karst systems are relevant in respect to groundwater vulnerability, and should consequently be taken into account (Goldscheider, 2005):

- Each karst system has its individual characteristics; generalisation is problematic.
- Karst systems are heterogeneous and anisotropic; interpolation of data is thus difficult and the reliability of a vulnerability map can be lower for karst than for other areas.
- There is both diffuse and point recharge. Adjacent non-karst areas may generate surface flow that may enter the karst aquifer via swallow holes (allogenic recharge).
- The epikarst, if present, controls the infiltration into the aquifer. It may store water and concentrate flow. The structure and function of epikarst is often difficult to assess.
- Karst aquifers may comprise conduits, fissures and intergranular pores. Contaminants can be transported very fast in the conduits or stored in the fissures and pores (matrix).
- Karst systems portray strong hydraulic and physicochemical reactions to hydrologic events.
- The water table and hydraulic gradient are often difficult to define, particularly in shallow and conduit systems.
- Karst catchments are often large and hydraulically connected over long distances. Karst catchments may overlap and the flow paths (proved by tracer tests) may cross each other.

#### **Weaknesses of the PI Method**

The protective cover factor takes into account the total annual recharge dependent on the annual precipitation, and the infiltration conditions factor takes into consideration the predominant flow process. This depends on the properties of the area and the precipitation regime, namely the time distribution of precipitation. This may not be possible to calculate for data limited areas due to the high numbers of calculated parameters.

The classification of dominant flow processes (I factor) is not exactly certain. Although it follows a stepwise procedure, its classification does not leave room for a possible flow process outside the listed range. Also, the saturated hydraulic conductivity values only range between  $>10^{-4}$  and  $<10^{-6}$ . Values outside this range are also difficult to place within the stated documented values.

For the protective function of the PI method, Daly *et al.* (2000b) suggest modification of the overlying layers on the basis of the protective property multiplied by thickness (m), and finally permeability as a means to evaluate the protective properties (see also Goldscheider, 2002). They further recommend using grain size distribution (GSD) and protective properties of subsoil material, which the GLA method (Holting *et al.*, 1996) has linked with permeability and provided standard values for. This indirectly means that the P factors of the PI method can be re-assessed by simply determining the GSD and multiplying it by the thickness. Therefore, for simplification and usage in data lacking areas, protective cover as used in the

PI method can be evaluated using standard values as presented in Kunoth (2000), multiplied by lithology thickness.

### 2.3.4 The EPIK Method

The EPIK method developed by Doerfliger *et al.* (1999), takes four factors into account: epikarst development (E), protective cover (P), infiltration conditions (I) and karst network development (K). Each factor is given a ranking index, where after a weighting coefficient is attributed to each of the indexed factors according to their degree of protection. The epikarst (E) is a subsurface, a highly fissured and karstified zone, which can extend between decimetres and tens of metres. Its main functions are water storage and flow concentration. The degrees of epikarst development are assessed based on geomorphologic karst features. Three classes are distinguished:

- $E_1$  Swallow holes, dolines, karrenfields.
- $E_2$  Intermediate zones between the aligned dolines, dry valleys.
- $E_3$  The rest of the catchment.

The protective cover (*P*) includes the soil and other non-karstic formations overlying the karst aquifer. Four categories are defined:

- $P_1$  0–20 cm of soil and/or low permeability formations.
- $P_2$  20–100 cm of soil and/or low permeability formations.
- $P_3$  More than 1 m of soil and/or low permeability formations.
- $P_4$  More than 8 m of low permeability formations, or more than 1 m of soil on 6 m of low permeability formations.

The infiltration (*I*) takes into consideration the type of recharge into the karst aquifer. Areas with diffuse infiltration are considered less vulnerable than areas that drain by concentrated recharge via a swallow hole. Four classes are distinguished:

- $I_1$  Perennial or temporary swallow holes and sinking streams, including the beds and banks of the streams, as well as artificially drained sectors within the catchment of these streams.
- $I_2$  Naturally drained areas inside the catchments of swallow holes or sinking streams with steep slopes (more than 10% for arable areas, more than 25% for meadows and pastures).
- $I_3$  Areas inside the catchment of swallow holes or sinking streams with gentle slopes (less than 10% or 25%, respectively); low lying areas outside such a catchment which collect run-off, and steep slopes which generate this run-off.
- $I_4$  Rest of the area.

The karst network development (K) is classified in the following ways:

- $K_1$  A moderate to well-developed karst network with decimetres to metres wide conduits.

$K_2$  A poorly developed or blocked karst network.

$K_3$  Fissured non-karstic limestone aquifers and systems that infiltrate in porous media.

The calculation of the EPIK rating protection index and vulnerability index is shown in Table 2.4 and Table 2.5 respectively.

The protection index F is calculated with the formula:

$$F = 3 \cdot E + P + 3 \cdot I + 2 \cdot K \quad \text{Equation 2.1}$$

Table 2.4: Rating used to calculate EPIK protection index

$E_1$	$E_2$	$E_3$	$P_1$	$P_2$	$P_3$	$P_4$	$I_1$	$I_2$	$I_3$	$I_4$	$K_1$	$K_2$	$K_3$
1	3	4	1	2	3	4	1	2	3	4	1	2	3

Table 2.5: EPIK vulnerability and protection index

Vulnerability	Protection Factor	Protection
Very high	$F < 19$	S1 (source protection zone)
High	$19 < F < 25$	S2 (inner protection zone)
Moderate	$F > 25$	S3 (outer protection zone)
low	$F > 25, P = P_4, I = I_{3,4}$	Rest of the catchment

### Weaknesses of the EPIK Method

A major disadvantage of EPIK is that it can only be used in karst areas. Other shortcomings of the EPIK method, as discussed by Goldscheider *et al.* (1999), include:

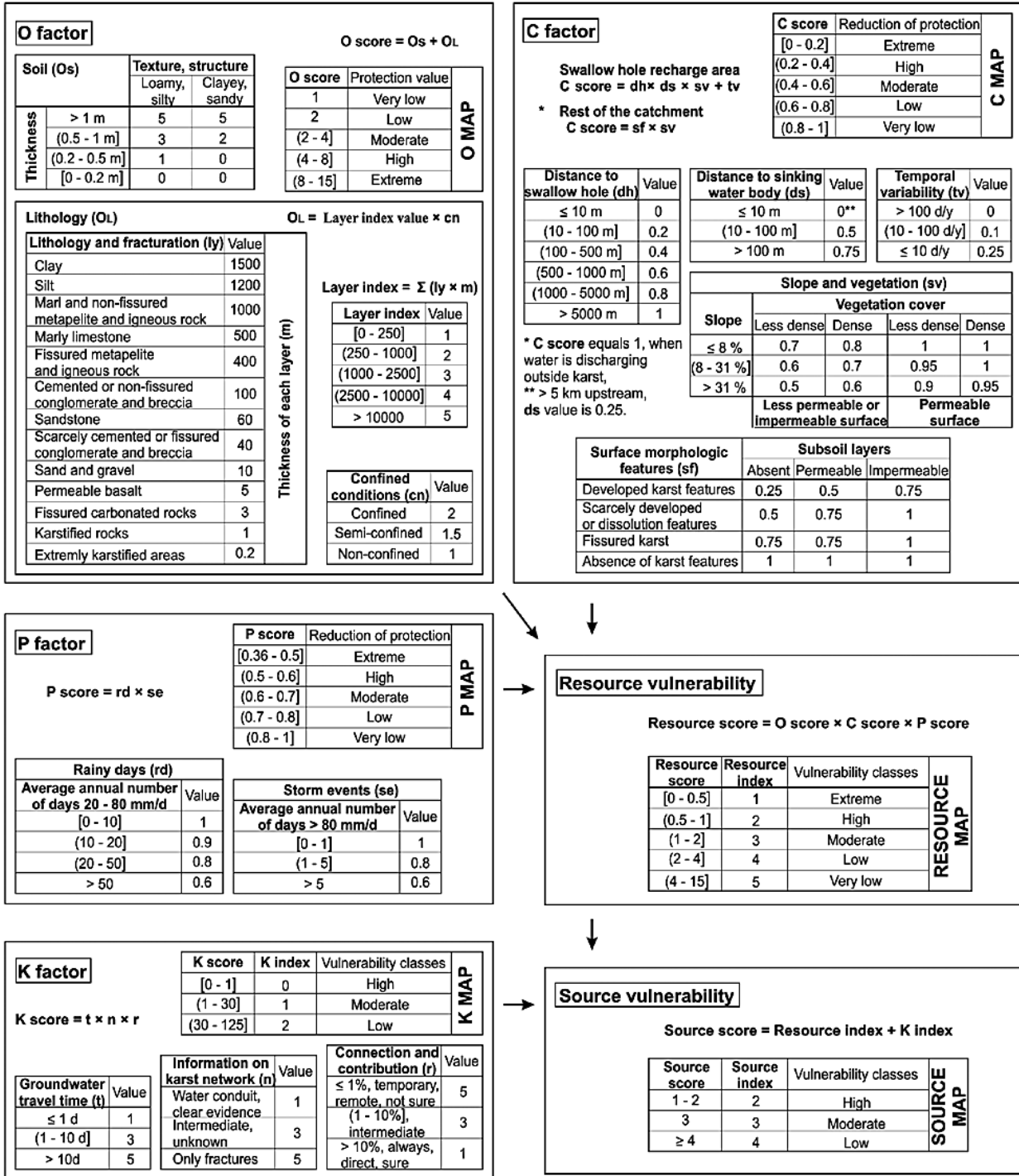
- Important parameters such as recharge and thickness were omitted.
- Epikarst (E) was based on the geomorphology of the karst, which is unreliable.
- Weighting system was contradictory.
- Zero was missing, making the minimum value of each attribute as one, even if its effect on protection was zero.
- The EPIK formula was not always applicable and not defined for all hydrogeological settings.

### 2.3.5 The Slovene Approach

The Slovene Approach is thus far the most complete interpretation of the European approach (Ravbar, 2007; Ravbar and Goldscheider, 2007). It can be used for vulnerability mapping and also includes an assessment of contamination hazards, an evaluation of the importance or value of the groundwater and different types of risk maps. The Slovene Approach was developed for source and resource vulnerability mapping since it is built on the PI method. It is complete, realistic and direct. The Slovene Approach is based on the framework of the COP method (Figure 2.5 and Figure 2.6), and partly based on the PI method (Vias *et al.*, 2006; Andreo *et al.*, 2006). The complete parameters involved in the assessment of the Slovene Approach are shown in Table 2.6.



**SLOVENE APPROACH**  
**INTRINSIC VULNERABILITY**



No.	Hazards	Classification criteria	Ranking factor (Qn)				
			0.8	0.9	1	1.1	1.2
<b>1.</b>	<b>Infrastructural development</b>						
1.1.	Waste water (urbanisation)	Population density (inhabitant/km <sup>2</sup> )	< 10	[10 - 50)	[50 - 100)	[100 - 500)	≥ 500
1.2.	Waste disposal (unprotected/illegal)	Volume (1000 m <sup>3</sup> )	< 0.1	[0.1 - 1)	[1 - 5)	[5 - 10)	≥ 10
1.3.	Fuels	No. Pumps	< 2	[2 - 5)	[5 - 10)	[10 - 15)	≥ 15
		Amount of storage (t)	< 0.5	[0.5 - 1)	[1 - 5)	[5 - 10)	≥ 10
1.4.	Transport and traffic, roads	No. Vehicles/day	< 100	[100 - 1,000)	[1,000 - 5,000)	[5,000 - 10,000)	≥ 10,000
	Railway	No. Trains/day	< 10	[10 - 25)	[25 - 50)	[50 - 100)	≥ 100
1.5.	Recreational facilities	No. Visitors/day	< 10	[10 - 100)	[100 - 500)	[500 - 1,000)	≥ 1,000
1.6.1.	Graveyard	Size (1000 m <sup>2</sup> )	< 5	[5 - 10)	[10 - 50)	[50 - 100)	≥ 100
1.6.5.	Military installations and dereliction	Size (km <sup>2</sup> )	< 1	[1 - 5)	[5 - 10)	[10 - 25)	≥ 25
<b>2.</b>	<b>Industrial activities</b>						
2.1.	Mining (in operation and abandoned)	Volume (1000 m <sup>3</sup> )	< 0.1	[0.1 - 1)	[1 - 5)	[5 - 10)	≥ 10
2.2.	Excavation sites	Volume (1000 m <sup>3</sup> )	< 0.1	[0.1 - 1)	[1 - 5)	[5 - 10)	≥ 10
2.4.	Industrial plants (none mining)	Water consumption (1000 m <sup>3</sup> /year)	< 1	[1 - 5)	[5 - 10)	[10 - 50)	≥ 50
2.5.	Power plants (wind turbines)	Power (kw)	< 50	[50 - 100)	[100 - 500)	[500 - 1,000)	≥ 1,000
2.6.	Industrial storage	Volume (1000 m <sup>3</sup> )	< 0.1	[0.1 - 1)	[1 - 5)	[5 - 10)	≥ 10
2.7.	Diverting and treatment of waste water	Capacity in PU (Person unit)	< 500	[500 - 1,000)	[1,000 - 1,500)	[1,500 - 2,000)	≥ 2,000
<b>3.</b>	<b>Livestock and agriculture</b>						
3.1.	Livestock	Livestock in LU (Livestock unit)	< 5	[5 - 10)	[10 - 50)	[50 - 100)	≥ 100
		Livestock density (LU/ha cultivated land)	< 0.5	[0.5 - 1)	[1 - 1.5)	[1.5 - 2)	≥ 2
3.2.	Agriculture	Livestock in LU (Livestock unit)	< 5	[5 - 10)	[10 - 50)	[50 - 100)	≥ 100
		Livestock density (LU/ha cultivated land)	< 0.5	[0.5 - 1)	[1 - 1.5)	[1.5 - 2)	≥ 2
		Annual consumption of manure or liquid manure (m <sup>3</sup> /ha cultivated land)	< 1	[1 - 5)	[5 - 10)	[10 - 15)	≥ 15
		Annual consumption of mineral fertilizers (kg/ha cultivated land)	< 1	[1 - 10)	[10 - 50)	[50 - 100)	≥ 100
		Annual consumption of pesticides (kg/ha cultivated land)	< 1	[1 - 5)	[5 - 10)	[10 - 50)	≥ 50

Source: Ravbar and Goldscheider (2007).

Figure 2.6: Ranking factors of selected hazards used in the Slovene Approach

Table 2.6: Factors and data required for the four selected vulnerability methods in mapping Slovene karst catchment

Methods	Factors	EPIK	Simplified Method	PI	Slovene Approach
Karst unsaturated zone	Top soil thickness	+	+	+	+
	Top soil texture	-	-	+	+
	Top soil structure	-	-	+	+
	Subsoil permeability	+	+	+	+
	Subsoil thickness	+	+	+	+
	Depth of the unsaturated zone	-	-	+	+
	Fracturing	-	-	+	+
	Epikarst development/geomorphological features	+	-	+	+
	Confined situation	-	-	+	+
Recharge conditions	Concentration of flows	+	+	+	+
	Slope gradient	+	-	+	+
	Land use/vegetation cover	+	-	+	+
	Autogenic recharge	+	+	+	+
	Allogenic recharge	+	+	+	+
	Temporary variability	-	-	-	+
Karst saturated zone	Presence of active karst network	+	-	-	+
	Hydrological characteristics of a source	+	-	-	+
	Tracer test interpretation	+	-	-	+
Resource vulnerability		-	+	+	+
Source vulnerability		+	-	-	+

Source: Ravbar and Goldscheider (2009).

### 2.3.6 The DRASTIC Method

The DRASTIC empirical method was developed by Aller *et al.* (1987) to evaluate the pollution potential of groundwater systems on a regional scale. The method is the most widely used groundwater vulnerability method for mapping a wide range of contaminants (Hamm, 1999; Fritch *et al.*, 2000; Piscopo, 2001; Al-Adamat *et al.*, 2003; Thirumalaivasan *et al.*, 2003; Lobo-Ferreira and Oliveira, 2003; Ramos-Leal and Rodriguez-Castillo, 2003; Murat *et al.*, 2004; Vias *et al.*, 2005; Herlinger and Viero, 2006; Stigter *et al.*, 2006 and Rahman, 2008). DRASTIC has also been widely modified to suit specific investigations (Akhavan *et al.* 2011; Shirazi *et al.* 2013). The DRASTIC index is calculated roughly analogous to the likelihood that contaminants released from the surface will reach the groundwater.

The primary purpose of DRASTIC is to provide assistance in resource allocation and prioritisation of many types of groundwater-related activities and to provide a practical educational tool. DRASTIC can be used to set priorities for areas to conduct groundwater monitoring. For example, a denser monitoring system might be installed in areas where aquifer vulnerability is higher and land use suggests a potential source of pollution. DRASTIC can also be used with other information (such as land use, potential sources of contamination and beneficial uses of the aquifer) to identify areas where special attention or protection efforts are warranted.

The model has four assumptions:

- The contaminant is introduced at the ground surface.
- The contaminant is flushed into the groundwater by precipitation.
- The contaminant has the mobility of water.
- The area being evaluated by DRASTIC is 100 acres or larger.

DRASTIC was not designed to deal with pollutants introduced in the shallow or deep subsurface, by methods such as leaking underground storage tanks, animal waste lagoons, or injection wells. The methodology is not designed to replace on-site investigations or to site any type of facility or practice. For example, DRASTIC does not reflect the suitability of a site for waste disposal. Although DRASTIC may be one of many criteria used in siting decisions, it should not be the sole criterion.

DRASTIC was established on the Delphi technique (Aller *et al.*, 1987). To assess the level of risk, this technique utilises the practical and research experiences of professionals in the area of interest. DRASTIC was divided into four categories through the rating system: low, moderate, high and very high. The higher the DRASTIC rating the greater the prospect of aquifer contamination.

### 2.3.6.1 DRASTIC Index

DRASTIC considers seven hydrogeological factors:

(1) **D**epth-to-water; (2) net **R**echarge; (3) **A**quifer media; (4) **S**oil media; (5) **T**opography (slope); (6) **I**mpact of the vadose zone media; (7) hydraulic **C**onductivity of the aquifer.

Each of the hydrogeologic factors is assigned a rating of 1 to 10 based on a range of values. The ratings are then multiplied by a relative weight ranging from one to five. The most significant factors have a weight of five; the least significant have a weight of one. The ranges and ratings for each hydrogeologic factor are listed in the Table 2.7 and the following formula shows an addition to the DRASTIC method.

$$\text{DRASTIC Index} = D_R D_W + R_R R_W + A_R A_W + S_R S_W + T_R T_W + I_R I_W + C_R C_W$$

*Equation 2.2*

Where D, R, A, S, T, I and C are the seven parameters of the model, the subscripts R and W are the corresponding ratings and weights, respectively. DRASTIC applications are probably the best known and widely used method of vulnerability mapping. Its application includes mapping contaminant and groundwater protection.

DRASTIC has been widely modified to suit different problems. The modifications include the addition of land-use conditions, sewage, pesticides and other agricultural contaminants. The DRASTIC model was used for vulnerability assessment in Portugal by using hydrogeological parameters and the final map of the DRASTIC model was developed in ARC/INFO GIS software on a 1:500 000 scales (Lobo-Ferreira & Oliveira, 1997). Groundwater pollution vulnerability using DRASTIC/GIS was carried out in Midnapur, West Bengal. The DRASTIC index for both generic and industrial municipal and pesticide pollutants was derived and vulnerability maps were prepared for both (Shahid, 2000).

Recent studies have used DRASTIC in a Fuzzy logic-based environment for pesticide modelling to account for uncertainty (Chen and Kao, 1997; Dixon *et al.*, 2002). Fuzzy rule-based models provide comparable results with less input data, as well as improved vulnerability prediction when DRASTIC factors are used (Dixon, 2001, 2004, 2005). Incorporation of fuzzy rules and Neural Network (NN) with DRASTIC variables improved vulnerability prediction for pesticides.

### Weaknesses of the DRASTIC method

Several drawbacks of the DRASTIC method include:

- It is not based on a clear conceptual model such as the origin–pathway–target model.
- Several of the factors are redundant, such as the factors A and C, because hydraulic conductivity is directly dependent on the aquifer medium.
- DRASTIC is also criticised for not being a multidimensional approach. The one-dimensional approach of this method might be sufficient to assess the vulnerability of a typical alluvial aquifer where water and contaminant percolate vertically from the land surface down to groundwater, but not so for karst areas where water and contaminant bypass protective function through lateral flow into swallow holes.
- DRASTIC over-emphasis slopes.
- DRASTIC index score intervals do not readily allow for continuous data.
- Maps are difficult to update.

Table 2.7: Assigned weights for DRASTIC hydrogeologic factors

Rating	Depth of water (m) D × 5	Net recharge (mm/y) R × 4	Aquifer media A × 3	Soil media S × 2	Topography T × 1	Impact of vadose zone I × 5	Hydraulic conductivity (GPD/ft <sup>2</sup> ) C × 3
10	0–1.5		Karst limestone	Thin or absent, gravel	0–2	Karst limestone	<2 000
9	1.5–4.5	>250	Basalt	Sandstone and volcanic	2–3	Basalt	
8		180–250	Sand and gravel	peat	3–4	Sand and gravel	1 000–2 000
7	4.5–9		Massive sandstone & limestone	Shrinking and/or aggregate clay/alluvium	4–5	Gravel, sand	
6		100–180	Bedded sandstone & limestone	Sandy loam, schist, sand karst volcanic	5–6	Limestone, gravel, sand, clay	700–1 000
5	9–15		Glacial	Loam	6–10	Sandy silt	
4			Weathered Met./Igneous	Siltyloam	10–12	Metamorphic gravel and sandstone	300–700
3	15–23	50–100	Metamorphic/Igneous	Clay loam	12–16	Shale, silt and clay	
2	23–31		Massive shale	Muck acid, granitoid	16–18	Silty clay	100–300
1	>31	0–50		Non shrink and non-aggregated clay	>18	Confining layer, granite	1–100

Source: Al-Hanbali and Kondoh (2008).

### 2.3.7 The AVI Method

Another method of aquifer vulnerability assessment is the Aquifer Vulnerability Index (AVI) of Van Stempvoort *et al.* (1993). This method was approved by the Canadian Prairie Provinces Water Board. The AVI methodological strength relies on vadose zone characterisation which has been noted as being the most important single parameter in aquifer vulnerability evaluation (McLay *et al.*, 2001; Herbst *et al.*, 2005). It can be directly related to the physical properties of the vadose zone (Ross *et al.*, 2004). The AVI computes aquifer vulnerability on the basis of the hydraulic resistance ( $c$ ), as a ratio between the thickness of each sedimentary unit above the uppermost aquifer ( $d$ ), and the estimated hydraulic conductivity of each of these layers ( $K$ ). Hydraulic resistance is calculated by:

$$c = \sum_{i=1}^n \frac{d_i}{K_i}$$

Equation 2.3

Where:

- $n$  = number of sedimentary units above the aquifer
- $d_i$  = thickness of the vadose zone
- $K_i$  = hydraulic conductivity of each protective layer
- $K$  = unit of length/time (m/s or m/d)
- $c$  = travel time with dimension in seconds

The hydraulic resistance  $c$  (vulnerability index) is an inverse indicator of vulnerability: This is vertical flow of water through the protective layers. This can be used as a rough estimate of vertical travel time of water through the unsaturated layers. It is important to note that significant parameters controlling the travel time like hydraulic gradient and diffusion are not considered in AVI. Even if there are a lot of methodologies that consider the processes occurring in the vadose zone more accurately, the AVI method is one of the best (Lasserre *et al.*, 1999; Connell and Daele, 2003). The AVI index is perhaps most suitable at a large regional scale vulnerability assessment (Zwahlen, 2004).

#### Weaknesses of the AVI Method

- The AVI method is not regarded as a complete vulnerability method.
- The  $c$  is hydraulic resistance of fluid and not the only factor resisting fluid movements.
- The method is too simplified.

### 2.3.8 The SINTACS Method

The SINTACS method, proposed by Civita in 1994 and many times enhanced until the fifth remodification (Civita and De Maio, 2000), is partially derived from DRASTIC. It uses the same seven parameters, but is more flexible as to ratings ( $R$ ) and weights ( $W$ ). It provides five weight classifications: normal impact, severe impact, drainage (by streams), karst

(aquifers) and fissured (aquifers). The SINTACS index (or contamination potential) is a sum of the rating of each of the seven parameters multiplied by the associated weight.

#### **Weaknesses of the SINTACS Method**

- SINTACS assumed rating and weight to parameters like the DRASTIC method.
- Selected parameters are not the only important parameter affecting aquifer vulnerability.

#### **2.3.9 The GOD Method**

This is another vulnerability method with acronyms coined from the first word of its parameters. GOD was proposed by Foster (1987). GOD takes into account the type of groundwater occurrence (**G**) (e.g. none, confined, unconfined), the overlying lithology (**O**) (e.g. loam, gravel, sandstone, limestone) and the depth of the groundwater table (**D**). GOD is rated between 0 and 1. The overall values for vulnerability assessment is derived by multiplying the three factors which consequently ranges between 0.0 (negligible) and 1.0 (extreme). The main advantage of the GOD method is that it can be applied to any type of aquifer, except in the karst areas. The special nature of epikarst and vertical shaft is also another problem when using this method in karst environment. Other shortcomings include the over-rating of the factor D, for example a depth of 100 m to the water table is assigned as moderate vulnerability (0.4).

#### **2.3.10 The PaPRIKA Method**

This method is designed for resource and source vulnerability assessment based on the concept of EPIK, PI, RISK and COP, some of which were discussed earlier. PaPRIKA factored in the functional and structural conditions of aquifer. The **P** means protection, which includes soil cover, unsaturated zone and epikarst aquifer behaviour. **R** represents the rock type, **I** stand for infiltration and **KA** is the karstification factor (Doerfliger, 1994; Doerfliger, 2010). PaPRIKA allows for additional factors such as groundwater travel time and active conduit network on the vulnerability map. A significant point with PaPRIKA is the soil characteristics (texture, structure and thickness), non-saturated zone (thickness, lithology and fracture degree) and epikarst aquifer which were factored into the protective cover assessment. The degree of fracturing of the aquifer body with the lithology accounts for the R factor, while the slope with karst accounts for the infiltration factor. Chemical variability was added to the karst degree with discharge of spring, as well as velocity rates showed by artificial tracing techniques. PaPRIKAs major disadvantage is that recharge was not considered and the larger factor space was given to karstic terrains.

Other methodologies developed for vulnerability assessment incorporate the use of sophisticated tools such as neuro-fuzzy techniques (Dixon, 2005) or the fuzzy quantification approach combined with the Ordered Weighted Average procedure (Gemitzi *et al.*, 2006). Both the above techniques validated their methodologies comparing the results with water quality data trying to form a sensitivity analysis. Neukum *et al.* (2008) discussed the inappropriateness of the qualitative methods for vulnerability assessment and presented a validation methodology based on simple numerical modelling and field investigations.

A simplified approach to vulnerability was done by Nguyet and Goldscheider (2006). This approach was first applied to the tropical karst area in Vietnam. A similar simplified approach applied to data limited environments (Ravbar and Goldscheider, 2007) considered the importance of groundwater source and resource of particularly the Slovene Approach. The simplified approach and Slovene Approach characterised and delineated the site investigated using lithological, geomorphological mapping, geophysical survey, structural and tracer test to evaluate the karst aquifers

Brouyere *et al.* (2001) suggest that the three practical questions, to which a vulnerability assessment has to answer, are the following: If pollution occurs, when will it reach the target, at which concentration level and for how long will the target be polluted? It is suggested to use a so-called vulnerability cube. The three axes of the cube are the transfer time, the maximum concentration and the duration of a contamination. Vulnerability mapping should be based on assessing all the intrinsic properties which control the impulse response of the system to a DIRAC-type input of a conservative contaminant.

Frind *et al.* (2006) applied a standard numerical flow and transport code to provide relative measures of intrinsic well vulnerability based on solute breakthrough curves. Neukum and Azzam (2009) presented a methodology which comprised of four indicators to estimate vulnerability based on properties of solute breakthrough curves at the groundwater table. A modification of the above method is presented by Yu *et al.* (2010), providing an index system for vulnerability assessment.

## **2.4 Travel Time in Vulnerability Pathways**

Vulnerability pathways are the summation of layers between the ground surface and the water body, particularly the water table in resources vulnerability assessment. It can also be from the groundwater surface through the unsaturated and saturated layers below the ground to a drinking well for source vulnerability assessment. Pathways in vulnerability assessment are important because it determines the flow characteristics and flow alterations of percolating fluids. Pathways assessments are physically based and not much work has been done on vulnerability pathways like other subjective vulnerability methods.

Time scales of groundwater flow provide a basis for design of physically based groundwater vulnerability indices. According to Focazio *et al.* (2002), physically based methods take into account the physical process of flow and transport and do not have to rely on deterministic simulations. The physically based (process-based, objective) methods were initially seen as requiring “analytical or numerical solutions to mathematical equations that represent processes governing contaminant transport” (NRC, 1993). It has the disadvantages of managing large data, problems with upscaling and downscaling of results and difficulties with representation of preferential flow.

The travel time concept in vulnerability assessment has been used with different terminologies in the literature. Transit time, turnover time, residence times and seepage time are some of these terminologies. The idea of vulnerability assessment by travel time consideration was recommended by Fried (1987) for the second phase of elaboration of



hydrogeological maps of Groundwater Resources of the European Community. Travel time was already used by some countries to produce the vulnerability map of Valence, France (BRGM, 1979); in the Netherlands (Meinardi, 1982), Denmark (Villumsen *et al.*, 1982) and in the United Kingdom (The British Geological Survey since 1984). These maps were produced with residence time in the unsaturated zone based on the assumption that the contaminant and the physical properties are not different to that of water.

Four vulnerability categories were proposed based on the above travel time concept in the maps: greater than 20 years; one to 20 years; one week to one year; less than one week. Based on the methodologies of the abovementioned groundwater vulnerability maps, Anderson and Gosk (1987) considered their applicability and discussed whether vulnerability could be quantified as depending on the travel time of pollutants to the aquifer. They stated that the travel time of a pollutant from the source to the aquifer plays an important role in vulnerability mapping and can be used as vulnerability indicators only for situations where removal of the pollutant is dependent on time.

A simplified methodology for the estimation of vertical and horizontal travel and flushing timescales to nitrate threshold concentrations in Irish aquifers was presented by Fenton *et al.* (2011). The concept was based on time-lag of contamination (nutrient literally) transport from source to receptor via hydrological and hydrogeological pathways. Horizontal travel time was estimated for first occurrence of nutrients in a surface water body with assuming piston-flow model under steady state conditions. The authors ascertain that an appraisal of catchment time-lag issues offers a more realistic scientifically based timescale for expected water quality improvements in response to mitigation measures implemented under the WFD (2010).

The particle tracking model for contaminant travel time in pathways was used by Eberts *et al.* (2012) and Sousa *et al.* (2013). In Eberts *et al.* (2012), particle tracking was compared to lumped parameters and were used for evaluating the vulnerability of production wells to contamination. To explore differences between the models and their ability to predict contaminant responses in each production well, computed age distributions were applied to a hypothetical slug input of a conservative contaminant entering the aquifer across the entire area contributing to the recharge and lasting 25 years. Selected characteristics of the breakthrough curves from the particle tracking and lumped-parameter models for each investigated well were compared to determine which, if any, of the model differences notably affect contaminant predictions.

According to Witczak *et al.* (2007) the time-lag for vertical transport of conservative contaminants from the surface to shallow aquifer can be a basis for vulnerability classification. These time-lags can be calculated as either the ratios of exchangeable water content in the unsaturated zone to recharge flux (typically natural infiltration) or from conductivity and active porosity of soil layers above the saturated zone of the aquifer.

The use of hydrochemical data to estimate groundwater vulnerability was first proposed by Bachmat and Collin (1987). They expressed vulnerability by only one factor as the anticipated change in concentration of a given substance in the groundwater per unit efflux

of the mass of the substance to the ground surface. They argued that the resulting change of pollutant concentration is a function of travel time of the substance from the ground surface to the groundwater. The travel time through the unsaturated zone is a function of the thickness of the unsaturated zone (composed of sequence of some lithological differentiable, homogeneous layers) and the average downward velocity of the pollutant (similar to the AVI method of Van Stempvoort *et al.*, 1993).

They finally suggested three models to arrive at the velocity of the pollutant depending on the levels of complexity:

- **The piston-flow model**, which assumes that the pollution moves at the average velocity of the water, i.e. velocity is equal to the vertical specific discharge of the water divided by the effective moisture content of the layer.
- **The advection-dispersion model** (Bear, 1979), which assumes that the pollutant is advected at the average velocity of the water and dispersed owing to the fluctuation of the velocities of the individual water particles.
- **The pollutant-specific velocity model** where the pollutant moves with its own velocity, which may differ to that of the carrier (Gvirtzman *et al.* 1986).

The residence times of groundwater in the upper aquifer were evaluated based on the WEKU model (Kunkel and Wendland, 1997) which in turn is based on the Darcy equation. Residence times determined for unconsolidated rock areas typically ranged between 10 and 25 years, whereas residence times <5 years were assessed for consolidated rock areas. The residence times of percolate water in soil were derived from the water storage capacity of soils (field capacity) and the percolate water rate (Herrmann *et al.*, 2012).

In karst areas transit time was developed for physically-based lateral flow within the uppermost weathered zone (epikarst) and high velocities of vertical infiltration at discrete infiltration points (e.g. sinkholes) or lines (e.g. dry valleys, faults) (Brosig *et al.*, 2008). The Transient Time Method considers lateral water flow along the slope within the epikarst towards final infiltration points in dry valleys/ wadis. It takes into account the assumption that surface water run-off within karst catchment areas only occurs during or shortly after storm events. Infiltrating water is assumed to flow almost immediately into the epikarst compartment with sink holes as the end point. By applying this method, the travel time of water is calculated by the ratio of travel path length between the infiltration point and the corresponding wadi and the average pore water velocity.

#### **2.4.1 Travel Time Formulas**

A simple method to assess unsaturated and saturated zone time-lag in the travel time from ground surface to receptor was proposed by Sousa *et al.* (2013). They described some techniques for estimating the travel time in unsaturated and saturated zones using advective travel time. In the saturated zone, particle tracking techniques and straight-line approximation based on Darcy's equation were proposed. For the unsaturated zone, three techniques were proposed to calculate the saturated term  $S(z)$ :

- Applying the Van Genuchten equation, while assuming no flow conditions in the unsaturated zone.
- One-dimension variable saturated modelling.
- Tabulated values from surface to aquifer advective time (SAAT) and vulnerability techniques developed by Province of Ontario (2006) into the general formula:

$$tu = \int_0^L \frac{n_{ef}(z) \cdot S(z)}{R} dz$$

Equation 2.4

Where:

$tu$  = the travel time in the unsaturated zone

$L$  = the thickness of the unsaturated zone, which can be estimated using data from the observation well

$R$  = the recharge

$n_{ef}$  = the effective porosity estimated from the field or from literature.

$S$  = water saturation

The proposed method was applied to a field site located in a glacial aquifer system in Ontario, Canada. This method is useful to decide whether to incorporate unsaturated processes in conceptual and numerical models and can be used to roughly estimate the total travel time between points near ground surface and a groundwater receptor.

One-dimensional transient time (steady-state flow, transient transport) was created especially for quantitative intrinsic vulnerability assessment in the VULK model for karst settings (Sinreich *et al.*, 2007; Zwahlen *et al.*, 2004). The concept of dominant transit time (maximum concentration –  $C_{max}$ ) and attenuation (inverse of relative maximum concentration  $C_0/C_{ma}$  where  $C_0$  is input concentration) used as the VULK key output parameters (Figure 2.7) representing the three proposed criteria for assessing vulnerability includes:

- When should the pollution start?
- To which level?
- For how long?

An assessment of intrinsic vulnerability of conservative contaminants was attempted by Saayman *et al.* (2007). They based their study on the evaluation of vertical travel time from land surface to the aquifer. They proposed calculating of the travel time using a simple formula

$$T_{time} = \frac{Z \cdot \theta}{V_d}$$

Equation 2.5

Where:

$T_{time}$  = travel time (years)

$Z$  = vadose zone depth (m)

$\theta$  = average moisture content or volumetric water content  
 $V_d$  = the average recharge rate (m/day)

Witkowski and Kowalczyk (2004) also used this equation to assess the groundwater vulnerability of conservative contaminants in Poland. Saayman *et al.* (2007) applied their findings to two study sites in South Africa: namely the Goedehoop irrigation site near Secunda and the Coastal Park waste disposal site near Cape Town.

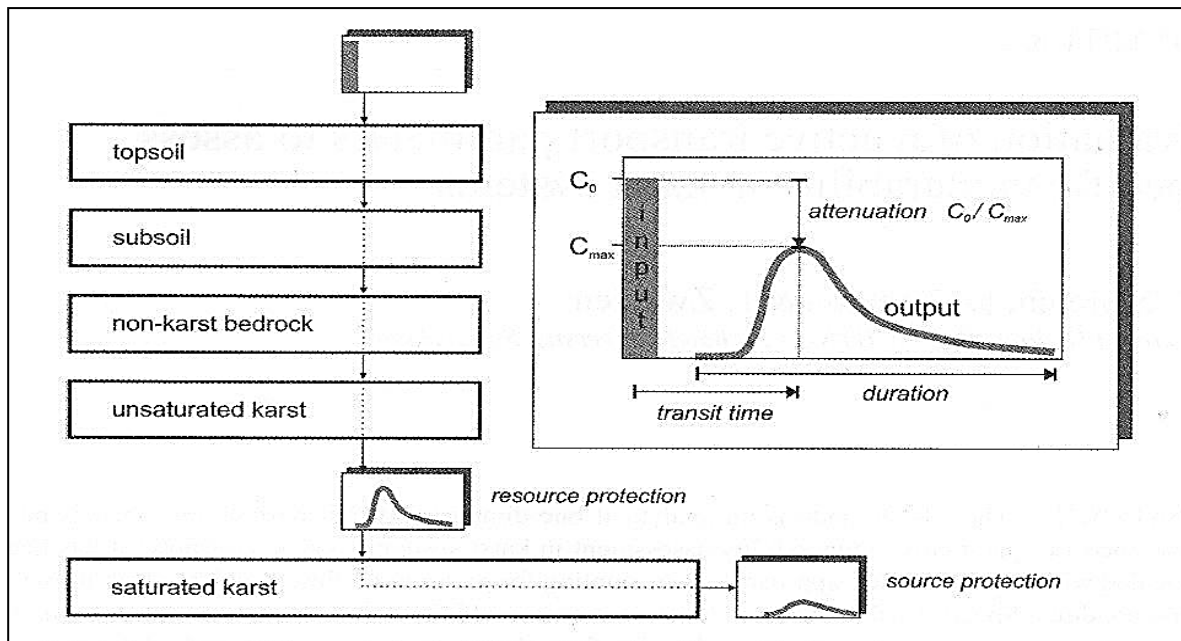


Figure 2.7: The VULK model source and resource vulnerability idea

Three models for calculating travel time of contaminant were presented by Krogulec (2004). The migration time was based on the time of water exchange in a rock formation assuming piston flow. Model 1 was on the infiltration time through the unsaturated zone as proposed by Wosten *et al.*, (1986); Haith and Laden (1986); Witczak and Zurek (1994).

$$t_a = \sum_{i=1}^n \frac{m_i \cdot (w_o)}{I_e}$$

Equation 2.6

Where:

- $m_i$  = thickness of successive layers of unsaturated zone profile [m]
- $t_a$  = travel time through the vadose zones
- $w_o$  = average volumetric moisture of successive layers of unsaturated zone
- $I_e$  = infiltration of atmospheric precipitation deep into the soil profile [ $m^3/m^2 \times year$ ] obtained through multiplication of infiltration rate ( $\omega_i$  [%]) by the volume of precipitation.

The second model was based on volumetric moisture content of sediments to calculate infiltration time. The second model can be calculated according to Bindemans formula:

$$t_a = \sum_{i=1}^n \frac{m_i n_o}{\sqrt[3]{I_e^2 K'}}$$

Equation 2.7

Where:

$n_o$  = effective porosity

$K$  = vertical hydraulic conductivity of unsaturated zone

The rest of the parameters ( $m_i, I_e, t_a$ ) is the same as the earlier models.

The Bindeman equation states that infiltration time, excluding thickness of unsaturated zone that is taken into account in all formulas, primarily depends on the infiltration intensity and effective porosity, but is of lesser importance on infiltration coefficient.

The third model presented to evaluate infiltration time was the formula proposed by Macioszczyk (1992). The model modified the earlier formulas:

$$t_a = \sum_{i=1}^n \frac{m_i w_o}{\sqrt[3]{I_e^2 K'}}$$

Equation 2.8

Seepage time was used by Rozkowski *et al.* (2004) to evaluate the vulnerability of vadose layers for a carbonate aquifer in Cracow, Poland. The seepage time was based on Bindemans simple formula and calculated using the Witczak and Zurek (2002) modified formula:

$$t = \frac{1000 \cdot w \cdot m}{W}$$

Equation 2.9

Where:

$t$  = seepage time (year)

$w$  = rock moisture volume

$m$  = thickness of isolation cover (m)

$W$  = infiltration intensity (mm/year).

The time of the vertical seepage through the lithological strata covering the rocks was calculated with the formula and modified in order to adapt to the *multilayer* profile as follows:

$$t_v = [(m_1 w_1) + (m_2 w_2) + (m_3 w_3) + m_4 w_4) + (m_5 w_5)] * 1000/W$$

Equation 2.10

Where:

$t_v$  = time of vertical seepage to the phreatic zone (years)

$W$  = infiltration intensity of atmospheric precipitation (mm/year)

$m_{1-5}$  = thickness of the succeeding lithological layers

$w_{1-5}$  = rock moisture volume.

Five classes were distinguished based on this vertical seepage through the vadose zone:

- Very high – seepage time less than two years.

- High – seepage time of two to five years.
- Medium – seepage time from 5 to 25 years.
- Low – seepage time from 25 to 100 years.
- Very low – seepage time more than 100 years.

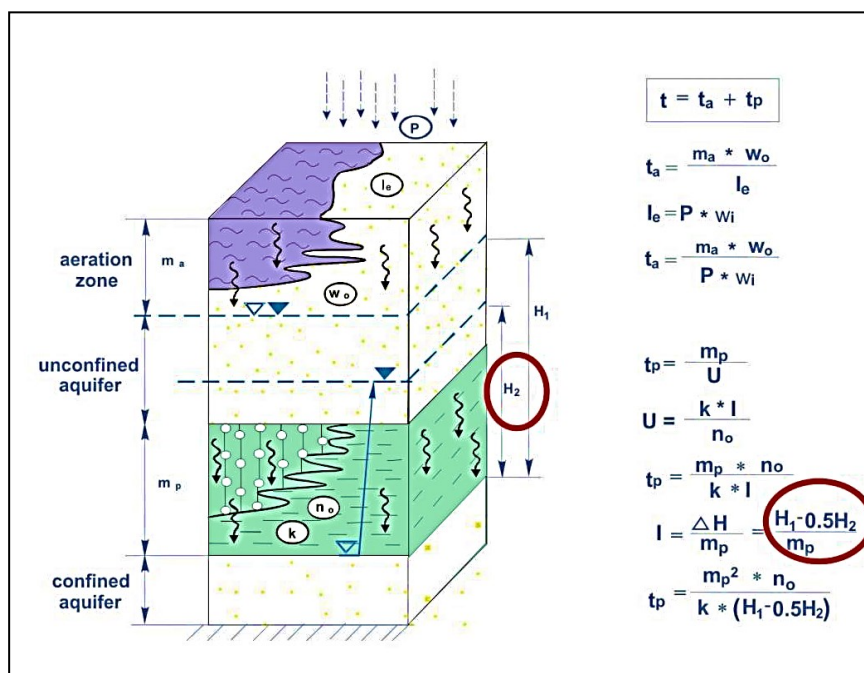
Kleczkowski *et al.* (1990) attempted the vulnerability mapping on a country-wide basin called Major Groundwater Basins (MGWB) based on qualitative and quantitative criteria. These criteria include:

- The presence of at least one well having a yield greater than 70 m<sup>3</sup>/h.
- Total groundwater abstraction of one intake greater than 10 000 m<sup>3</sup>/d.
- Transmissivity greater than 10 m<sup>2</sup>/h.
- Good water quality (Witczak *et al.*, 2007; 2010).

Travel time of contaminant was depicted through the recharge area (Figure 2.8 and Figure 2.9).

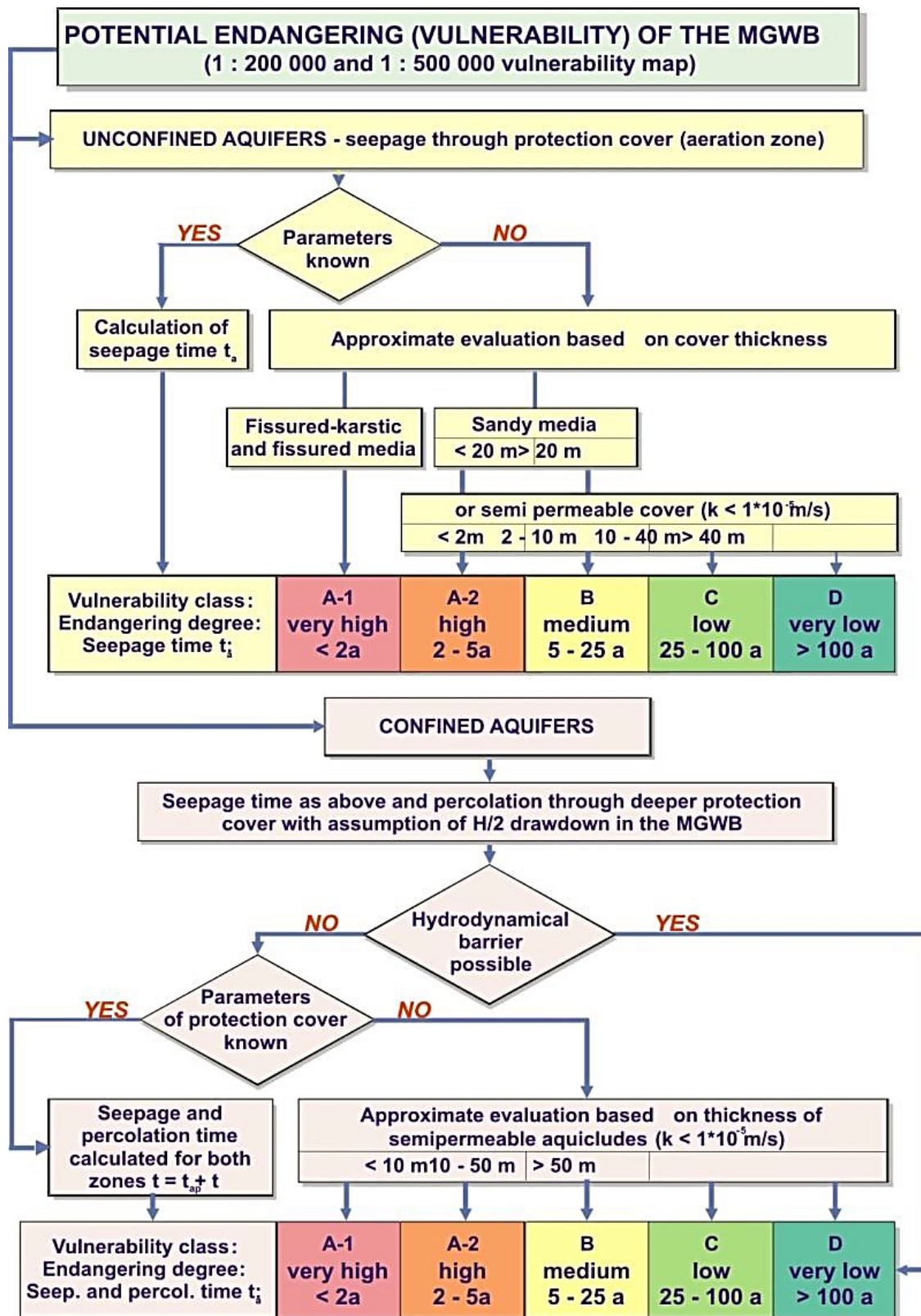
Intrinsic vulnerability was based on the vertical surface to aquifer and the horizontal transport time of the contaminant to the borders of MGWB using the piston-flow model (Witczak *et al.* 2011). The intrinsic vulnerability of the MGWBs and their recharge areas was classified as follows:

- High vulnerability – with travel time shorter than 5 years, requiring extreme protection and so-called Maximum Protection Areas (MPA).
- Moderate vulnerability – with travel time of 5–25 years, requiring high protection and so-called High Protection Areas (HPA).
- Low and very low vulnerability – with travel time longer than 25 years, requiring usual protection and so-called Standard Protection Areas.



Source: Witczak *et al.* (2004); Kleczkowski *et al.* (1990).

Figure 2.8: Scheme of the Major Groundwater Basins vulnerability assessment



Source: Witczak *et al.* (2004); Kleczkowski *et al.* (1990).

Figure 2.9: Scheme of the Major Groundwater Basins vulnerability assessment

## 2.5 Validation of Vulnerability Methods

There is no agreed method of validation of aquifer vulnerability methods known yet. Different authors have used different convenience techniques to validate proposed vulnerability methods. Common methods of validation, as highlighted by Daly *et al.* (2002), Gogu *et al.* (2003) and Neukum *et al.* (2008), include hydrographs, chemographs, bacteriological analyses, tracer techniques, water balances, calibrated numerical simulations and analogue studies. Artificial tracers were used by Jeannin *et al.* (2001) as addition techniques for the validation of vulnerability maps.

Goldscheider *et al.* (2001) proposed three criteria: peak time, recovery (R) and maximum concentration normalised by the injected tracer mass ( $c/M$ ), all obtained from tracers breakthrough curves. Ravbar and Goldscheider (2009) also used lithium chloride (LiCl) and potassium iodide (KI) released over the surface of limestone beds and partly covered by vegetation, as tracers to validate four vulnerability methods. They proposed two validation criteria based on Perrin *et al.* (2004) and Andreo *et al.* (2006). The time of the first tracer detection and the normalised tracer recovery  $R_N$ . This criterion is defined as:

$$R_N = \frac{1}{M} \int_{i=0}^{\infty} c dt = \frac{R}{Q}$$

Equation 2.11

Where:

$R_N$  = normalised tracer recovery

$R$  = recovery

$Q$  = spring discharge

$c/M$  = injected tracer mass

$R$  = directly proportional to the spring discharge  $Q$ .

Neukum *et al.* (2008) discussed the inappropriateness of the qualitative methods of vulnerability assessment and presented a validation methodology based on simple numerical modelling and field investigations.

Rahman (2008) employed a single parameter sensitivity analysis and map removal sensitivity analysis. Map removal involves removing one or more data layers and observing the variation in vulnerability. He noted that net recharge shows the highest sensitivity upon removal in the groundwater vulnerability index for DRASTIC. This is because of the mean variation index and high theoretical weight assigned to net recharge parameters. Other parameters sensitivity orders were the removal of topography, hydraulic conductivity, soil media and aquifer media.

Single parameter sensitivity involves comparing the theoretical weights with that of effective weight of a vulnerability map. This was also used by Babiker *et al.* (2005). The effective weight of DRASTIC was reported to exhibit some deviation from that of the theoretical weight, and the effective weight is a function of the value of the single parameter with



regards to the other six parameters. Rahman (2008) reported net recharge and depth-to-water layers as the most effective parameters in the vulnerability assessment of DRASTIC models. This was followed by the hydraulic conductivity and topography, respectively, with other parameters such as aquifer media, soil media and impact of vadose zone, showing lower effective weight.

Ramos-Leal and Castillo (2003) presented the aquifer vulnerability validation study for the Turbio River Valley in Mexico using the effective weighting  $W_{xvi}$  (Napolitano and Fabbri, 1996; Gogu and Dassargues, 2000b).

$$W_{xvi} = \frac{X_{ri}X_{wi}}{V_i} * 100$$

Equation 2.12

Where:

$X_{ri}$  and  $X_{wi}$  are the ranges and the assigned weights for each parameter  $X$ , and  $V_i$  is the vulnerability index of each point.

Ramos-Leal and Castillo (2003) went even further and proposed another validation method, namely vulnerability variation  $V_{vxi}$  by Lodwick *et al.* (1990), derived by parameter omission.

$$V_{vxi} = \frac{V_i - V_{xi}}{V_i} * 100$$

Equation 2.13

Where:

$V_{vxi}$  = variation index omitting a parameter  $X$  (D,R,A,S,T,I or C)

$V_i$  = Vulnerability index in the point  $i$

$V_{xi}$  = vulnerability index calculated without a parameter,  $X$  (D,R,A,S,T,I,C).

The two formulas are different but equivalent.

## 2.6 Challenges and Expected Contributions to Vulnerability Assessments

The most commonly accepted subjective vulnerability method is the DRASTIC method. Despite DRASTIC being well-known and the most widely used method, merely because of its simplicity, it has continuously been subjected to criticism. One of the major reasons for this criticism is the subjectivity DRASTIC introduced and the oversimplification in the hydrogeological characterisation. However, data gathering in the computation of DRASTIC parameters is challenging in many African countries aquifers (data limited areas). Opinions differ about the DRASTIC method. In fact, some authors such as Barber *et al.* (1993) and Merchant (1994), argued that an equivalent DRASTIC result might be obtained using fewer parameters, with several advantages in accuracy, precision and costs (Napolitano and Fabbri, 1996).

Travel time or transit time concepts were used more in the physically based vulnerability methods which were mainly for steady state conditions. Environmental tracers involving arrival time serve as some of the yardsticks in measuring the travel time. Numerical modelling simulating field conditions were used to arrive at the travel time of some methods. However, laboratory simulation options have not been fully utilised. Even though laboratory factors in overall vulnerability assessment may be tasking and site-specific, it is another avenue to explore in vulnerability assessment.

It is permissible to ignore short travel time of very shallow aquifers (Basu *et al.*, 2012; Eberts *et al.*, 2012) in vulnerability studies. Short travel time makes no difference between the source and receptor and is better assumed under saturated conditions. Sousa *et al.* (2013) further support this assumption if travel time is negligible in the overall pathway travel time.

Likewise, disagreement over the concept of precipitation as to increase or decrease in groundwater vulnerability is important to state. Methods such as PI and DRASTIC maintained that a decrease in groundwater vulnerability occurs when increasing precipitation infiltrates into groundwater. The methods argument was that an increase in recharge provides higher dilution and consequently decreased vulnerability. The SINTACS method by Civita (1994) specifically proposes reduction in vulnerability if recharge is higher than 300–400 mm/year, while DRASTIC proposes values >250 mm/year. This means more recharge means more dilution and decreased vulnerability. However, the COP argument is more tenable in this study, because it relates travel time of contaminant with vulnerability. The COP places the importance of quantity to dilution. Precipitation of 800 to 1 200 mm increases vulnerability, because more precipitation will be available to recharge the groundwater. In addition, the up side of precipitation inclusion in vulnerability methodology is that most methods accept rainfall quantity and annual recharge as interrelated and an important factor in assessing groundwater vulnerability.

The challenges of using most of these earlier mentioned vulnerability methods is that they were designed to include most factors influencing vulnerability and sometimes duplicate key intrinsic parameters. This allow for capturing of all possible avenues by which contaminants infiltrate from the ground surface to the water table. However, satisfying these conditions may become a daunting task for data limited areas. Data gathering for vulnerability assessment can be economically expensive, labour intensive and there is a shortage of qualified geohydrologists, particularly in data limited areas. Therefore, there is a need for a simplified vulnerability method that can address data limited areas.

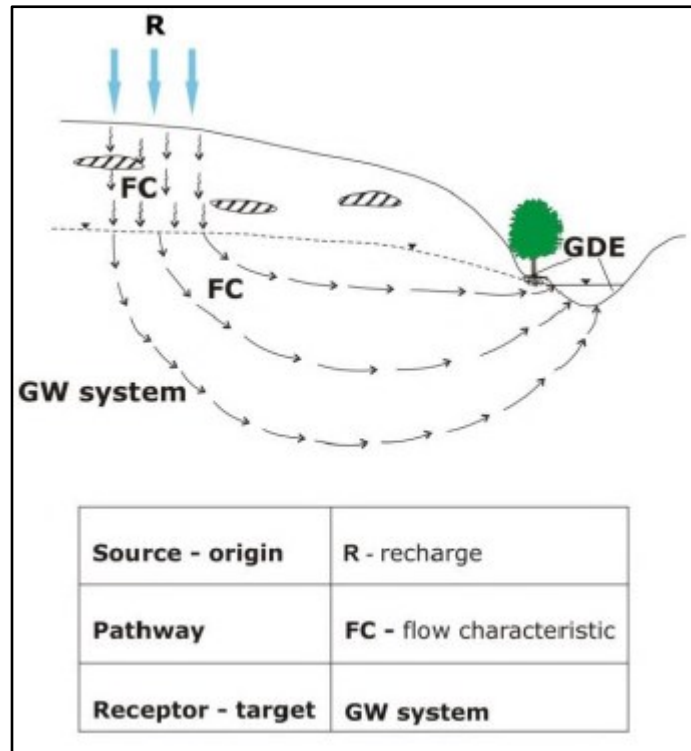
Another area of challenge using established vulnerability methods, particularly the subjective methods, is the lack of physical precision of most methods. This is the disadvantage aspect of most of the established subjective methods, because in reality, the heterogeneity nature of most lithologies can create a wide gap between predicted map and actual field occurrence. This is despite the validation of most methods, which is why no two vulnerability methods give the same results when applied to assess an area. It is therefore suggested that, if possible, separate vulnerability methods factoring in-situ properties should be designed for every area intended to be assessed.

It is noticed that out of all of the vulnerability methods developed, the DRASTIC, PI and COP have widely been applicable, particularly the latter two in the karst aquifers. The PI method and its modifications application have been officially used in not less than eight European countries (Goldscheider, 2005). Therefore, DRASTIC and PI will be applied to assess the vulnerability of the Dahomey Basin. They will also guide in the formulation of new methods to be proposed in mapping data limited areas, which this research intend to address.

For intrinsic vulnerability mapping of an area, it is important to take into account the inherent properties of the areas under investigation into the vulnerability methodology. Since these properties are quite large and cannot all be factored into the vulnerability methods, it is best to use a methodology that will factor in inherent parameters through which the groundwater is contaminated. One of these methods is the travel time concept, which relate directly or indirectly parameters through which water or contaminant flows. However, one major disadvantage of intrinsic vulnerability methodologies is not considering the specific properties of contaminants.

Transport of any contaminant always depends on the interaction between the specific properties of the contaminant and the specific properties of the area and the media it passed through. For instance, pesticide mass transport will depend on the type and content of organic matter, mass transport and mobility of bacteria, particularly in soakaway, will depend on the media pore sizes and the pathogen residence time. Mass transport of heavy metals depends on the cation exchange capacity of the media and nitrate movement influenced by the media redox potentials.

The basic principle of the intrinsic vulnerability of the COST Action 620 were assessed on the assumption of groundwater vulnerability based on the properties controlling the transport of a conservative contaminant which behaves like water molecules (Daly *et al.* 2002; Goldscheider, 2002). These include factors such as dilution, dispersion, and advective transit time, which relates when a substantial amount of contaminant can get to the water table. This means that the actual parameters needed in determining the arrival time on the field for intrinsic vulnerability is the permeability and lithological thickness for intrinsic vulnerability and an addition of relevant factors of contaminants (e.g. redox potential, type and content of clay minerals and organic matter) for specific vulnerability mapping (Goldscheider, 2002). Therefore, site-specific intrinsic vulnerability that is to be proposed in this research will be based on the permeability of overlying lithology above the water table and the overall depth from the surface to the water table. This simple vulnerability methodology is similar to the Work Packages (WP) of the GENESIS Project (2013) shown in Figure 2.10.



Source: [www.thegenesisproject.eu](http://www.thegenesisproject.eu).

Figure 2.10: Basic concepts defining the intrinsic vulnerability in relation to Work Packages (WP) of the GENESIS project

## 2.7 Characterisations of Study Sites for Vulnerability Assessment

Appropriate geological and geohydrological characterisations are important for groundwater vulnerability assessment. These characterisations include processes that influence contaminant movement from point of release to either surface of groundwater (resource assessment) or a drinking well body (source assessment). Major parameters characterised are the hydraulic conductivity, vegetation, slopes, depth-to-water table, soil types, aquifer types, nature of recharge, precipitation, run-off, topsoils, and so on.

Characterisations for groundwater vulnerability studies can be grouped into three broad processes (Daly, 2002):

- Processes that occur on the land surface.
- Processes occurring within the vadose zones.
- Processes occurring within the aquifer systems.

The three processes can be investigated using geohydrological approaches. Geophysics exploration, geochemical investigations, hydrochemical monitoring, hydrological investigations and numerical modelling are some of the basic geological processes used to characterise a study site for vulnerability assessment.

## 2.8 Conclusion

Groundwater vulnerability investigations are means by which the degree of susceptibility of an aquifer can be measured and protected. The groundwater vulnerability methodologies were proposed based on different purposes which aim towards the protection of the aquifers at water table or at the well sources. The subjective and physically based methods are the most widely used methodologies. Some of the subjective methodologies discussed are COP, DRASTIC, PI, GOD and EPIK. The subjective methods' major shortfalls are in their mode of rating. Travel time is the main component of the physically based methods. Groundwater vulnerability estimation relies on the knowledge of the precipitation, geomorphology and geology over an area to be assessed. For that reason, the geology of the Dahomey Basin above the water table which this research is attempting to characterise and its degree of vulnerability will be discussed in the next chapter.

# **CHAPTER 3**

## **PHYSIOGRAPHY AND GEOLOGY OF THE DAHOMEY BASIN**

### **3.1 Introduction**

The Dahomey Basin is a marginal basin belonging to the Gulf of Guinea (Figure 3.1) and extends from southeastern Ghana through Togo and the Benin Republic to the western side of the Niger Delta in Nigeria. The Dahomey Basin is a shelf depositional environment sedimentary basin. A sedimentary basin is a thick sequence of sedimentary rock underlying the earth surface. Sedimentary basins act as hosts to mineral resources (e.g. oil, gold, coal and natural gas) and many of them have been explored for their economic importance. A sedimentary basin also houses large volumes of groundwater resources that are explored to serve human needs. Hence, studies involving sedimentary basins are very important.

For the purpose of this study, it is necessary to discuss the background physiography settings, including the geography and geology of the study area. The geology includes the stratigraphy, sedimentology and structural characteristics of the Dahomey sedimentary basin in relation to the geohydrological characteristics of the basin. Understanding the climatic and geological characteristic features of this sedimentary basin can help predict the extent of vulnerability of shallow groundwater to contamination in the basin.

### **3.2 Description of the Study Area**

#### **3.2.1 Location, Climate and Geology of Nigeria**

This study was carried out in the southwestern part of Nigeria. The study area is located along the West African coast margin. Nigeria is bounded in the north by the Niger Republic, Cameroon to the east, the Chad Republic to the northeast, the Republic of Benin to the west and the Atlantic Ocean to the south. The country's population is estimated to be around 170 million by 2015 (NPC, 2014). The major river is the Niger, which originates from the Foutadjalon Highland in the Guinea Republic and the Benue from Mt. Cameroun. Other major rivers include Kaduna, Sokoto, Gongola, Ethiopia, Ogun and Eboine.

The dominant climatic type over Nigeria is tropical. The tropical climate gives Nigeria the two prevailing seasons of wet (rainy) and dry. It is hot and wet most of the year in the southeast, dry in the southwest and hot and very dry in the savanna north. The precipitation of Nigeria decreases from south to north. The rainy season extend from March to November in the south and mid-May to September in the far north of Nigeria. The southeast receives rainfall of about 3 000 mm (120 inches) in a year, compared to 1 800 mm (70 inches) in the southwest and less than 500 mm (20 inches) in the far north.

The general relief of Nigeria is dominantly plains. The plains are interjected by plateaus and hills, such as the Jos Plateaus and north-central highland in the north, Udi-Nsukka Plateaus

in the east and southwestern highlands in the west. The vegetation of Nigeria consists of a mangrove and freshwater swamps along the coast, a tropical rainforest belt in the south, a tropical grassland belt in the centre and semi-desert vegetation at the border tips of the Sahara desert.

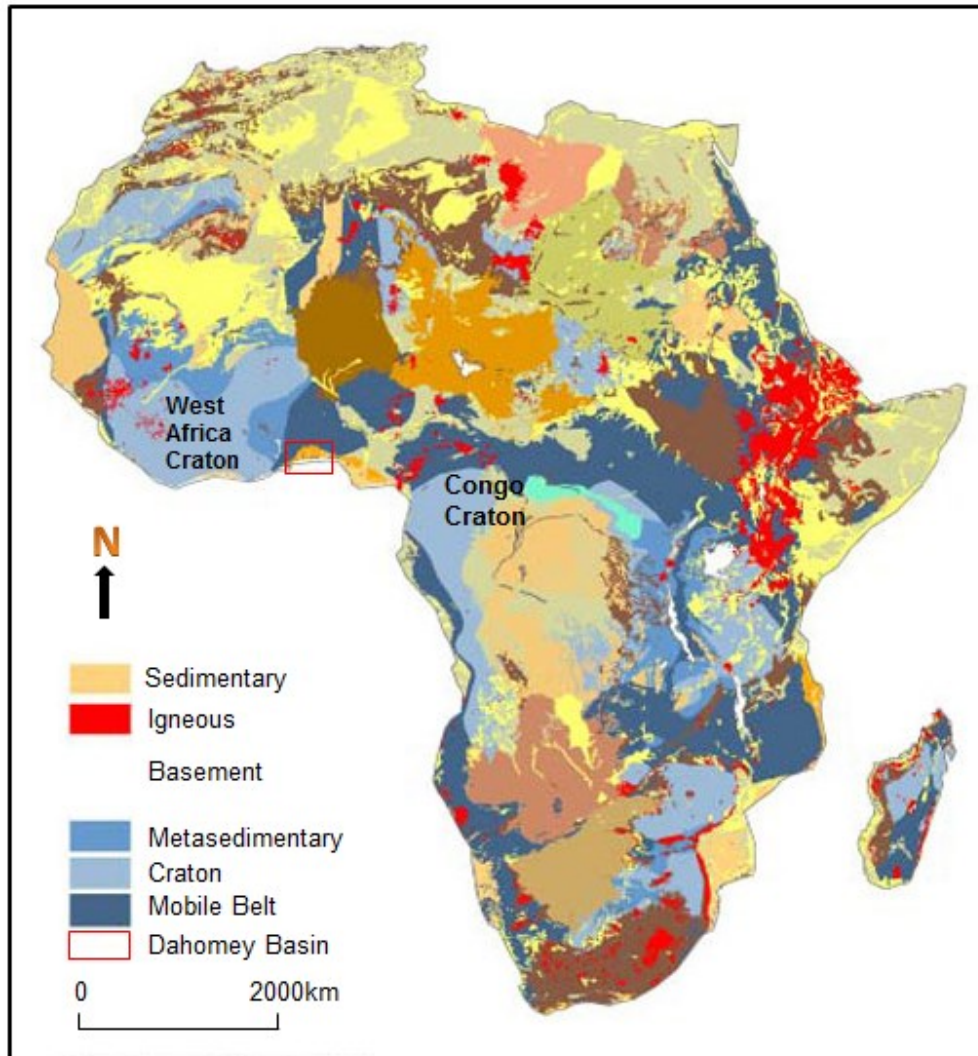
Nigeria's geology can be grouped into two categories: Basement Complex rocks and sedimentary rocks. Apart from their characteristic features and mineralogical compositions, this is necessary for identification and description, and most researchers have employed this grouping over the years. The Basement Complex rocks of Nigeria are found around the northern and southwestern parts of the country. Most are of Precambrian age. Rahman (1988) particularly argued that the Basement Complex of southwestern Nigeria is of late Precambrian to Early Paleozoic Orogeny.

The southwestern Nigerian Basement Complex extends westward and is continuous with the Dahomeyide of the Benin-Togo-Ghana region to the west. Here it bounds the West African Craton and have been categorised into six litho-tectonic zones or terrains in Benin and Togo (Schluter, 2005). Major rock types in these litho-tectonics zones are migmatites, syenites, granites, marbles, gneisses, micas, schists, quartzites and amphibolites. Most of the rock types are similar in structure to those found in Western Nigeria, which will be discussed in detail at a later stage.

The Dahomeyide Orogeny is dated Kibaran with some evidence of Pan-African ages. The northern Basement Complex is predominantly Archean to Lower Paleozoic consisting of migmatite-gneiss-quartzite complex with imprints of Liberian, Eburnean and Pan-African tectonic events. Other rock types include schists, phyllites, banded iron formations, marble, amphibolites and younger granite complexes that are noted for its tin and columbite mineralisation.

The Nigerian Basement Complex lies within the Pan-African Mobile Belt to the east of the West African Craton, and northwest of the Congo Craton which has been affected by the 600 million years Pan-African Orogeny (Figure 3.1). The entire belt lies in the reactivated region, which resulted from the plate collision between the West African Craton and the active Pharusian continental margin (Rahman, 1988). The Basement Complex is believed to be polycyclic (where rocks are found in the same environment with a different age and mode of occurrence) and has responded to different tectonic episodes which ranges from Archean to Late Proterozoic.

The sedimentary basin in Nigeria occupies nearly half of the country's land mass and can be classified into two broad groups: The marginal sag basins which are the Niger delta and the Dahomey Basin (where this study is carried out) and the Intra-continental Basin comprising of the Benue Trough, Bida Basin, Chad Basin and Iullummeden Basin (Figure 3.2). These basins range in age from Uppermost Jurassic to Quaternary. They host several mineral resources, including the petroleum rich Niger delta, Lower Benue Trough and Lead-Zinc mineralisation of Benue Trough. They also host several other minerals such as coal, limestone barite, iron ore and Tarsand.



Source: Modified after MacDonald (2012) and NERC (2015).

Figure 3.1: Location of Nigerian Basement and sedimentary rocks

### 3.2.2 Location, Climate and Geology of Southwestern Nigeria

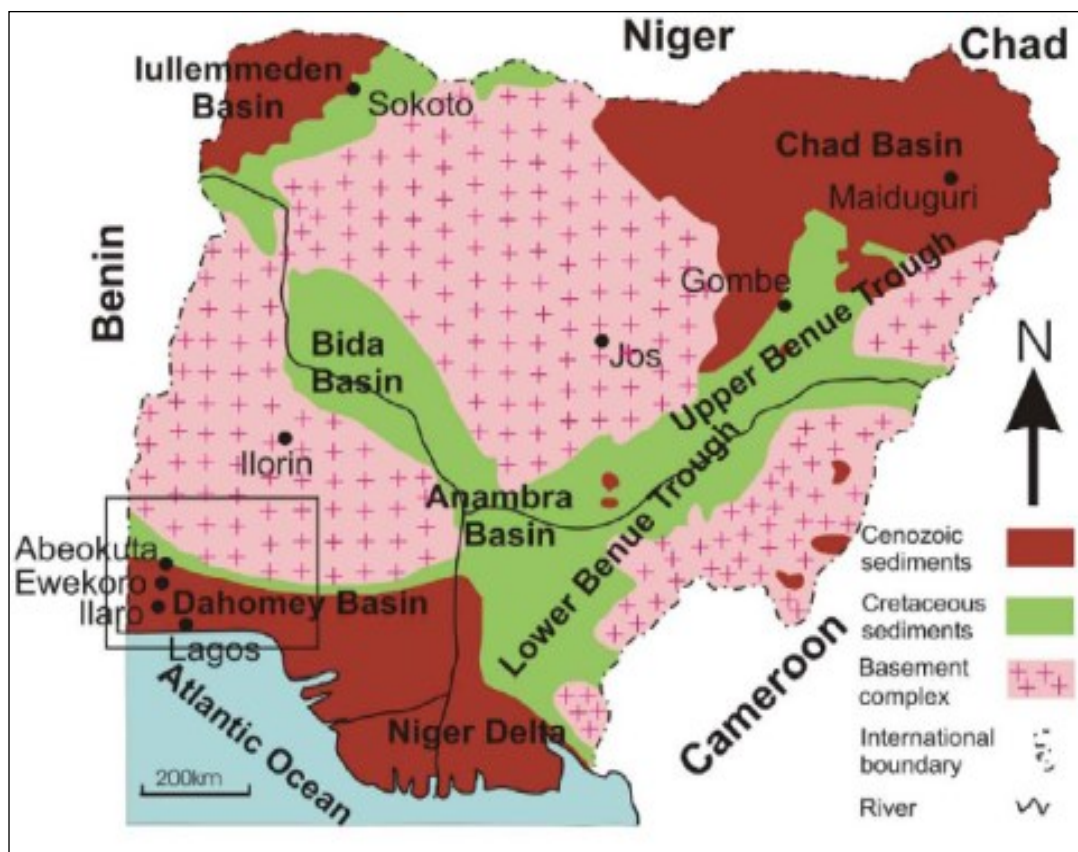
Southwestern Nigeria is located along the tropical climatic belt and it is criss-crossed from east to west by the rainforest belt and a derived savannah in the north. Average diurnal temperature ranges from 22 to 32 °C. The two seasonal periods result from the Harmattan wind of the Sahara desert and the Inter Tropical Convergent wind (ITCZ). The major rivers in southwestern Nigeria are the Rivers Ogun, Oyan, Ewekoro, Oba, Ofiki and Opeki. The rivers flow southward into the Atlantic Ocean.

Two broad groups of rock (as discussed earlier) occupy the southwestern part of Nigeria, the southwestern varied suite of Basement rocks and the Dahomey sedimentary basin (Figure 3.2). The Basement rocks have been classified according to their petrological, lithological and age determination criteria (Oyawoye, 1964; Grant, 1970; Odeyemi, 1976; Annor, 1986). Rahman (1988) attempted classification based on the petrology and recognised the following units:



- The Migmatites Gneiss complex.
- The Older granite.
- The Charnockitic rocks.
- The Schist belt.
- Unmetamorphosed dolerite dyke.

The migmatite-gneiss complex rock is the most common rock in the southwestern Basement rocks. It comprises of gneiss, quartzite, calc-silicates, biotite to hornblende schists and amphibolites. They consist of the three main components: (1) early gneiss, which are foliated, hornblende quartzo-feldspathic of granodioritic composition, (2) mafic amphibolites and biotite hornblende schists and (3) granitic to felsic components of aplitic to pegmatite, which occur as concordant or discordant veins. Banded gneiss is the most common of these rocks and it consists of alternating parallel light and dark coloured bands. The box in Figure 3.2 indicates the study area and sedimentary formation under study.



Source: Oyawoye (1964).

Figure 3.2: Map of Nigeria showing the Basement and sedimentary rocks distribution

Older granite rocks exhibit circular to elliptical bodies in a schist environment and more elongated bodies in migmatite-gneiss terrains. The older granite appears to be related to the environment in which the granite is emphasised. The older granite is a compound name and includes rocks of a wide range of compositions that includes granites, granodiorites, adamellites, quartz, monzonites, syenites and pegmatites. Granitic-granodioritic compositions are the most common (Jones and Hockey, 1964). The regional north–south strike was

confirmed and stipulated that the fundamental structure of southwestern Nigeria is an anticlinorium with a northwards plunging migmatitic core. The initial folding was along a northwest trending axis and was followed by a second folding. Grant (1970) recognised it with axial plane trace of the early antiforms.

Minor occurrence of pegmatite and microcline are widely reported throughout the Basement Complex of southwestern Nigeria. The composition of microcline and quartz pegmatite are frequently found associated with gneisses and older granites but is conspicuously absent from the main areas of the slightly migmatised to unmigmatised paragneisses and meta-igneous rocks. Most dolerite and syenite occur as dykes and they are believed to be the youngest rocks of the Basement Complex rock. Grant (1970) obtained a whole rock Rb/Sr Isochron age of  $2\,205 \pm 70$  million year ago (mya) for the Ibadan granite-gneiss, which was emplaced into a banded gneiss quartzite complex. He also published a whole rock Isochron age of  $1\,150 \pm 140$  mya for granite gneiss from Ile-Ife. These findings by Jones and Hockey (1964) and Grant (1970) suggest that no Orogeny younger than the Pan African has affected the rocks in Nigeria or its neighbouring West African countries.

### **3.2.3 Location, Climate and Geology of the Dahomey Basin**

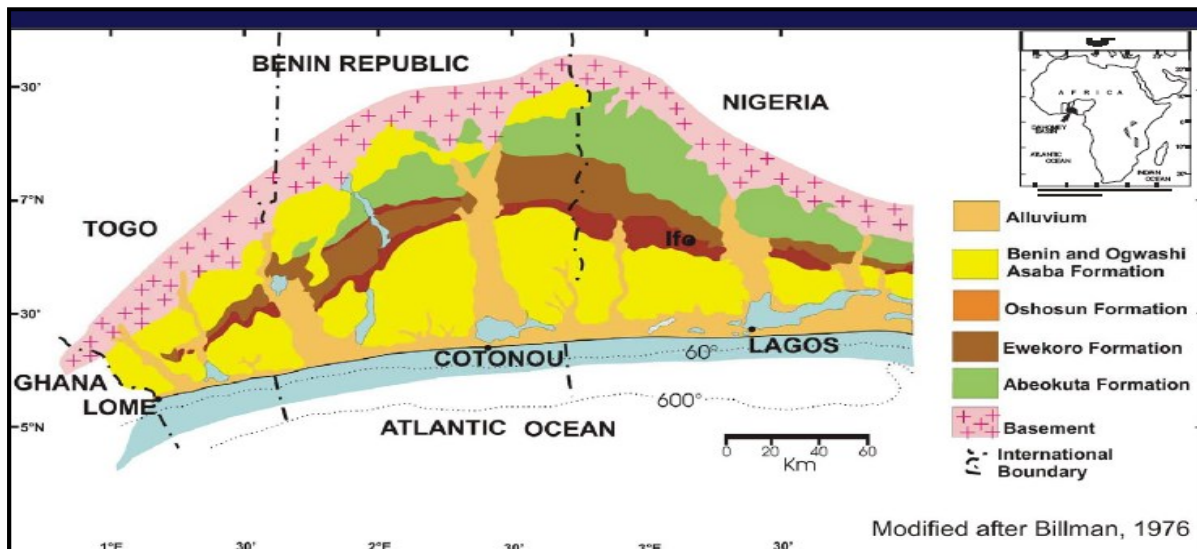
The Dahomey Basin is one of the sedimentary basins on the continental margin of the Gulf of Guinea. It extends from Volta delta in Ghana in the west, where it is referred to as the Keta basin, to the Okitipupa Ridge in Nigeria in the east. It is a marginal pull-apart basin or marginal sag basin (Kingston *et al.*, 1983). The eastern half of the basin occurs within the Nigerian territory and is the study area for this research (Figure 3.3). The axis of the basin and the thickest sediments occur slightly west of the border between Nigeria and the Republic of Benin (Slanky, 1962; Billman, 1992).

The Dahomey Basin vegetation ranges from a rainforest belt at the northern-most end, to swampy mangrove vegetation in the south. Rivers and lagoons dominate the southern end of the basin, particularly in Nigeria and the Benin Republic where almost half of the basin is water-logged.

During the Mesozoic the Dahomey Basin was initiated. This initiation was probably responsible for the splitting of the Africa-South America lithospheric plate separated by the continental margin and the subsequent opening of the Atlantic Ocean in the Cretaceous era (Burke *et al.*, 1971, Whiteman, 1982). The basin contains an extensive wedge of Cretaceous to Recent sediments of up to 3 000 m. The sediments thicken from the onshore margin (where the predominantly clastic Cretaceous sediments rest conformably on the Basement Complex rocks of southwestern Nigeria) to the offshore. Within the offshore area; thick, fine grained, Cenozoic sediments cover the basin (Whiteman, 1982; Schlumberger, 1985).

The Dahomey Basin is bounded on the west by a fault and other tectonic structures associated with the landward extension of the Romanche Fracture Zone. Its eastern limit is similarly marked by the Benin Hinge Line, a major fault structure marking the western limit of the Niger Delta Basin. The latter is also a landward extension of the Chain Fracture Zone. To the east of the Benin Hinge Line is the Okitipupa Ridge (Adegoke, 1969). The basin is filled

with a number of horst and graben structures in north–south to northeast–southwest trending faults. The most significant fault is the Okitipupa Ridge, which marks the eastern margin of the basin.



Source: Billman (1976).

Figure 3.3: Generalised geological map of the Dahomey Basin

The basin was formed during the first stage of initial continental rifting where the crust were thinning, arching and faulting around Middle Jurassic. A series of graben formed and were filled with lacustrine and alluvial marine sediments transgressed during the Albian. The depression occurred because of rift generated Basement subsidence during the early Neoconian period. The subsidence gave rise to the deposition of a very thick sequence of continental grit and pebbly sands/ conglomerate, over the entire basin (Omatsola and Adegoke, 1981). By the Cretaceous times, African and South American plates were totally split with a spreading ridge and Oceanic crust separating the continent. This gives rise to a passive basin with marine sediment prograding southward over a gentle sagging basin.

This continued until the Santonian period of the Cretaceous era before another major tectonic episode, linked to the closure of the Benue Trough folding, occurred. The folding led to tilting, blocked faulting of the granites, gneisses and associated pegmatites. Numerous sediments of the basin formed a series of horst and graben structures, while considerable erosional activity accompanied the upliftment and block faulting. The extensive lower cretaceous pre-drift sediments were almost completely eroded from the horsts. The basin became quiet during the Maestrichtian period and experienced only gentle subsidence. By this time, the environment changed rapidly from continental to estuarine. This was initially through brackish to open marine conditions, resulting in the deposition of a relatively thick sequence of sand with interbeds of organic shales. The Paleocene rocks were laid down during Eocene times; the sea regressed extensively in the Niger Delta, but less extensively in the Dahomey Basin (Jones and Hockey; 1964, Ogbe, 1970; Omatsola and Adegoke, 1981).

### 3.3 Stratigraphy Succession of the Eastern Dahomey Basin

The stratigraphic correlation succession, as observed from palynological data of the borehole penetrating the eastern Dahomey Basin, recognises Precambrian to Recent sediment (Omatsola and Adegoke, 1981). The succession from the oldest to the youngest strata includes:

- The Abeokuta Formation.
- The Ewekoro Formation.
- Akinbo Formation.
- Oshosun Formation.
- Ilaro Formation.
- Coastal Plain Sands (Benin formation).
- Alluvium.

Although researchers have carried out extensive work on the eastern section of this basin, they are yet to agree on a number of issues including the age of most of these formations. They do, however, all recognise their successions (Nton, 2001).

#### 3.3.1 Abeokuta Formation

This is the oldest recognised sedimentary rocks of the Dahomey Basin and was deposited during the first marine transgression in Maestrichtian. The formation consists mainly of ill-sorted ferruginous grits, siltstones and mudstones with shale-clay layers. The formation is believed to be deposited in turbulent shallow sea during a humid tropical climate. The origin is marine, partly brackish water and partly fresh water (Kogbe, 1976). The formation is grouped into three sub-formations: Ise Formation, Afowo Formation and Araromi Formation.

The **Ise Formation** consists of conglomerates with grits at the base and is overlain by coarse to medium-grained loose sand with interbedded kaolinite. The conglomerates are unimbricated and ironstones occur at some locations. Both the cross bedding azimuth of the sandstones and the pebble alignments point to a NE paleocurrent system (Nton, 2001). The age range is from Neocomian to Albian. The Ise Formation marked the end of the regressive phase of Benue Trough during Albian. The Formation conformably lies above the Basement rocks of southwestern Nigeria (Figure 3.4) and exposed outcrop can be observed at Abeokuta town. The formation holds a lot of groundwater due to the high amount of pore spaces in the conglomerate and grit in the formation.



Figure 3.4: Ferruginised Ise (Abeokuta) Formation resting conformably on weathered granite gneiss in Abeokuta town

The **Afowo Formation**, which overlies the Ise Formation, is mostly composed of coarse to medium-grained sandstones, with variable but thick interbedded shales, siltstones and claystones (Figure 3.5). The sandy facies are tar-bearing around Okitipupa, while the shales are organically rich (Enu, 1990). The shale component increases progressively from bottom to top, and the lower part of the formation is transitional with mixed brackish to marginal horizons alternating with well-sorted, subrounded, clean and loose fluviatile sands (Billman, 1976). This indicates a littoral or estuarine near shore environment of deposition in which water level fluctuated rapidly. The medium-grained loose sands, sandstone and sand grits with interbeds of kaolinitic clay of the Afowo Formation were deposited during the Turonian to Maastrichtian period (Omatsola and Adegoke, 1981). The Afowo Formation conformably overlies the Ise Formation; but the Afowo Formation sometimes conformably overlies the Basement Complex rocks in some locality.



Figure 3.5: Afowo Formation of the Dahomey basin

The Araromi Formation is the youngest formation in the Abeokuta Group of Cretaceous rocks (Figure 3.6). It is composed of fine- to medium-grained sands at the base and overlaid by shales and siltstone beds with thin interbedded limestones and marls (Ogbe, 1970; Okosun, 1998). Lignitic sands are also common in the sequence. The shales are light grey to black (Billman, 1976). The Araromi Formation was deposited by the marine transgression

that started at the end of the Maastrichtian stage/ period, which continued through the Paleocene period (Adegoke, 1969). This formation, together with the underlying Afowo and Ise Formations, constitutes what Omatsola and Adegoke (1981) proposed as the Abeokuta Group and is shown stratigraphically in Figure 3.13.



Figure 3.6: Ferruginised Araromi Formation sand quarry

### 3.3.2 Ewekoro Formation

The Ewekoro Formation overlies the Abeokuta Group conformably consisting of highly fossiliferous limestones (Adegoke, 1969, Adegoke *et al.*, 1970, Adegoke *et al.*, 1980). The formation turns to marl, and its arenaceous content increases towards the base and grades into the underlying predominantly sandy Abeokuta Group. Around Ibeshe, the limestone becomes harder and exhibit crystalline features with little or no pore spaces. The outcrop is exposed at the WAPCO quarry at Ewekoro and Shagamu (Figure 3.7). According to Ogbe (1970), the Ewekoro Formation is an extensive limestone body that is traceable over a continuous distance of about 320 km from Ghana in an easterly direction towards the eastern margin of the Dahomey Basin in Nigeria (Adekeye *et al.*, 2005).

The Ewekoro Formation is also extensively mined in the Benin Republic for cement production. It is thickly bedded and colour banded (Figure 3.7). Adegoke *et al.* (1970) estimates the thickness of the quarry type section at around 11–12.5 m and subdivided it into three units, while Ogbe (1970) added the fourth unit:

- Red Phospahtic Biomicrite.
- Algal Biosparite.
- Shelly Biomicrite.
- Sandy Biomicrosparite.

Apart from the quarry exposures there are very rare outcrops, except those intercepted in several boreholes. It is associated with a shallow marine environment due to an abundance of coralline algae, gastropods (Figure 3.7), pelecypods, echinoids fragments and other skeletal debris. It is believed to be Paleocene (Nton, 2001).

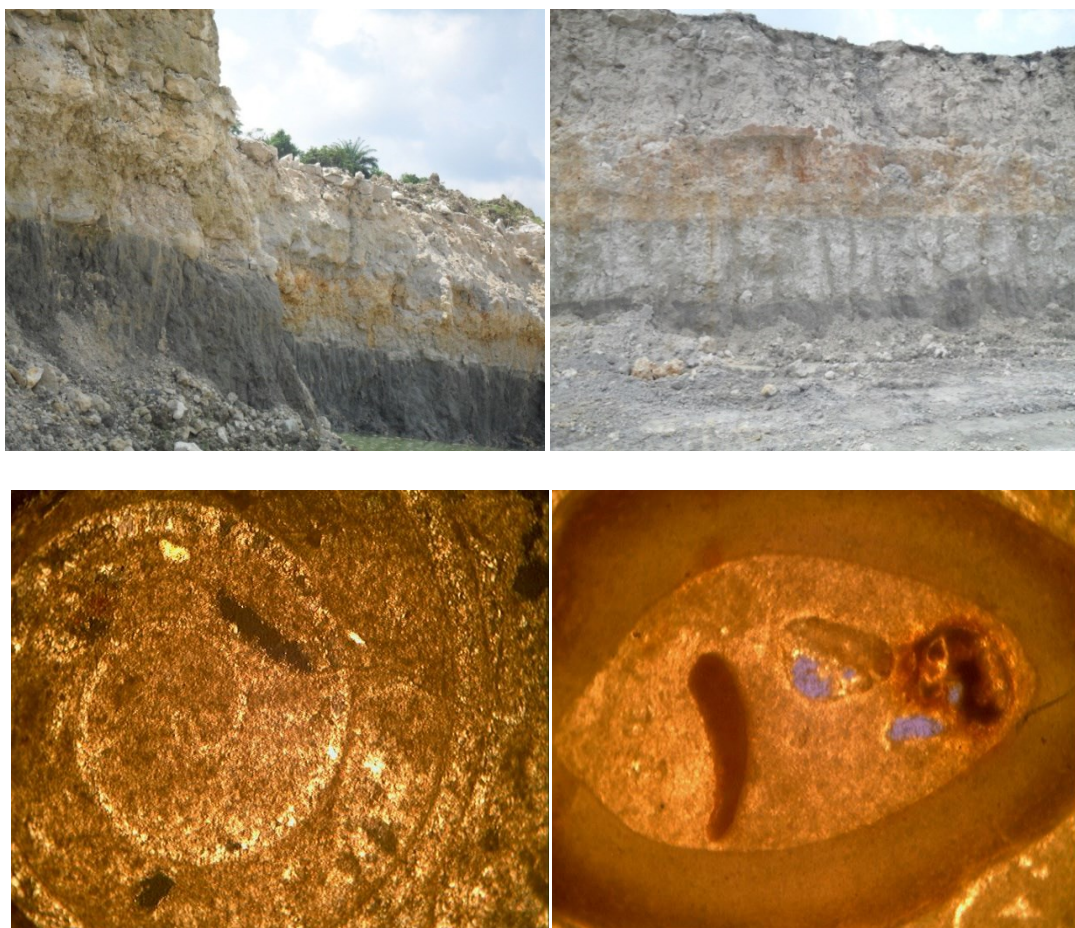


Figure 3.7: Colour banded limestone rock and calcareous fossils from the Ewekoro limestone, showing the well-preserved cylindrical shape of Gastropods

### 3.3.3 Akinbo Formation

The Akinbo Formation is a distinct rock of predominantly greenish-grey shale. The sequence is more of clayey shale. The formation overlies the Ewekoro Formation with a laminar glauconitic band rock as base. At the Ewekoro quarry type section the shales are grey, fissile, clayey and concretionary (Figure 3.8 & Figure 3.9). The top of the Akinbo Formation is marked by pure grey, gritty sand, lacking red mottling and with little clay. It is about 8-9 m thick at the Ewekoro type locality and has an average of 18 m in boreholes westward into Benin and Togo (Slanky, 1962; Antolini, 1968). The shale also appeared sheared, which was due to a disturbance and exposure to cracks that can be a pathway for groundwater movement (Figure 3.9). Nton (2001) observed a gentle dip of  $<50^{\circ}$ SW.

Most groundwater drillers and residents report a frequent borehole collapse at Shagamu, which is due to the shale shearing nature during time of deposition. East of Ijebu-Ode, the formation replaces the Ewekoro Formation, which thins out westward; the age of the formation ranges from Paleocene to Eocene. The shale becomes arenaceous and gradationally passes into mud towards the base of the limestone. The stratigraphic succession of the Akinbo Formation is shown in (Figure 3.13).



Figure 3.8: Thickly laminated and very rich fossiliferous shale



Figure 3.9: Shale showing the preferential path for groundwater flow

### 3.3.4 Oshosun Formation

The Oshosun Formation overlies the Akinbo Formation and is composed of the following: greenish-grey or beige clay, light greyish, white to purple clay and unconsolidated clayey shale with an interbed of sandstone. The shale is thickly laminated and glauconitic (Okosun, 1998). Borehole observations suggest its thickness to be around 30–35 m (GSN borehole no. 1582) and the formation is predominantly marine environment of deposition and not of lagoon as postulated by Russ (1924). The top is unconsolidated and a friable mixture of sandstone and clay which serves as the unconfined aquifer bed (Figure 3.10). The basal bed consists of the following facies: sandstone, mudstone, claystone, and shales. This formation is compositionally phosphorite (Nton, 2001) and thin beds of limestone or marl are locally



present in the formation. The shales found in the formation were deposited in a well-oxygenated deep marine environment. The age is Paleocene to Eocene. The Oshosun Formation stratigraphy is presented in (Figure 3.13).

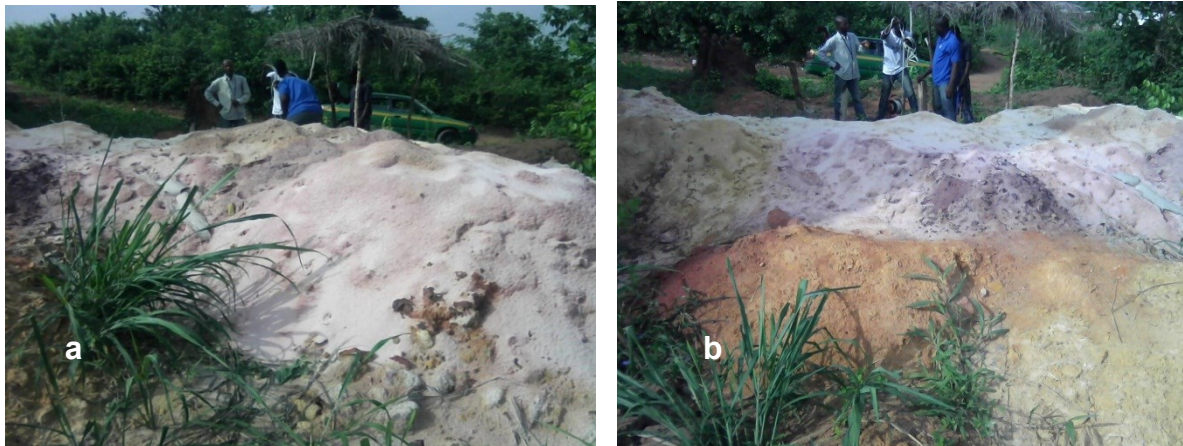


Figure 3.10: Unconsolidated sand grit and clay of Oshosun Formation

### 3.3.5 Ilaro Formation

The Ilaro Formation presents a different geology when compared to earlier rock types that were discussed. The formation is directly overlying the Oshosun Formation and was formed during the Middle to Late Eocene age (Adegoke, 1969; Kogbe, 1976; Ako *et al.*, 1981). It consists of predominantly coarse sands of estuarine, deltaic and continental environments, which display a rapid lateral facies change (Slansky, 1962; Jones and Hockey, 1964). The sands are massive, white (sometimes yellowish) and poorly sorted and mineralogically composed of pure quartz grains (Figure 3.11a). The formation is known for its aquiferous potentials with an average thickness of 36–60 m. Section was reported at Hetin Sotta near the axis of western Nigeria and the Benin boundary. The sedimentation of the Oshosun Formation followed a regression that resulted in the deposition of sandstones at a unit of the Ilaro Formation.



Figure 3.11: (a) Whitish alluvial sand dug during well construction in Ilaro Formation; and (b) red mottling and friable grit of the Oshosun Formation

### 3.3.6 Coastal Plain Sand/ Benin Formation

The Benin Formation is the youngest stratigraphic sequence in the eastern Dahomey Basin. It consists of poorly sorted sands with lenses of claystones and mud. The sands are partly cross-bedded (Figure 3.12) and show transitional to continental characteristics. The age ranges from Oligocene to Recent (Reyment, 1965). Apart from the recent alluvium sediment that was deposited along the shore, the formation underlies the Lagos metropolis. Thicknesses of as much as 400 m were reported towards the coast (Agagu, 1985).

In summarising the stratigraphy of the Dahomey Basins, a comparison by two major authors, Jones and Hockey (1964) and Omatsola and Adegoke (1981), is presented in Figure 3.13.

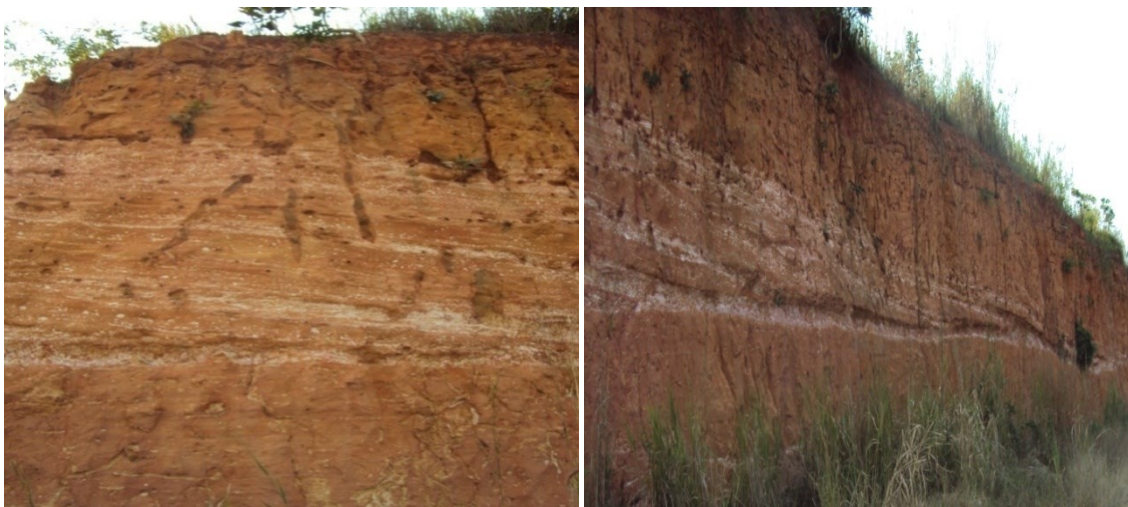
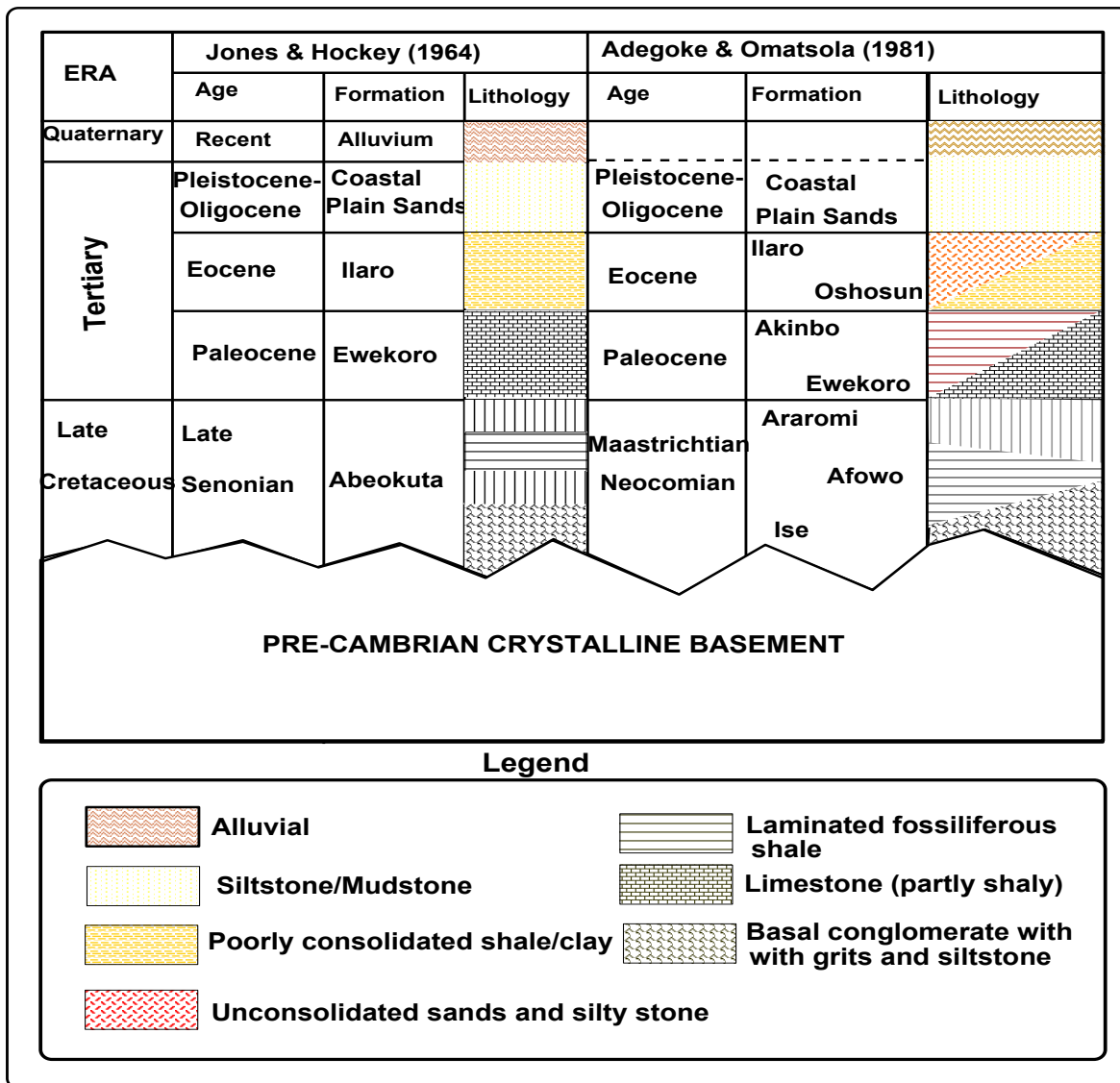


Figure 3.12: Cross stratification of Coastal Plain Sand (CPS)



Source: After Omatsola and Adegoke (1981).

Figure 3.13: Generalised stratigraphy of the Dahomey Basin

### 3.4 Conclusion

Groundwater characterisation involves the understanding of the basic geology hosting the water, particularly for sedimentary basins where clay rich sediments serve as aquifer boundaries. Groundwater occurrence in the Dahomey Basin is controlled by the geological formation and stratigraphic succession. The hydrogeology of the Dahomey basin will be discussed in later chapters. In this chapter, the formations' sediment compositions, mode of formation and age were discussed. This chapter also will assist in the characterisation of the Dahomey Basin vadose zones and groundwater vulnerability estimation.

# CHAPTER 4

## HYDROGEOLOGICAL CHARACTERISATION OF THE EASTERN DAHOMEY BASIN

### 4.1 General Introduction

Shallow unconfined groundwater resources can be investigated by studying and predicting deposited formations overlying an aquifer and the ease with which the formation allows contaminants to vertically flow to the groundwater table. Contaminants infiltrate vadose materials before reaching groundwater bodies. This has a direct influence on groundwater vulnerability to contamination by slowing and filtering the contaminant compositions. This is possible by the amounts of silt and clay material present in the deposited vadose materials. The deposited vadose material is called the pathway in the European model of groundwater vulnerability studies. The distribution and amount of sediments filtering capacity in the pathway can best be estimated from their grain size analysis (GSA) and textural properties.

Properties such as porosity, grain shape and hydraulic conductivity of the pathway materials are important in site characterisation. The importance of hydraulic conductivity, which will be discussed in detail in Section 4.3, is vital to travel time determination and groundwater vulnerability estimation. Furthermore, estimation of hydraulic conductivity, porosity, GSA, grain shape and soil textural properties will all be laboratory derived in Section 4.3. Laboratory determination of vadose properties is a reliable alternative method aside the in-situ field methods.

The vadose zone, a layer above the water table and a major component of the groundwater flow regime, contributes greatly to groundwater recharge and quality. The geo-electrical understanding of the vadose zone properties can be used in predicting surface and subsurface contaminant transport, groundwater flow and general aquifer characteristics (Heigold *et al.*, 1979; Kosinski and Kelly 1981; Urish 1981; Ponzini *et al.*, 1984; Frohlich *et al.*, 1996). Such vadose zone properties include depth-to-water table, individual bed thickness, clay presence and sediment types. Due to the geo-electrical methods wide applicability, interpreting results from resistivity of subsurface materials would be relatively easy and important in characterising the Dahomey Basin vadose zone.

Likewise, a proper understanding of groundwater quality and quantity, distribution and location is important in its protection. Groundwater, though relatively unseen, is an accessible water supply to most sub-Saharan African countries, the reason being that its development is simple and quality is relatively assured (MacDonald *et al.*, 2012). Therefore, the hydrogeochemical characteristics of groundwater in the Dahomey Basin will be investigated. From the above discussions, estimating the aquifer vulnerability of the eastern Dahomey Basin requires proper characterisation of the aquifer systems. Therefore, characterising the aquifer systems of the Dahomey Basin's hydrogeological properties in this chapter will be done using the following methods:

- Geophysical techniques.
- Hydrochemical analysis.
- Lithogeochemical investigations.
- Soil hydraulic properties.
- Groundwater hydraulics.

## 4.2 Geophysical Characterisation of the Dahomey Basin Vadose Zones

### 4.2.1 Surface Geophysics

A widely used surface geophysical method in groundwater studies is the geo-electrical method (Hallenbach, 1953; Koefoed, 1979; Kosinski and Kelly, 1981; Frohlich *et al.*, 1987; El-Waheidi *et al.*, 1992; Frohlich and Urish, 2002; Matias, 2002; Mhamdi *et al.*, 2006). Since the twentieth century, the geo-electrical method has increasingly been used in groundwater prospecting, but its application in vulnerability studies improved in the 80's and 90's (Kelly and Frohlich 1985; Kalinsky *et al.* 1993; Kirsh 2006; Casas *et al.* 2008). The application of the geo-electrical method to groundwater vulnerability studies is intended to characterise the following in the vadose zone:

- The depth of the vadose zones.
- Lithological delineation.
- Strata/ bed characteristics.
- Delineation of water table.

The displayed geo-electrical properties are used to characterise the sedimentary rock material and predict the protective capacity of material in the vadose zone, which is also termed aquifer protective capacity. Aquifer protective capacity is important in order to evaluate groundwater movement and quality in rock media. This is because the earth medium acts as a natural filter through its ability to retard and filter percolating ground surface polluting fluid (Olorunfemi *et al.*, 1999).

#### 4.2.1.1 Theoretical Background and Justification of the Resistivity Method

A wide range of geophysical techniques can be applied to investigate the vadose zones. The techniques target static, structural and dynamic characterisations of rock materials such as lithological boundaries, fracture zones, estimation of volumetric or gravimetric water content. These characterisations are carried out to determine specific rock properties: elastic moduli, mass density, dielectric permittivity and resistivity. Resistivity, an inverse of electrical conductivity is measured through electromagnetic induction, direct current (DC) resistivity and induced polarisation methods (Binley and Kemna, 2005).

The mapping of a lateral hydrogeological environment, such as the study area, requires direct contact of the equipment with the ground over a large area, which is time consuming. The time domain method, such as the electromagnetic method, is however, best suited for depth profiling in a short time and requires a large antenna loop making it ineffective and

limiting its use over many surface locations (Cassiani *et al.*, 2005). However, DC with electrical sources used in this research allows for spatial variations in electrical conductivity, because resolution is principally controlled by electrode spacing. In addition, the dynamic range of the DC method is broad, permitting application in highly resistive and highly conductive environments.

In vadose zone vulnerability mapping, DC can be used for tracking spatial changes in conductivity that results from changes in volumetric water content in the soil (Cassiani *et al.*, 2005). DC techniques measure electrical resistivity ( $\rho$ ) of earth material, but was established on the assumption that there is a relationship between soil volumetric water content, with either soil dielectric permittivity or electrical conductivity (Vereecken *et al.*, 2006). The resistivity of earth material, which is an inverse of conductivity, is roughly equal to the resistivity of the pore fluids divided by the porosity. This is otherwise known as the Archie's Law (1942). This law relates electrical resistivity of material to the shapes of the materials matrix grains, pore water, porosity and saturation of vadose zone.

#### 4.2.1.2 Vertical Electrical Sounding

Vertical Electrical Sounding (VES) is one of the best DC methods that can be adapted to determine resistivity of layered rock with depth. Sedimentary rocks are deposited as flat-lying layered structures over one another, with the effect of high compaction resulting from overlying weight of recent sediment over previously deposited sediment. This leads to the reduction of the volume of pore spaces and subsequently reduces porosity. The Schlumberger array is most commonly used in VES, especially in the determination of depth-to-water table and sedimentary bed identification (Figure 4.1). Layered sedimentary rock poses distinct characteristic properties from their composition. These differing materials cause them to show contrary electrical conductivity properties.

For groundwater vulnerability studies the choice of electrode arrays can sometimes be determined by the geological formation underlying the study area. The single VES method, which is best suited for horizontally layered rocks with very little lateral formation, can be interpreted using the 1D and 2D model and has been tested for its efficiency and accuracy (Ernstson and Kirsch, 2006).

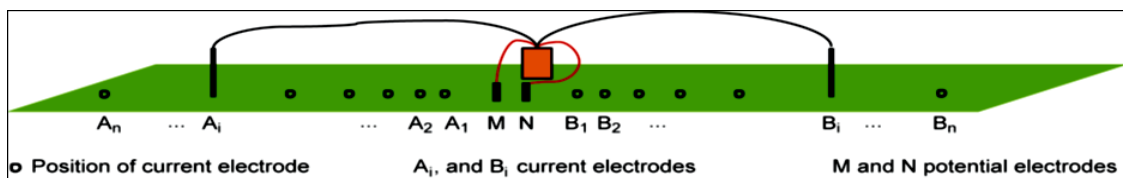


Figure 4.1: Sketch of the field setup for a VES in Schlumberger configuration

#### 4.2.2 Schlumberger Array

VES was employed because of its relative practical and methodological advantages. Schlumbergers configurations, which are closely associated with VES where current electrode A and B (Figure 4.1) are spaced according to the depth of underground layers

intended to be investigated, was confirmed to be best suited for this investigation. This was due to its sensitivity to shallow variation, which is the target in vadose zone characterisation (Ernstson and Kirsch, 2006).

The current electrodes (A and B) were logarithmically ranged from 1 m to 160 m. The VES method of electrical resistivity survey was chosen because it provides detailed information on vertical succession of individual thicknesses, resistivity and their different conducting zones (Kelly, 1977; Sorensen *et al.*, 2005). Dahlin and Zhou's (2004) recommendation of the use of schlumberger and a pole-dipole array then followed because of their high data density and gradient, but also because it is more sensitive to noise than the wenner and gamma array.

The equipment used included the resistivity meter which has been tested for its ability to probe up to one kilometre into the earth surface, provided the current and potential electrode followed spacing that prevents a faint detection of current by the inner potential electrode. The amount of current introduced was monitored and regulated throughout the field data acquisition. Stainless steel rods were used for both current and potential electrodes and good insulation of the cables was ensured in order to prevent leakages.

VES traverses were zoned according to the geological formation (Figure 4.2). Traverse A–B was along the Coastal Plain Sand, Traverse C–D along Ewekoro Formation, Traverse E–F along Abeokuta Formation and traverse G–H along the Ilaro/ Oshosun Formation.

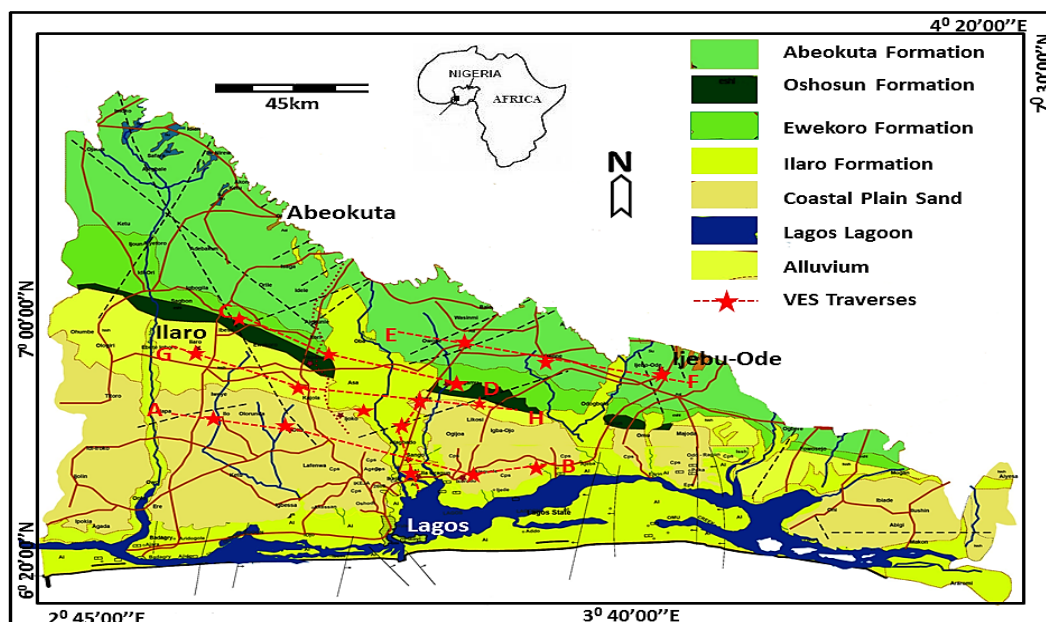


Figure 4.2: Restivity sounding points showing VES traverses superimposed on the geological map of the Dahomey Basin

The sounding location was chosen based on the following criteria:

- Near wells of known lithology and groundwater table.
- Nearly horizontal space for electrode spreading.
- Considerable distance from conductive materials on the ground surface and electrical overhead cables.

- Avoidance of topographic effect during spreading such as hilly, gorge or generally difficult terrains.

The assumption of a nearly horizontal layering was employed during the interpretation that was further aided by the identified well logs and water levels. Figure 4.3 shows the methodological framework followed in the interpretation of this data.

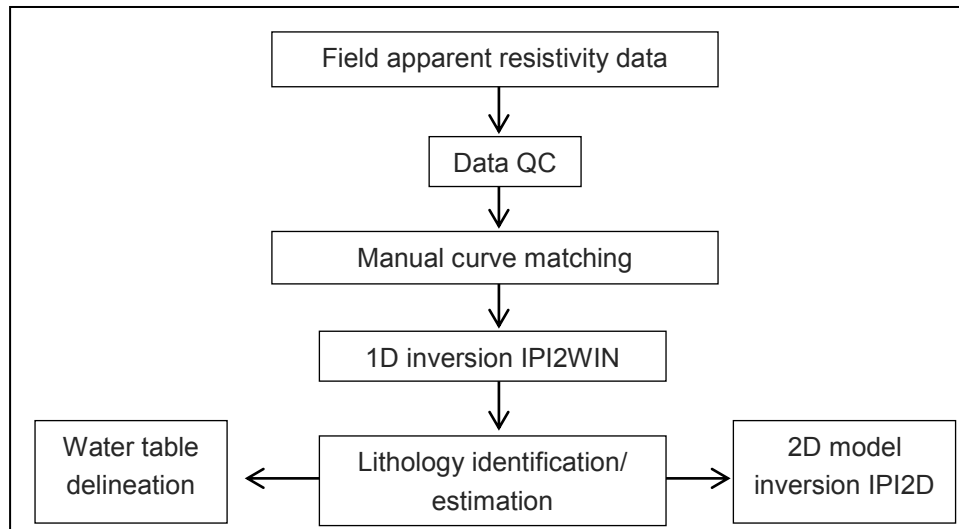


Figure 4.3: Methodology framework used in the interpretation of this section

### 4.2.3 Resistivity Data Evaluation

The data evaluation criteria are defined based on the research objectives. Geophysical evaluation in hydrogeological systems can only apply to available geophysical data and the geological conditions prevailing in the study area. Data evaluation depends on geophysical model parameterisation that was used. The zonation geophysical model parameterisation was used in this research (Linde *et al.*, 2006). The study area was zoned according to their formation and along their geological characteristics as classified by Omatsola and Adegoke (1981), Agagu (1985) and Jones and Hockey (1964). This was necessary for model parameters comparison and lithological correlation of the vadose zone and aquifer properties.

Zonation is best used in a sedimentary rock terrain where variations between beds in the formation are small compared to bed variations in different formations (Linde *et al.*, 2006). This was further demonstrated by Auken and Christiansen (2004) by using electrical methods in mapping large-scale sedimentary hydrogeological units. This approach allows direct comparison with borehole logs and is considered the best when a geological structure is apparent and formation boundaries are distinct (McLaughlin and Townley, 1996).

Data were inverted to 1D and 2D resistivity images using the IPI2WIN software. The inversion was done to interpret the primary resistivity data recorded from the field, with the aim of obtaining both lateral and vertical layer distribution of beds in the vadose zone. The software was based on the Newton algorithm (Bobachev *et al.*, 2003). The advantage of this



program is that individual layers are identified and connected along the sounding profile. The data processes also involve removal of false data and noise. Field VES data were plotted on a log paper, and partial curve matching was carried out.

The obtained layer and resistivity values were used as initial background values before inversion of the data into a 1D image. From the inversion, lithology, layer depth, overall thickness of vadose zone overburden as well as the lithology and layer resistivity/ conductivity were extracted. These extracted parameters were used in the lithological identification, vadose zone characterisation and hydrogeological implication. The sounding point along the same zones was connected together by using IPI-2D programs. The program effectiveness in inhomogeneous horizontally layered media allows suppressing the distorting influence of near surface inhomogeneity, thereby increasing the accuracy of the interpretation.

Borehole lithology was recorded, as well as the groundwater levels in each formation where sounding occurred. This was done in order to have a visual and exact composition of the vadose zone material, especially permeable layers, and to check the accuracy of the inverted model data. It should, however, be noted that the vadose zones characterisations, using the resistivity method, is dependent on the quality of the data which are regulated by other unseen factors.

#### **4.2.4 1D Inversion of Field Resistivity Data**

The field data for VES are presented in Table 4.1 and Table 4.2. The data present in these tables include the current electrode spacing ( $AB/2$ ), potential electrode spacing ( $MN/2$ ), the geometric factor ( $K$ ) and the apparent resistivity values  $R$  ( $\Omega m$ ) of each VES sounding point. In order to obtain a VES curve, the apparent resistivity is plotted against the corresponding half of the electrode spacing ( $AB/2$ ). Sounding curves that are produced over a horizontal stratified medium is a function of the resistivity, layer thickness and electrode configuration (Zohdy, 1974).

The IPI2WIN software (Bobachev, 2003) on the observed field resistivity data automatically inverted the curves. The estimated true resistivity calculated from the inverse procedure gives the measured apparent resistivity. The inversion advantage is that it minimises the difference between the modelled and measured apparent resistivity. Commonly known curve types including A, H, K and Q (Figure 4.4) reveals resistivity variation with depth and lithology. The selected representative geo-electrical curves obtained are indicated in Figure 4.5. The curves vary considerably throughout the study area. The black lines indicate the field curve, while the red and blue lines indicate inverted curves. It provides information about the relation between  $AB/2$  and apparent resistivity value. The blue curve gives information about resistivity value variation.

Table 4.1: Apparent resistivity values of formation from the Dahomey Basin

Current	Potential electrode	Geometric factor	Ves 1	Ves 2	Ves 3	Ves 4	Ves 5	Ves 6	Ves 7	Ves 8	Ves 9
AB/2 (m)	MN/2 (m)	K	R ( $\Omega$ m)	R ( $\Omega$ m)	R ( $\Omega$ m)	R ( $\Omega$ m)	R ( $\Omega$ m)	R ( $\Omega$ m)	R ( $\Omega$ m)	R ( $\Omega$ m)	R ( $\Omega$ m)
1	0.5	3.14	284	334	568	561	98	296	385	228	103
2	0.5	12.57	467	517	934	518	12	166	216	128	142
3	0.5	28.27	534	584	1068	426	5	202	263	155	156
5	0.5	78.55	644	694	1288	238	5	275	358	212	173
6	0.5	113.11	736	786	1472	172	6	301	391	232	201
6	1	56.56	746	796	1492	176	6	329	428	253	208
8	1	100.54	825	875	1650	102	7	364	473	280	215
10	1	157.1	887	937	1774	75	8	380	494	292	187
10	2.5	62.84	935	985	1870	54	8	432	562	332	181
15	2.5	141.39	1141	1191	571	56	11	525	683	404	178
20	2.5	251.36	1255	1305	628	61	12	595	774	458	138
25	2.5	392.75	1268	1318	634	78	15	625	813	481	89
30	2.5	565.56	1305	1355	653	105	17	872	1134	671	72
35	2.5	769.79	1270	1320	635	108	18	689	896	530	56
40	2.5	1005.44	1185	1235	593	107	23	718	933	552	53
40	7.5	335.15	1316	1366	658	109	24	812	1056	625	49
45	7.5	424.17	1278	1328	639	104	27	883	1148	679	39
50	7.5	523.67	1246	1296	623	61	36	925	1203	712	39
60	7.5	754.08	1002	1052	501	50	35	961	1249	739	44
70	7.5	1026.39	894	944	447	48	40	928	1206	7134	41
80	7.5	1340.59	1027	1077	514	33	37	906	1178	697	47
80	15	16.76	Nd	Nd	Nd	27	38	949	1234	730	50
90	15	18.85	Nd	Nd	Nd	23	41	846	1099	651	48
100	15	20.95	Nd	Nd	Nd	21	40	745	969	573	66
120	15	25.14	Nd	Nd	Nd	Nd	Nd	811	1054	624	77
140	15	29.33	Nd	Nd	Nd	Nd	Nd	689	896	530	87
160	15	33.51	Nd	Nd	Nd	Nd	Nd	552	718	425	Nd

Nd=no data

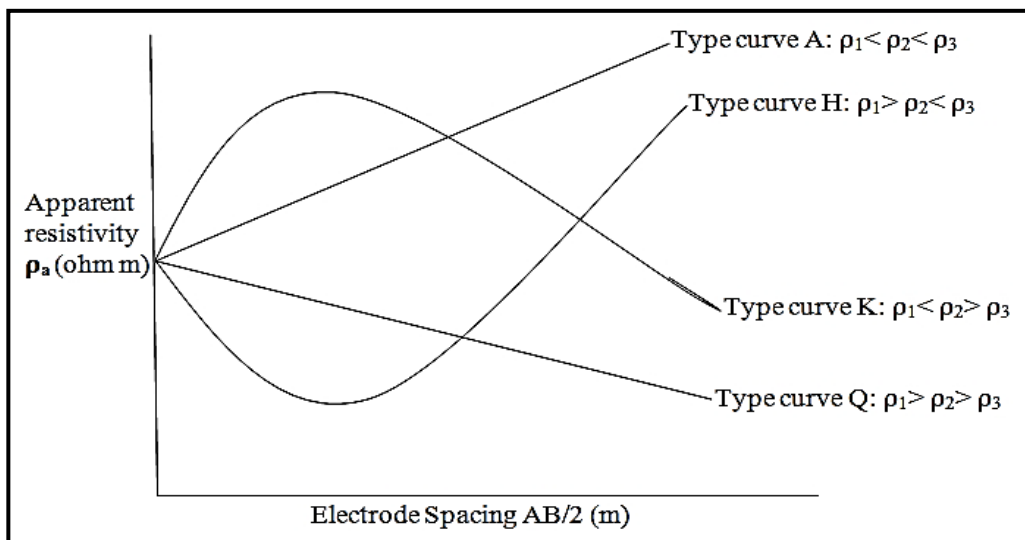


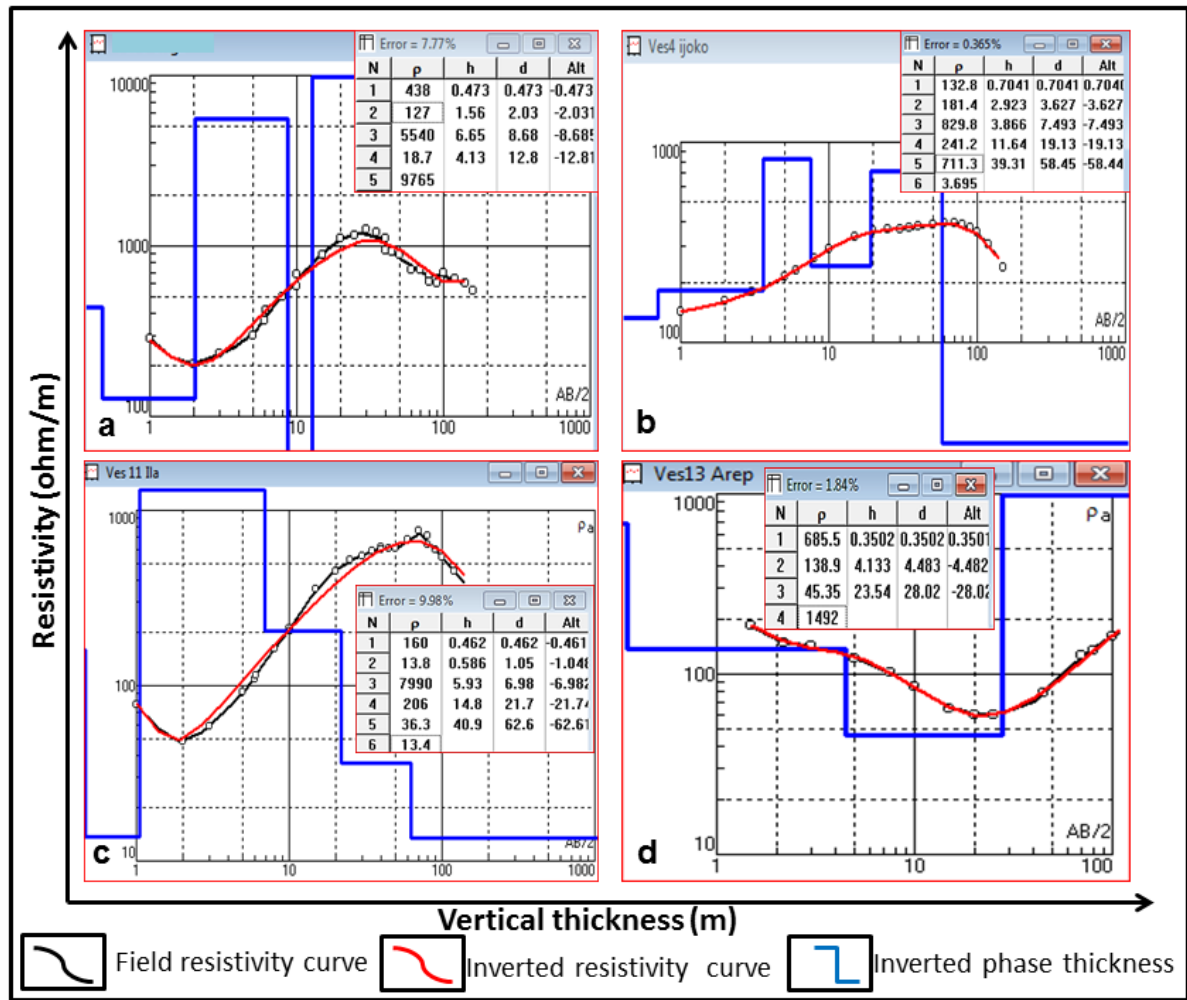
Figure 4.4: Diagram of resistivity curve types in layered structures

Table 4.2: Apparent resistivity values of formation from the Dahomey Basin

Current Electrode	Potential Electrode	Geometric Factor	Ves 10	Ves 11	Ves 12	Ves 13	Ves 14	Ves 15	Ves 16	Ves 17	Ves 18
AB/2 (m)	MN/2 (m)	K	R (Ωm)	R (Ωm)	R (Ωm)	R (Ωm)	R (Ωm)	R (Ωm)	R (Ωm)	R (Ωm)	R (Ωm)
1	0.5	3.14	184	78	94	144	159	397	398	385	103
2	0.5	12.57	136	48	58	157	172	486	431	522	142
3	0.5	28.27	114	59	71	186	201	590	409	562	156
5	0.5	78.55	102	92	110	205	220	699	393	614	173
6	0.5	113.11	102	109	131	193	208	694	354	722	201
6	1	56.56	81	115	138	234	249	700	327	684	215
8	1	100.54	81	162	194	258	273	951	394	827	187
10	1	157.1	49	212	254	294	309	943	403	838	178
10	2.5	62.84	32	204	245	301	316	576	421	910	138
15	2.5	141.39	28	356	427	353	368	596	484	905	89
20	2.5	251.36	32	452	542	367	382	646	559	1027	72
25	2.5	392.75	32	518	622	353	368	655	472	1062	56
30	2.5	565.56	38	547	656	359	374	736	578	1021	53
35	2.5	769.79	42	584	701	370	385	930	768	1081	39
40	2.5	1005.44	44	620	744	355	370	1193	1032	1182	39
40	7.5	335.15	50	599	719	388	403	1443	1146	2213	44
45	7.5	424.17	62	609	731	368	383	1525	1076	2017	41
50	7.5	523.67	71	856	1027	379	394	1502	911	93	47
60	7.5	754.08	70	681	817	386	401	1358	776	72	50
70	7.5	1026.39	80	765	918	379	394	1387	747	67	48
80	7.5	1340.59	97	721	865	429	444	1044	499	51	66
80	15	16.76	110	635	762	416	431	855	363	48	77
90	15	18.85	114	459	551	392	407	702	266	49	87
100	15	20.95	119	691	829	314	329	690	187	55	94
120	15	25.14	127	488	586	217	232	Nd	Nd	Nd	Nd

Nd = no data

Typical forms of these curves in the Dahomey Basin are HK, HKQ, AKQ, AK, AKH and QHA types. Most of the obtained sounding curves were of the HK ( $\rho_1 > \rho_2 < \rho_3 < \rho_4 > \rho_5$ ) as shown in Figure 4.5a, and AKQ type ( $\rho_1 < \rho_2 < \rho_3 > \rho_4$ ) in Figure 4.5b. These curve types indicate four to five lithologies. The dominant resistivity curves in the formation were as follows: Ilaro Formation (HKQ, HKA), Abeokuta Formation (AK, AKQ), Coastal Plain Sand (HAK, AK, AKQ), Alluvium (AKH, QHA) and Ewekoro Formation (HAK). The curves types' combinations show the presence of multiple layered rocks deposition. The HAK curves rose steeply into positive slopes, and such curves are a reflection of a highly resistive sedimentary rock at depth (Onuoha and Mbazi, 1998). The descending early curves, mostly below 10 m (Figure 4.5a and Figure 4.5c), indicate a resistive top soil underlain by a conductive material which can possibly be wet sandstones.



Key: a = HKA curve type, b = AKQ curve type, c = HKQ curve type and d = QH curve type.

Figure 4.5: Representative resistivity curve types in the Dahomey Basin

#### 4.2.5 Geo-electrical Sections

The key to the success of any geophysical data is the hydrogeological and geological information (Lashkaripour and Nakhaei, 2005). Ordinarily, geo-electrical sections constructed from VES data analysis do not always coincide with the corresponding actual geological sections. Layers of different lithology may display the same resistivity data and form a single geo-electrical layer. However, a good understanding of the underlying geology, most especially documented stratigraphic data and drillers geological logs data, can be used to differentiate these layers. A geo-electric section is thus determined through their respective individual layer resistivity and thickness. Figure 4.6 and Figure 4.7 indicate the geo-electric sections of the 18 geo-electric soundings obtained in the Dahomey Basin.

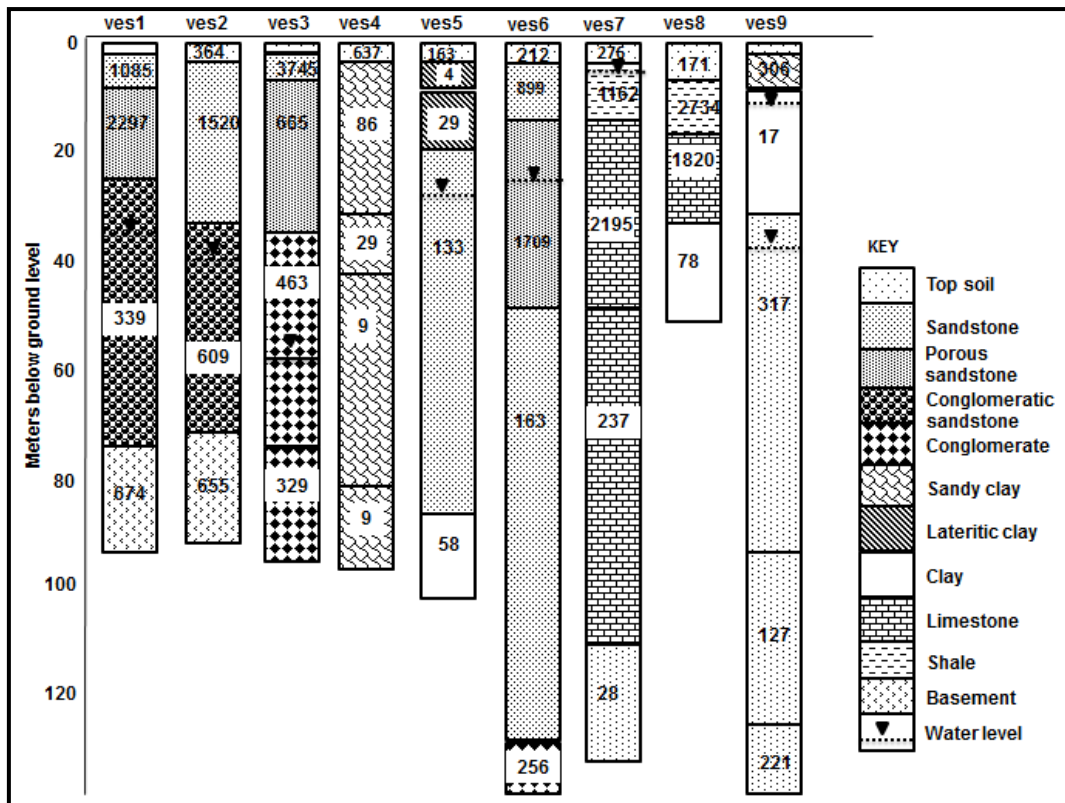


Figure 4.6: Interpreted geo-electric sections of the study area

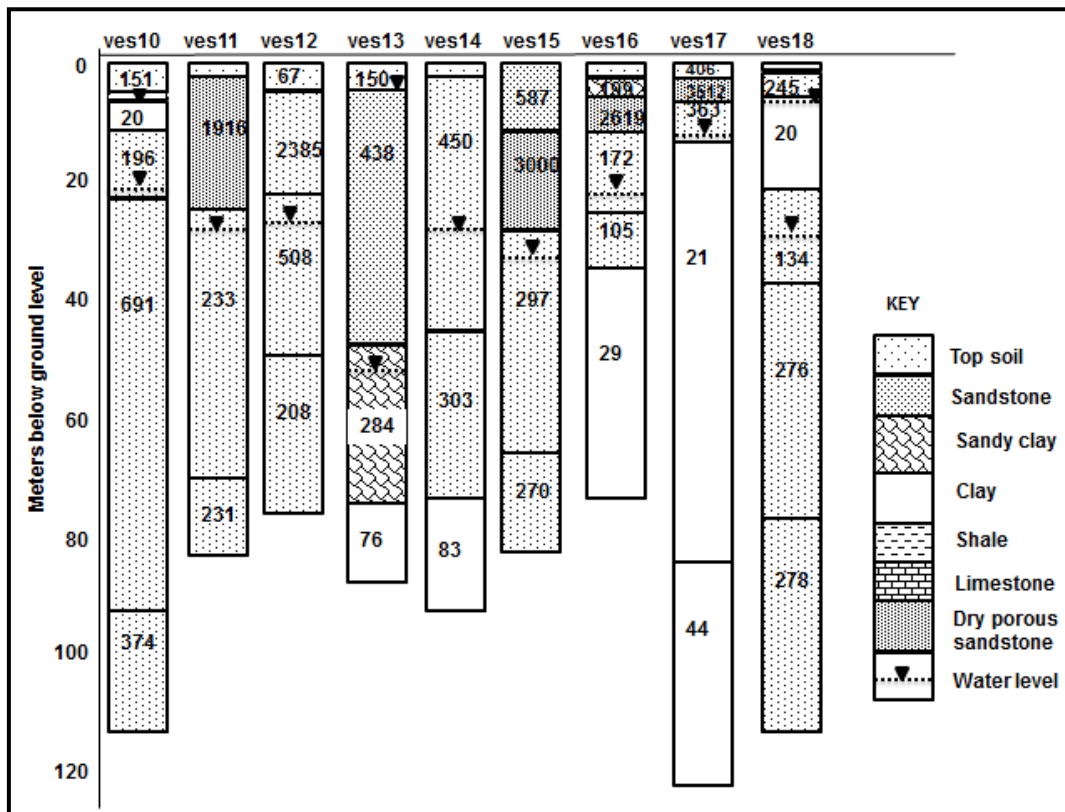


Figure 4.7: Interpreted geo-electric sections of the study area

The lithological units of these sections, as interpreted from VES data, include topsoil, sandy clay, conglomeratic sandstone, limestone, dry porous sandstone, weathered basement rock and lateritic clay. The top soils are sandstones consisting of lateritic sand and alluvium. Top soil resistivity ranges between 67 and 275  $\Omega$ m. Sandstones resistivity values range between 133 and 308  $\Omega$ m for the section filled with groundwater and 899 and 3 745  $\Omega$ m for the dry porous sandstones. Limestone resistivity values range between 237 and 2 195  $\Omega$ m while clay shows values below 100  $\Omega$ m. For a comparison of the Dahomey Basin, geo-electric values with documented lithology values are presented in Table 4.3.

Table 4.3: Apparent resistivity interpretation showing geo-electric parameters in  $\Omega$ m

Rocks and their resistivity values	Dahomey Basin	Telford et al. (1995)	John Milson (2003)
Clay/ shale	17–83	1–90	100–200
Sandstone	133–3745	1–1 000	200–8 000
Fresh water sand	133–308	50–1 000	
Limestone	237–2 195	10–10 000	500–10 000
Dry sand/ loose sand	899–3 745	2 000–100 000	500–50 000
Gravel/ conglomerate	339–609		100–600
Top soil	67–637		50–100

#### 4.2.6 Lithological Characteristics

Electrical resistivity contrasts existing between lithological sequences in the subsurface are often adequate to enable the delineation of geo-electric layers and bed identification as well as aquiferous or non-aquiferous layers (Schwarz, 1988; Dodds and Ivic, 1998; Lashkaripour, 2003). Interpreted results suggest a geo-electric sequence comprising of a subsurface geology characterised by deposition of lateral sedimentary rocks. Pseudo cross-sectional images from converted apparent VES data were produced and linked according to their geological formations and along traverses (Figure 4.9).

Furthermore, representative grain sizes of the formations were carried out (Figure 4.8). This was done to further verify the predominant sediment types in each formation and in relation to the interpretation of the pseudo-section (Figure 4.9). Electrical resistivity from this lithology can also further be correlated to their porosity, degree of saturation and void presence (Ako, 2002). The EWE Formation shows sandy clay resistivity values of 400–750  $\Omega$ m, which correlate to the aquiferous layers in ABK, CPS and 350–470  $\Omega$ m in ILA. Further information on each layers' aquiferous potential is presented in Table 4.4.

Table 4.4: Interpreted resistivity results of sounding points and closed water samples

Ves No	Sedimentary Formation	Vadose resistivity range ( $\Omega$ m)	Estimated resistivity depth-to-water table (m)	Actual measured water table (m)	Vadose zone thickness (m)
5, 6, 11, 12	llaro	4–2 385	22–25	21	20
7, 8	Ewekoro	171–2 734	25–40	2–4,35	30
1, 2, 3	Abeokuta	268–3 754	35–70	45–90	65
14,15,16,17	CPS	165–3 512	10–21	7–25	22
9,10, 13 18	Alluvium	11–438	2–4	3–6	3

### Traverse A–B (Coastal Plain Sand)

Coastal Plain Sand (CPS) reveals a sandstone regime with sand sizes ranging from coarse to fine-grained. Lithological sequences along traverse A–B reveal beds of sandy clay as the top soil, underlain by sandstone and porous sandstone. Combining the findings with that of the grain size distributions implies a high vulnerability formation with high groundwater recharge potential.

### Traverse C–D (Ewekoro Formation)

Analysis of the Ewekoro pseudo-section portrays a thick fine-grained shale/clay cover of about 6.5–10 m overlying the sandstone and limestone formations. Low aquifer vulnerability potential to contamination is assured for this formation. This is partly due to its high clay content and the general spread of its grain sizes (Figure 4.8). The formation will also have lower porosity because available pore spaces within a larger matrix will be filled with smaller grains of silt and clay, thereby reducing its recharge potentials.

### Traverse E–F (Abeokuta Formation)

The Abeokuta Formation (ABK) traverse indicates a lithological sequence comprising of a sediment matrix of conglomerate and dry porous sandstone, typical of a geological transition formation (Figure 4.9 E–F). Analyses of grain distribution indicate a coarse grain sand to gravel-size particles. This can be interpreted to contain a high porosity within the sediment matrix, high infiltrations and therefore high aquifer vulnerability.

### Traverse G–H (Ilaro/ Oshosun Formation)

The lithological pseudo-sections show gradation from a fine to coarse grain sequence of lateritic clay deposit overlying sandstones. Further evidence from grain size analysis suggests that the Ilaro Formations (ILA) display a combination of sand and appreciable silt sediments (Figure 4.8). A visual examination of the Ilaro Formation sediment reveals a presence of a pure quartz bed, which may be responsible for its high resistivity (Figure 4.9 G–H).

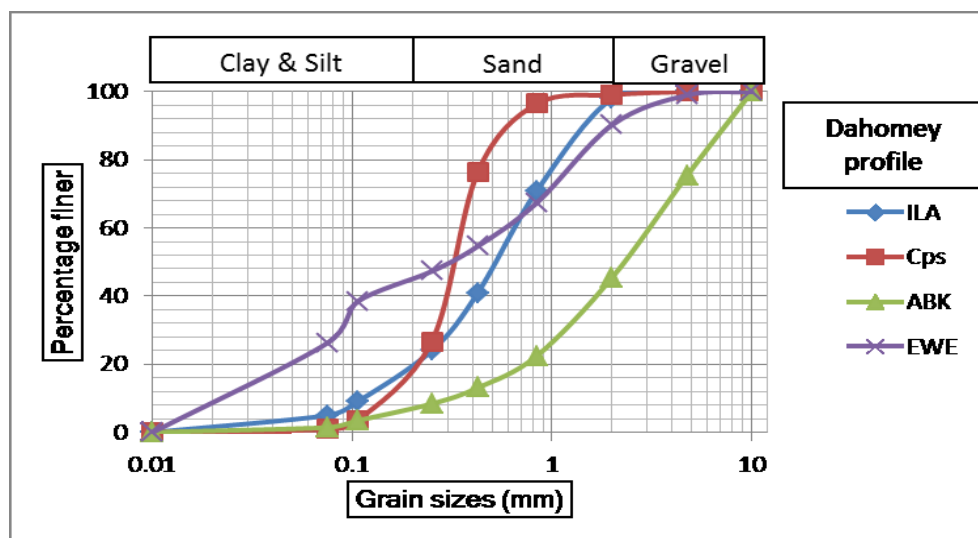


Figure 4.8: Grain size distribution of geological formations

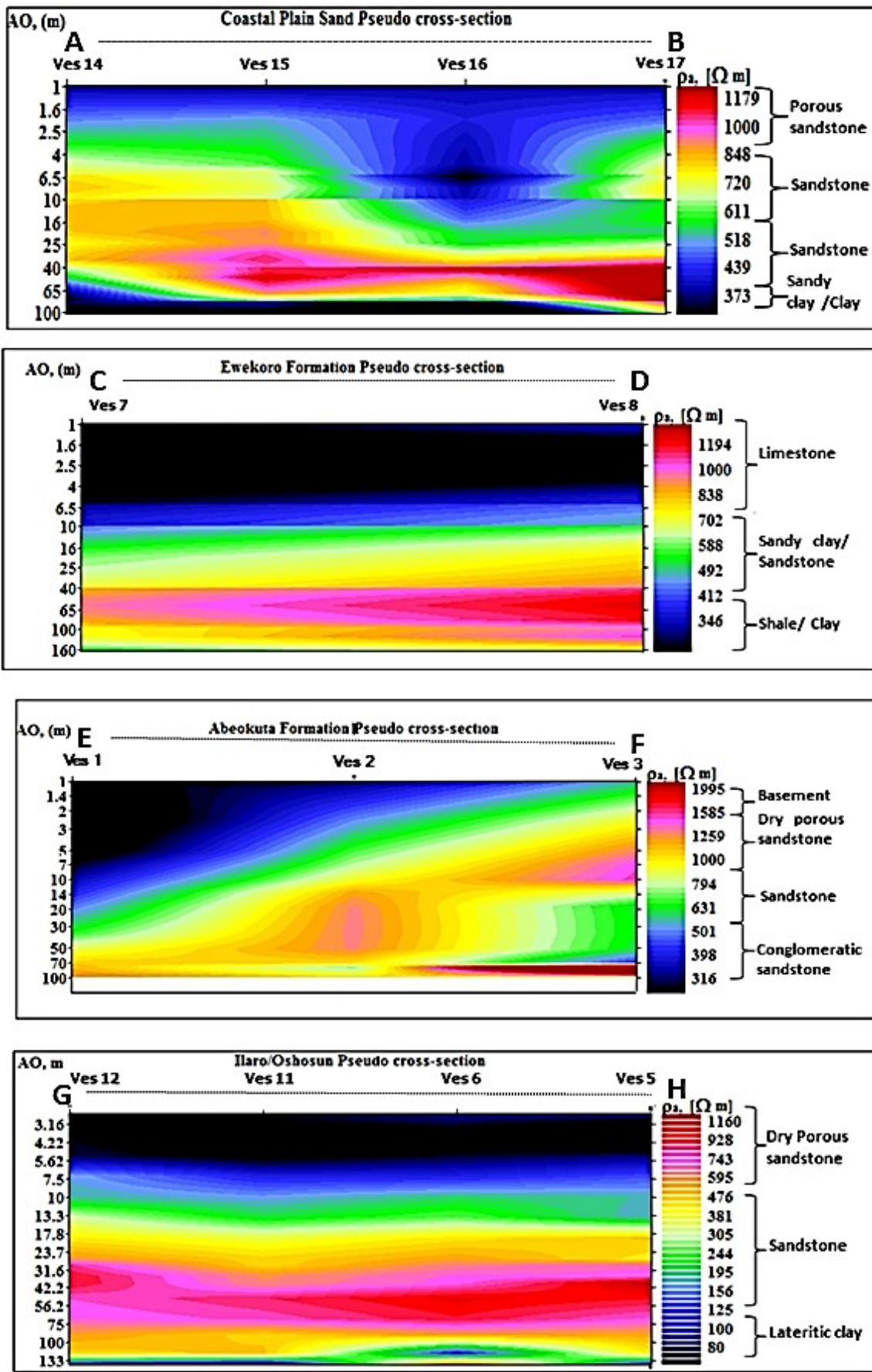


Figure 4.9: Pseudo-sections of geological formations



#### **4.2.7 Water Table Delineation and Vadose Zone Estimation**

As the study area is rain-fed, the water table is controlled by precipitation recharge which is delineated based on the soils, geological information and geo-electrical results. During the inversion, the average depth-to-water table taken, using a groundwater level indicator and available drillers log, were correlated and used as a constraint of the 1D-resistivity models. From this correlation, the true resistivity, depths and thickness of the expected water-bearing zones were recognised. The water table was estimated from these models and compared along their zonation (i.e. geological depositions and boundaries) as shown in Figure 4.1. Results show an estimated vadose thickness of 22–25 m for the Ilaro Formation, 25–40 m for the Ewekoro Formation, 35–70 m for the Abeokuta Formation, 2–5 m for the Alluvium and 10–21 m for the Coastal Plain Sands.

Table 4.4 presents the estimated resistivity and actual measured depth-to-water table and vadose zone thickness. In vadose zone delineation, the bulk electrical layer resistivity is frequently derived from interpretation of the VES curves that can be summarised from the pseudo-sections. The method of horizontal layer interpretation of VES curves is non-unique, namely various resistivity-depth models can produce the same VES curve. However, unsaturated thicknesses can be extracted from precise constructed geo-electrical sections. Experimental evidence shows that the bulk electrical resistivity of a rock sample increases with increasing electrical resistivity of the saturating fluid (Frohlich and Parke, 1989).

#### **4.2.8 Limitations**

- A major limitation in the use of resistivity in delineating the vadose zone is the problem of uncertainty. The possibility of misjudging and misinterpreting the resistivity values of different sediment for one another is high.
- Bed thickness accuracy is another limitation associated with using resistivity to estimate properties of the vadose zone. Resistivity tends to not detect thin underlying beds far from the surface.
- In addition, the distance between traverse points to one another is large and can introduce inaccuracy in the vadose lithological estimation. However, the objective of using resistivity was to identify deposited lithology and in comparison to the drillers logs and documented stratigraphy.

#### **4.2.9 Conclusion**

A hydrogeophysical investigation using geo-electrical methods in the Dahomey Basin is quite challenging, because the sediment composition involves a wide range of lithologies and a mixture of sediment of grain sizes. The sediment grain sorting ranges from poorly sorted to nearly homogeneous facies as well as a broad range of rock types including limestone, shale, sandstone and conglomerate. Extracted geo-electrical sections were used to differentiate the lithological characteristics of the basin with the guidance of borehole geological data. Inverted curve types were of the HAK, HKA, AK and AKQ types which suggest a multi-layered lithology. The depth of the water table and vadose zone estimations derived from the geo-electrical and litho-sections, and would be used in the evaluation of the Dahomey Basin vulnerability.

Table 4.5: Interpreted apparent resistivity, lithological unit and hydrogeological implications

Location	VES Points	Curve type	No of layers	Resistivity ( $\rho = \Omega m$ )	Thickness (m)	Depth (m)	Lithological Unit	Hydrogeological Implication
Iperu	1	AK	5	268	0.92	0.92	Top soil	Non-aquiferous
				1 085	7.48	8.4	Porous Sandstone	Non
				2 297	16.48	24.88	Porous Sandstone	Non
				339	49.89	74.77	Sandstone/ Conglomeratic Sandstone	Aquiferous
				674			Basement	Non
Ikenne	2	AK	4	364	1.46	1.46	Top soil	Non
				1 520	30.57	32.03	Sandstone	Non
				609	39.93	71.96	Sandstone/ Conglomeratic Sandstone	Aquiferous
				655			Basement	Aquiferous
Ijebu-Ode	3	AKQ	5	419	0.62	0.62	Top soil	Non
				3 745	1.72	2.34	Porous Sandstone	Non
				665	32.52	34.86	Sandstone	Aquiferous
				463	39.91	74.77	Conglomerate	Aquiferous
				329			Conglomerate	Aquiferous
Ijoko	4	KQKQ	5	637	1.69	1.69	Top soil	Non
				86	30.6	32.29	Sandy Clay	Non
				29	9.62	41.91	Sandy Clay	Non
				9	20.26	62.17	Sandy Clay	Non
				5			Sandy Clay	Non
Shagamu	5	QHA(K)	5	163	0.45	0.45	Top soil	Non
				4	3.61	4.06	Lateritic Clay	Non
				29	14.05	18.11	Lateritic Clay	Non
				133	69.03	87.14	Sandstone	Aquiferous
				58			Clay	Non
Shagamu	6	HAK	5	212	3.47	3.47	Top soil	Non
				899	11.89	15.36	Sandstone	Non
				1 709	32.3	47.66	Porous Sandstone	Non
				163	84.64	132.3	Sandstone	Aquiferous
				256			Conglomerate	Aquiferous
Papalanto	7	HAK	5	276	3.47	3.47	Top soil	Non
				1 162	11.5	14.97	Shale	Aquiclude
				2 195	32.31	47.28	Limestone	Non
				237	69.12	116.4	Limestone	Aquiferous
				28			Sandstone	Aquiferous
Ibeshe	8	HAK	4	171	6.34	6.34	Top soil	Non
				2 734	10.5	16.84	Shale	Aquiclude
				1 820	18.76	35.60	Limestone	Non-aquiferous
				78			Clay	

Location	VES Points	Curve type	No of layers	Resistivity ( $\rho = \Omega m$ )	Thickness (m)	Depth (m)	Lithological Unit	Hydrogeological Implication
Ibafo	9	AKH	6	106	1.34	1.34	Top soil	
				306	6.71	8.05	Clayey sand	Aquiferous
				17	22.06	30.11	Clay	Non-aquiferous
				317	64.6	94.71	Sand	Aquiferous
				127	43.1	137.81	Sand	Aquiferous
				221			Sand	Aquiferous
Mowe	10	QHA	6	151	3.34	3.34	Top soil	Aquiferous
				20	2.29	5.63	Clay	Aquitard
				11	5.86	11.49	Clay	Aquitard
				196	10.98	22.47	Sand	Aquiferous
				691	72.97	95.44	Sandstone	Aquiferous
				374			Sandstone	Aquiferous
Ilaro	11	HKQ	4	56	2.29	2.29	Top soil	
				1 916	21.75	24.04	Porous Sandstone	Non-aquiferous
				233	46.5	70.54	Sandstone	Aquiferous
				231			Sandstone	Aquiferous
Aje	12	HAK	4	67	2.31	2.31	Top soil	
				2 385	18.76	21.07	Porous Sandstone	Non-aquiferous
				508	29.55	50.62	Sandstone	Aquiferous
				208			Sandstone	Aquiferous
Arepo	13	HA	4	150	2.54	2.54	Top soil	
				438	43.78	46.32	Sandstone	Non-aquiferous
				284	28.59	74.91	Sandclay	Aquiferous
				76			Clay	Aquitard
Otta	14	HAK	4	165	2.61	2.61	Top soil	
				450	42.71	45.32	Sandstone	Non-aquiferous
				303	28.98	74.3	Sandstone	Aquiferous
				83			Clay	Aquitard
Agbado	15	AK	4	587	11.5	11.5	Top soil	
				3 000	16.96	28.46	Porous sandstone	Non-aquiferous
				297	37.64	66.10	Sandstone	Aquiferous
				270			Sandclay	Aquiferous
Ikorodu	16	QHK	6	428	2.32	2.32	Top soil	
				199	2.85	5.17	Sandy clay	Aquiclude
				2 619	10.17	15.34	Porous sandstone	Aquiclude
				172	9.96	25.30	Sandy clay	Aquiferous
				105	11.65	36.95	Sandy clay	Aquiferous
				29				
Agbowa	17	AKQ	5	406	2.11	2.11	Top soil	
				3 512	5.18	7.29	Porous Sandstone	Non-Aquiferous
				363	5.28	12.57	Sandstone	Aquiferous
				21	53.31	65.88	Clay	Aquitard
				44			Clay	Aquitard

Location	VES Points	Curve type	No of layers	Resistivity ( $\rho = \Omega m$ )	Thickness (m)	Depth (m)	Lithological Unit	Hydrogeological Implication
Ofada	18	AKH	6	96	0.81	0.81	Top soil	
				245	5.22	6.03	Sandstone	Aquiferous
				20	16.29	22.32	Clay	Aquitard
				134	15.93	38.25	Sanstone	Aquiferous
				276	40.53	78.78	Sandstone	Aquiferous
				278			Sandstone	Aquiferous

### 4.3 Vadose Zone Characterisations of the Dahomey Basin

#### 4.3.1 Introduction

In this section, the lithological characteristics of the Dahomey Basin vadose zone, including its petrophysical (textural and hydraulic), will be discussed. The vadose zone (pathway) component in groundwater vulnerability studies is central to the assessment of all the other factors that contribute to groundwater vulnerability estimations. Groundwater movement in the vadose zone is aided by some intrinsic properties. These properties include porosity, permeability, hydraulic conductivity, grains shape and sizes and the degree of cementation of the vadose material.

Hydraulic conductivity is obviously affected by structure as well as by texture, which is more important if the soil is highly porous, fractured, aggregated or stony, than if it is tightly compacted and dense (Mehuys *et al.*, 1975; Van Genuchten, 1980; Fies *et al.*, 2002; Wang *et al.*, 2002; Ma and Shao, 2008). Hydraulic conductivity depends not only on porosity, but also on size of the conducting pore. For example, gravelly or sandy soil can have much greater conductivity than a clay soil with narrow pore spaces, even though the total porosity of clay is greater than that of sandy soil. Cracks, worm holes and decayed roots channels which are present in soils, most especially near root zones, are not considered in this section.

This section therefore aims at investigating the textural and hydraulic properties of the vadose zone above unconfined aquifer systems in the Dahomey Basin. This is in relation to their possible attenuation on groundwater vulnerability contamination.

#### 4.3.2 Procedure

The procedure used in this section involves field sampling of the vadose zone and laboratory analysis.

##### 4.3.2.1 Field Sampling

The field sampling was done in stages. The first stage involved the observation and sampling of disturbed samples for grain size analysis (GSA). Samples were collected from different strata above the water table. This was followed by the collection of undisturbed samples for laboratory permeability testing using core samplers. Undisturbed samples were obtained by slowly pushing thin-walled tubes, and by having sharp cutting ends and tip relief into the soil. This was achieved during the hand-dug well construction method that is common in the Dahomey Basin since the water table is shallow (Figure 4.10d, g, j & l). Ten

centimetre core samples were taken for each observable change in lithology, colour and texture with each sample representing observed homogenous strata. It should be noted that due to the unconsolidated nature of some formations, these techniques could not be applied to all lithologies, particularly alluvium and porous sand formations (Figure 4.10i).

Further lithological measurement and observations that aided the descriptions of the basin were obtained from sand quarrying sites (Figure 4.10c&f), construction pit (Figure 4.10h) and drillers used during borehole construction. Numerous disturbed soil samples were collected from drillers across the basin during borehole construction. Some of the boreholes penetrated both the unconfined and confined aquifers systems. The drillers' logs were used to check and correlate the lithological properties and phreatic zone thickness across the study area. Lithologies above the shallow water table were strictly targeted for analysis.



Figure 4.10: Selected sampling sites across the Dahomey Basin

### 4.3.2.2 Laboratory Analysis

This stage involved the laboratory testing of sediments to determine grain sizes and hydraulic conductivity ( $K$ ). The GSA test was performed to determine the percentage of different grain sizes present within a soil. The mechanical sieve analysis was used to perform this experiment. It determines the distribution of the sands (coarse, medium, fine sand), silt and gravel. Finer percentage is plotted against grain sizes (mm) on a log-log graph to generate the soil distribution curves. The GSA was determined according to the specifications of Fishers Scientific US Standard series ASTM E-11. The GSA is grouped according to the formation in the basin, Abeokuta Formation (ABK), Ewekoro Formation (EWE), Ilaro Formation (ILA), Oshosun Formation (OSH) and Coastal Plain Sand (CPS).

### 4.3.2.3 Empirical Determination of Hydraulic Conductivity

Hydraulic conductivity ( $K$ ), which is a measure of soil permeability, was determined empirically from the GSA and experimentally using a permeameter. The empirical formula method employed in this research includes:

$$Hazen (1911) = K_{Hazen} = C (d_{10}^2) \quad \text{Equation 4.1}$$

$$Beyer (1964) = K_{Beyer} = \left[ \frac{g}{v} \right] C_b x (d_{10}) \quad \text{Equation 4.2}$$

$$Harleman et al. (1963) = \left( \frac{\rho g k}{\mu \gamma} \right), k = 6.54 x 10^{-4} x d_{10}^2 \quad \text{Equation 4.3}$$

$$\text{Matthess \& Ubel (2003) = } K = 0.00357 \times d_{50}^2 \text{ (Seelheim 1880, after Matthes \& Ubell 2003)} \quad \text{Equation 4.4}$$

$$Breyer (1964) = K = \frac{g}{\gamma} x 6.0 x 10^{-4} \log_{10} \frac{500}{U} d_{10}^2 \quad \text{Equation 4.5}$$

$$C_u = \frac{d_{60}}{d_{10}} = \text{Coefficient of Uniformity} \quad \text{Equation 4.6}$$

Where:

$C_u$  = dimensionless coefficient based on grain size and sorting character

$K$  = hydraulic conductivity

$d_{10}$  = grain diameter (cm) of the 10% fraction of the grain size distribution

$d_{50}$  = grain diameter (cm) of the 50% fraction of the grain size distribution

$d_{60}$  = grain diameter (cm) of the 60% fraction of the grain size distribution

$C_b$  = a coefficient defined as  $6.0 \times 10^{-4} \times \log_{10} (500/C_u)$

$\rho$  = density of the fluid water = (1)

$\mu$  = viscosity of the fluid water (0.01 g/cms).

$g$  = acceleration 9.8 m/s or 980 cm/s<sup>2</sup>

$$U = (d_{60}/d_{10}) = \text{Uniformity}$$

*Equation 4.7*

C = a factor which depends on a uniformity (U) modified version of Beyer (1964) after Holting 1996 (Table 4.6).

Table 4.6: Range of uniformity and coefficient value

U	C
1.0–1.9	$110 \times 10^{-4}$
2.0–2.9	$100 \times 10^{-4}$
3.0–4.9	$90 \times 10^{-4}$
5.0–9.9	$80 \times 10^{-4}$
10.0–19.9	$70 \times 10^{-4}$
>20	$60 \times 10^{-4}$

Other empirical formulas which can be used, as well as their disadvantages, include Fair and Hatch (1933) and Kozeny-Carman (1956). They were designed for a uniformly graded soil with serious drawback for clay. These drawbacks include: no pores are sealed off, pores are distributed at random and pores are reasonably uniform in size.

#### 4.3.2.4 Estimation of Hydraulic Conductivity by Permeameter

There is no universal acceptable way of determining hydraulic conductivity, but experimental measurements can be obtained in the laboratory. Dirksen (1999b) states that measurements of hydraulic properties can be made in the laboratory, unless there are overriding reasons to perform them in-situ. This will include the presence of strongly layered soil profile, large unstable structural elements and an abundance of stones. Vogel and Roth (2001) put forward that direct measurements of the hydraulic functions are only feasible on the scale of core samples treatable in the laboratory. Laboratory measurements may however be affected by hydraulic effects not present in the field (Munoz-Carpena *et al.*, 2002). Hydraulic conductivity determined with the permeameter is the saturated hydraulic conductivity ( $K_{sat}$ ).

The fundamental principle and physical description of groundwater flow in any medium is based on Darcy's law (Hubert, 1956). The premises for Darcy's law to be successful are:

- That flow is laminar, no turbulent.
- That the medium is fully saturated.
- That flow is in a steady state, with no temporal variation.

The  $K$  can in principle be obtained in the laboratory either through hydrostatic, steady-state or transient state flow systems. In steady state flow, the flux, gradient and water content are constant in time, whereas they vary in transient flow systems. Hence, measurements based on steady state flow are more convenient and more accurate (Hillel, 1998). The laboratory set-up for this experiment mirrored the steady state flow (Figure 4.11a) and followed the description of Klute and Dirksen (1986) and Dane and Topp (2002). The  $K_{sat}$  was also determined experimentally with the use of Impact brand SL305 which combined constant and falling head permeameter.

The  $K_{sat}$  was measured by applying constant hydraulic head differences across the sample and measuring the resulting steady flux of water. Soil samples were saturated in the permeameter pressure chamber after applying a vacuum of approximately 20 inches Hg (33.5 kPa) for fifteen minutes, which was done to remove trapped air in the specimen and voids (Figure 4.11a). After evacuation, water gradually saturates the vacuum in the chamber and passes the outlet into a cylinder until a steady flow condition is established. After obtaining equilibrium flow conditions, a measurement and time of a given quantity of water to flow through the chamber was taken. Hydraulic conductivity was derived using the following equation:

$$K_{sat} = \frac{QL}{Ath}$$

*Equation 4.8*

Where:

$K_{sat}$  = Coefficient of saturated hydraulic conductivity (cm/s)

$Q$  = Quantity of water discharge in ml

$L$  = Length of sample in cm

$t$  = Total time for discharge in seconds

$h$  = Vertical distance between funnel overflow and chamber outflow port in cm

$A$  = Area of cross section of specimen = 31.65 cm<sup>2</sup>

It should be noted that these laboratory techniques is best suited for measurement of undisturbed soil cores samples as shown in Figure 4.11 from the field. This is compared to the measurement of fragmented and artificially packed samples even though controversies on repacked soils remained unresolved (Lebron and Robinson, 2003). There is, however, no field technique available to truly provide strictly undisturbed samples and the type of sediment will also dictate the sampling techniques.

#### **4.3.2.5 Porosity Determination**

Porosity of soil or rock can be defined as the fraction of a given volume of material that is occupied by void space or interstices. Porosity is usually expressed as the ratio of volume of voids  $V_v$  to the total unit volume  $V_t$  of a soil or rock such that

$$n = \frac{V_v}{V_t}$$

*Equation 4.9*

Where

$n$  = the porosity

$V_v$  = the void in the soil or rocks

$V_t$  = the total volume of soil or rocks



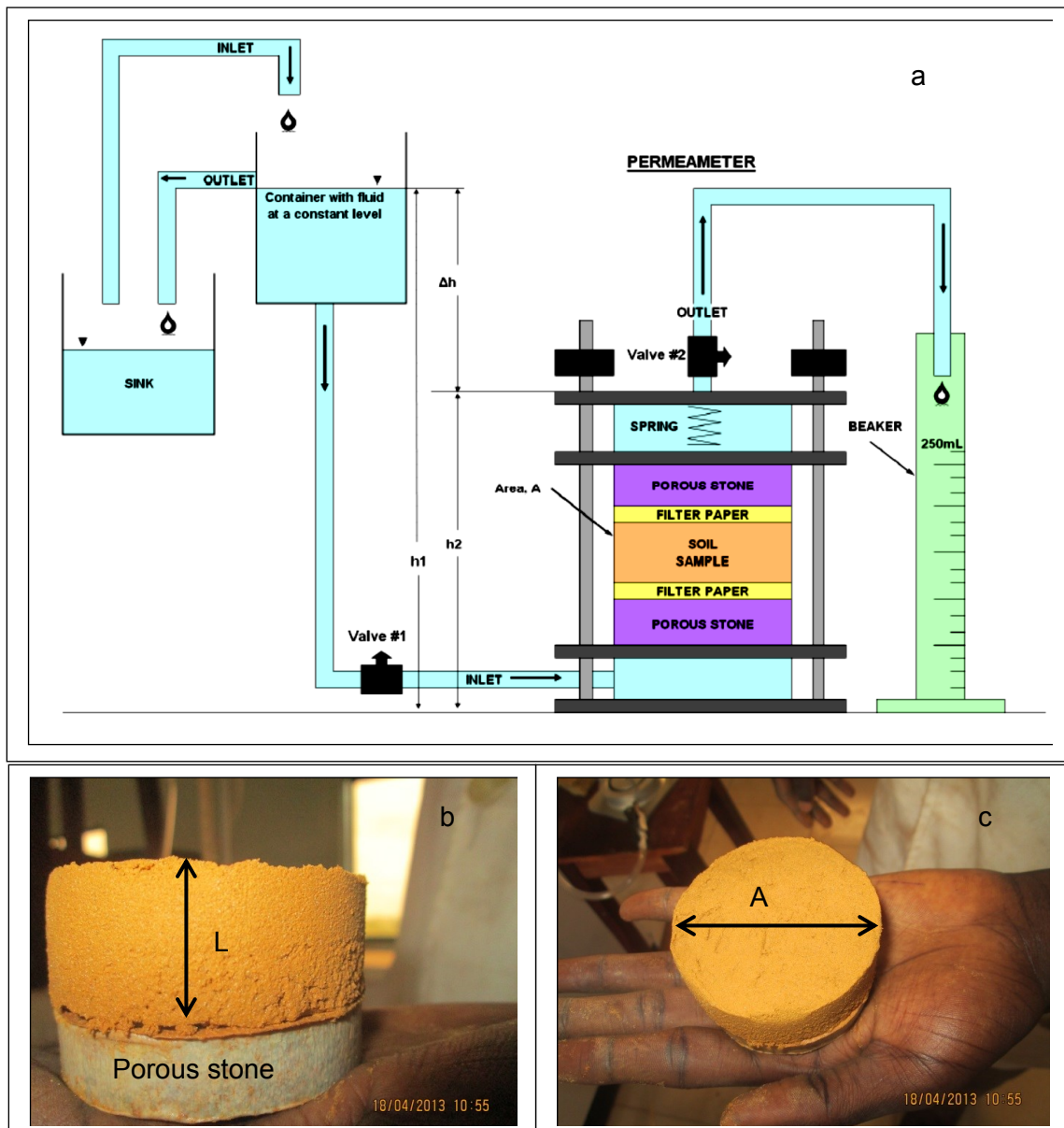


Figure 4.11: (a) Schematic diagram of permeameter experimental set-up; (b) length of core sample  $L$ ; (c) Cross sectional area  $A$

Porosity was determined with the oven dry method. This occurred after the known quantity of soaked soil samples were oven dried at  $25\text{ }^{\circ}\text{C}$  and the weight was determined before and after oven drying. Most rocks and soil sediments usually contain voids that are either filled with air or water, or both. Therefore, three void conditions are possible: dry, partially saturated and saturated voids. In aquifer vulnerability studies the vadose layer porosity is assumed to be filled with water, which is the major transport of contamination. The volume of water that fills pores are controlled by the shape and arrangement of the grains, degree of sorting, compaction, cementation, degree of pore connectivity, fracturing and solution weathering. Further analysis in this study involved the use of a Scanning Electron Microscope (SEM) and optical microscopes to identify the grain shape, which is another important factor for water movement in the vadose zone characterisation.

### 4.3.3 Grain Size Analysis

GSA is one of the best methods to classify the textural property of the vadose zone structure. Unconsolidated sediments such as those in the study area consist of a wide range of particle sizes ranging from gravel to sand, and silt and clay. Soil with flattened and smooth distribution curves which cuts across particles sizes without discontinuity are widely termed well-graded and poorly sorted soil. Soil with preponderance of a single particle size, mostly those indicating a step like distribution curve, are known as uniformly graded and well-sorted. For a better interpretation, the GSA results will be discussed according to the formations.

#### 4.3.3.1 Abeokuta Formation (ABK)

The ABK Formation sediments are mainly of coarse texture, poorly graded and well-sorted, except for ABK B (Figure 4.12). This lithological layer is well-graded and poorly sorted. The texture cuts across the gravel, sand, silt and clay texture range. The attenuation of the layer ABK B to vulnerability is greater than that of the other layers, especially layer ABK C that has a larger gravel percentage of 55%. This is because the pore spaces within the large particles of gravel are filled with sand, silt and clay.

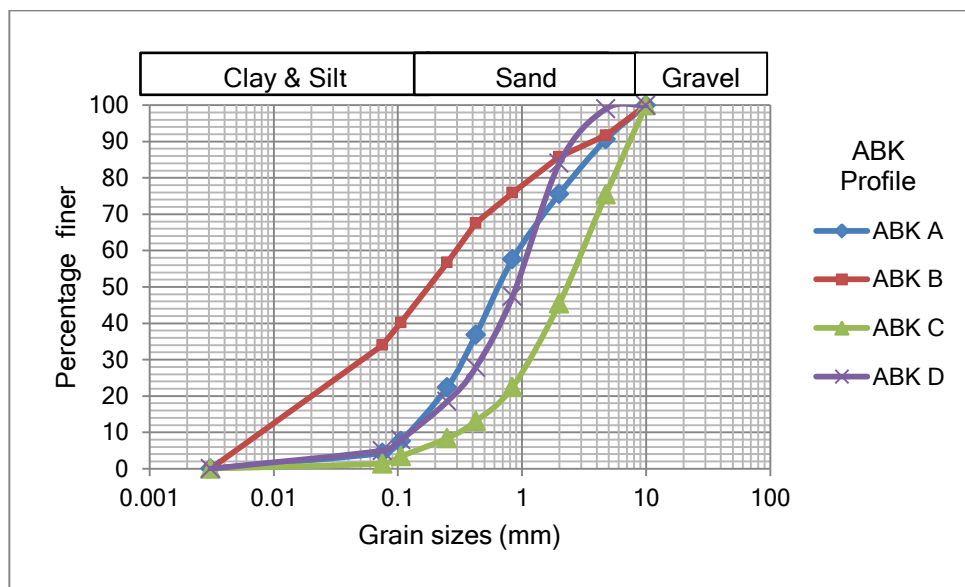


Figure 4.12: Grain size distribution and sediment textural characteristics of the Abeokuta Formation

#### 4.3.3.2 Ilaro Formation (ILA)

The ILA Formation is distinct quartz rich sandy estuarine to deltaic and continental coarse sediment (Jones, 1964). The grain sizes indicate sandy classes of 49–54% coarse, 21–22% medium grain and 19–20% fine to very fine. These lithological layers have no clay presence (Figure 4.13). The sediments are well-sorted and uniformly graded. The contaminants attenuation capacity is expected to be weak, while the soil lithologies show similar textural characteristics.

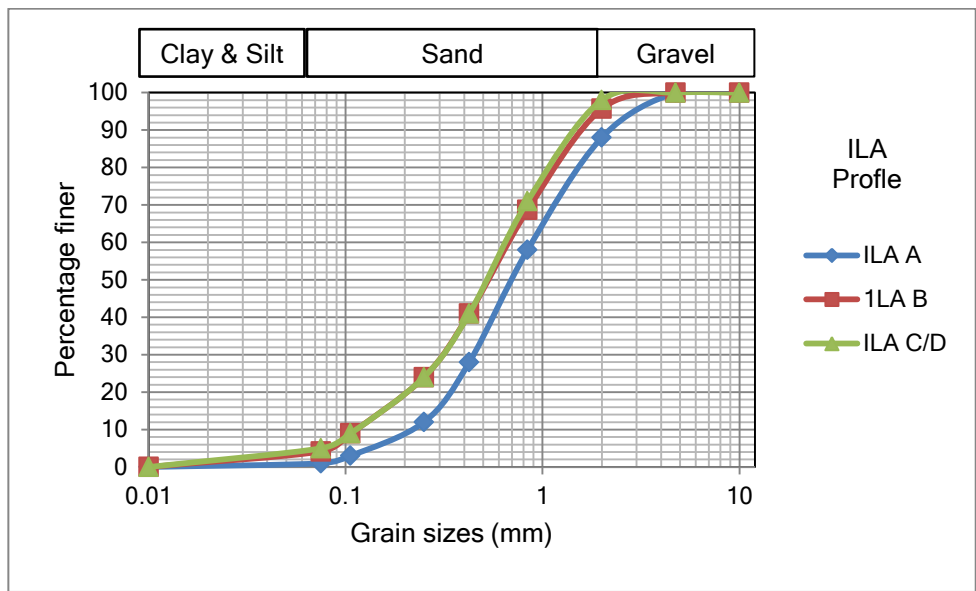


Figure 4.13: Grain size distribution and sediment textural characteristics of the Ilaro Formation

#### 4.3.3.3 Oshosun Formation (OSH)

The Oshosun Formation sediment is represented by OSH. The Ilaro Formation overlies the formation, but unlike estuary and deltaic environment of ILA, OSH is of marine environment (Adegoke, 1969). The formations textural characteristics are also para-cyclic between fine to medium and coarse grain sizes; 53% of lithology A (Figure 4.14) is fine grained sand, while 46% of lithology B is coarse grained sand, with the presence of silt and clay particles. The majority of the sand range of lithology C and D are fine to medium sand grain with 40–58%, respectively.

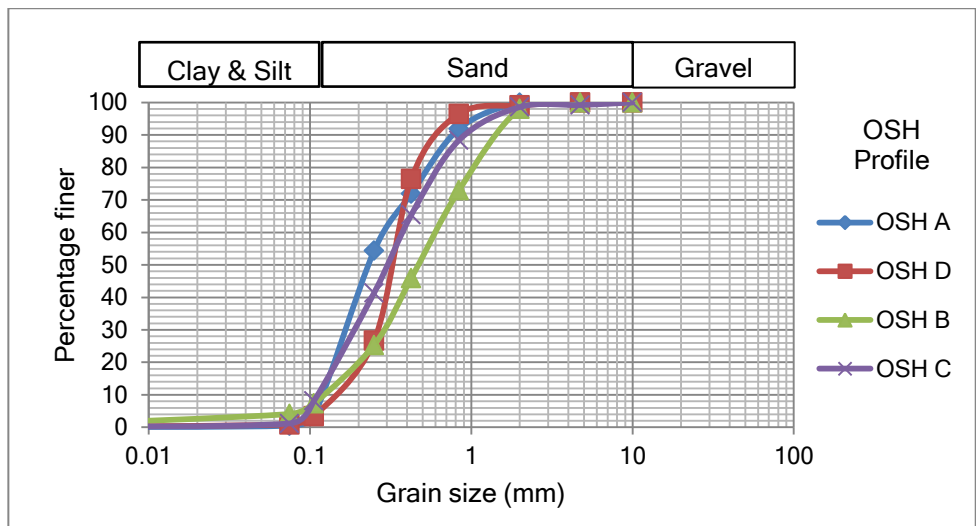


Figure 4.14: Grain size distribution and sediment textural characteristics of the Oshosun Formation

#### 4.3.3.4 Coastal Plain Sand (CPS)

Sediment texture ranges for the CPS vadose zone are generally well-graded and poorly sorted. The sand composition ranges from 84–92%, clay from 1–8%, silt from 2–5%, while gravel range from 2–6%. The sand clast majority are characteristically different from lithology to lithology.

CPS A is fairly distributed between fine, medium and coarse grain sand sizes with values of 31%, 23% and 38%, respectively. CPS B and C display 30%, 35%, 28%, 32%, 21% and 31% for fine, medium and coarse grain sand, respectively. The lithology CPS D consists more of medium grain sizes of 52%, while fine and coarse grains record 10% and 28%, respectively (Figure 4.15). Observation from the field shows the CPS D as the water filled upper level of the unconfined aquifer overlying the main aquiferous lithology CPS E (Figure 4.20).

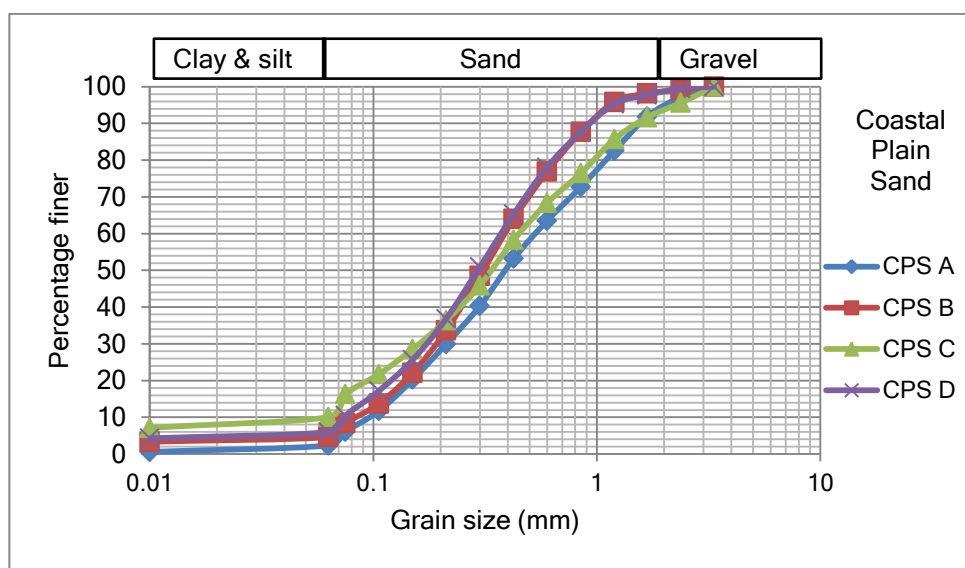


Figure 4.15: Grain size distribution of the Coastal Plain Sand

#### 4.3.3.5 Ewekoro Formation

Figure 4.16 shows the percentage distribution of different vadose lithologies in the Ewekoro Formations in the Dahomey Basin. Well-graded sediments tend to have a lower porosity and therefore have lower permeability than uniformly graded sediments. This is because there are fewer finer particles to fill pore spaces between larger particles. For silt–clay sizes, the particles, and the pore spaces between them, are very small and permeability is very low. This slows movement of water. Unlike uniformly distributed sand with bigger particle sizes and larger pore spaces between them, they tend to have higher permeability and faster water movement.

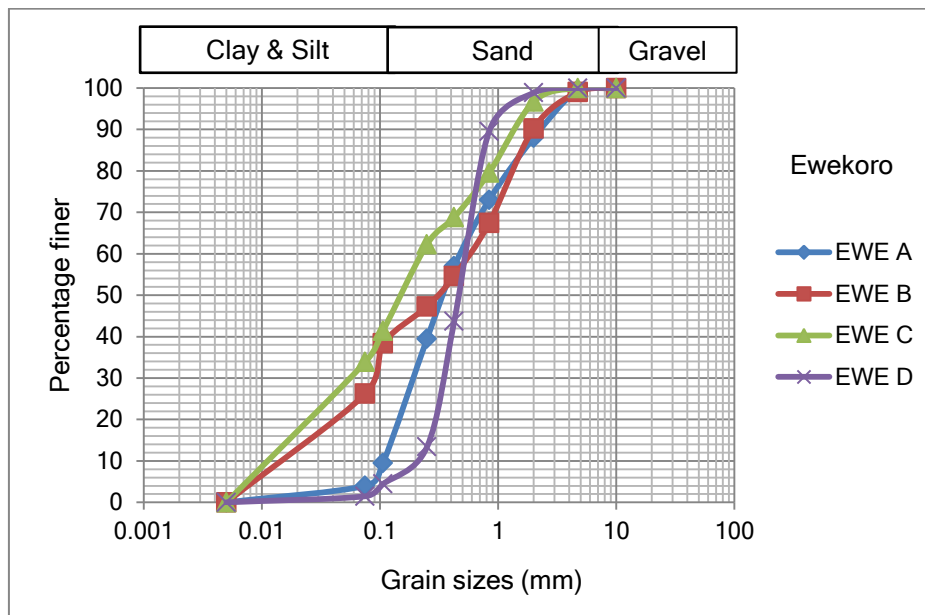


Figure 4.16: Grain size distribution and sediment textural characteristics of the Ewekoro Formation

The Ewekoro Formation, which is predominantly limestone and glauconitic rocks, presents a complicated unit of rock sequence to most stratigraphers (Adegoke, 1977). Lithology was lumped with the thickly bedded shale sequence overlying the formation. The shale is impermeable to fluid with an average thickness of 18 m and 8–9 m at some type locality (Kogbe, 1976). However, percolating groundwater is stored on the pure grey, gritty sand lacking red mottling, and white little clay overlying the shale. In addition, the limestone formation further north is devoid of this shaly formation and allows the infiltration of water. The lithology EWE B and C consist of the most finely grained materials of 7%, 17%, 66%, 2%, 30% and 65% for clay, silt and sand materials, respectively. Table 4.7 shows the complete range of particles sizes and percentages present in the formation, while Figure 4.17 displays the percentage of gravel, sand, silt and clay that make up the composition of each lithology under study.

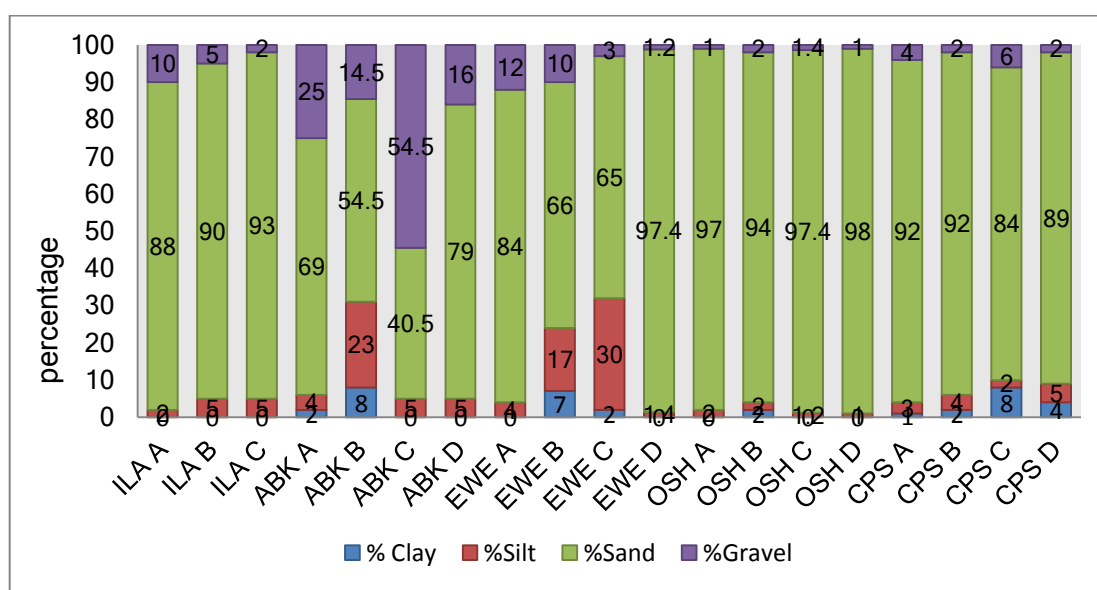


Figure 4.17: Textural percentage classification from lithology of the Dahomey Basin

Table 4.7: Grain size classification of the Dahomey Basin vadose sediment

	Depth (m)	Clay	Fine Silt	Medium silt	Coarse silt	V.Fine sand	Fine sand	Medium sand	Coarse sand	V.coarse sand	Gravel	% Clay	%Silt	%Sand	%Gravel	Soil Type
RANGE		0.0039	0.0039–0.0156	0.0156–0.031	0.031–0.0625	0.0625–0.125	0.125–0.25	0.25–0.5	0.5–1.0	1.0–2.0	2.0–4.0					
ILA A	3	-	-	-	2	4	8	22	30	24	10	0	2	88	10	Sand
ILA B	8	-	-	2	3	5	15	21	28	21	5	0	5	90	5	Sand
ILA C/D	15	-	-	2	3	5	14	22	32	20	2	0	5	93	2	Sand
ABK A	5	2	1	1	2.	3	13.5	21.5	18	13	25	2	4	69	25	Sand
ABK B	25	8	8	8	7	11	14.7	13.3	8	7.5	14.5	8	23	54.5	14.5	Sandy clay loam
ABK C	45	-	1	2	2	3	0.4	6.6	12	18.5	54.5	0	5	40.5	54.5	Sand
ABK D	60	-	-	2	3	4	9.5	13.5	22	30	16	0	5	79	16	Sand
EWE A	5	-	-	2	2	6.5	29	23.5	13	12	12	0	4	84	12	Sand
EWE B	12	7	4	3	10	16	7.3	10.7	12	20	10	7	17	66	10	Sandy clay loam
EWE C	20	2	5	12	13	10	20.3	8.7	11	15	3	2	30	65	3	Sandy loam
EWE D	27	-	-	-	1.4	4.6	7.4	34.6	46	4.8	1.2	0	1.4	97.4	1.2	Sand
OSH A	5	-	-	-	2	3	49.4	23.6	16	5	1	0	2	97	1	Sand
OSH B	10	2	-	1	1	4	17	27	26	20	2	2	2	94	2	Sand
OSH C	17	-	-	-	1.2	7.8	32.4	30.6	20	6.6	1.4	0	1.2	97.4	1.4	Sand
OSH D	25	-	-	-	1	3	22.7	58.3	13	1	1	0	1	98	1	Sand
CPS A	2	1	-	1	2	10	21	23	20	18	4	1	3	92	4	Sand
CPS B	7	2	1	1	2	8	21	35	22	6	2	2	4	92	2	Sand
CPS C	11	8	-	1	1	13	19	21	19	12	6	8	2	84	6	Loamy sand
CPS D	15	4	1	3	1	9	20	32	22	6	2	4	5	89	2	Loamy sand

#### 4.3.4 Textural Characteristics

The textural properties of sediment from the lithology of the Dahomey Basin were derived from the GSA, as discussed above. The percentage of clay, silt and sand contained in each lithology as calculated from the GSA is plotted and shown in Figure 4.18. The majority of the lithology is of sand clast texture, except for EWE B, EWE C, ABK B, CPS C and CPS C. EWE B and ABK B are of sandy clay loam, while EWE C is of sandy loam. The difference in these two classes is the amount of clay present in them. Clay particles serve as the greatest hindrance to groundwater pollution because of its high porosity and low permeability. The sandy clay loam contains more clay than sandy loam, and is therefore better in aquifer attenuation capability, provided other physical properties such as hydraulics, infiltration and thickness of the unsaturated zone are right. Loamy sand contains clay and silt percentages lower than the sandy loam and sandy clay loam. The order of soil attenuation capacity from soil textural classification is therefore sandy clay loam > sandy loam > loamy sand > sand.

Water-holding capacity in soil is another important factor in soil attenuation capacity. Soil water-holding capacity is determined by soil texture and structure. A decrease in water-holding capacity is significant in sandy soils with large pore openings, because it increases infiltration, which supports faster contaminant migration. Soil that is impermeable to percolation and subsequent infiltration allows water to stay in contact with the topsoil or subsoil for a longer period, provided there is no surface run-off. This allows soil micro-organisms to work on the percolating contaminated water. Well-graded soils reduce infiltration and possibly reduce contaminated water that may pollute groundwater resources.

The amount of water passing through any particular soil is predominantly influenced by soil texture and structure. The soil texture and structure governs the size of the pore spaces that in turn controls how tightly the water is bound. For any given rain event, heavy soils made up of fine grained, clay or silt-sized grains will retain more water due to reduced permeability. This reduces the effect of contaminated water infiltration compared to a thin, free draining soil such as the coarse and gravelly sandstones.

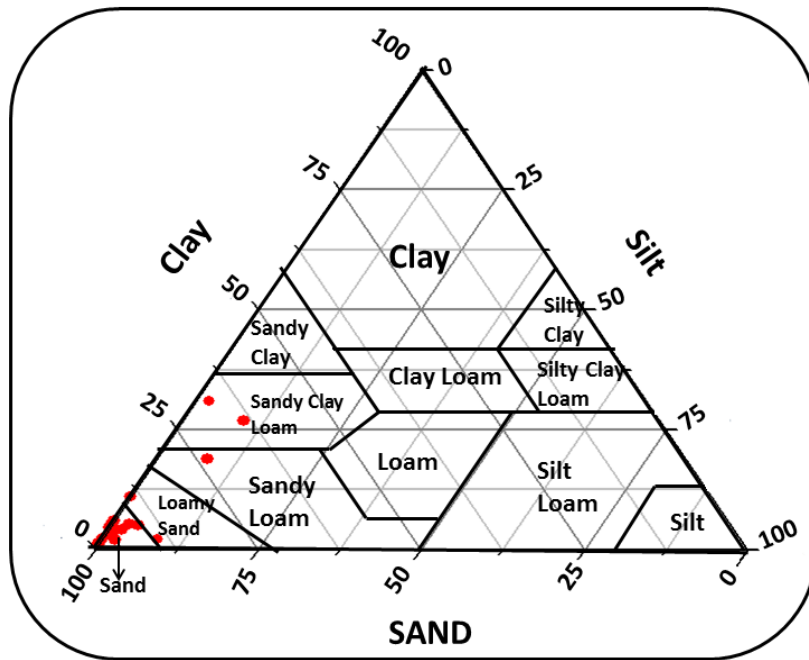


Figure 4.18: Textural classification of sediment from the Dahomey Basin

### 4.3.5 Hydraulic Conductivity Estimation from Grain Size Analysis and Permeameter

The  $K$  of the Dahomey basin sediment will be discussed under two laboratory scenarios. These scenarios are the grain size analysis (GSA) and  $K_{sat}$  estimate from a permeameter test.

#### 4.3.5.1 Grain Size Analysis Derived Hydraulic Conductivity

Determination of  $K$  from the GSA is an empirical method of estimating the rate of pore fluid movement. For an easy description and determination of the Dahomey Basin vadose zone  $K$ , the GSA was grouped according to their lithology and grain size property, as described in the methodology. This was after observations of stratigraphic and lithological order of the sediment deposition. It is important to calculate the saturated  $K$  of the vadose zone, because for attenuation of any contaminated water to occur, the lithological layers must contain attenuation capability, which include the  $K_{sat}$  parameter. Aside from the vadose zone  $K$ , the thickness of the vadose layers, the size and arrangement of its soil particles (pore size distribution and grain size distribution) are the physical parameters that largely determine how water traverses in any particular soil.

Figure 4.19 shows the hydraulic conductivities derived from these empirical methods using the GSA. The result indicates that the Hazen (1911), namely the  $K_{Hazen}$  method, shows the upper limit  $K$ , while the lowest  $K$  was derived from the Seelheim (1880) after Matthes and Ubell (2003), namely the Matthes & Ubell Hydraulic Conductivity ( $K_{m\&u}$ ). The differences in their  $K$  are due to the grain size distribution and sorting character.  $K_{Hazen}$  is too large and the  $d_{10}$  grain size percentile (Table 4.10) is non-uniform, unlike the  $d_{50}$  grain distribution and



sorting character advanced by the methods of  $K_{m\&u}$ . The uniformity of values  $d_{50}$  as used in  $K_{m\&u}$  is shown in Figure 4.19.

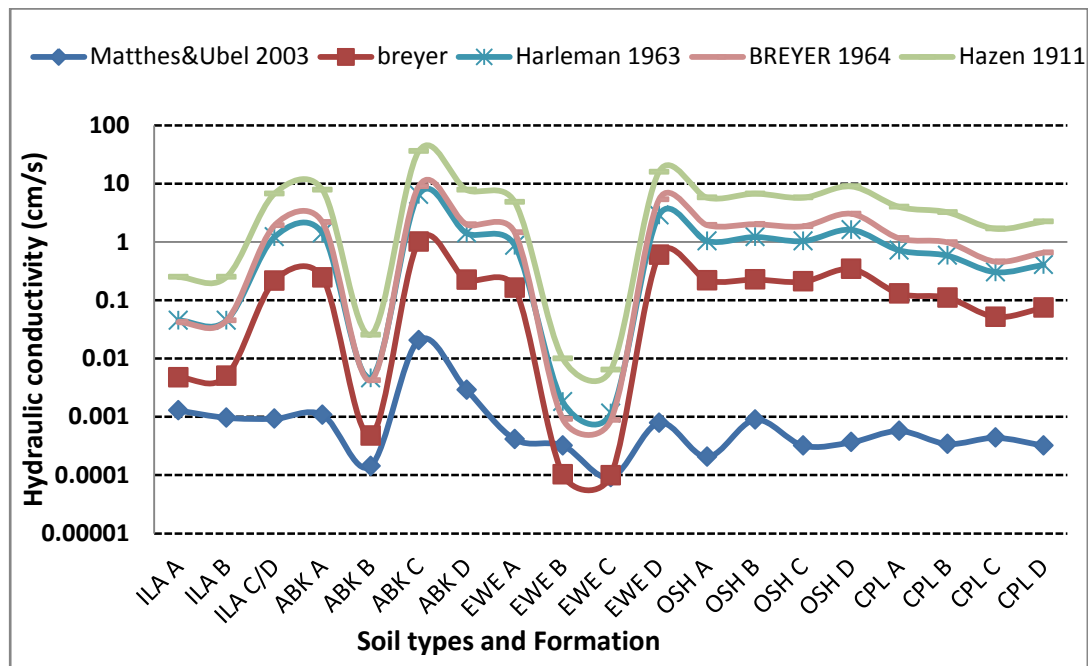


Figure 4.19: Empirical hydraulic conductivities derived from GSA for vadose lithology

Estimated  $K_{m\&u}$  values have a closer correlation with the estimated values of Fetter (2001) as presented in Table 4.8. (See the sediment type of each formation in Table 4.7). The  $K$  of the Dahomey Basin differs with few magnitudes of difference, but within the proposed range of Freeze and Cherry (1979) and Dominico and Schwartz (1990) which was documented in metre per second. The empirical method of Harleman *et al.* (1963) includes the perspective of intrinsic permeability ( $k$ ) with a fixed value ( $k = 6.54 \times 10^{-4} \times d_{10}^2$ ). Harlemans *et al.* (1963) method is, however, valid for materials of very uniform particle sizes and shapes (Figure 4.19).

Table 4.8: Hydraulic conductivity of selected sediments

Material or sediment type	Fetter 2001 (cm/s)	Dominico & Schwartz 1990 (m/s)	Freeze and Cherry 1979 (cm/s)
Well-sorted gravel	$10^{-2}$ –1	$10^{-4}$ – $10^{-2}$	$10^{-1}$ –100
Well-sorted sands	$10^{-3}$ – $10^{-1}$	$10^{-7}$ – $10^{-3}$	$10^{-4}$ –1
Silty sands, fine sands	$10^{-5}$ – $10^{-3}$	$10^{-7}$ – $10^{-4}$	$10^{-5}$ – $10^{-1}$
Silt, sandy silt, clayey sands	$10^{-6}$ – $10^{-4}$	$10^{-9}$ – $10^{-5}$	$10^{-7}$ – $10^{-3}$
Clay	$10^{-9}$ – $10^{-6}$	$10^{-11}$ – $10^{-9}$	$10^{-10}$ – $10^{-6}$

Possible vulnerability implications of the derived hydraulic conductivity from GSA is that lithology of the EWE formation, particularly EWE B and EWE C, has the lowest hydraulic conductivity (including the  $K_{Hazen}$  and  $K_{m\&u}$ ). This is due to the high amount of clay that is present in these lithologies (Table 4.8). This means that the EWE B and C lithology is expected to have a low aquifer vulnerability potential based on hydraulic conductivity. This

does not necessarily translate to low hydraulic conductivity when the lithological average is considered. EWE lithological profile average gives 0.0035 cm/s in the  $K_{m&u}$ , while the lowest  $K$  for the  $K_{m&u}$  is the OSH and CPS with 0.00046 and 0.00042 cm/s, respectively. This implies longer vertical infiltration and lower vulnerability while ABK and ILA record the highest hydraulic conductivity for  $K_{m&u}$  with 0.0061 and 0.001 cm/s respectively. This also implies to faster vertical infiltration of water when other infiltration parameters are considered.

A slightly different scenario, however, plays out for the  $K_{Hazen}$  hydraulic conductivity calculation, which is the upper limit among the formulae, used in the hydraulic conductivity empirical calculation methods. Unlike the  $K_{m&u}$  where the ILA records the highest hydraulic conductivity,  $K_{Hazen}$  of ILA lithology records the lowest  $K$  of 2.42 cm/s (Table 4.9). The highest  $K$  values were recorded for OSH with 9.03 cm/s and ABK with 12.9 cm/s, respectively. Similarities in these two extreme values, namely upper and lower empirical  $K$ , is that ABK lithology in both scenarios was high and that CPS  $K$  was low. However, it should be noted (as stated earlier) that the reason for the differences in these two extreme scenarios (upper and lower limit) was in the percentage of grain size values used in their formulae computation. Further highlight on the differences will be discussed in the limitations of the methods.

Table 4.9: Average hydraulic conductivity values of the formations

Lithology/Formation	$K_{Hazen}$ (cm/s)	$K_{m&u}$ (cm/s)
ILA	2.42	0.001
EWE	5.21	0.0035
ABK	12.9	0.0061
OSH	9.03	0.00046
CPS	2.79	0.00042

Also of note are the topsoil influence and the impact of soil compaction on the infiltration front and saturated hydraulic conductivity (this is very important and will be discussed in Chapter 5). Water movement tends to flow along the easiest path which sometimes could be horizontal rather than vertical. Particle sizes may also play a role in horizontal infiltration of water in the vadose zone. The bigger the particle sizes, the larger the pore spaces, and the higher the  $K_{sat}$ , while the finer and smaller the particle sizes, the lower the pore spaces and lower the  $K_{sat}$ .

$K$  may also tend to be slower due to sediment consolidation and compaction, as water infiltration percolate the topsoil and spread to lower lithology (Adams and Foster, 1991; Robins, 1998). This may sometimes vary depending on the sedimentary covers with layers of different deposition and sediments. The rate of  $K$  in the lithology under study, namely  $K_{sat}$  of the infiltrating front in aquifer vulnerability estimations, however, also depends on the thickness of its vadose zone.

#### 4.3.5.2 The Impact of Coefficient of Uniformity

Coefficient Uniformity (Cu) is defined as the homogeneity of sediments (Kasenow, 2002). Table 4.10 displays the particles size diameter and its Cu for the lithology of the Dahomey

Basin. Large Cu corresponds to a large range in particle sizes (poorly sorted or well-graded), while a small Cu coefficient corresponds to well-sorted or poorly graded material (Kasenow, 2002). With a Cu of 1, it means a perfectly sorted material. When Cu is well-sorted and poorly graded its ability to reduce contaminant migration, which is the target in aquifer vulnerability estimation, is reduced. EWE B shows the highest Cu value of 120 (Table 4.10). EWE B is texturally a sandy clay loam, namely it contains appreciable clay particles (Table 4.7) with ABK B and EWE C. These lithologies have higher Cu values compared to other lithologies.

The higher the coefficient of unconformity, the more irregular the pore spaces generally are. This means a high specific inner surface area and higher tortuosity with higher irreversible water content leading to low effective porosity, which means low hydraulic conductivity and therefore low aquifer vulnerability (Kirsh and Hinsby, 2006). *This experimental empirical hydraulic conductivity analysis has determined that the finer grain sizes sediment present in a lithology, the more its influence on hydraulic conductivity, and hence the better its ability to retard contaminant in aquifer vulnerability studies.*

Table 4.10: Percentile values of lithology of the Dahomey Basin sediment

Lithology	Sampling depth (m)	10	20	30	40	50	60	70	80	90	100	Cu = $d_{60}/d_{10}$
ILA A	3	0.025	0.35	0.4	0.52	0.6	0.9	1.03	1.06	1.11	1.35	36.00
ILA B	8	0.025	0.2	0.32	0.41	0.52	0.76	0.84	1.04	1.06	1.3	30.40
ILA C/D	15	0.13	0.2	0.33	0.43	0.51	0.75	0.86	1.02	1.05	1.2	5.77
ABK A	5	0.14	0.22	0.35	0.4	0.55	0.9	1.6	2.7	4.8	9	6.43
ABK B	25	0.008	0.02	0.06	0.15	0.2	0.3	0.45	1.2	4.5	10	37.50
ABK C	45	0.3	0.75	1.3	1.8	2.4	3	4	5.5	7	10	10.00
ABK D	60	0.14	0.3	0.47	0.7	0.9	1.3	1.5	1.8	2.6	4.5	9.29
EWE A	5	0.11	0.16	0.19	0.26	0.34	0.5	0.7	1.3	2.4	5	4.55
EWE B	12	0.005	0.05	0.09	0.13	0.3	0.6	1	1.5	2	5	120.00
EWE C	20	0.004	0.035	0.06	0.11	0.16	0.23	0.5	0.85	1.5	2.5	57.50
EWE D	27	0.2	0.3	0.35	0.4	0.47	0.54	0.6	0.7	0.85	1.2	2.70
OSH A	5	0.12	0.15	0.17	0.2	0.24	0.3	0.4	0.55	0.8	2	2.50
OSH B	10	0.13	0.2	0.3	0.38	0.5	0.6	0.8	1.1	1.5	2.2	4.62
OSH C	17	0.12	0.15	0.2	0.25	0.3	0.38	0.5	0.62	0.9	2	3.17
OSH D	25	0.15	0.22	0.28	0.3	0.32	0.37	0.4	0.47	0.6	1.5	2.47
CPS A	2	0.1	0.016	0.21	0.3	0.4	0.54	0.8	1.2	1.6	3.2	5.40
CPS B	7	0.09	0.15	0.2	0.25	0.31	0.38	0.5	0.65	0.95	2.3	4.22
CPS C	11	0.065	0.095	0.17	0.25	0.35	0.45	0.65	1	1.6	3.5	6.92
CPS D	15	0.075	0.13	0.16	0.24	0.3	0.38	0.5	0.65	0.95	2.3	5.07

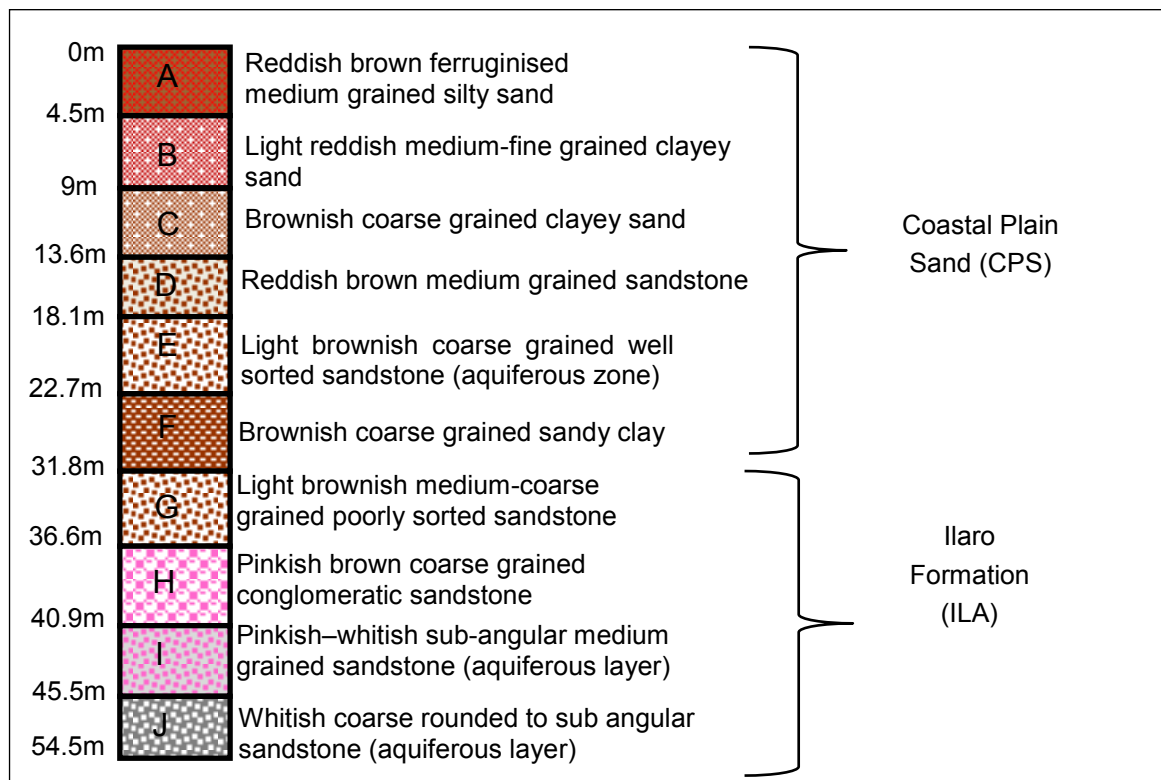


Figure 4.20: Lithological borehole profile cutting through the CPS and ILA Formation

#### 4.3.5.3 Permeameter Derived Hydraulic Conductivity

Laboratory permeameter hydraulic conductivity ( $K_p$ ) presented in Table 4.11 is a simulated laboratory  $K_{sat}$ , as explained in the methodology section. A comparison of the mean  $K_p$  and empirical  $K$  is shown in Figure 4.22 and Table 4.12 of the lithology under study. A good correlation exists between  $K_p$  and the empirical  $K$  for the EWE Formation. The correlation noted between  $K_p$ - $K_{Hazen}$  and  $K_p$ - $K_{Harleman}$  is 92%.  $K_p$ - $K_{breyer}$  and  $K_p$ - $K_{BREYER}$  show a correlation value of 90%, and EWE's lowest correlation was between  $K_p$  and  $K_{m\&u}$  with a correlation of 85%. The best correlation in the lithology of the Dahomey Basin (Figure 4.22) was noted in the ILA Formation (Table 4.12). Correlated values noted were the  $K_p$ - $K_{Hazen}$ ,  $K_p$ - $K_{Harleman}$ ,  $K_p$ - $K_{breyer}$  and  $K_p$ - $K_{BREYER}$  indicating 100%, while a low correlation was noted between  $K_p$  and  $K_{m\&u}$  with a correlation of 33%.

Table 4.11: Hydraulic conductivity values of the permeameter experiment and a comparison to empirical methods

Lithology/Formation	$K_p$ (cm/s)	$K_{Hazen}$ (cm/s)	$K_{m\&u}$ (cm/s)
ILA	0.0393	2.42	0.001
EWE	0.0073	5.21	0.0035
ABK	0.1261	12.9	0.0061
OSH	0.0217	9.03	0.00046
CPS	0.0105	2.79	0.00042

Table 4.12: Permeameter hydraulic conductivity ( $K_p$ ) correlation with empirical methods

Lithology	$K_{m\&u}$	$K_{breyer}$	$K_{Harleman}$	$K_{BREYER}$	$K_{Hazen}$
ILA	33%	100%	100%	100%	100%
EWE	85%	90%	92%	90%	92%
ABK	7.6%	1.2%	1.8%	10%	6%
OSH	71%	6%	20%	6%	20%
CPS	44%	10%	6%	10%	6%

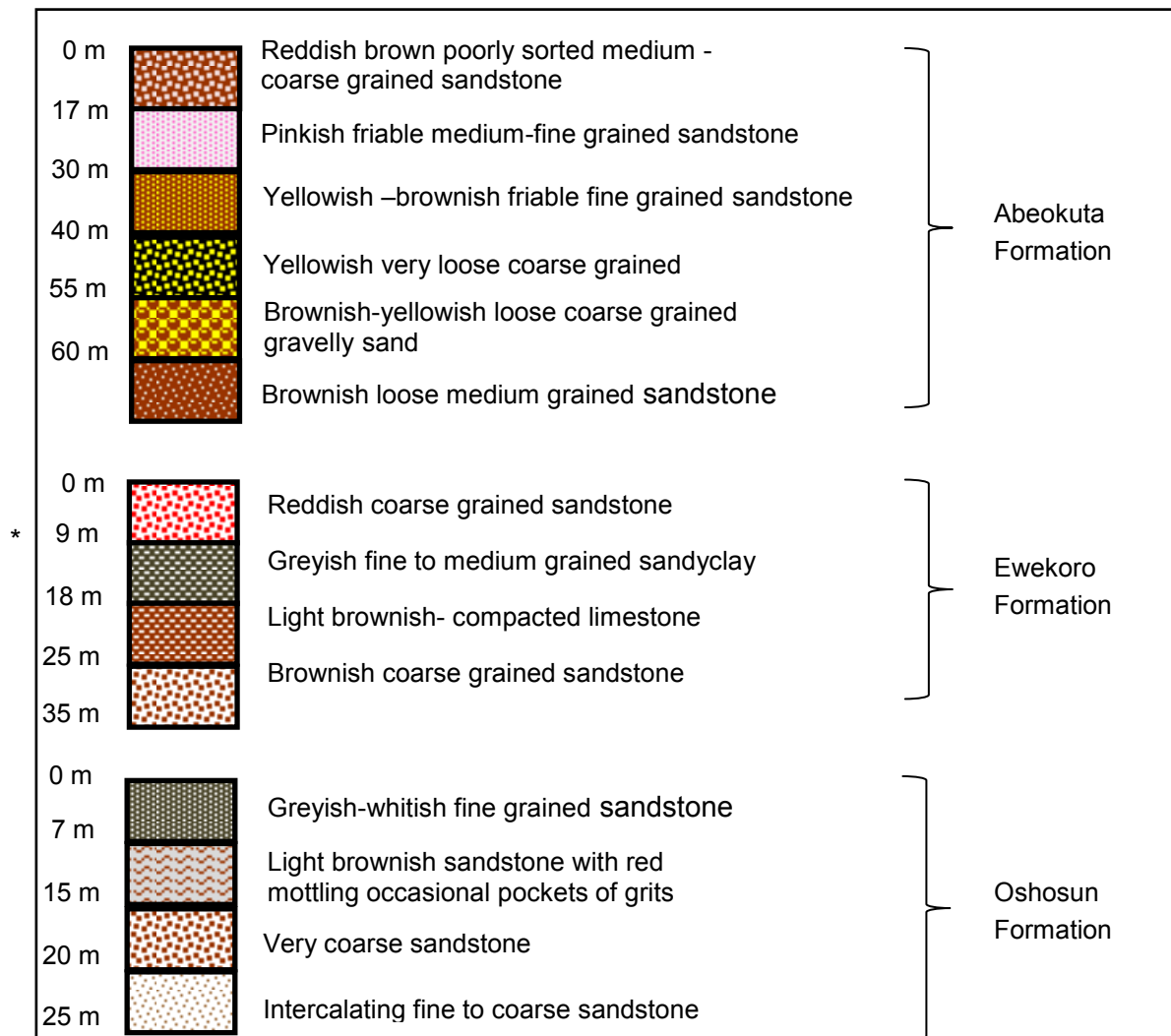


Figure 4.21: Lithological log of Ewekoro, Abeokuta and Oshosun Formations

The major reason for this low correlation in  $K_p$ - $K_{m\&u}$  is the uniformity in the grain size of ILA. ILA is a well-sorted sediment composed predominantly of coarse-medium sand (Figure 4.24 c-d).  $K_{Hazen}$  and  $K_{Harleman}$  has a better correlation, with the laboratory saturated  $K_p$  showing an influence of finer particles ( $d_{10}$ ) on  $K$ , unlike the  $K_{m\&u}$  that uses ( $d_{50}$ ) in its formula. However,  $K_{Hazen}$  cannot be relied on because of its outrageous values which is sometimes outside the documented values of the previous experiment.

Most of the soil in the Dahomey Basin are unconsolidated sediments. This means that some sediment firmness and consolidation are not strong enough for core sampling. The core samples were therefore principally carried out on consolidated samples. This, however, means that some unconsolidated samples were analysed and repacked before the experiment could take place. Among these samples is the sample of well-sorted sediment of the Ilaro and Oshosun Formations. Hydraulic conductivity ( $K$ ) based on grain size correlations is rough, but  $K$  from the permeameter results in this research is used as a benchmark in selecting the  $K$  from the GSA, and *vice versa*. Reynolds *et al.* (2000) noted that laboratory permeameter hydraulic conductivity ( $K_p$ ) can be used to calibrate or compare the  $K$  determined from other methods. This was done in the study.

The  $K_p$  will be used in the estimation of aquifer vulnerability in this study. The essence of calculating the different vadose sediment empirical hydraulic conductivity, however, suggests another easier, simpler and accurate way by which vadose  $K$  can be calculated in the Dahomey Basin for aquifer vulnerability studies. With the different empirical formulae used to calculate the empirical hydraulic conductivities,  $K$  of Matthes and Ubel (2006) has the best correlations with the permeameter  $K$  and the documented standard  $K$ . Therefore, GSA empirical derived  $K_{m&u}$  can be used by other researchers who cannot afford the hydraulic conductivity determination through the rigorous field and laboratory permeameter experiments in the study area. ABK, however, shows no close correlation between  $K_p$  and the empirical formula. This does not rule out the possibility of using empirical GSA for  $K$  determination in the ABK. It is advised that the intended researcher can use methods best fitted for the empirical formulae of hydraulic determination for the ABK.

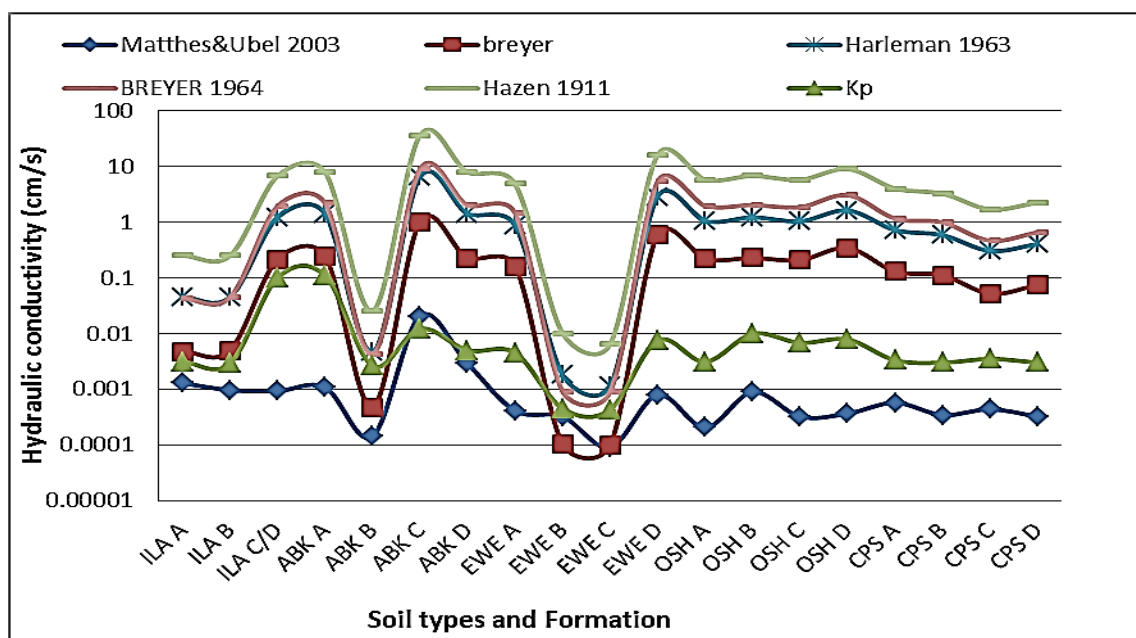


Figure 4.22: A comparison between permeameter hydraulic conductivity ( $K_p$ ) and empirical hydraulic conductivity

#### 4.3.5.4 General Limitations of Laboratory Hydraulic Conductivity

Hydraulic conductivity determined in the laboratory with the empirical methods and permeameter are not without some limitations. The major limitations that cause differences in the  $K$  values, as compiled by Vienken and Dietrich (2011) are:

- Grain size range.
- Level of uniformity ( $U = d_{60}/d_{10}$ ) which is a degree of heterogeneity of the sediments.
- Abundance of clay particles.
- Shape of particles (sand particles are largely rounded and clay particles are usually laminated).
- Empirical  $K$  is only applicable to soils that are similar in nature to those tested in the original study.
- Most samples used to develop the empirical values are not in-situ, and the samples may not be exactly representative, particularly for soils in the Dahomey Basin.

#### 4.3.5.5 Limitations and Strengths of the Breyer Method

- $K$ -unit was determined in m/s.
- Grain diameter  $d_{10}$  is in mm and is the most important parameter.
- The formula is best applicable to sediment of  $Cu < 20$ .  $K$  derived outside this limit is unreasonable. Therefore, it cannot be used for soils of EWE B, ABK B, ILA A and ILA B because the  $Cu > 20$ .
- It has been tested on the usefulness in correlating GSA and pumping tests.
- $K$ -values are too high and above the documented standard  $K$ . Therefore, it cannot be used in calculating aquifer vulnerability of the Dahomey Basin.

#### 4.3.5.6 Limitations and Strengths of the Hazen Method

- $K$ -unit is in m/d giving large unreasonable values when converted to cm/s.
- The most important parameter is  $d_{10}$  and it is measured in mm.
- The formula is applicable to sediments of  $Cu < 5$  and between sediment grains of 0.1 and 3.0 mm. This suggests that the Hazen Method is not suitable for ILA, ABK, CPS and EWE soils.
- It is best used on uniformly graded sand samples, but it can also be used for fine sand and gravel with uniformity of  $< 5$ .
- $K$  Hazen values cannot be used for the aquifer vulnerability test of the Dahomey Basin, because it is not reliable and above the documented standard  $K$ .

#### 4.3.5.7 Limitations and Strengths of Modified Seelheim by Matthes and Ubel Method

- $K$ -unit is in m/s and not cm/s, and the  $d_{50}$  is in mm.
- The most relevant parameter is the  $d_{50}$ ; this suggests a proper representation of sediments.
- It has no application range due to high diameter.
- It has been tested on sand, clay and chalk.

- Constant value of 0.00357 was used, but in the real sense, the value can only be applied to the original work it was developed for.
- The constant values also depend on some external factors not considered such as temperature, and secondary particle characteristics such as angular and surface roughness.
- $K$  derived by this method is within the range of the documented standard  $K$ . However, it is not the best  $K$  derived, but can be used by the researcher if the permeameter experiment cannot be used, however, the extra conditions such as change in grain sizes, level of uniformity and shape of the particles must be considered.

#### 4.3.5.8 Limitations and Strengths of Permeameter Hydraulic Conductivity

- Errors are introduced when replicating in-situ conditions, particularly for granular soils due to sample disturbance and stress changes.
- Most soils of the Dahomey Basin have weak cementing structures between the soil particles due to mineral deposits holding the structures together. The mineral deposits fill pore spaces, but break down when testing and can lead to erroneous results.
- The permeameter measurement is in cm/s.
- The method is still the best method of simulating the original field condition, because it involves core samples of representatives' lithology in its undisturbed form, and the resultant  $K$  from permeameter is within the range of many documented standard hydraulic conductivity. Therefore, the  $K$  permeameter will be used in this study for aquifer vulnerability evaluation.

#### 4.3.6 Porosity and Shape Estimation

The hydraulic conductivity is a function of both the porous medium structure and the flowing liquid. As grain size or sorting decreases, the proportionality between pore radii and porosity begins to fail, as does the proportionality between porosity and hydraulic conductivity (Kirsh, 2006). For example: Clays typically have very low hydraulic conductivity (due to their small pore radii), but also have very high porosities (due to the structured nature of clay minerals). This means clays can hold a large volume of water per volume of bulk material. They do, however, not release water rapidly and therefore have low hydraulic conductivity, which is good for contaminants attenuation.

Porosity is not a function of grain size, but rather grain size distribution. Porosity, however, decreases with an increase in grain sizes within unconsolidated sediments (Kirsh, 2006). For a proper classification of porosity in non-uniform soils, the sorting plays an important role. Well-sorted (poorly graded) material is highly porous compared to poorly sorted (widely graded) material, because small particles can fill the pore spaces between the larger particles, and by doing so reduces porosity and groundwater movement. Therefore, porosity of well-sorted material is higher than porosity of poorly sorted material.  $C_u$  has the greatest effect on porosity, as porosity increases with an increase in  $C_u$  (Kasenow, 2002).



Table 4.13 shows the porosity values determined by oven-dried methods for sediments of the Dahomey Basin, and expected porosity range according to Freeze and Chery (1979). These porosities are within the range of textural class of the sediment. For example, EWE B and ABK B are sandy clay loam soil and has a porosity of 0.31 and 0.24 which is within the expected porosity of 0.30–0.45, except for 0.24 porosity value of ABK B. ILA, OSH and CPS lithology are of sand range and their expected porosity should be within 0.05–0.30 (Freeze and Chery, 1979). In the Dahomey Basin, ABK Formation soils have a tendency to portray good attenuation, because the grain sizes cut across gravel, sand, silt and clay particles that have reduced porosity, and subsequently retard water movement. This is different when compared to the uniformly deposited medium sand grains of the Ilaro and Oshosun Formations.

In unconsolidated materials, porosity is principally governed by three properties of the media: Grain packing, grain shape and grain size distribution. Shape is probably the most fundamental property of any particle, but is unfortunately one of the most difficult to quantify (Kasenow, 2002). Shape is frequently assessed in terms of roundness and sphericity, which may be estimated visually by comparison to standard images (Figure 4.23a). The effect of packing may be observed with the degree of compactness, and it ranges from 0.26 (stable structure) to 0.47 (unstable structure) in porosity. The uniformly arranged grains in a similar packing arrangement will always yield a lower porosity than material with high  $C_u$ .

Table 4.13: Selected hydraulic conductivity and porosity values of the Dahomey Basin soils and expected range of porosity

Lithology	Hydraulic conductivity (K)	Porosity (n)	Expected porosity range (Freeze and Cherry, 1979)
EWE B	$4.5 \times 10^{-4}$	0.31	0.30–0.45
ABK B	$2.62 \times 10^{-3}$	0.24	0.30–0.45
ABK C	$1.22 \times 10^{-2}$	0.15	0.05–0.30
ILA A	$3.1 \times 10^{-3}$	0.19	0.05–0.30
ILA C	$1.0 \times 10^{-1}$	0.36	0.05–0.30
OSH A	$3.1 \times 10^{-3}$	0.20	0.05–0.30
OSH B	$9.89 \times 10^{-3}$	0.25	0.05–0.30
CPS A	$3.3 \times 10^{-3}$	0.09	0.05–0.30
CPS C	$3.5 \times 10^{-3}$	0.15	0.05–0.30

The roundness and uniformity of grains in the ILA Formation (Figure 4.24c&d) suggest that the sediments have travelled a farther distance before depositions. Due to its shape, the ILA Formation will display less resistance to infiltration of water and therefore indicate faster groundwater movement. Silty clay sediments of EWE sediments (Figure 4.25a&b) will also likewise portray size uniformity. The EWE B particles size of 20  $\mu\text{m}$  shows a higher porosity of 0.31, and lower  $K$  of  $4.5 \times 10^{-4}$  cm/s. Table 4.13 indicates that EWE B lithology has the capacity to filtrate contaminants and will serve as a better aquifer protective lithology. ABK sediments (Figure 4.24a&b) and CPS (Figure 4.25c&d) shows the lithology's good prospect for contaminant attenuation that is due to their varying grain sizes.

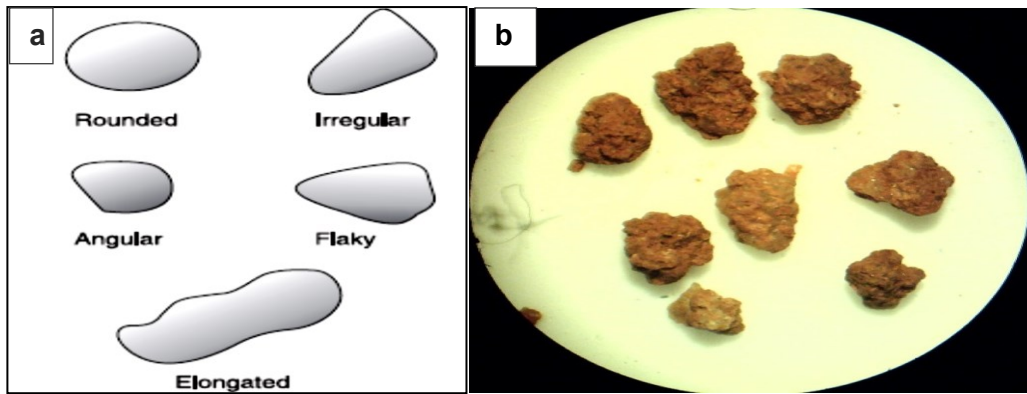


Figure 4.23: Common shapes present in sediments (a) and the irregular shape of OSH (b)

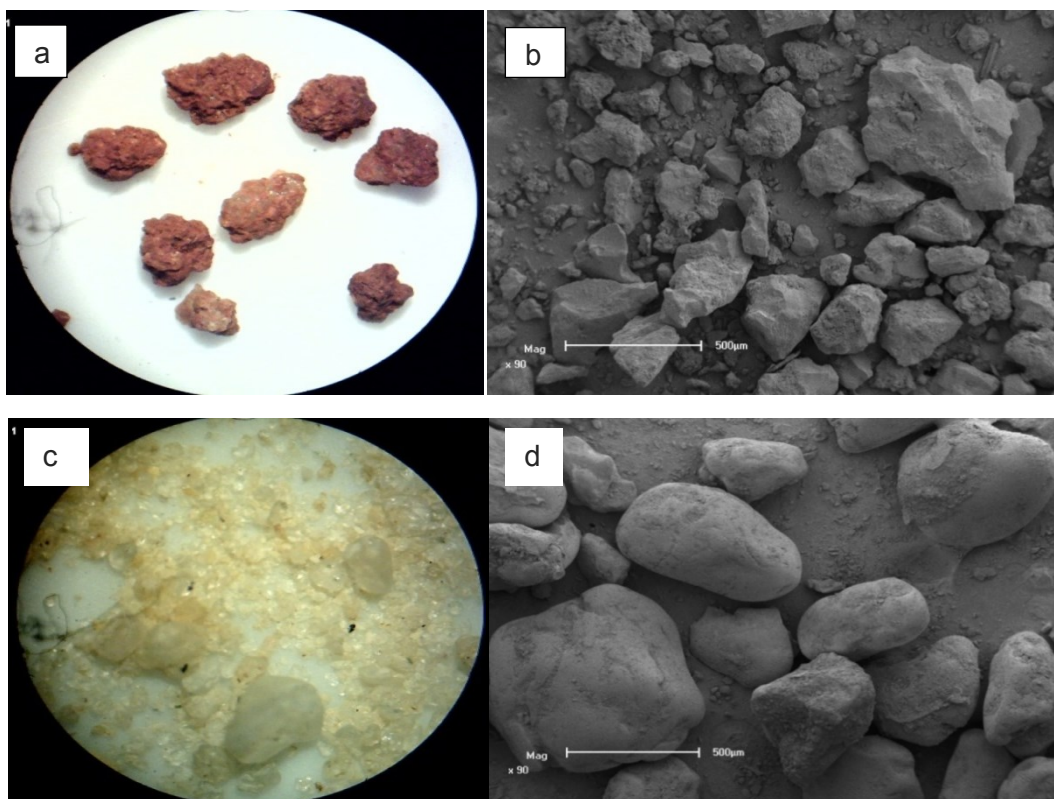


Figure 4.24: Grain shape of ABK (a&b) and ILA (c&d)

Note the pure quartz uniformity and subrounded grain sizes of the ILA sediment and the straight edges of the ABK grain in Figure 4.24.

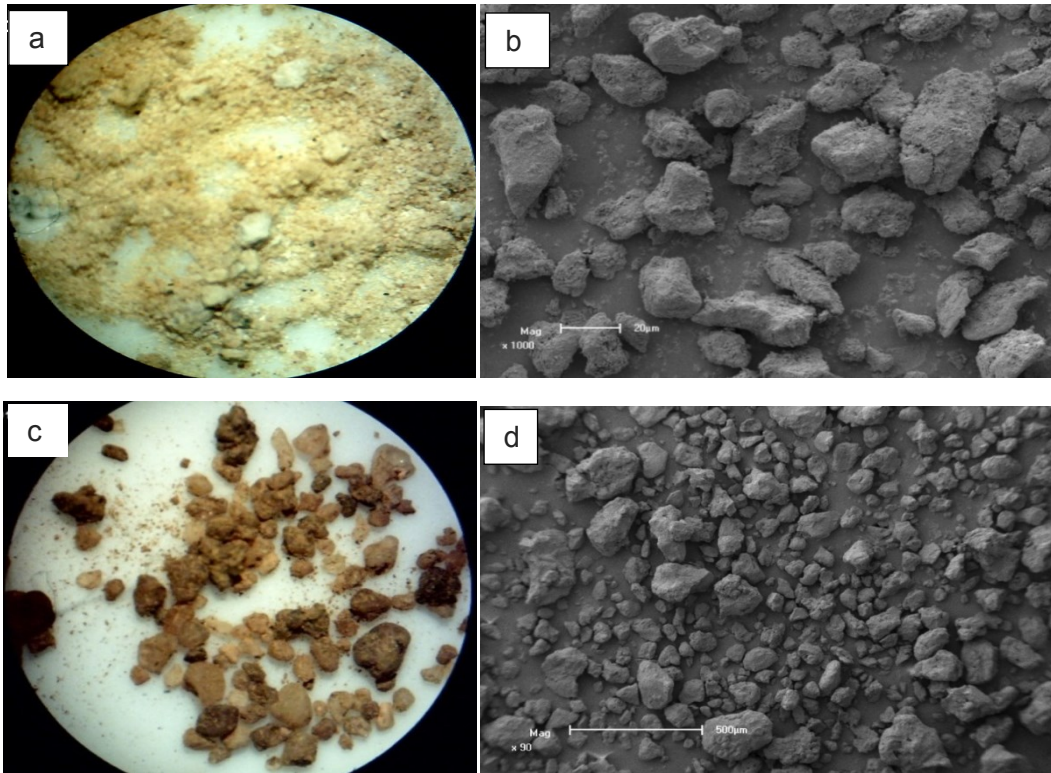


Figure 4.25: Shapes of EWE (a&b) and CPS (c&d).

Note the magnification of ( $\times 1\,000$ ) for the EWE and magnification of ( $\times 90$ ) for CPS. Also note the reddish brown ferruginisation colouration of the formation.

#### 4.3.7 Conclusion

The importance of the vadose zone in groundwater protection was discussed in this section. The section has indicated the important factors controlling the Dahomey vadose sediment, which includes the grain shape and grain size distribution. These two factors influence the hydraulic conductivity, intrinsic properties and the vadose attenuation capacity and these properties ultimately control the protective cover potential of the basin. In addition to the sediment grains and shapes, vadose grain size distribution and laboratory permeameter testing on Dahomey soil characterisations were presented. The saturated permeameter hydraulic conductivity values will be used for the calculation of aquifer vulnerability studies of the Dahomey Basin. The above textural description of the Dahomey Basin vadose materials excludes its geochemical attenuation characteristics, which will be discussed in the next section.

### 4.4 Lithogeochemical Characterisations of the Dahomey Basin Sediments

#### 4.4.1 Introduction

Geogenic and geochemical interactions between the vadose zone materials and infiltrating fluids are critical factors that further determine the attenuation capacity above an aquifer and

groundwater quality of the aquifer systems. In the Dahomey Basin, wetting, drying and salt crystallisation are the main processes that aid the fragmentation of rock to soil. Tropical regions of the world experiencing high temperatures and rainfall, combined with the presence of organic matter, will accelerate the rate at which the hydrolysis process occurs. Hydrolysis is a reaction of primary minerals with water and pronounced more in tropical regions than the cold and dry regions. It leads to the removal of most soluble ions, thereby degrading the original mineral structures into clay minerals (Hillel, 1998).

Hydrolysis also releases elements from minerals and then combines it to create new minerals (clays). This is the process that leads to the formation of montmorillonite, kaolinite and smectite which are critical attenuation components of soil for vulnerability evaluation. Therefore, this section determines the vadose zones geochemical properties that could retard contaminant infiltration, including the clay type and properties present in each formation.

#### **4.4.2 Geochemical Analysis**

One way to determine the chemical composition of sediments is the use of the X-ray fluorescence technology (XRF). XRF is a well-established, non-destructive laboratory and field screening method for the detection, identification and delineation of metal oxides and contaminants in the subsurface sediments. In XRF analysis the photoelectric effect is used. Fluorescent x-rays are produced by radiating the soils with an x-ray source, which has a definite excitation energy that will partly be absorbed by the target elements resulting in an energy emission in the form of x-rays. Each element hereby emits a unique x-ray at a characteristic energy level or wavelength.

Elements in the samples can be identified qualitatively by analysing the energy of the characteristic x-rays, while a quantitative analysis can be performed by measuring the intensity of the x-ray. This is as the intensity of the x-rays is proportional to the concentrations elemental oxide determination that was done with the Axios<sup>max</sup> PANalytical XRF machine (WDXRF). This was after the sediments were disaggregated by using mortar and pestle and passed through a 2 mm sieve, which was done in order to remove pebbles and twigs. Grinding was also conducted to reduce the particles sizes and passed through a 63 µm sieve. The sieved samples were further used to determine the clay mineralogical compositions with a PANalytical Empyrean XRD machine.

##### **4.4.2.1 Chemistry of Vadose Zone Sediments**

Table 4.14 shows the XRF results of major metals that are present in the soils of the Dahomey Basin. ABK, CPS and EWE Formation soils contain a significant amount of aluminium oxides, which is an indication of the presence of clay particles and better attenuation capacity. This is because clay rich soils have reduced permeability and a larger surface area. Soils of the ILA and part of OSH show predominance of silica. Silica-rich soils have poor water-holding capacity and therefore have poor attenuation capacity, but are among the most prolific aquifers. Sediments of ABK and CPS show a balance between the principal rock-forming minerals. Good representative percentages of SiO<sub>2</sub>, Al<sub>2</sub>O<sub>3</sub> and Fe<sub>2</sub>O<sub>3</sub>

suggest greater possibility of contaminant attenuation compared to the ILA and OSH sediments that are predominantly of silica.

Table 4.14: Major metals of soils from the Dahomey Basin

Layers	SiO <sub>2</sub>	Al <sub>2</sub> O <sub>3</sub>	Fe <sub>2</sub> O <sub>3</sub>	CaO	MgO	MnO	Na <sub>2</sub> O	K <sub>2</sub> O	P <sub>2</sub> O <sub>5</sub>	TiO <sub>2</sub>
ABK A	61.22	26.41	9.04	0.04	0.69	0.11	0.15	0.09	0.12	1.944
ABK B	59.14	29.33	8.8	0.01	0.22	0.08	0.15	0.11	0.12	1.984
ABK C	66.86	22.64	6.76	0.01	0.6	0.07	0.16	0.06	0.09	2.187
CPS A	60.86	28.2	7.86	0.15	0.39	0.08	0.15	0.12	0.2	1.981
CPS B	56.94	31.63	8.44	0.01	0.03	0.07	0.15	0.01	0.12	2.045
CPS C	62.39	29.25	5.08	0.01	0.61	0.06	0.16	0.03	0.12	1.893
OSH A	98	0.55	0.47	<0.01	<0.01	<0.01	<0.01	<0.01	0.02	0.06
OSH B	55.45	31.39	9.47	0.25	0.68	0.09	0.15	0.07	0.37	2.107
OSH C	97.01	2.31	0.18	0.02	0.16	0.05	0.16	0	0.04	0.164
OSH D	95.62	1.95	1.37	<0.01	<0.01	<0.01	<0.01	0.02	0.02	0.13
ILA A	97.42	0.71	0.53	0.03	<0.01	<0.01	<0.01	0.01	0.02	0.1
ILA B	97.71	0.71	0.64	0.06	<0.01	<0.01	<0.01	0.01	0.03	0.1
ILA C	94.94	1.47	1.8	0.01	0.01	<0.01	0.03	0.02	0.04	0.18
EWE A	87.99	1.34	7.85	0.03	<0.01	<0.01	<0.01	0.02	0.43	0.08
EWE B	83.58	7.94	3.67	0.02	0.04	<0.01	<0.01	0.03	0.06	0.47
EWE C	67.53	18.19	3.53	0.13	0.21	<0.01	0.04	0.51	0.24	1.39
EWE D	75.90	0.25	0.27	23.20	0.33	<0.01	0.01	0.01	0.03	0.01

#### 4.4.3 Clay Type and Implication for Groundwater Vulnerability

The x-ray diffraction diffractogram was used in identifying minerals such as kaolinite, hematite, goethite, quartz, mica and anatase present in the vadose lithology above the water table. The XRD diagrams (Figure 4.26 and Figure 4.27) depict various peaks for different clay minerals. The presence of fine grain sized material, such as clay or silt, and the percentage of organic matter within the soil cover can decrease intrinsic permeability, and retard or prevent contaminant migration via physico-chemical processes, namely absorption, ionic exchange, oxidation and biodegradation. In addition, soil organic matter can act as cation adsorption sites and is part of the hydrophobic sorption of organic compounds (Sililo *et al.*, 2001).

The dominant clay mineral type, kaolinites (Al<sub>4</sub>Si<sub>4</sub>O<sub>10</sub>(OH)<sub>8</sub>) (Table 4.15), is generally classified into 1:1 minerals. These non-expanding clay types do not allow water or ions into its structure and cannot be cleaved or separated. Kaolinite is made up of more silica and alumina sheets and is held together by rigid hydrogen bonding multi-layered lattice that

formed hexagonal platelets. The exposed platelet faces and edges have a low specific surface, and thickness ranges from 0.02 to 0.05  $\mu\text{m}$  and a diameter layer of 0.1 to 2  $\mu\text{m}$ , thereby making them exhibit low plasticity and cohesion (Hillel, 1998). Due to these properties, they also do not swell, and are likely to exhibit less resistance to some contaminants making them less competent when compared to other clay minerals in contaminant attenuation purposes.

Hydrological conditions of the Dahomey Basin support the kaolinite formation and clay mineral production due to the basin; longer period of exposure to rainfall. The nature of the basin topography supports water flows from different surfaces to the larger rivers connecting the Atlantic Ocean in the south, which further supports the formation of kaolinite whereby silica and alkali minerals are simultaneously depleted from rocks with alumina enrichment (Table 4.15). Weathering under acidic conditions is also responsible for kaolinisation. Kaolinite is the chief clay mineral in most residual and transported clays.

Table 4.15: Representative mineralogical composition from lithology in the Dahomey Basin

Sample	Formation	Quartz	Kaolinite	Anatase	Rutile	Hematite	Goethite	Muscovite	Vermiculite
1	ILA A	XX	x		<x	X			
2	ILA B	XX	xx	<x			X	<x	
3	ILA C	XX	xx			X	<x		
4	EWE C	X	XX	<x			X		
5	CPS	X	XX	<x	<x		X	<x	x
6	CPS B	X	XX	<x		X	X		
7	OSH A	XX	XX	X					
8	OSH B	X	XX	X		xx			
9	EWE A	XX	xx	X		x			
10	ABK A	X	XX	X		Xx			
11	ABK B	X	XX	X		x	X		

**Key:**

XX	Dominant mineral	>50%
X	Major mineral	20-50%
xx	Minor mineral	10-20%
x	Accessory mineral	2-10%
<x	Trace mineral	<2%

A reddish nature is observed in the majority of the profiles, especially the top soil of ABK, CPS and OSH (Figure 4.10, Figure 4.20 and Figure 4.21), and is from the sesquioxides of iron and aluminium oxides, a consequent of weathering and clay fraction with the formulas  $\text{Fe}_2\text{O}_3 \cdot n\text{H}_2\text{O}$  and  $\text{Al}_2\text{O}_3 \cdot n\text{H}_2\text{O}$ , respectively. Limonite, hematite and goethite are examples of the hydrated iron oxides while gibbsite is the observed aluminium oxide (Table 4.15). The sesquioxides form cementing materials between several soil particles of differing size aggregates and reduced pore spaces, which is why they are important soil properties for contaminants attenuation purpose. Their poor electrostatic properties, however, exhibit less adsorptive capacity and plasticity and are comparable to most silicate clays such as kaolinite, thereby exhibiting less competent to contaminant attenuation.

Clay mineral production is a complex chemical process that occurs with other favourable factors. This includes climate in humid and sub-humid tropical climates where rainfall exceeds 1 500 mm, such as the study area. The rainfall dissolves minerals in rocks and elements carried away in the order of their solubility, ranging from sodium, potassium, calcium, magnesium, iron, silicon and aluminium. The other remaining elements, particularly trace metals, combine with clay minerals (Hillel, 1998). This implies that trace and heavy metals contained in rock during their formation are leached into clay minerals and are a reliable source of heavy minerals in groundwater.

Pronounced leaching gives rise to smectites with traces of silicon, iron and magnesium, while vermiculites are developed in moderate leaching. Strong leaching in well-drained environments, however, removes silica and other soluble cations favouring the formation of kaolinite. Climatic zones affect the type and nature of clay minerals formed; kaolinite is common in the equator belts, while smectites are associated with both Mediterranean and tropical zones, and vermiculites in temperate zones. Chlorites are found in the colder regions (Hillel, 1998).

To conclude, elements in contaminated water are less mobile in soils that provide a large quantity of sorption sites for exchange (Table 4.16). Oxides of Fe, Al and Mn can provide chemisorption sites for cations and anions in contaminated sources. Layer silicate minerals will likewise provide exchange sites for cations and a few chemisorption sites for both cations and anions (Sililo *et al.*, 2001).

Table 4.16: Cation Exchange Capacity of sediment

Clay type	Cation Exchange Capacity [meq/100g]	pH-dependence
Kaolinite	3–15	++
Halloysite	5–10	
Montmorillonite	80–120	~
Glauconite	5–40	
Illite, chlorite	10–40	+
Smectite	80–150	~
Vermiculite	100–150	-
Zeolithe (vulcanite, marine sediments)	100–400	-
Goethite, hematite	–100	~
Mn(IV)- / Fe(III)-oxyhydroxides	100–740	+
Humic acids	100–500	+
Organic matter	Per 100 g C <sub>org</sub>	51*pH–59

Source: After Merkel and Planer-Friedrich (2002); Appelo and Postma (1999).

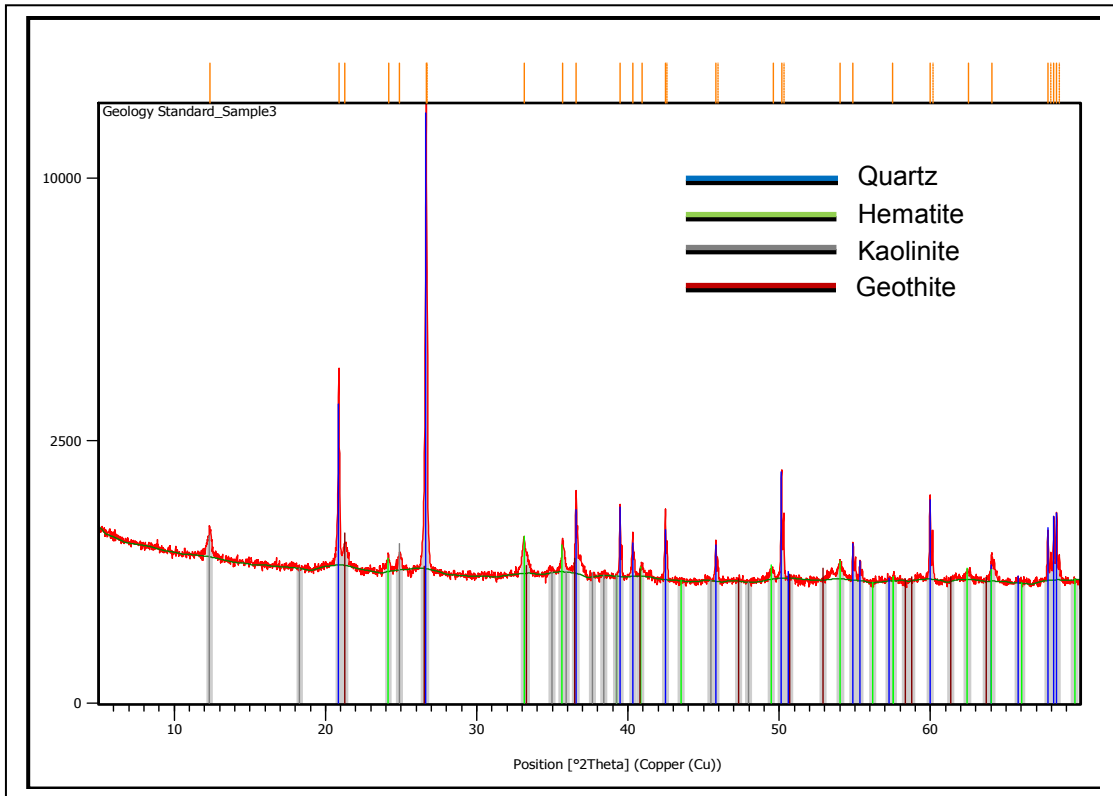


Figure 4.26: XRD diagram for CPS B lithology in the Dahomey Basin

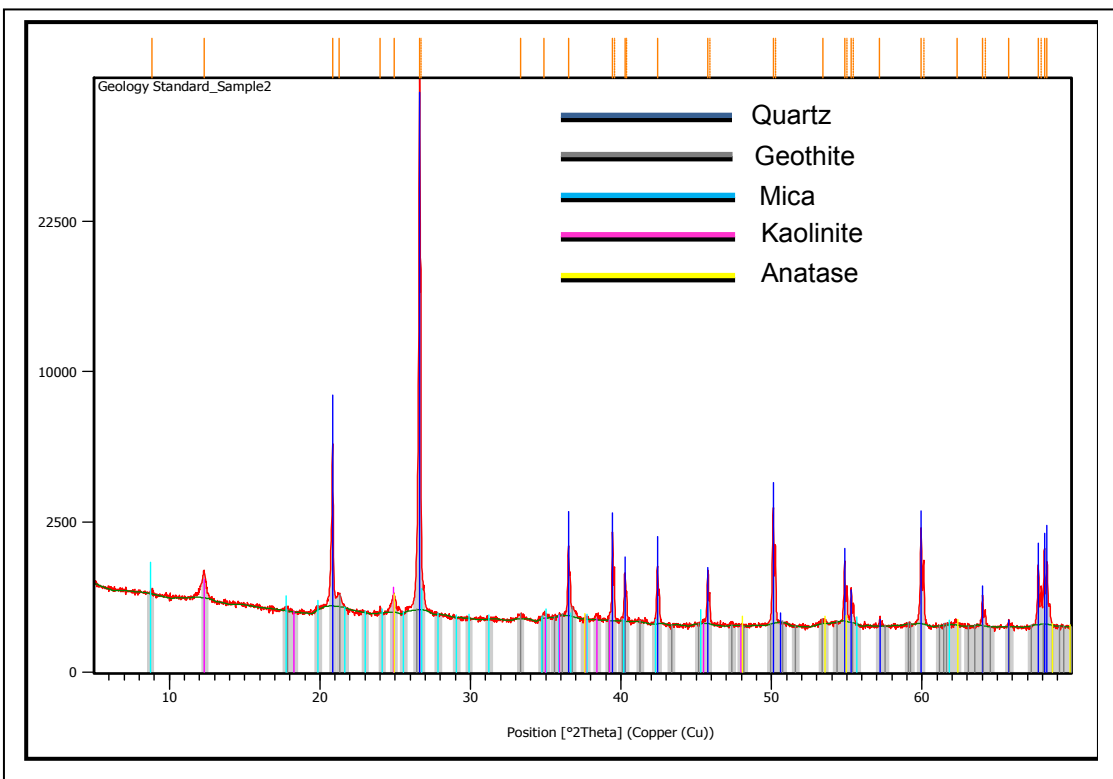


Figure 4.27: XRD diagram for ILA B sediment in the Dahomey Basin



#### 4.4.4 Conclusion

In addition to the sediment grains and shapes, the Dahomey Basin vadose sediment chemistry shows a dominance of iron, quartz and aluminium as reflected by silica oxide, aluminium oxide and iron oxide. The XRD indicates that lithology with predominant quartz shows a greater risk of groundwater contamination. Clay-rich sediments and sediments with appreciable aluminium oxide, however, indicate good contaminant attenuation and protective cover for the Dahomey Basin aquifers.

### 4.5 Characterisations of the Groundwater Bearing Unit of the Dahomey Basin

#### 4.5.1 Rainfall Pattern

An evaluation of shallow aquifer vulnerability requires estimations of groundwater recharge mechanism. Different sources contribute to groundwater recharge. For regional estimation, exact groundwater recharge can be challenging and inaccurate. Aquifer vulnerability to contamination is controlled largely by recharge-transporting contaminants to the aquifer (Robins, 1998); delineating zones of high recharge is therefore important in order to define zones vulnerable to contamination.

The groundwater recharge used in this section focuses more on rainfall quantity estimations. This is because groundwater recharge in the study area is through the natural mode, namely downward flow of water through the unsaturated zone (Adelana *et al.*, 2008; Oke *et al.* 2013). The study area, being a coastal basin and tropical humid region, is characterised by shallow water tables and gaining streams with groundwater discharged through evapotranspiration and base flow to streams. The recharge rate in the area is often limited by the ability of the aquifers to store and transmit water and climatic conditions.

Climate variability affects rainfall patterns in the Dahomey Basin. The movement of the Inter-Tropical Convergence Zone (ITCZ) influences the rainfall. The ITCZ is a zonation boundary that separates the equatorial maritime air mass over the Atlantic Ocean and the subtropical continental air mass over the Sahara. The seasons (wet and dry) are derived from the two air masses. The dry season results from Harmattan, a name given to the dry Sahara air mass ranging from November to March. January and February are the driest months. The dry air blows over the basin to the Atlantic Ocean with resultant little or no rainfall during the period. The ITCZ movement northward results in heavy precipitation with the rainfall amount decreasing northwards.

Precipitation increases from north to south in the Dahomey Basin. Measured rainfalls at the southern part of the Dahomey Basin in Lagos exceed the northern end rainfall at Abeokuta. Figure 4.28 shows the rainfall pattern collected from Nigeria's Meteorological Agency stationed at three strategic parts of the Dahomey Basin. The graph shows an annual rainfall pattern of twenty years in the three major cities of the basin. Abeokuta is located on the northernmost tip of the Dahomey Basin and lies on the basement rock of southwestern Nigeria and the Abeokuta Formation. Ijebu-Ode is located on the eastern end of the basin closer to Lagos, while Lagos is located along the coast of the Atlantic Ocean. Annual

recharge average estimates could be put at 1 800 mm for Lagos, 1 600 mm for Ijebu-Ode and 1 200 mm for Abeokuta (Table 4.17).

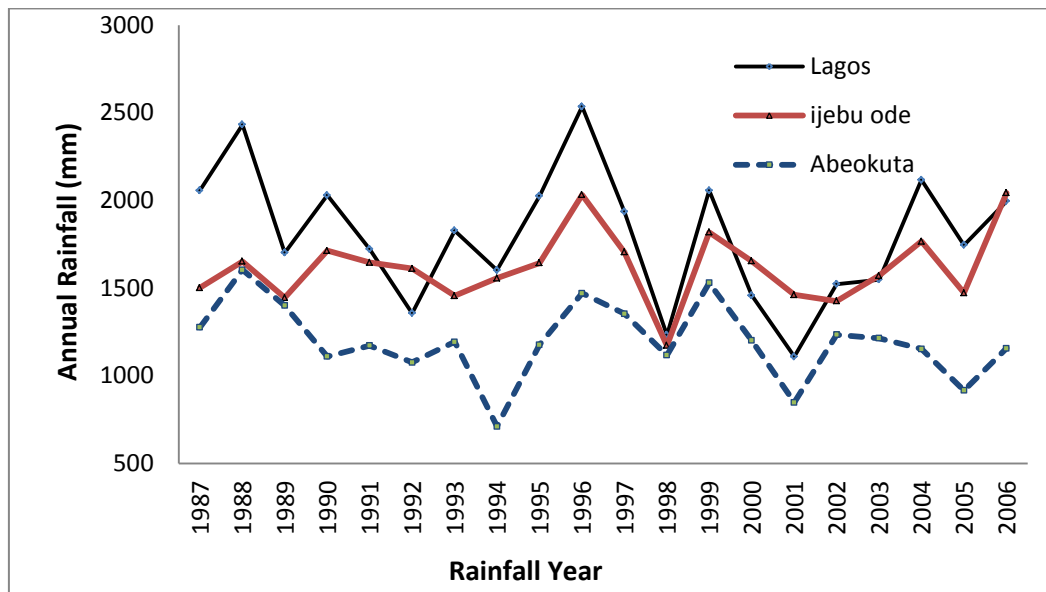


Figure 4.28: Twenty years' annual rainfall pattern of three prominent cities in the Dahomey Basin

Table 4.17: Twenty years' rainfall data of three major cities in the Dahomey Basin

Year	Lagos (mm)	Ijebu ode (mm)	Abeokuta (mm)
1987	2 057.0	1 501.9	1 277.1
1988	2 432.1	1 653.2	1 604.4
1989	1 702.6	1 445.5	1 401.0
1990	2 030.2	1 713.8	1 111.0
1991	1 722.9	1 646.9	1 173.1
1992	1 357.6	1 611.8	1 076.7
1993	1 828.2	1 456.9	1 193.6
1994	1 602.3	1 556.9	712.2
1995	2 025.3	1 643.8	1 177.5
1996	2 535.9	2 032.4	1 471.6
1997	1 936.8	1 705.7	1 354.9
1998	1 232.9	1 172.8	1 118.4
1999	2 056.9	1 819.4	1 530.4
2000	1 458.9	1 655.0	1 201.9
2001	1 110.0	1 462.3	849.2
2002	1 523.2	1 426.5	1 235.1
2003	1 549.0	1 572.0	1 214.7
2004	2 117.4	1 766.6	1 153.3
2005	1 745.6	1 473.3	917.5
2006	1 996.2	2 043.6	1 157.2
Average	1 801.05	1 618.015	1 196.54

#### 4.5.2 Groundwater Level and Monitoring

The groundwater levels in the Dahomey Basin vary from north to south. The topographical elevation decreases toward the Atlantic Ocean at the southernmost part of the basin. Surface, unconfined shallow and deep groundwater flow towards the Lagos lagoon, which connects the sea at the southern end of the basin. Due to the nature of the Dahomey geology, the water table gets shallower towards the end of the sea, with the hydraulic head behaving in a similar manner. The nature of the geological formation plays an important role in this. Loose alluvium recorded the shallowest depth and they deposited as the base rock for most rivers in the basin. The alluvium depositions recorded the lowest topography values and they are the most vulnerable aquifers in the basin due to their shallow depth.

The water-bearing strata of Lagos consists of sand, gravel, or a mixture, which range from fine through medium to coarse sand and gravel (Adeleye, 1975). Four major aquiferous units are tapped for the purpose of water supply in the Lagos metropolis (Jones and Hockey, 1964). The first aquifer extends from the ground level to roughly 12 m below the ground layers of clay and sand (Figure 4.30). This aquifer is prone to contamination because of its limited depth. The second aquifer encountered is between 20 and 100 m below the sea level. The third aquifer encountered is in the central part of Lagos at a depth ranging from 130 to 160 m below the sea level. The fourth aquifer is located at an elevation of approximately 450 m below the sea level. Only a few boreholes tap water from this aquifer (Jones and Hockey, 1964).

This account differs from Onwukas' (1990) observations. He classified three main hydro-stratigraphic units in the groundwater of the Dahomey Basin:

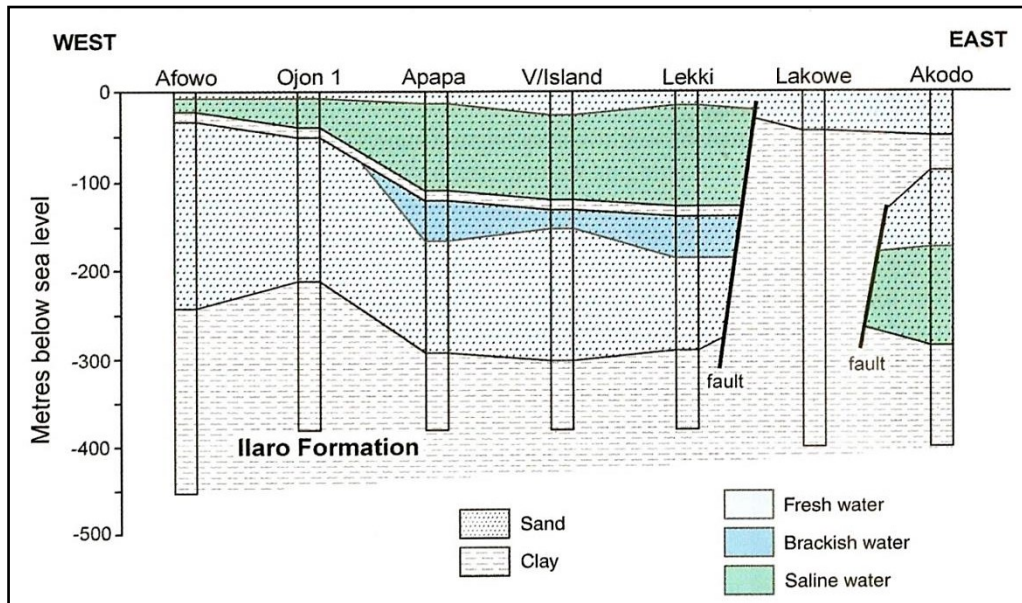
- Upper Aquifer (Alluvium and Coastal Plain Sands).
- Middle Aquifer (Ilaro and Ewekoro Formations).
- Lower Aquifer (Abeokuta Formations).

In most parts of Lagos, the hydrogeological units is the alluvium and Coastal Plain Sands, which are underlain in places by the Eocene Middle Aquifer (Tijani *et al.*, 2005), while the Abeokuta Formations are the main hydrogeological units in Ijebu-Ode and south of Abeokuta City. The Abeokuta Formations are lying conformably on the Basement Complex rocks of southwestern Nigeria. The depth-to-water level of the Dahomey Basin coastal aquifers is shallow and below 3 m along the coast (Figure 4.29) and ranges from 25 to 70 m in the Abeokuta Formations. Clay and shale deposits form the impermeable horizons for the shallow aquifers in the basin (Longe *et al.*, 1987). Alluvial aquifers along the valleys of the Yewa and Ogun rivers show substantial groundwater potential. Record of water levels below 3 m were noted by Jones *et al.* (1964) and 2.4 m was measured in Ofada areas.

Figure 4.30 show the water level monitoring of the Coastal Plain Sands (also called Benin Formation) in the Dahomey Basin. Two water levels were identified here, and it is of note that the distance from the sea and the Lagoon contributed to this depth. The Epe monitoring borehole is closer to the sea and the Lagos lagoon as compared to the Ikeja monitoring borehole. The shallow groundwater level rises from February to July and peaks from around April to May. The groundwater rises and peaks correlate with the start and peak of the rainy

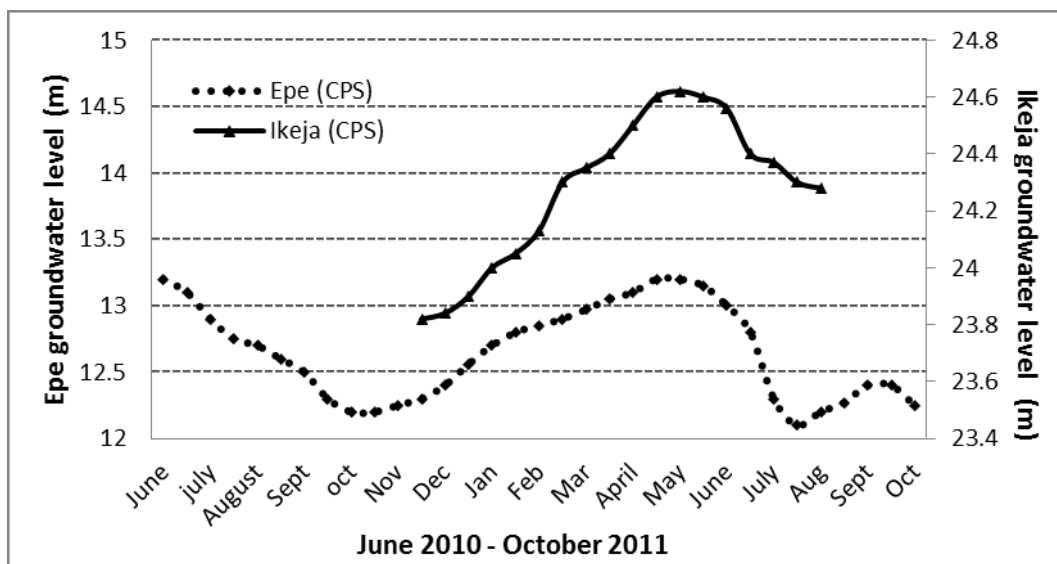
season in the Dahomey Basin. Adelana *et al.* (2008) reported a range of 0.4 to 21 m below ground level for the water table in Lagos, and an annual fluctuation of less than 5 m.

Few boreholes are generally used for groundwater monitoring by the Nigeria Hydrological Service Agency (NIHSA) for the Lagos metropolis and Dahomey Basin. The agency is responsible for groundwater monitoring in Nigeria by law and their lack of geohydrological data limits groundwater research. Groundwater monitoring of the Dahomey Basin is an avenue to explore for further research in the basin.



Source: After Adelana *et al.* (2008).

Figure 4.29: Schematic hydrogeology cross section along the coastal areas of the Dahomey Basin



Source: Nigerian Hydrological Services Agency.

Figure 4.30: Groundwater monitoring borehole hydrograph of the Coastal Plain Sand at the Epe and Ikeja stations from June 2010 to October 2011

### 4.5.3 Aquifer Abstraction Rate

The current abstraction rate of the unconfined shallow aquifers was the target of characterisation. This was difficult to achieve, particularly in most parts of the Dahomey Basin containing a multi-layered aquiferous zone. This was because constructed boreholes in the basin penetrated more than one aquifer. Table 4.18 presents the current borehole abstraction rate of major geological formations of the Dahomey Basin. The abstraction rate of the CPS and Ilaro Formation is the highest. The CPS and ILA aquifers yield an average of 18-55.3 m<sup>3</sup>/hr. Groundwater abstracted from the Abeokuta Formation are of two categories based on the formation proximity to the southwestern Basement rocks.

Table 4.18: Current abstraction rate of selected locations in the Dahomey Basin

S/N	Location	Formation	Depth (m)	Stastic water level (m)	Abstraction rate (m <sup>3</sup> /hr)	Pump Capacity
1	Kajola	ABK	154	2.4	36.3	1 HP
2	Ade Abk	ABK	60.9	35	4.8	1.5 HP
3	Onikoko	ABK	152.4	50	3.5	1 HP
4	Idi-Aba	ABK/Basement	79.2	6	6	2 HP
5	Alamala	ABK/Basement	79.2	11	9.8	3.5 HP
6	*Ijebu-Ode	ABK	69.9	46.2	10.8	Nd
7	*Meko	ABK/Basement	57.9	42.3	1.6	Nd
8	Ijako	ILA		22	22	0.75 HP
9	*Ilaro 1	ILA	132	20.4	26	Nd
10	*Ilaro 2	ILA	39	18	14.4	Nd
11	*Ilaro 3	ILA	37.5	18	13.1	Nd
12	Ijoko	CPS	55	25.5	25	0.75 HP
13	Ogijo	CPS	230	10	21	1 HP
14	Mokoloki	CPS	128	8.4	28	1 HP
15	Ijofin	CPS	114	12.3	20	1 HP
16	*Ikeja	CPS	99	22.8	55.3	Nd
17	*Otta	CPS	52.2	20	22.5	Nd
18	Owode	OSH		18	18	0.75 HP
19	*Ibeshe	EWE	121.3	57.6	10.2	Nd
20	*Igbogila	EWE	70.5	11	28.5	Nd
21	*Ewekoro	EWE	90	Nd	58.5	Nd
22	Ofada	Alluvium	133	2.6	21.5	1 HP
23	*Ibefun	Alluvium	28.5	3	49.2	Nd
24	*Ibefun 2	Alluvium	45	7.5	25	Nd

Nd = no data

\*Source: Offodile (2014)

Some part of the Abeokuta Formation is the region in the Dahomey Basin lacking sustainable well yields. The shallow aquifer part of the Abeokuta Formation directly overlying the Basement rocks; record the lowest abstraction rate in the basin (1.6 m<sup>3</sup>/hr). While part of the Abeokuta Formation containing thick-deposited sediments gives a yield of 10–36.3 m<sup>3</sup>/hr. Most of the low yielding Abeokuta Formation aquifer lies in the weathered

regolith overlying the Basement rocks. The current abstraction rate of the Alluvium and EWE Formations is between 21.5-49.2 m<sup>3</sup>/hr and 10-58 m<sup>3</sup>/hr (Offodile, 2014). Asiwaju-Bello and Oladeji (2001) confirmed storage of  $2.87 \times 10^3$  m<sup>3</sup> for the Alluvium aquifers of the Dahomey Basin. A representative diagram of the groundwater abstracted superposed on the geological formations is shown in Figure 4.31. Adelana *et al.* (2008) reported that there is pressure on the groundwater resources of Lagos, and about 75% of groundwater abstracted in Lagos for domestic and industrial purposes is obtained from the second aquifer (Coastal Plain Sand).

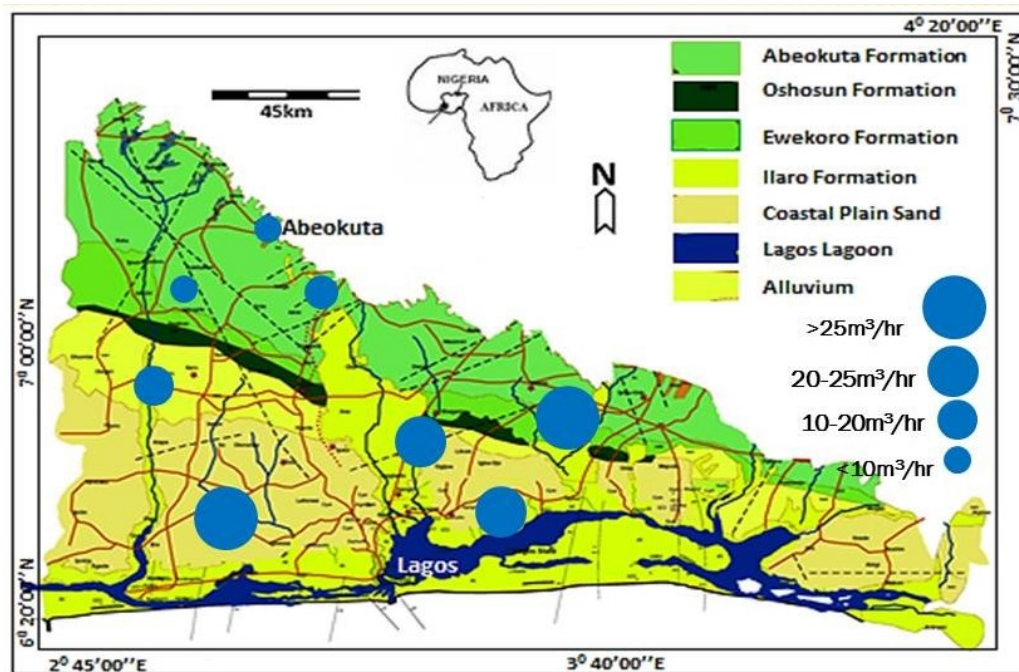


Figure 4.31: Representative groundwater abstraction rate distribution of the Dahomey Basin aquifers

#### 4.5.4 Conclusion

As a coastal tropical basin, most of the rivers in the Dahomey Basin flow towards the sea down south with the rivers gaining from groundwater. Groundwater level control is predominantly by geology and recharge, which is precipitation driven. The groundwater level varies across the basin and is mainly controlled by the in-situ geology and distance from the sea. The rock types control the amounts of groundwater available for abstraction in the Dahomey Basin aquifers. The rainfall pattern decreases from the coast toward the northernmost end of the basin. Average precipitation includes 1 800 mm in Lagos, 1 600 mm in Ijebu-Ode and 1 200 mm in Abeokuta. It is therefore concluded in this section that the precipitation, abstraction rate and groundwater level are characteristics of the rock type and climatic condition over the Dahomey Basin. The chemical constituent of the recharge source and effect of in-situ rock materials on the groundwater are important determinants in establishing groundwater vulnerability occurrence. Further discussion on this topic will be presented in the next section.

## **4.6 Hydrogeochemical Characterisations of the Dahomey Basin Aquifer**

### **4.6.1 Introduction**

Hydrogeochemical characterisations of groundwater systems, both in time and space, play a significant role in deciphering the variations of physical and chemical characteristics of groundwater. Evaluating the suitability of groundwater quality for vulnerability purposes involves an understanding of the hydrogeochemical characteristics, including the chemical composition of groundwater. Chemical characteristics of groundwater develop due to various reasons, among which include water rock interaction, nature and mode of recharge and anthropogenic influence (Mercado, 1985; Satpathy *et al.*, 1987; Helstrup *et al.*, 2007; Chattopadhyay and Singh, 2013). Chemical characteristics of groundwater can directly be linked to groundwater quality (Tijani, 1994; Babiker, 2007).

This section presents the shallow groundwater characteristics through a hydrogeochemical and microbiological framework. The section intends to highlight the Dahomey Basin's different water quality and hydrochemical dynamics and reasons responsible for it. More so, due to the peculiarity of the Dahomey aquifer as a coastal basin with a high population density, its hydrogeochemical characterisation is important in vulnerability studies. Groundwater is the major source of water for many rural and urban communities in Africa, including the Dahomey Basin (Giordano, 2009; MacDonald and Calow, 2009). Groundwater quality indices can serve as pollution or tracer indicators for vulnerability validations. Therefore, the assessment and monitoring of shallow groundwater quality at a well, within urban and rural settings, have the advantages of ascertaining the level of groundwater risk, and the extent of shallow groundwater vulnerability to contamination.

### **4.6.2 Sampling and Experimental Analysis**

Groundwater sampling was conducted during February/ March 2011 and October/ November 2012. This allowed the groundwater samples to spread across the two seasons: dry (Season 1) and wet (Season 2). Seasonal sampling is significant because it allows for groundwater elemental concentration monitoring. (During the dry season, groundwater experiences less dilution whereas during the rainy season, groundwater is significantly recharged by rainfall.) The inappropriate use of water quality data can contribute to inaccuracies in a groundwater vulnerability assessment. Water quality conditions represented by a single water sample collected from a given well may or may not represent the same water quality conditions sampled from the same well at another time, or another well (even if the wells are in proximity).

Collected samples include shallow hand-dug groundwater and deep borehole waters. The shallow hand-dug wells are targeted more in this research, because it is the most vulnerable to contamination, compared to deep hand-dug wells or deep confined boreholes. It is also the most accessible to the rural populace that uses the water. Unfiltered water samples were collected in sterilised plastics bottles per site using a bailer, and transported in a refrigerated box to the laboratory between 1 and 8 °C prior to analysis. All the sampling bottles were

washed and rinsed two to three times by using sampling water. Unfiltered water samples were collected in 100 ml bottles acidified with nitric acid for determination of cations and trace metals. The groundwater was not filtered before adding acid, because filtering may remove some contaminants that exist in a dissolved state or colloidal materials that are mobile in some groundwater conditions.

#### **4.6.2.1 Hydrochemical Data Collection and Analysis**

Anion determination water samples were collected in 500 ml bottles, unfiltered and unpreserved, and stored below 8 °C prior to analysis. Microbial loads were determined from the third sampling bottles. Physico-chemical properties (electrical conductivity (EC), total dissolved solids (TDS), temperature, dissolved oxygen (DO) and pH) were determined insitu using Hanna multi-parameters (model HI991300), whereas Hannah (model HI9147) equipment was used for DO. Ion Chromatography (IC) was used to analysed for anions. Nitrate, phosphates, bicarbonate, chloride and sulphate were measured after chromatography separation using conductivity detectors.

Major metals and trace metals were determined using the Inductively Coupled Mass Spectrometer (ICP-MS) and Inductively Coupled Optical Emission Spectrometry (ICP-OES). In order to improve accuracy and to prevent cloudiness of the water, water samples were filtered to less than 0.45 µm using a Pall Corporation GN-6 metricell sterilised membrane. Minute particles of clay sizes were removed before analysis. ICP-OES is useful in measuring higher concentrations, such as high levels of contamination. When lower levels of contamination are present, ICP-MS provide lower detection limits for measurement. In addition, cell-based ICP-MS provides an additional tool for the removal of interferences that might prevent detection of a contamination incident.

#### **4.6.2.2 Microbiological Data Collection and Analysis**

Bacteriological samples were collected using sterile sampling bottles. These were transported to the laboratory in an ice chest. Following the standard procedures, microbial analyses were carried out at the Microbiology Laboratory of Al-hikmah University, Ilorin, Nigeria. The groundwater samples were examined for total heterotrophic counts, total E. coli count, total Salmonella/ Shigella count and faecal coliform count under the microscope. They were then compared to standards as stipulated by the World Health Organisation (WHO, 2011) and the National Agency for Food and Drug Administration and Control (NAFDAC, 2004). Analyses were in accordance to the Nigerian and WHO standards. The accuracy of the methods for all determinants is better than ±10%, the bias is within ±3%, and the repeatability at the 95% confidence interval is better than at 5%. The analyses were repeated to make certain results correct.

#### **4.6.3 Hydrochemical Data Evaluation**

Data for major cations determined by ICP-OES/ICP-MS and anions determined by IC were checked for accuracy by calculating an ionic charge balance and also by checking the ratio of conductivity to TDS. The accuracy was further checked by the TDS and pH values. If carbonate is absent the pH should be less than 8, and TDS divided by measured



conductivity should be between 0.55 and 0.75 (Hem, 1985). Normal statistical parameters, for example mean minimum, maximum and standard deviation, were calculated for the water quality samples. The parameters include pH, TDS, EC, Ca, Na, Al, HCO<sub>3</sub>, Cl, Mg, TH, NO<sub>3</sub> and SO<sub>4</sub>.

#### 4.6.4 Ionic Ratio

Hydrochemical processes can be understood by calculating the ionic ratios and changes in the groundwater chemistry. Several processes and factors are responsible for hydrochemical characters displayed by groundwater, among which include the water rock interaction, dissolution, dilution, ion exchange, anthropogenic contamination and seawater effect through precipitation and salinisation (Satpathy *et al.*, 1987; Westbrook *et al.*, 2005; Frohlich *et al.* 2008; Kim *et al.*, 2009; Vengosh, 2013). A summary of the hydrochemical analysis for the rainy and dry seasons sampling is presented in Table 4.19.

Table 4.19: Physical and chemical parameters of the Dahomey Basin groundwater presented in mg/l

Parameters	Season 1 (Dry season)				Season 2 (Wet season)				WHO
	Min Values	Max Values	Mean Value	SD	Min Values	Max Values	Mean Value	SD	
pH	6.3	8.4	7.19	0.51	5.02	7.67	6.36	0.71	
EC	23	1026	224.67	270.7	22.1	1298.0	198.7	253.8	
TDS	17.25	769.5	168.49	203.0	12.0	648	103.1	126.2	
DO					0.3	7.5	2.04	1.86	
TH	5.36	183	42.64	43.2	4.927	160	37.61	40.8	
Ca	0.75	71.8	14.44	17.02	0.57	62.59	12.52	16.31	75
Mg	0.3	17.8	3.22	4.38	0.22	25.55	3.21	4.84	30
K	0.022	52.5	8.42	12.59	0.6	89.27	8.18	17.05	300
Na	1.8	158.7	24.09	36.2	3.75	117.51	17.71	21.28	200
NO <sub>3</sub>	18.75	25.7	21.95	1.68	0.1	2.63	0.74	0.92	50.0
SO <sub>4</sub>	5.24	12.96	8.06	2.16	0.04	20.05	1.42	3.71	500
Cl	106.5	1739	506.65	372.6	72.0	162.0	104.3	23.07	250
HCO <sub>3</sub>	72.2	758.1	244.80	117.5	13.25	91.5	39.02	17.39	
Si	0.566	21.84	8.562	3.96	3.14	9.58	5.17	1.13	
Co	0.0003	0.023	0.0035	0.004	0.002	0.002	0.002	0.002	
Cu	0.0022	0.265	0.058	0.050	0.007	0.19	0.05	0.04	2.0
Al	0.014	12.37	0.923	2.249	0.05	0.92	0.27	0.215	0.2
As	0.005	0.011	0.005	0.0009	0.007	0.009	0.008	0.003	0.01
Cr	0.0009	0.389	0.027	0.078	0.006	0.006	0.006	0.006	0.05
Fe	0.01	17.44	0.774	2.91	0.005	8.473	0.965	2.098	50.0
Zn	0.003	0.467	0.071	0.08	0.013	0.204	0.060	0.043	3.0
Mn	0.002	0.447	0.108	0.14	0.001	0.270	0.080	0.078	0.5
Ni	0.004	0.197	0.015	0.037	0.014	0.084	0.048	0.017	0.02

The Dahomey Basin records longer months of rainfall and higher precipitation due to its location along the tropical equatorial climate belts. Chloride concentrations in coastal aquifers tend to be constant and are used as tracer due to its conservative tendencies and high solubility property (Ramos-Leah and Rodriguez-Castillo, 2003). Comparative studies of anions/ cations with chloride and TDS are accepted techniques in identifying salinity variations in an aquifer (Wei *et al.*, 2008; Matthew *et al.*, 2011; Chattopadhyay and Singh, 2013). It is therefore important to understand the characteristics of the chloride that will be used as a vulnerability validation tool in the research in Chapter 8.

Higher values of Mg/Cl with TDS (Figure 4.32b) in Season 2 support recent groundwater recharge from precipitation, while Season 1 values indicate a mixed behaviour. Cl/sum of anion plots with TDS (Figure 4.32c) indicate a rainwater source with a value of >0.8 and TDS is <100. This pattern is indicated in Season 2 samples plotting above the 0.8 marks and Season 1 showing rock weathering. A common recharge source of rain water could be deciphered for both waters with plots of Na/(Na+Cl) values below 0.5 (Figure 4.32d) by Hounslow (1995). Low TDS and ion exchange processes controlled the mechanism of the water. A predominance of Na/Cl and TDS (Figure 4.32a) with a molar ratio of 0.86 for Season 2 over 0.37 for Season 1, suggests a diluted seawater recharge source (Vengosh, 2013).

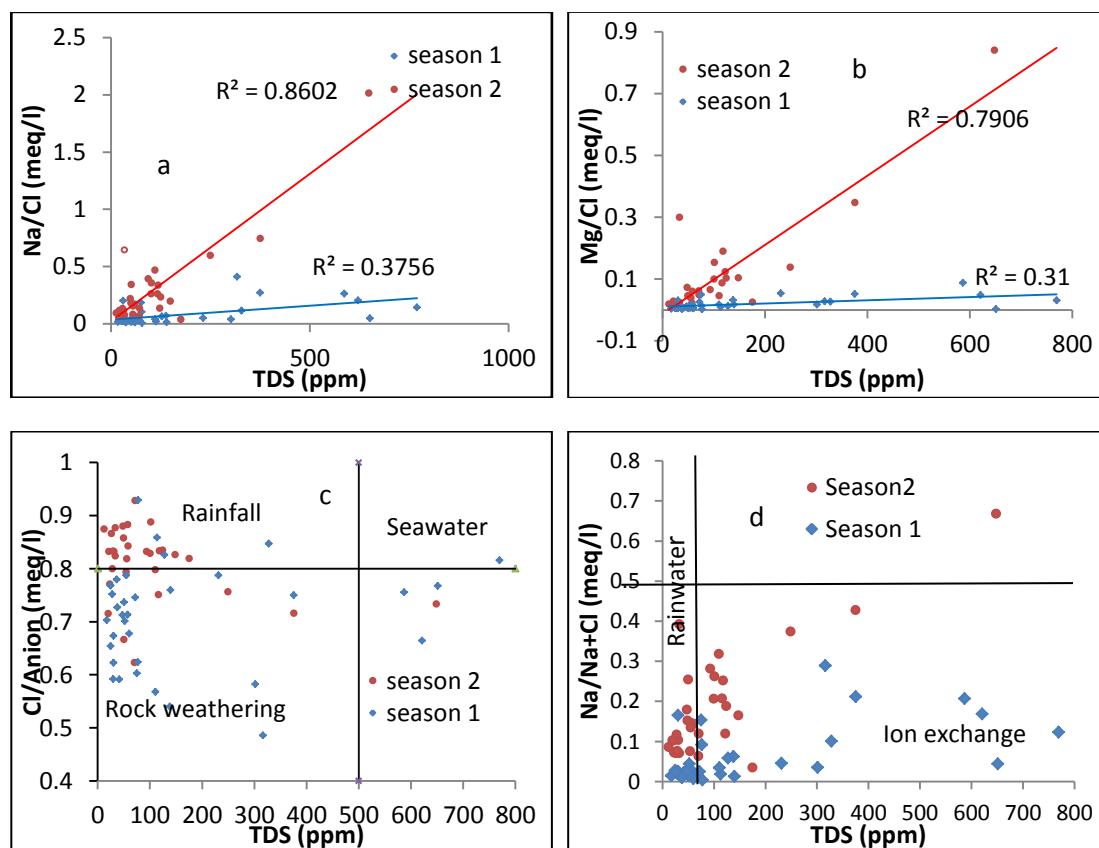


Figure 4.32: Ionic ratio of groundwater samples

Hem (1989) noted climates influence and variations on hydrochemical characteristics, water quality (Si, Cl and other solutes ions) and annual regime. These variations are shown in Figure 4.33. Higher concentrations of aqueous silica and a by-product of weathering were noted for a dry Season 1 and a more regular pattern in the wet Season 2. These variations were followed by the chloride concentration in both seasons meaning that intense weathering occurs more in the dry season, than in the wet season. Chloride variations in both seasons also show the chloride background concentrations in the Dahomey Basin and its conservative characteristics. This can be used to validate aquifer vulnerability maps. It also suggests that background chloride concentration in the Dahomey Basin decreases in the wet season due to dilution, and increases in the dry season due to evaporation. This further substantiates the reason why dissolved solid and chemical constituents of water wells

were higher in the dry season. However, these variations represent changes in the background groundwater quality.

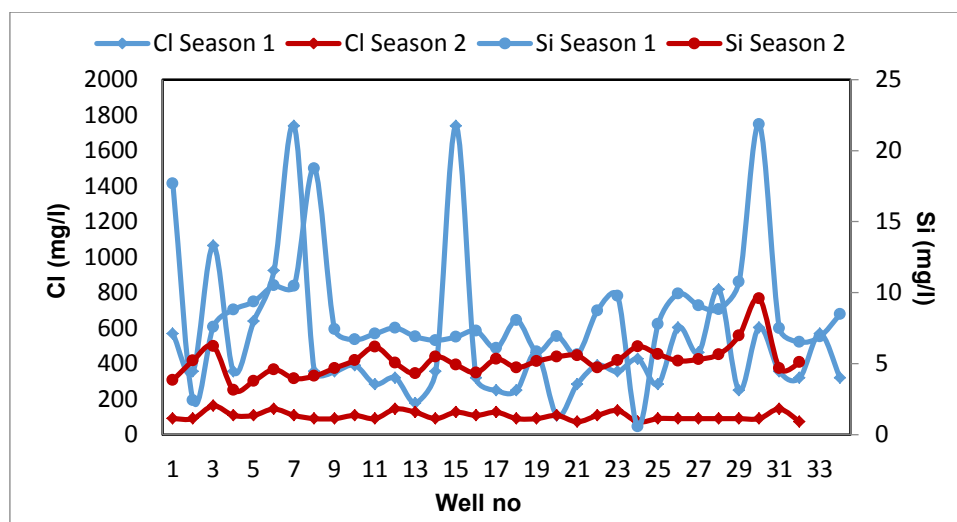
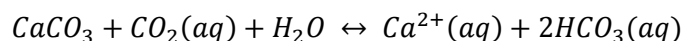


Figure 4.33: Seasonal variation of Si and Cl for the Dahomey Basin

#### 4.6.5 Hydrogeochemical Facies and Evolving Water Quality

An interpretation of the expanded Durov diagram (Figure 4.34) shows that groundwater in the area is generally of Ca-Cl, Na-Cl and Mg-Cl water types. Water rock interactions and possible chemical reactions of precipitation, dissolution and cation exchange are responsible for the variations in the chemical composition of groundwater samples. Since precipitation average a minimum of 1 200 mm over the whole Dahomey Basin (Section 4.5), and recharge is by downward flow of water through the unsaturated zone (Oke *et al.*, 2013), geochemical processes in the groundwater will depend on the in-situ rock type and chemical constituents of the recharge sources, most especially rainfall.  $Ca^{2+}$ ,  $Mg^{2+}$  and  $HCO_3^-$  are contributed to the groundwater through dissolution of carbonate rocks such as calcite or dolomite.



Limestone + carbon dioxide + rain water = calcium + bicarbonate

*Equation 4.10*

The Piper plots (Figure 4.35) indicate ion exchange processes where calcium and magnesium in the water samples is replaced by sodium. The plot shows a trend where plotted waters start from a constant calcium end and parallel to the magnesium line curve towards the sodium apex. This also indicates more calcium being exchanged compared to magnesium. However, anions showing a dissimilar trend suggest a possibility of other reaction processes in the water apart from ion exchange. The majority of the cations water plots in the mixing zone (D on the cation plot) indicate contribution of weathering to the groundwater. It also points to the inhomogeneity of aquifer materials. Chloride dominance over other anionic sources on the piper plot suggests sea influence due to proximity and precipitation from the sea.

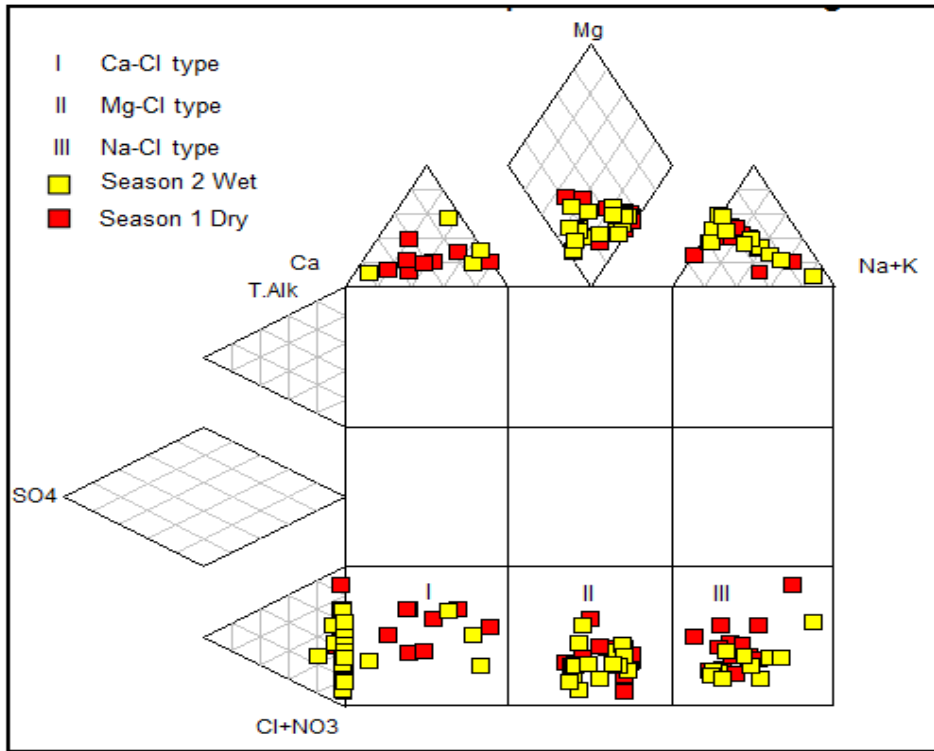


Figure 4.34: Expanded Durov diagram

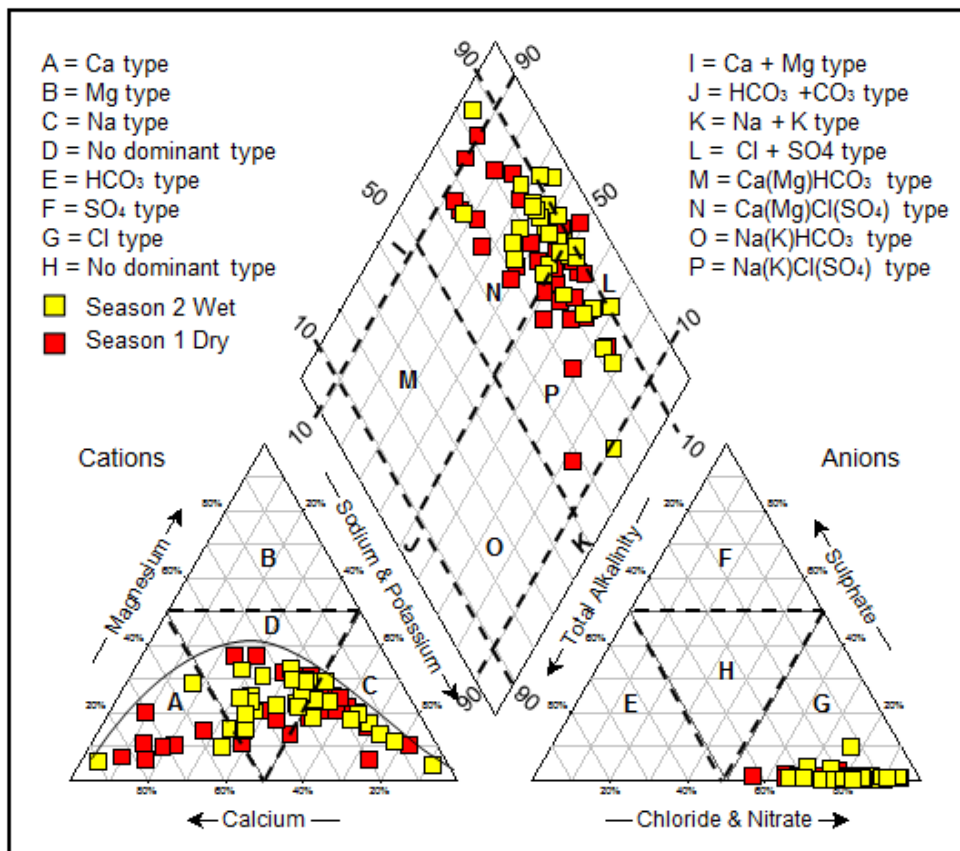


Figure 4.35: Piper diagram showing the interpretation of water chemistry

Likewise, Ca-Mg-Cl water types were predominant in the limestone rich Ewekoro Formation and sandstone with intercalated limestone in the Abeokuta Formation in the northern areas of the basin. Na-Cl water types dominate the southern areas closer to the sea with clayey and sandstone formations. In addition, Na-Cl water types were noticed for most cities, including those lying on the Abeokuta and Ewekoro Limestone Formations. These agree with findings from similar research of the western section of the Dahomey Basin in Ghana (Glover *et al.*, 2012).

The Na-Cl water types within the Abeokuta and Ewekoro Formations indicate anthropogenic sources, for example urbanisation, septic release and wastewater. This is because the background water type in the formations is a Ca-Cl water type due to beds of limestone in the formation. Vengosh (2013) has discussed salinisation induced by a direct anthropogenic effect and further explanations will be made under the sources of chloride in the next subsection. The general water types trend from calcium-magnesium-chloride water types to sodium-chloride water types (Table 4.20). This is an indication of rainfall recharge sources and an urbanisation effect on the shallow groundwater and ion exchange processes (Salama 1993, Rajmohan and Elango, 2004).

The water type is further supported by meq/l ratio of  $\text{Na}/(\text{Na}+\text{Cl})$  value  $<0.5$  with low TDS (Hounslow, 1995), thereby suggesting recent rainwater input (Figure 4.32d). The low TDS also implies that the chloride origin could not be brine, despite the water recording  $<0.5$  ratio for  $\text{Na}/(\text{Na}+\text{Cl})$ . This is because rainwater contains low dissolved constituents. Further evidence in support of ion exchange and precipitation of the groundwater evolution is supported with the Gibbs (1970) diagram. Most of the groundwater samples in the two seasons plotted in the rock dominated field (Figure 4.36), whilst a few, particularly in Season 2, plotted in the precipitation field. This demonstrates water rock interaction and precipitation as the main factors responsible for the geochemical processes controlling the groundwater chemistry.

The Ca-Cl water type is because of base-exchange reactions of aquifer materials with diluted saline water in Season 1 (dry). The cation exchanger in the aquifer is the limestone, clay minerals, oxyhydroxides and organic matter. Ca adsorbed on surface of these materials react with the diluted saline waters, Na replaces part of the Ca on the solid surface, Ca is released and Na is taken up by the solid phase. The composition then changes from Na-Cl into Ca-Cl water type. The  $(\text{Ca}+\text{Mg})/\text{Cl}$  ratio doubles the  $\text{Na}/\text{Cl}$  ratio in the water (Custodio, 1997; Jones *et al.* 1999; Appelo and Postma, 2005). Vengosh *et al.* (2002) noted that under such conditions, the relative enrichment of calcium and magnesium, normalised to chloride concentration, should be balanced by relative depletion of sodium (Figure 4.377 a). Similar to reasons adduced to Ca-Cl water is the plot of  $\text{Ca}/(\text{SO}_4+\text{HCO}_3) > 1$  by Vengosh (2013). Dry season samples are greater than one and a few of the wet water samples is above one, with the majority of wet samples being less than one. This means the sodium ions dominated the rainy season water.

Hem (1989) observed the action of differential permeability of clay and shale sediments in saline waters. Na-Cl water type predominate formations compose of sandstone and

intercalated clay. Cl is held back, while water molecules passed through clay layers and might accumulate until high concentrations are reached. The selective behaviour of such layers also influences the residual concentration of cations. The stronger retained ions in such a solution would be the ones most strongly attracted to cation exchange sites.

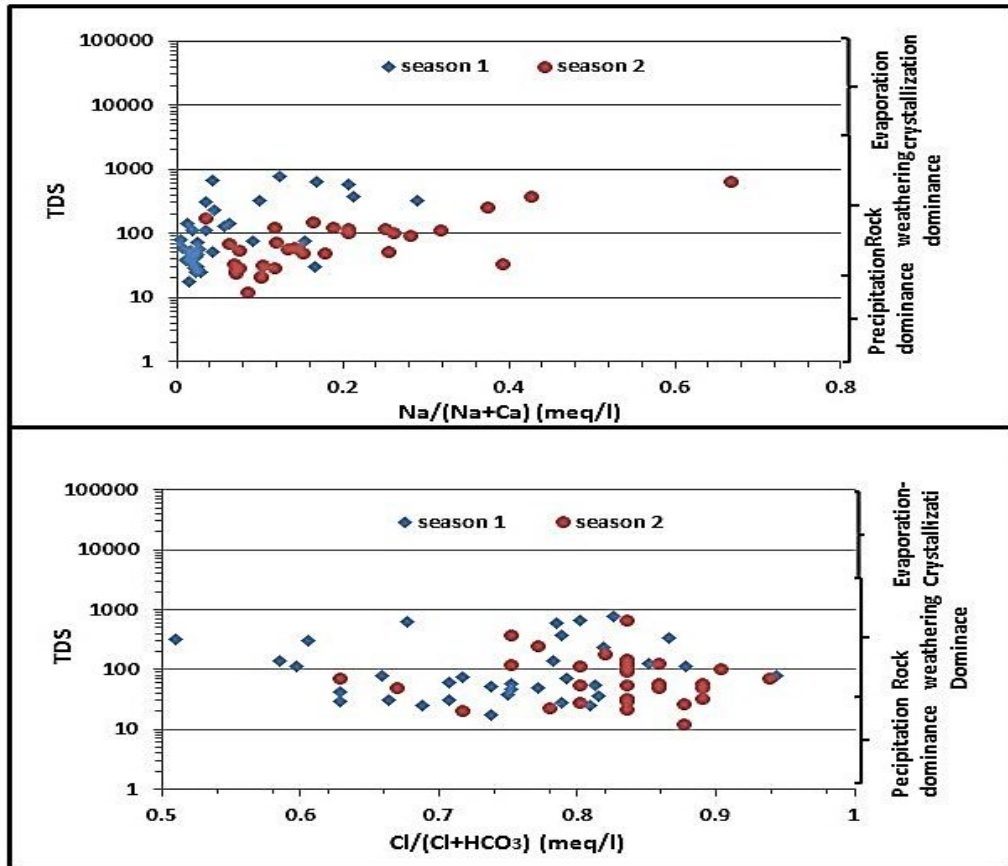


Figure 4.36: Gibbs' plots of groundwater samples from the Dahomey Basin

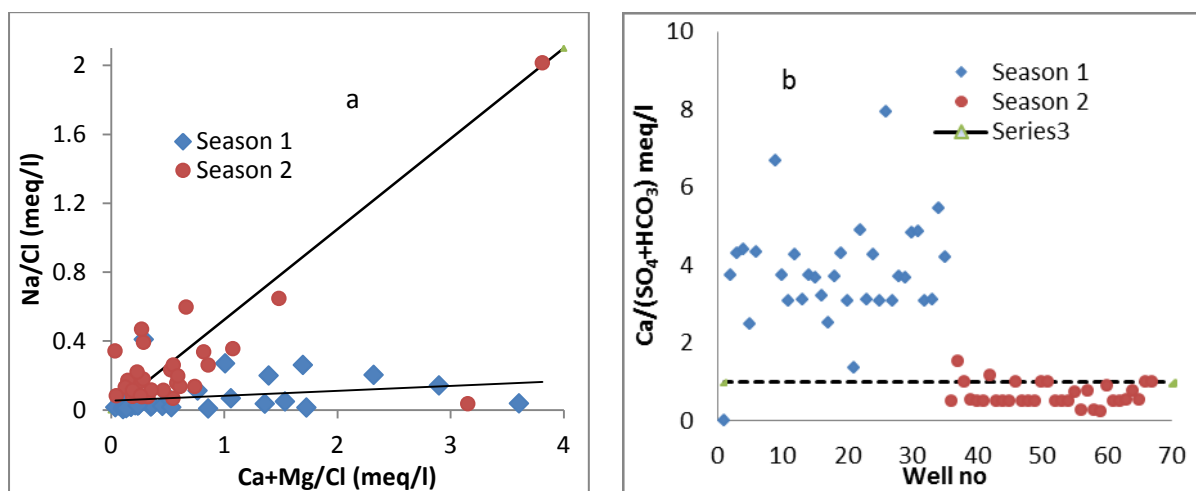


Figure 4.37: (a) Plot of Ca+Mg/Cl vs Na/Cl ratio; (b) Plot of Ca/(SO<sub>4</sub>+HCO<sub>3</sub>)

Table 4.20: Water quality and hydrochemical facies of the Dahomey Basin

Sam- ple	Rock Type	TH	Salinity	E Durov	Piper	pH	EC	TDS
Season 1								
1	ABK	M hard water	V.High	Mg-Cl	Ca-(Mg)-Cl	7.5	309	231.1
2	ABK	Soft water	High	Ca-Cl	Ca-Cl	7.5	80	60
3	EWE	Soft water	High	Mg-Cl	Cl+SO4	7.1	151	113.2
4	ILA	Soft water	Medium	Na-Cl	Na-(K)-Cl	7.2	33	24.7
5	CPS	Soft water	Medium	Mg-Cl	Ca-(Mg)-Cl	6.4	73	54.7
6	CPS	M hard water	V.High	Na-Cl	Na-(K)-Cl	7.5	828	621
7	CPS	Hard water	V.High	Na-Cl	Na-(K)-Cl	7.9	1026	769.5
8	ALLUVIUM	V hard water	V.High	Ca-Cl	Ca-(Mg)-Cl	6.9	402	301.5
9	ALLUVIUM	Soft water	Medium	Na-K-Cl	Na-(K)-Cl	6.6	69	51.7
10	ILA	Soft water	Medium	Na-Cl	Na-(K)-Cl	6.9	37	27.7
11	ABK	Soft water	High	Na-K-Cl	Na-(K)-Cl	7.1	102	76.5
12	ABK	Soft water	High	Mg-Cl	Cl+SO4	7.1	103	77.2
13	EWE/OSH	Soft water	High	Mg-Cl	Ca-(Mg)-Cl	7	76	57
14	EWE/OSH	Soft water	High	Ca-Cl	Ca-(Mg)-Cl	7.1	184	138
15	EWE	Soft water	Low	Na-Cl	Na-(K)-Cl	6.7	23	17.2
16	ALLUVIUM	Soft water	High	Mg-Cl	Ca-(Mg)-Cl	7.2	96	72
17	CPS	Soft water	Medium	Ca-Cl	Ca-(Mg)-Cl	7.3	40	30
18	CPS	Soft water	Medium	Ca-Cl	Ca-(Mg)-Cl	6.3	55	41.2
19	CPS	Soft water	Medium	Mg-Cl	Ca-(Mg)-Cl	6.9	48	36
20	CPS	Soft water	High	Na-Cl	Na-(K)-Cl	7.4	100	75
21	CPS	Soft water	Medium	Na-Cl	Na-(K)-Cl	6.6	39	29.2
22	CPS/ILA	Soft water	V.High	Na-K-Cl	Na-(K)-Cl	7.5	500	375
23	CPS/ILA	M hard water	Medium	Na-Cl	Na-(K)-Cl	7.6	40	30
24	EWE/OSH	Soft water	V.High	Na-Cl	Na-(K)-Cl	8.4	868	651
25	EWE/OSH	M hard water	V.High	Mg-Cl	Ca-(Mg)-Cl	8.3	782	586.5
26	ILA	Soft water	V.High	Na-K-Cl	Na-(K)-Cl	8.2	422	316.5
27	ILA	Soft water	High	Mg-Cl	Ca-(Mg)-Cl	7.4	170	127.5
28	CPS	Soft water	V.High	Na-Cl	Na-(K)-Cl	7.6	437	327.7
29	EWE	M hard water	High	Ca-Cl	Ca-(Mg)-Cl	7.4	147	110.2
30	EWE	M hard water	High	Ca-Cl	Ca-(Mg)-Cl	7.1	186	139.5
31	EWE	Soft water	Medium	Ca-Cl	Ca-(Mg)-Cl	6.4	67	50.2
32	ALLUVIUM	Soft water	Medium	Ca-Cl	Ca-(Mg)-Cl	6.9	63	47.2
33	ABK	Soft water	Medium	Ca-Cl	Ca-(Mg)-Cl	7.1	50	37.5
34	ABK	Soft water	Medium	Mg-Cl	Ca-(Mg)-Cl	6.5	33	24.7
Season 2								
1	ABK	Soft water	V.High	Mg-Cl	Ca-(Mg)-Cl		230	122
2	ABK	Soft water	High	Ca-Cl	Ca-(Mg)-Cl	5.55	137	70
3	EWE	V hard water	V.High	Ca-Cl	Ca-(Mg)-Cl	7.67	330	175
4	ILA	Soft water	V.High	Mg-Cl	Ca-(Mg)-Cl	5.02	242	124
5	CPS	Soft water	High	Na-Cl	Cl+SO4	5.8	115	57
6	CPS	V hard water	V.High	Mg-Cl	Ca(Mg)-Cl	7.3	745	375

Sam-ple	Rock Type	TH	Salinity	E Durov	Piper	pH	EC	TDS
7	CPS	Soft water	High	Na-K-Cl	Na-(K)-Cl	5.8	124	58
8	ALLUVIUM	Soft water	V.High	Mg-Cl	Ca-(Mg)-Cl	5.8	238	118
9	ALLUVIUM	Soft water	High	Na-Cl	Na-(K)-Cl	6.5	180	93
10	ILA	Soft water	High	Na-Cl	Na-(K)-Cl		97	49
11	ABK	Soft water	Medium	Ca-Cl	Ca-(Mg)-Cl	6.2	40	20
12	ABK	Soft water	Medium	Mg-Cl	Cl+SO4	7.13	68	33
13	EWE/OSH	Soft water	Medium	Na-Cl	Na-(K)-Cl	7.2	24	12
14	EWE	Soft water	High	Ca-Cl	Cl+SO4	6.69	111	55
15	EWE	Soft water	Medium	Mg-Cl	Ca-(Mg)-Cl	6.8	47	23
16	ALLUVIUM	Soft water	V.High	Mg-Cl	Ca-(Mg)-Cl	5.38	232	116
17	CPS	Soft water	Medium	Mg-Cl	Ca-(Mg)-Cl	6.21	53	26
18	CPS	Soft water	High	Mg-Cl	Ca-(Mg)-Cl	6.23	201	100
19	CPS	Soft water	Medium	Mg-Cl	Ca-(Mg)-Cl	6.6	61	31
20	CPS	Soft water	Low	Na-Cl	Na-(K)-Cl	5.24	22.1	110
21	CPS	Soft water	High	Na-Cl	Cl+SO4	6.01	97	48
22	CPS/ILA	Soft water	Medium	Na-Cl	Na-(K)-Cl	6.6	55	28
23	CPS/ILA	Soft water	High	Mg-Cl	Cl+SO4	6	144	71
24	EWE/OSH	Soft water	High	Mg-Cl	Cl+SO4	7.6	203	101
25	EWE/OSH	Hard water	V.High	Mg-Cl	Ca-(Mg)-Cl	7.05	1298	648
26	ILA	Soft water	Medium	Mg-Cl	Ca-(Mg)-Cl	7.2	43	21
27	ILA	Soft water	Medium	Mg-Cl	Ca-(Mg)-Cl	6.3	57	29
28	CPS	Soft water	V.High	Na-Cl	Na-(K)-Cl	5.51	496	249
29	EWE	M hard water	Medium	Mg-Cl	Ca-(Mg)-Cl	6.5	67	33
30	EWE	Soft water	V.High	Mg-Cl	Ca-(Mg)-Cl	5.45	295	148
31	EWE	Soft water	High	Na-Cl	Na-(K)-Cl	7.2	108	54
32	ALLUVIUM	Soft water	High	Na-Cl	Na+K			

#### 4.6.6 Source of Chloride in Groundwater

Chloride is the dominant anion in groundwater systems. Chloride decreases with an increase in bicarbonate in groundwater (Figure 4.38a). An investigation of the chloride sources is important in order to verify the water sources and recharge on the one hand, and the groundwater quality, on the other. Identifying chloride sources is important in the validation of groundwater vulnerability.

Chloride is a conservative mineral and assumed to originate from the sea. Chloride in groundwater is deposited through wet and dry depositions through precipitation and rainout effect (Hainsworth *et al.*, 1994; Guan *et al.*, 2010). A low Ca/Mg ratio of 0.18 suggested by Hem (1992) may indicate salt-water intrusion. This means value much above the ratio suggest fresh water. The low value of one for the majority of Season 1 samples, suggest an influence of the sea through precipitation on the shallow groundwater. This is possible because of the high Cl concentration in seawater that enriched marine drift with Cl, while the higher values recorded during Season 2 prove the effect of dilution in the wet season (Figure



4.38b). It should, however, be noted that the dominant chemical compositions of fresh groundwater should be Ca-HCO<sub>3</sub> due to its geology sources, but Vengosh (2003) noted its variability depending on climate, region and air mass/ wind direction. Chloride that is not accounted for by precipitation (Table 4.21) can logically be assigned to leaching of sediments or evaporite and pollutions caused by humans.

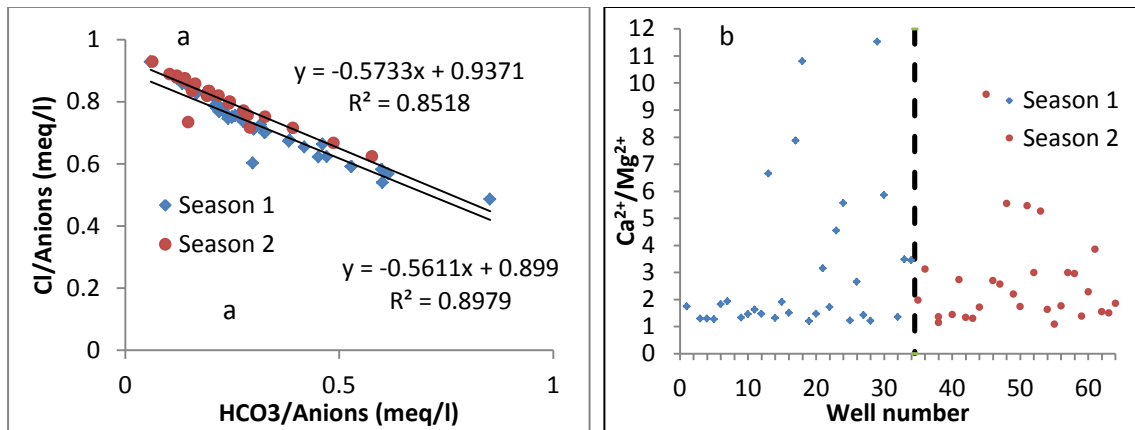


Figure 4.38: (a) Dominant anion ratio plots and (b) plots of Ca<sup>2+</sup>/Mg<sup>2+</sup> ratio

Table 4.21: Rainwater chemistry in (meq/l)

	Ca <sup>+2</sup>	Mg <sup>+2</sup>	Na <sup>+</sup>	K <sup>+</sup>	Cl <sup>-</sup>	HCO <sub>3</sub>	NO <sub>3</sub>	SO <sub>4</sub>	pH	EC	TDS
	meq/l	meq/l	meq/l	meq/l	meq/l	meq/l	meq/l	meq/l	meq/l	meq/l	meq/l
Agege	0.043	0.037	0.067	0.006	0.044	0.028	0.0048	0.037	5.17	14.82	9.7
Alagbado	0.177	0.104	0.094	0.014	0.099	0.111	0.0187	0.074	5.86	35.6	26.7
Lagos Island	0.029	0.031	0.063	0.003	0.017	0.021	0.0010	0.033	5.14	10.1	7.6
Epe	0.05	0.041	0.070	0.004	0.017	0.021	0.0019	0.031	5.19	10.7	8
Shagamu	0.225	0.148	0.104	0.016	0.113	0.115	0.0274	0.081	5.9	39.72	29.8

The predominance of chloride waters, particularly in the dry season, may be because of several processes other than precipitation:

- Advection and diffusion of saline fluid entrapped in an aquitard connected to an active aquifer (Vengosh, 2013).
- Dissolution of soluble salts, such as halite within the aquifer. This possibility is low, because the result of geochemical modelling shows halite under saturation in the waters (Table 4.23).
- The presence of anthropogenic sewage/ wastewater and septic tank effluent, especially in poor urban slums. Water samples from congested areas show high chloride and TDS, particularly during the dry season. Further, highlight on the urbanisation effect on groundwater quality areas of the Dahomey Basin and West African cities was reviewed by Ocheri *et al.* (2014), Taylor *et al.* (2005) and Adelana *et al.* (2003, 2004, 2005, 2008).
- Dissolution of evaporite minerals in the aquifer or vadose material after regression of marine waters.

The last two points are the most probable situation. This is because the Dahomey Basin is a regressive marine depositional environment and the basin formations resulted from marine transgression and regression (Adegoke, 1969; Adegoke *et al.*, 1970; Adegoke *et al.*, 1980; Nton, 2001). The formation of the basin has been discussed extensively in Chapter 3. Dissolution of evaporite minerals has been fingered to be responsible for similar basins with the geologic structure, for example the Dahomeyan Plain of Accra (Glover *et al.*, 2012), the Ogallala Formation of Texas in the United States of America (USA) (Mehta *et al.*, 2000), the Damman aquifer in Kuwait (Al-Ruwaiy, 1995) and the Nubian sandstone aquifer in Sinai and Negev (Rosenthal *et al.*, 1998).

The deduction from the above is that chloride and other ions in the dry season water shows a mixture of several processes, including water rock interactions and evaporation, more than that of the rainy season water. This suggests an intense reaction between chloride and other ions in the groundwater during the dry season. Therefore, the dry season chloride will be employed as a groundwater vulnerability validation tool in Chapter 8.

#### **4.6.7 Microbiological Load in Groundwater of the Dahomey Basin**

The African shallow aquifer system has always been at risk to a surface contaminant. In a study by Xu and Usher (2006), 11 African countries were assessed for aquifer pollution vulnerability, and microbiological contaminants ranked among factors polluting shallow groundwater. Microbiological contaminants move as suspended particles through the subsurface water. Polluted groundwater harbours a population of bacteria, protozoans and virus pathogens. The importance of microbial contaminants in aquifer vulnerability studies is necessary because most pathogens survive longer in aquatic environments and can therefore serve as a validation tool. Goel (2006) reported *Salmonella* survival a considerable distance from their release in rivers.

Table 4.22 shows the total viable plate counts obtained from Season 2 water samples. The table indicates the total result of organisms on each plate of different locations and the type of agars used for total heterotrophic, *Escherichia coli* (*E. coli*) and *Salmonella Shigella* count. According to the WHO (2002) and the Nigerian Administration for Food and Drug Control (NAFDAC, 2011) standard, a satisfactory value standard limit set for drinking water that is free of microorganisms is  $1.0 \times 10^3$  CFU/mL. The highest value of total heterotrophic is  $7.0 \times 10^4$ , total *E. coli* count  $6.0 \times 10^4$  and total *Salmonella/ Shigella* counts of  $6.0 \times 10^4$  were detected in the water samples. These are not in line with the standard limit for drinking water.

The results indicate higher THBC–total heterotrophic bacteria counts and TECC–Total *E. Coli* counts for water sourced from populated urban settlements compared to peri-urban settlements. Likewise, shallow large diameter wells shows a higher pathogen content than the deep boreholes. This demonstrates the higher contributing factors of dug wells to the vulnerability tendency of the shallow aquifer system. Surface water recharging groundwater also shows greater microbial load. The microbiological polluting sources include pit latrines,

graves, waste disposal and poor urban planning. It is important to consider population and urban settings when characterising microbial influences on shallow aquifers.

Consumption of these contaminated waters containing faecal matter may result in severe health hazards. Salmonella bacteria are common species implicated in water-borne diseases to man and animal (Goel, 2006). Common Salmonella infections are typhoid, paratyphoid and food poisoning. Shigella is the causative agent of bacillary dysentery, while infantile diarrhoea, caused by E. coli, is common among little children.

Microorganisms, however, also serve useful purposes in groundwater attenuation. The shallowest groundwater contains dissolved oxygen near the water table. This shallow groundwater supports aerobic microorganisms that can degrade a wide range of organic compounds, including petroleum hydrocarbons. Zhang *et al.* (2006) noted that the extent of bio-degradation would depend on the oxygen concentration. Groundwater with a higher DO records less microbiological loads (Table 4.22). This, however, varies with the type of microbial load, but the higher the THBC, the lower the dissolved oxygen and the biodegradation tendency. THBC and DO can serve as validation tools for the aquifer vulnerability.

Table 4.22: Total Plate Count on general and differential media counts (Total Viable CFU/mL×10<sup>3</sup>)

Sample code	DO	THBC	TECC	TSSC	Sample code	DO	THBC	TECC	TSSC
1 BW	7.5	1.0×10 <sup>3</sup>	1.0×10 <sup>3</sup>	1.0×10 <sup>3</sup>	16 BW	2.0	1.0×10 <sup>3</sup>	1.5×10 <sup>4</sup>	0×10 <sup>3</sup>
2 BW	6.0	1.5×10 <sup>4</sup>	1.8×10 <sup>4</sup>	0×10 <sup>3</sup>	17 BW	0.5	5.2×10 <sup>4</sup>	2.0×10 <sup>4</sup>	0×10 <sup>3</sup>
3 BW	5.2	1.0×10 <sup>3</sup>	3.0×10 <sup>4</sup>	0×10 <sup>3</sup>	18 BW	1.7	1.0×10 <sup>4</sup>	1.0×10 <sup>4</sup>	0×10 <sup>3</sup>
4 WW	3.8	2.0×10 <sup>4</sup>	1.0×10 <sup>3</sup>	0×10 <sup>3</sup>	19 BW	0.8	2.0×10 <sup>4</sup>	1.0×10 <sup>3</sup>	0×10 <sup>3</sup>
5 WW	2.3	3.0×10 <sup>3</sup>	3.0×10 <sup>4</sup>	0×10 <sup>3</sup>	20 WW	0.5	2.2×10 <sup>4</sup>	6.0×10 <sup>4</sup>	0×10 <sup>3</sup>
6 WW	5.2	1.0×10 <sup>3</sup>	2.0×10 <sup>3</sup>	0×10 <sup>3</sup>	21 WW	1.2	2.0×10 <sup>3</sup>	4.0×10 <sup>4</sup>	0×10 <sup>3</sup>
7 WW	2.2	3.5×10 <sup>4</sup>	2.0×10 <sup>3</sup>	0×10 <sup>3</sup>	22 WW	2.0	1.8×10 <sup>4</sup>	9.0×10 <sup>3</sup>	0×10 <sup>3</sup>
8 WW	2.4	4.5×10 <sup>4</sup>	5.0×10 <sup>4</sup>	0×10 <sup>3</sup>	23 WW	4.7	4.0×10 <sup>4</sup>	2.0×10 <sup>4</sup>	0×10 <sup>3</sup>
9 WW	1.3	7.0×10 <sup>3</sup>	4.0×10 <sup>3</sup>	0×10 <sup>3</sup>	24 BW	0.8	3.0×10 <sup>4</sup>	5.0×10 <sup>3</sup>	0×10 <sup>3</sup>
10 BW	0.6	4.0×10 <sup>3</sup>	2.0×10 <sup>3</sup>	5.0×10 <sup>3</sup>	25 WW	0.6	2.9×10 <sup>4</sup>	2.0×10 <sup>4</sup>	2.5×10 <sup>3</sup>
11 WW	0.9	2.0×10 <sup>4</sup>	1.0×10 <sup>3</sup>	0×10 <sup>3</sup>	26 BW	2.5	2.0×10 <sup>4</sup>	2.0×10 <sup>3</sup>	0×10 <sup>3</sup>
12 WW	0.9	3.0×10 <sup>3</sup>	5.0×10 <sup>3</sup>	0×10 <sup>3</sup>	27 WW	1.8	2.1×10 <sup>4</sup>	2.1×10 <sup>4</sup>	0×10 <sup>3</sup>
13 WW	0.4	2.2×10 <sup>4</sup>	2.0×10 <sup>4</sup>	0×10 <sup>3</sup>	28 WW	0.6	2.0×10 <sup>4</sup>	3.1×10 <sup>4</sup>	0×10 <sup>3</sup>
14 BW	1.6	1.0×10 <sup>3</sup>	1.0×10 <sup>4</sup>	1.0×10 <sup>3</sup>	29 WW		7.0×10 <sup>4</sup>	1.0×10 <sup>3</sup>	0×10 <sup>3</sup>
15 BW	0.6	1.0×10 <sup>3</sup>	1.2×10 <sup>4</sup>	3.0×10 <sup>3</sup>	30 BW		6.0×10 <sup>4</sup>	1.0×10 <sup>3</sup>	0×10 <sup>3</sup>

Key:

- BW = Borehole water
- WW = Well water
- DO = Dissolved oxygen
- THBC = Total heterotrophic bacteria counts
- TECC = Total E. coli counts
- TSSC = Total Salmonella/ Shigella counts

#### 4.6.8 Aqueous Geochemical Characteristics

Major elements and trace metals are transported in compounds through groundwater. Concentrations of groundwater anions and cations form complex associations. Aqueous complexes characterisations are important in vulnerability studies, because the bioavailability and toxicity of metals in groundwater depends on aqueous speciation or

complexation of the metals (Langmuir, 1997). Water rock interactions are also responsible for higher dissolution of solids in the Dahomey Basin groundwater.

The Saturation Index (SI) is used to predict possible chemical reactions and evolution of the groundwater. The SI result is used as an indicator of rock types that where responsible for the chemical constituents dominant in the water chemistry (Belkhiri and Mouni, 2013). Saturation index (SI) of water samples was calculated as:

$$SI = \log_{10} (IAP/K_{sp})$$

*Equation 4.11*

Where IAP is the ion activity product and  $K_{sp}$  is the solubility product at a given temperature.

The derived SI values are interpreted as follows: When Si is below 0, the water is undersaturated with respect to the mineral in question. If Si is 0, it means that the water is in equilibrium with the mineral, while SI values greater than 0 means a supersaturated aqueous solution with respect to the mineral in question. The SI result of groundwater samples is presented in Table 4.23.

The results show that the Dahomey Basin water samples are supersaturated with respect to quartz (0.72–4.37), albite (1.86–9.07), kaolinite (5.89–14.19), goethite (3.08–10.2) and hematite (8.21–22.63). This indicates the effect of weathering and ferrugenisation. They are undersaturated with respect to halite and gypsum (evaporite minerals). Calcite and dolomite varies between oversaturated, neutral and undersaturated, in line with water from limestone predominant rock types, transitional zones and rock types rich in sandstone. Chloride and bicarbonate ions dominate the study area, but the source of the chloride concentrations are not limited by mineral equilibrium and could not be from brine water, as shown in Table 4.26, with an undersaturation of halite. This gives credence to the other sources of chloride in the groundwater.

Calcite was supersaturated with samples from the Abeokuta and Ewekoro Formations that are sandstone–limestone mixed rocks, but was undersaturated with water samples from the Alluvium, Ilaro and Benin Formations which are predominantly sandstone. Calcite precipitation is reported to occur in a basin with decreased salinity, namely mixing of low and high salinity waters (Bricker, 1971; Dreybrodt, 1988). This may agree with the rock types of the Ewekoro and Abeokuta Formations. The Ewekoro Formation is predominantly thick-bedded limestone rocks, while the Abeokuta Formation contains lenses of limestone beds.

In relation to groundwater geochemical vulnerability, further examinations and influences of the quartz–albite–iron rich minerals dominating all the rock types in the Dahomey Basin is important. Quartz is known to be very resistant to weathering, but weather to form clay formations (Goldich, 1938). The degree at which quartz-rich aquifers is susceptible to vulnerability is determined by other factors such as the degree of cementation with other minerals, grain shape, compaction and type of external contaminant. Shale, limestone, sandstone and alluvium are the major rock types in the Dahomey Basin (Chapter 3) and contain varying degrees of quartz in their composition. They weathered to form kaolin-rich clay (XRD in earlier section) which is important in groundwater vulnerability attenuations.

Super-saturation of kaolinite and its precipitation also suggests possible attenuation capacity, mostly during the dry season when the groundwater level is low. The saturation index also shows that dissolution is higher in the dry season (Season 1) than the rainy season (Season 2). This is especially for minerals such as albite, calcite and quartz (Table 4.23). Therefore, the water samples of the dry season will best be suited to validate vulnerability maps of the Dahomey Basin to background concentration of natural processes in the groundwater.

Water chemistry in carbonate terrains, especially limestone aquifers, is complicated by the fact that they are more affected by the chemistry of the aquifer materials, which includes dolomites and iron. When high calcites with magnesium-rich components are placed in water, they initially dissolve congruently (the entire solid dissolves), but as the concentration of ions in the solution increases, dissolution becomes incongruent (Plummer and Mackenzie, 1974; Bischoff *et al.*, 1987). Saturated indices plot (Figure 4.39) show that for equilibrium to be achieved and precipitation of calcite to occur, the magnesium calcite dissolution rate must double that of the calcium calcite in the study area. There is consensus that calcites containing some magnesium are more stable than pure calcite (Drever, 2002).

Kaolinite and albite super-saturation in the water sample show that the clay minerals are being washed into the groundwater system from either the vadose zone or the clay within the aquifer system. Under-saturation of halite suggests that the salinisation water type of the groundwater is not from chloride present in the deposited minerals.

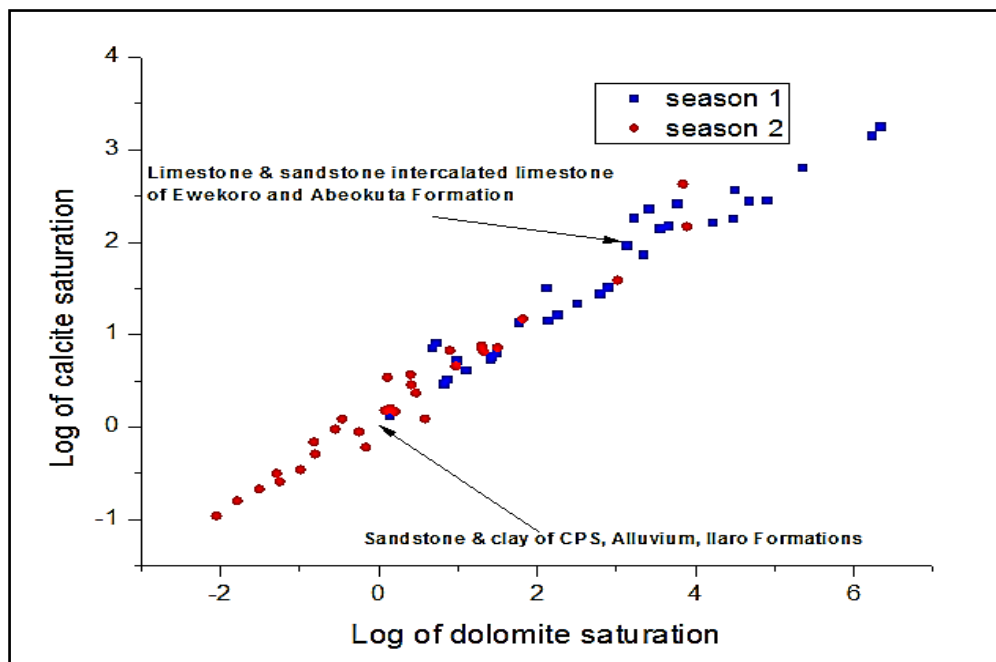


Figure 4.39: Saturated indices of calcite dissolution and precipitation

Table 4.23: SI indices values of the Dahomey Basin groundwater

Sample	Rock type	Quartz	Calcite	Albite	Dolomite	Kaolinite	Goethite	Hematite	Halite	Gypsum
Season 1		SiO <sub>2</sub>	CaCO <sub>3</sub>	NaAlSiO <sub>8</sub>	CaMg(CO <sub>3</sub> ) <sub>2</sub>	Al <sub>2</sub> Si <sub>2</sub> O <sub>5</sub> (OH) <sub>4</sub>	Fe <sub>3</sub> <sup>+</sup> O(OH)	Fe <sub>2</sub> O <sub>3</sub>	NaCl	CaSO <sub>4</sub> (H <sub>2</sub> O)
1	ABK	2.24	2.45	6.94	4.67	11.4	9.62	21.28	-3.95	-0.61
2	ABK	1.38	2.27	3.24	3.21	9.53	9.49	21.01	-5.13	-0.83
3	EWE	1.92	1.45	6.41	2.79	12.77	8.48	19.00	-3.83	-1.16
4	ILA	1.91	0.77	5.17	1.41	10.6	8.85	19.73	-4.54	-1.92
5	CPS	1.99	0.47	4.47	0.82	10.54	6.22	14.46	-4.3	-1.5
6	CPS	2.14	2.81	8.57	5.34	13.68	8.71	19.43	-2.96	-0.79
7	CPS	2.12	0.26	9.07	6.33	13.47	9.4	20.85	-2.57	-0.67
8	ALLUVIUM	2.29	2.37	7.45	3.4	14.19	8.04	18.10	-4.49	-0.4
9	ALLUVIUM	1.85	0.62	4.57	1.09	10.48	6.27	14.56	-4.35	-1.46
10	ILA	1.8	0.52	4.6	0.86	10.54	7.53	17.09	-4.52	-1.91
11	ABK	1.78	1.22	5.27	2.25	10.51	7.98	18.00	-4.21	-1.66
12	ABK	1.85	1.16	4.53	2.13	10.12	7.51	17.05	-4.65	-1.29
13	EWE/OSH	1.79	1.97	4.86	3.12	10.52	8.01	18.04	-4.78	-0.62
14	EWE/OSH	1.79	1.51	3.97	2.11	10.27	6.56	15.14	-4.85	-2.19
15	EWE	1.89	1.52	5.48	2.89	11.74	8.74	19.53	-4.05	-1.67
16	ALLUVIUM	1.77	0.86	4.69	1.48	10.18	8.67	19.39	-4.69	-1.13
17	CPS	1.71	0.13	4.21	0.13	9.55	8.73	19.51	-4.9	-1.32
18	CPS	1.87	0.86	4.29	0.67	11.32	6.31	14.66	-4.96	-1.09
19	CPS	1.72	0.74	4.21	1.4	10.27	7.43	16.89	-4.6	-1.76
20	CPS	1.76	1.34	5.01	2.5	9.8	8.93	19.83	-4.73	-1.01
21	CPS	1.68	0.73	3.91	0.98	10.57	6.61	15.27	-4.91	-1.58
22	CPS/ILA	1.92	2.22	7.72	4.21	13.07	9.09	20.21	-3.51	-0.84
23	CPS/ILA	1.96	2.57	7.46	4.49	12.52	9.22	20.47	-3.73	-0.83
24	EWE/OSH	0.72	2.18	1.86	3.65	5.89	8.36	18.75	-4.21	-1.76
25	EWE/OSH	1.85	2.46	6.94	4.89	10.35	9.78	21.59	-3.67	-1.47
26	ILA	1.98	1.87	6.02	3.33	10.53	8.84	19.71	-3.78	-1.14
27	ILA	1.91	0.92	7.63	0.72	11.18	9.35	20.74	-3.4	-0.78
28	CPS	1.93	2.26	6.89	4.47	11.23	9.33	20.70	-3.29	-1.13
29	EWE	2.01	2.42	5.77	3.76	11.18	8.99	20.00	-4.78	-0.85
30	EWE	2.33	2.15	8.47	3.54	15.95	10.28	22.59	-4.46	-0.72
31	EWE	1.87	3.16	5.34	6.22	13.31	6.52	15.07	-4.8	-1.07
32	ALLUVIUM	1.78	0.81	4.78	1.48	11.11	8.42	18.86	-4.67	-1.54
33	ABK	1.82	1.14	4.76	1.76	10.86	8.65	19.33	-4.64	-1.79

Sample	Rock type	Quartz	Calcite	Albite	Dolomite	Kaolinite	Geothite	Hematite	Halite	Gypsum
34	ABK	1.84	4.77	11.46	8.67	19.23	8.0	19.4	-4.78	-1.89
Season 2										
1	ABK	1.13	0.18	-3.16	0.08	7.1	5.87	13.78	-4.98	-0.85
2	ABK	1.64	-0.02	3.07	-0.55	11.07	5.78	13.6	-5.29	-1.43
3	EWE	1.69	2.63	4.77	3.84	10.01	10.06	22.16	-5.11	-1.8
4	ILA	1.4	-0.96	1.89	-2.05	9.42	3.08	8.21	-4.59	-1.25
5	CPS	1.49	-0.46	3.85	-0.99	11.76	5.03	12.09	-4.72	-2.52
6	CPS	1.57	-0.67	3.8	-1.51	11.05	5.02	12.08	-4.47	-2.73
7	CPS	1.55	0.85	5.06	1.3	9.78	8.95	19.92	-4.14	-0.25
8	ALLUVIUM	1.51	0.17	5.21	0.21	12.54	6.68	15.75	-4.51	-2.26
9	ALLUVIUM	1.61	-0.05	4.49	-0.25	12.2	4.9	11.82	-4.58	-2.67
10	ILA	1.67	0.37	5	0.47	11.8	7.31	16.64	-4.68	-3.09
11	ABK	1.67	0.54	4.27	0.11	11.44	6.34	14.72	-5.05	-2.14
12	ABK	1.64	0.88	5.09	1.3	11.5	9.84	21.71	-4.82	-2.03
13	EWE/OSH	1.51	2.17	4.12	3.89	9.66	10.29	22.63	-4.84	-2.58
14	EWE	1.66	0.83	4.9	0.9	11.64	7.86	17.76	-4.9	-2.01
15	EWE	1.66	0.66	4.47	0.97	11.06	8.54	19.11	-4.92	-2.36
16	ALLUVIUM	1.52	-0.29	3.55	-0.8	11.35	3.84	9.74	-4.55	-2.35
17	CPS	1.66	0.09	4.1	0.58	11.36	6.54	15.1	-4.92	-2.35
18	CPS	1.62	0.46	4.95	0.41	12.47	7	16.02	-4.62	-1.37
19	CPS	1.62	0.57	4.3	0.4	10.98	7.48	16.99	-5.02	-2.06
20	CPS	1.62	-0.8	3.1	-1.79	9.84	3.59	9.24	-4.29	-3.04
21	CPS	1.66	-0.59	4.18	-1.25	11.42	5.79	13.6	-4.92	-1.73
22	CPS/ILA	1.59	0.2	4.16	0.15	10.58	7.03	16.10	-4.81	-2.48
23	CPS/ILA	1.64	-0.16	4.21	-0.82	11.5	5.84	13.71	-4.62	-1.14
24	EWE/OSH	1.75	1.17	5.6	1.82	10.49	11.3	24.61	-4.73	-1.54
25	EWE/OSH	1.59	1.59	6.44	3.02	11.7	9.11	20.25	-3.89	0.04
26	ILA	1.67	0.82	4.58	1.32	10.32	9.08	20.19	-5.02	-2.32
27	ILA	4.37	0.09	4.37	-0.46	11.96	7.04	16.10	-5.16	-2.27
28	CPS	1.69	0.86	5.6	1.5	12.13	7.12	16.27	-4.32	-1.06
29	EWE	1.74	-0.22	4.37	-0.16	11.37	4.25	10.54	-4.34	-1.9
30	EWE	1.89	-0.5	4.68	-1.29	12.51	5.64	13.32	-4.81	-1.38
31	EWE	1.61	0.45	3.08	0.68	7.41	7.48	16.99	-4.79	-2.72
32	ALLUVIUM	1.63	-0.94	2.65	-2.1	8.37	3.75	9.54	-4.75	-2.9

#### **4.6.9 Conclusion**

The hydrochemical characteristics of the Dahomey Basin were assessed based on the chemical concentrations that are present in the aquifer. The shallow unconfined groundwater indicates both the roles of anthropogenic, and geogenic influences of the Dahomey Basin groundwater quality. Elements such as chloride, total dissolved solids, electrical conductivity, salinity and microbial load records concentrations of concern. Water types include Na-Cl water at the southern end of the study site and areas closer to the sea, and Ca-Mg-Cl water types at the northern end. Geological and geohydrological information derived from the characterisation of the Dahomey Basin presented in this chapter will be used in the applications and validation of the proposed vulnerability method for data scarce areas, and in the assessment of the basin intrinsic properties with other vulnerability methods.



# CHAPTER 5

## PROPOSED SIMPLIFIED VULNERABILITY APPROACH FOR DATA SCARCE AREAS

### 5.1 Introduction

A major decision in the development of vulnerability methods is the availability of input data for the hydrogeological system under consideration. Different geological environments require different vulnerability methods. For example, karst landforms or fractured terrains require vulnerability methods that factors in the karstification and nature of fractures in their respective vulnerability methods (Goldscheider *et al.*, 2000; Goldscheider, 2002). There are challenges when using the most established vulnerability methods to assess areas with limited data. Therefore, there is a need to establish a simple groundwater vulnerability methodology that addresses the challenges of limited hydrogeological data. The developed vulnerability method must be designed to use few hydrogeological parameters to assess groundwater vulnerability. The developed vulnerability method could target the assessment of resources (regional water table) or sources (well or spring); the protection of groundwater resources, target pathways and layers above the groundwater table. Sources protection target water in springs or wells, including mostly horizontal pathways in the aquifer (Goldscheider *et al.*, 2000).

### 5.2 The Concept of the Rainfall–Travel Time Method

The subjective vulnerability method that is developed to address this gap is the Rainfall–Travel time (RTt) method. This method is based on the diffuse recharge through a specified soil thickness with the assumption of precipitation as the driving force in the vertical infiltration and subsequent percolation that recharges the groundwater. The RTt method employs the objective as well as subjective based vulnerability techniques. The major condition in the use of the RTt method is to understand the basic parameters, namely soil, rock, hydraulic conductivity, porosity, bed thickness and topography. The RTt method stands on the basis that the rate of rainfall infiltration and lithology must be known, and the dissolved solute contaminants in the infiltrating water would travel at the same infiltration rate as water (Figure 5.1 and Figure 5.2).

The RTt acronym is derived from the initial letters of the factors used in the formula: Rainfall (R) and advective travel time (Tt) of fluid. This concept was originally defined by the European Groundwater Vulnerability Approach, origin–pathway–target (Daly, 2002; Zwahlen, 2004). The European approach states that vulnerability methods must be flexible and allow for local conditions, including geology, information availability, time and resources. In data scarce areas, resources and scientific information availability is the most challenging. This European approach is the basic concept behind many other methods such as COP (Vias *et al.*, 2006), PI (Goldscheider *et al.*, 2000), the Slovene approach (Ravbar, 2007; Ravbar and Goldscheider, 2007) and the Irish approach (Daly and Drew, 1999).

The basis for using the European approach is because it can be applied using different levels of available data. This is applicable to the purpose of the research, which is to develop a vulnerability assessment method designed for data scarce areas. The RTt method is designed for onsite vulnerability assessment and is accompanied with a spreadsheet (Appendix A) that can calculate the vulnerability impact while mapping.

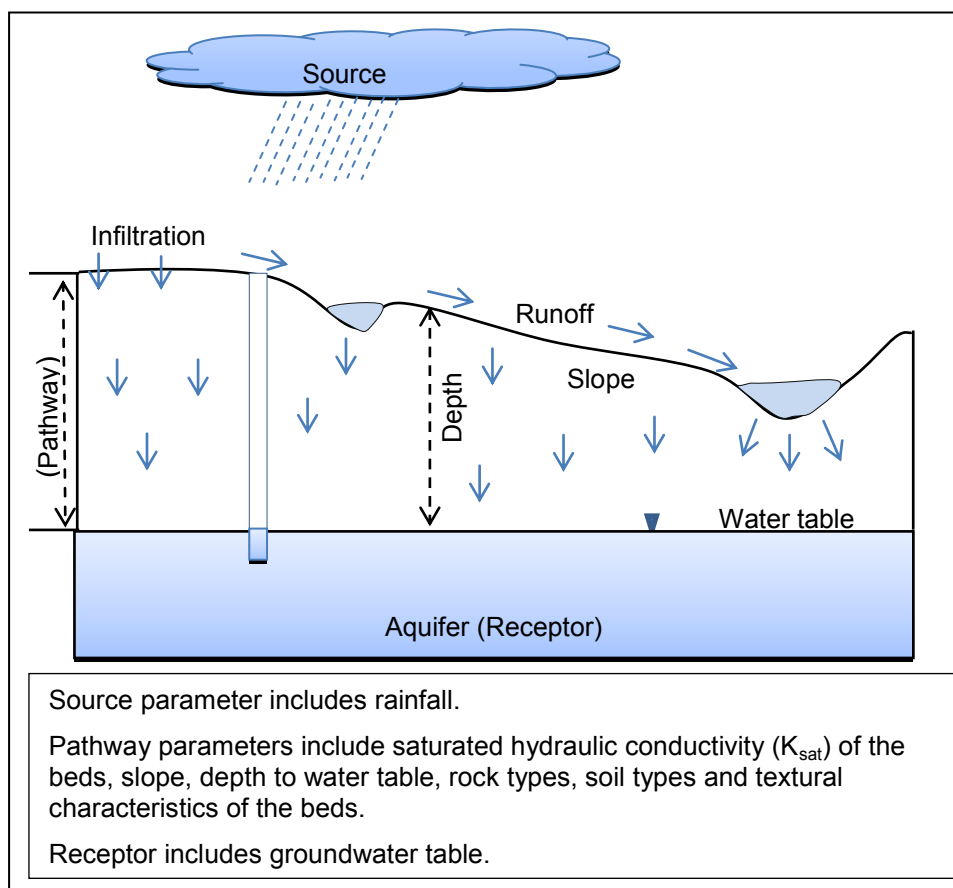


Figure 5.1: Idealised illustration of the RTt model derived from the Source–Pathway–Receptor concept of the European Vulnerability Approach

The R-factor is the amount of precipitation that a site receives, which therefore represents the potential for infiltration and subsequent percolation into the aquifer. This is determined by the estimation of the mean rainfall, which depends on the climatic conditions. The Tt-factor is the assumed advective travel time expected of infiltrating water to move from the surface to the water table. The travel time of concern in the RTt method is the first arrival time of contaminated water from the ground surface, assuming the contaminants travel at the advective groundwater velocity (Figure 5.2).

The RTt method is designed with few parameters, following the concept of the source–pathway–receptor model (Figure 5.1). Due to the limitation of the parameters employed in the formulation of the RTt method, it cannot be used as a complete vulnerability tool (because comprehensive vulnerability assessment requires all possible information on

aquifer vulnerability). It should be noted that the RTt method is designed for regions with scarce or limited data. Areas assessed with the RTt method should always be reassessed with other vulnerability methods whenever new data is available. This should be done in order to account for the weaknesses contained in the method. However, since no vulnerability method is completely effective, areas that have been assessed with the established vulnerability methods can also be reassessed with the RTt method.

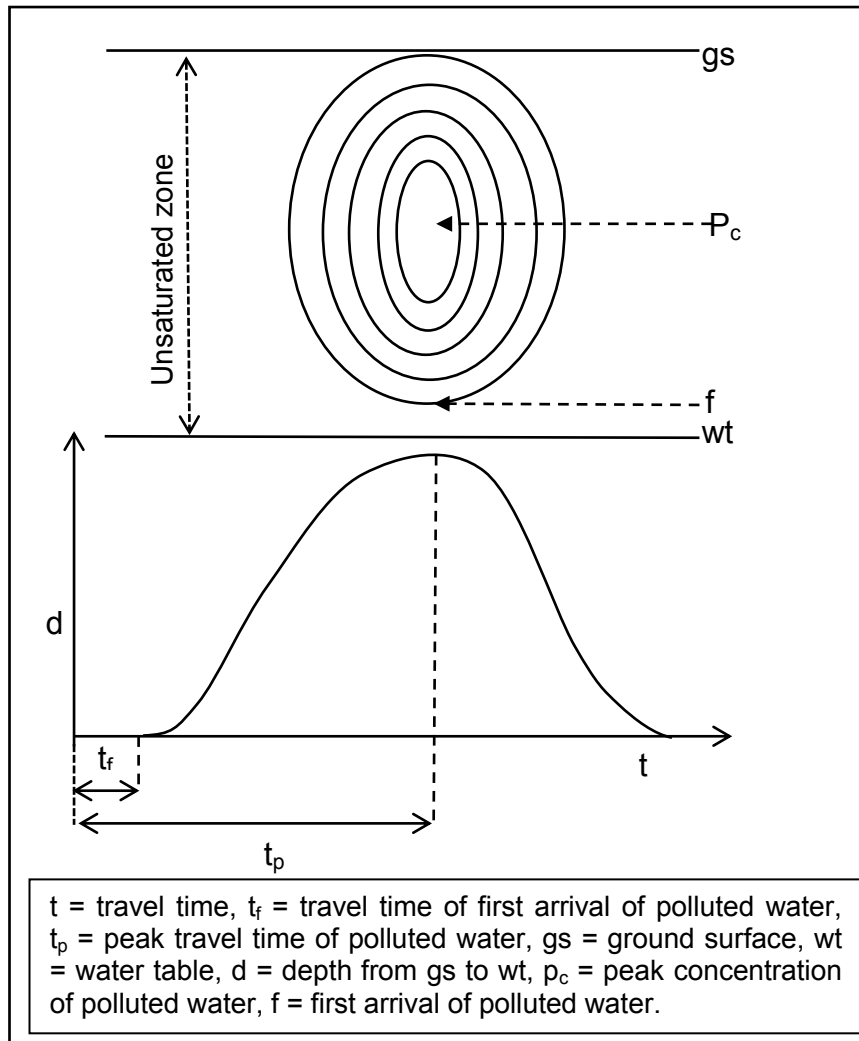


Figure 5.2: Conceptualised flow of contaminated water in the RTt vulnerability method

### 5.3 The Rainfall Factor

The R-factor in the RTt method evaluates the amount of water from precipitation available to percolate and migrate down to the groundwater. Precipitation was chosen because of the following reasons:

- It is accessible to many researchers (Mahe *et al.*, 2008).
- It is inexpensive to collect over wide areas.

- It is the most suitable parameters that can substitute contaminant travelling from the ground surface to the water table. This is because water usually transports contaminants.

It is noticed that most established vulnerability methods consider the intensity, duration, temporal distribution and frequency of precipitation (Daly, 2002), which data is difficult to measure, but important to complete vulnerability estimation. Higher rainfall quantities and intensities mean more surface flow, higher transport velocities, shorter transit times, more turbulent flow, effective transport of sediments, microbial pathogens and particle-bound chemical contaminants, and thus higher vulnerability (Ravbar and Goldscheider, 2007).

However, precipitation quantity and distribution will only be considered in the RTt method due to the above reasons. Quantification and distribution of precipitation is very important in the RTt method because it influences infiltration. Precipitation considered here is the annual rainfall average over a wide area (regional scale). This gives a sense of rainfall distribution and the amount of water that can potentially recharge aquifers while transporting surface contaminants into the aquifer.

An issue identified with the rainfall in vulnerability studies is the dilution effect. Vias *et al.* (2006) states in the COP method that precipitation of up to 800–1 200 mm increases vulnerability, because the transit time of contaminants from surface to groundwater is likely to be more important than the dilution process. The COP method argued that if annual precipitation exceeds 1 600 mm, it is expected for dilution to be dominant (Vias *et al.*, 2006). This is against the idea of Civita (1994) in SINTAC method who proposed a reduction in vulnerability when recharge is higher than 300–400 mm/year. However, the RTt method assumed that irrespective of dilution, this does not reduce the concentrations of migrating contaminant travelling to the water bodies. RTt is concerned mainly with the first arrival at the water table (Figure 5.2). Therefore, areas with annual precipitation exceeding 1 600 mm will conceptually have an increased potential for infiltration on the ground surface and therefore groundwater recharge. The method assumes that there will be no run-off, whilst areas of precipitation below 400 mm will have less percolation and groundwater recharge (Table 5.1).

### **5.3.1 Rating and Assumption of the Rainfall Factor**

The R-factor is rated based on the quantity of precipitation received over an area. The R-factor assumes that the higher the amount of rainfall over an area, the greater the potential infiltration, percolation and the subsequent groundwater recharge, while the opposite is equally true. These assumptions, however, cannot be generalised. Its usage should be based on factors such as climatic condition over an area, intensity of precipitation, slope and top soil conditions. For example, in arid regions receiving less than 400 mm of precipitation and which have high evapo-transpiration, groundwater recharge through precipitation is generally limited. In general, groundwater recharge through precipitation is possible in the arid region if there is high rainfall intensity within a very short period, thereby creating pools of water readily available to infiltrate and percolate the subsurface than flow

through surface run-off. This is assuming that other factors such as soil types and topography are right. These conditions are not considered in the R-factor rating.

In the RTt method, rainfall is assumed as the driving force for infiltrating contaminants. This means rainfall is expected to be available before vertical seepage is possible, as contaminants are usually transported in water. The R-factor rating therefore assigned the maximum weight value of five to areas exceeding 1 600 mm, and a lowest weight of one to areas receiving less than 400 mm of rainfall (Table 5.1). Similar to assigning the maximum weight of rainfall, is the stagnant water bodies or released stagnated pollutant on the land surface. However, in regions where the amount of rainfall is annually very low (<400 mm/year), the lowest weight value will be assigned. Low R-factors also include areas which experience high precipitation over a very short time. In general, when the rainfall intensity is greater than the infiltration rate, the rainwater is likely to run off rather than infiltrate to recharge the groundwater. This will also depend on the nature of the surface topography.

*Table 5.1: Rainfall rating of the RTt method*

<b>Rainfall (mm)</b>	<b>Weight</b>
>1 600	5
1 200–1 600	4
800–1 200	3
400–800	2
<400	1

### **5.3.1.1 Local Adaptation**

The rating in Table 5.1 is proposed for mapping regional vulnerability or wide (regional) hydrogeological areas, particularly in data limited areas. However, actual recharge can substitute for the rainfall at local scale. The recharge can be measured using the various groundwater recharge methods such as the chloride mass balance method, water balance method, water table fluctuations method and so on (Risser *et al.*, 2005). The use of recharge would enable the application of the RTt method at local scales and the rainfall-travel time would become recharge-travel time method. This is mainly because unlike rainfall, which is generally estimated to be the same for particular region, recharge also spatially varies over small areas as influenced by subsurface heterogeneity. Table 5.2 shows the proposed recharge rating factors for the RTt method.

*Table 5.2: Recharge rating of the RTt method*

<b>Recharge (mm/year)</b>	<b>Weight</b>
>400	5
300–400	4
200– 300	3
100–200	2
<100	1

### 5.3.2 Conditions Influencing Percolation

Conditions that determine if rainwater will recharge groundwater, or flow as run-off, are presented by Goldscheider (2002). The most notable conditions include:

- Infiltration with subsequent percolation.
- Surface flow.
- Subsurface flow.

The dominating process out of these will depend on both the soil properties of the site and the characteristics of the rainfall event, as well as the previous precipitation history and the degree of saturation of the soil.

Diffuse infiltration of rainwater from the surface into the soil and the subsequent downward percolation through the soil is the dominant hydrological process if the rainfall intensity is less than the capacity of the soil to absorb the water. Also, if the hydraulic conductivity of the total soil profile is high enough to allow downward movement of the water. Gentle slopes, dense vegetation, especially forest cover and coarse textured soils with thick organic horizons, and stable peds favour infiltration (Dyck and Peschke, 1995).

Surface flow (run-off) occurs when not all of the rainwater is able to penetrate the soil surface. There are two main types of surface flow:

- **Hortonian run-off** occurs when the intensity of a rainfall event exceeds the infiltration capacity of the topsoil and the surplus rainwater flows away on the surface. The necessary condition for Hortonian run-off is that the intensity of the rain is significantly higher than the vertical hydraulic conductivity of the topsoil. The amount (depth) of surplus water that is sufficient to produce surface run-off is dependent on the slope of ground surface (Peschke *et al.*, 1999).
- **Saturated surface flow** arises when a rainfall event is sufficiently long and intense to saturate the soil and exhaust its absorption capacity. This can also occur if the soil was saturated due to previous precipitation and the additional precipitation cannot infiltrate, but flows away on the surface. This process is favoured when lower permeability layers are present below thin, relatively high permeable topsoil. The necessary condition for this type of flow is that the total amount of precipitation is more than the effective porosity; similar to Hortonian run-off. The amount of surplus water that is sufficiently high to produce surface run-off depends on the ground surface gradient (Merz, 1996).
- **Subsurface flow** occurs when the vertical hydraulic conductivity of the topsoil is high enough to allow the infiltration of rainwater, while lower permeability layers in or below the soil does not allow the further downward percolation to continue. In this case, the layers above the low permeability zone become temporarily saturated, allowing movement parallel to the slope. The velocity of the subsurface flow is strongly dependent on the slope gradient, the hydraulic conductivity of the topsoil and on preferential flow paths.

These conditions are not directly factored into the rating method of the R-factor, because it is based on potential infiltration that will result from the rainfall. However, the processes are important since they indirectly influence infiltration and eventual percolation. An understanding of the infiltration processes will therefore give an insight if percolation is occurring with a rating of five or Hortonian run-off or the subsurface process is dominant with a rating of one.

## 5.4 The Travel Time Factor

Travel time in the RTt vulnerability method is the rate of flow (assuming that infiltration rate equals fluid velocity as presented in Figure 5.1 and Equation 5.1 to 5.4) between the source and receptor, which is the land surface and the water table. This is called the pathway in the European vulnerability approach (Daly, 2002). Water infiltrates into the subsurface and percolates through the unsaturated zone into the groundwater system. Flow in the pathway is dominated by advection, diffusion and dispersion (Sousa *et al.*, 2013). The RTt method considers only the advective flow component of the mass transport mechanism that is mainly dominated by vertical flow from the surface (Gargini and Pranzini, 1994). The RTt method is physically based and conservative for a one dimensional vertical movement (Figure 5.3).

Travel time in the pathway may be faster or slower depending on the lithological and soil properties. Other external influences include worm burrows and plant roots, but these are beyond the scope of this method. Therefore, the unsaturated front in the pathway is negligible and it is assumed that the unsaturated front behave as the saturated front based on advective travel time presented by Sousa *et al.* (2013), since we are concerned with the first arrival of contaminated water (Figure 5.2). Flow conditions may take many forms in saturated or near saturated scenarios for vertical percolation of water. Based on the advective flow, travel time in saturated front (discussed below) is therefore done under some important assumptions.

### 5.4.1 Travel Time Factor Assumptions

Travel time (Equation 5.3) in the proposed method is based on the flow of the saturated infiltrating front. Two methods are commonly used in estimating travel time in saturated front, namely (1) particle tracking association using development and calibration of three 3D flow models, and (2) direct application of Darcy's law observing some basic assumptions (Sousa *et al.*, 2013). Since the aim of the research is to develop an alternative way to classify vulnerability with special focus on data scarce or limited areas, the common Darcy's concept with simplified assumptions is used.

The simplified assumptions for the saturated flow conditions are:

- Annual precipitation must be known with an average estimate over a long period of time (average of 20 years) and it is assumed that rainfall recharge the aquifer (steady state condition).
- That flow will be vertical from the surface to the receptor. There are no flow barriers or artificial recharge. This has been illustrated in Figure 5.1 and Figure 5.3.

- The overall depth-to-water table is known.
- Hydraulic properties at each site are homogeneous and isotropic.
- The aquifer is unconfined.

With this assumption, the vertical hydraulic conductivity equals the saturated hydraulic conductivity, and elevation head control downward flow. This has been demonstrated by Sousa *et al.* (2013) using the Van Genuchten no-flow condition. This assumption allows an approximate calculation of the saturation profile without the need for simulating unsaturated flow, but takes into account the different soil properties and their position in relation to the water table. However, in a normal saturated pathway, flow tends to be horizontal rather than vertical (Wilson *et al.*, 2014). The velocity of horizontal flow is controlled by hydraulic head difference, soil texture, soil type, pore spaces and permeability of the soil. These conditions are also assumed to control vertical flow. Therefore, this research proposes using a saturated permeameter hydraulic conductivity, assuming the travel time for the saturated infiltrating front by means of a modified Darcy's model.

If the unsaturated flow is to be considered, which is not the case in this research, the basic conditions important in the estimation of unsaturated zone travel time are the depth-to-water, the hydrologic condition prevailing over an area, moisture content in soil and soil property present in the area (Saayman *et al.*, 2007; Witczak *et al.*, 2007). These above simplified conditions are very important particularly when considering the advective travel time of the saturated front on a regional scale. The travel time is then calculated based on the diffusive flow recharge model and the modified Darcy's equation. The diffusive flow recharge model is based on the premise that water moves vertically downward through the unsaturated zone, pushing existing water and solute to greater depths with no mixing or variation in velocity (Figure 5.3). This has been demonstrated by surface to aquifer advective time (SAAT) by the Province of Ontario (2004).

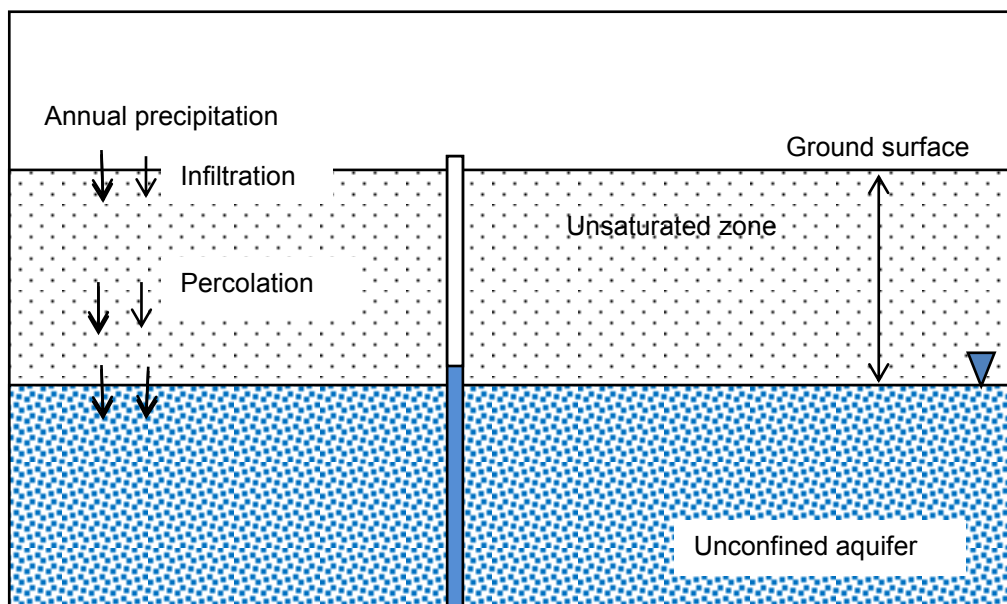


Figure 5.3: Diffusive flow model illustration for groundwater movement



Travel time is related to the following parameters:

$$Tt \propto D$$

$$Tt \propto S$$

$$Tt \propto 1/I$$

*Equation 5.1*

Where:

$I$  = Infiltration rate or true fluid velocity which is derived from the division of hydraulic conductivity by the effective porosity ( $I = K/\theta$ ).

Increase in travel time is directly proportional to increase in depth (D) and slope (S) and is inversely proportional to the infiltration rate (I). Low depth to water table will lead to smaller travel time of contaminant. If infiltration rate is low, travel time of contaminated water will be high. High infiltration rate will result to low travel time. A higher travel time is expected for a higher slope. This is due to possible surface runoff.

Therefore:

$$Tt = K \frac{D * S}{\left(\frac{K_{sat}}{\theta}\right)}$$

*Equation 5.2*

Where K = the proportionality constant.

Slope is not directly linked to travel time for infiltrating groundwater. This is because it depends on factors such as infiltration and gravity, but will be an influence if water will infiltrate or run off. Due to slopes indirect relationship with travel time, it was assigned the lowest weight in the travel time rating. Slope was added to the overall depth because head difference is a determinant factor for precipitating water to either run off or pond, and infiltrate under gravitational effect. The head differences in this instance are the water run-off from a higher slope to a lower slope. Rate of infiltration is expected to be higher from a lower slope to a higher slope in the course of surface or subsurface horizontal movement before or during percolation. The overall travel time is then given by the following equation:

$$Tt = \sum_{i=1}^n \frac{D * S}{\left(\frac{K_{sat}}{\theta}\right)}$$

*Equation 5.3*

Where:

$Tt$  = Travel time (secs)

$D$  = Depth from the ground surface to aquifer (m)

$K_{sat}$  = Hydraulic conductivity at saturation of successive layers (cm/s)

$\theta$  = Porosity of the medium (unitless)

$S$  = Slope (elevation head difference: dh/dl) in meters

$n$  = Numbers of layers between the ground surface and the top of the aquifers

Based on the Darcy concept and as was proposed earlier, that  $K_{sat}$  under a steady state condition derived from Darcy's laboratory experiment with undisturbed core samples in permeameter is divided with the porosity and substituted as the infiltration rate.

The  $K_{sat}$  can be achieved using

$$K_{sat} = \frac{QL}{Ath}$$

Equation 5.4

Where:

$K_{sat}$  = Saturated hydraulic conductivity (m/day)

$Q$  = Quantity of water discharge in ( $m^3$ )

$L$  = Length of sample in (m)

$t$  = Total time for discharge in (days)

$h$  = Vertical distance between funnel overflow and chamber outflow port in (m)

$A$  = Area of cross section of specimen ( $m^2$ )

Darcy's equation describes groundwater movement in the saturated zone as the bulk flow of water through a medium of both soil particles (solids), and pores of cross-sectional area ( $A$ ) under gradient ( $h$ ) which is also known as Darcy velocity, Darcy flux ( $q$ ) or saturated hydraulic conductivity ( $K_{sat}$ ). It is important to highlight that Darcy velocity is different from fluid velocity which is the actual true velocity after taking effective porosity into consideration. This is because water does not flow through the entire cross-sectional area (USEPA, 1988) and the actual flow area is less than the bulk. Therefore, the true fluid velocity is higher than the Darcy velocity.

The proposed RTt approach considers the advective flow component to be one driving the transportation of contaminants from the surface through infiltration and thus the fluid velocity in the equation (Equation 5.3). This is based on the premise that once the first arrival of contaminants has reached the aquifer, then, the aquifer is already under threat even though it is not the peak of concentration as driven by seepage or pore velocity (Figure 5.2). The advective flow is equivalent to fluid velocity and contrasted to the infiltration rate ( $I$ ). The saturated hydraulic conductivity represents the ratio of available bulk water movement through the soil and the pore and not specifically that of the pore only.

#### 5.4.1.2 Limitations of Saturated Hydraulic Conductivity

Substituting the laboratory  $K_{sat}$  for field  $K_{sat}$  has its limitations. This is due to many field factors that are not present in the laboratory. They include (Campbell *et al.* 1990):

- Scale: Measurement done in the laboratory scale does not necessarily reflect behaviour of the larger field scale.
- Field heterogeneity: The hydraulic conductivity of geological material may change considerably across site and this may not be reflected accurately.
- Fractures: Joints, faults, desiccation cracks and fractures may be a very significant influence on the hydraulic conductivity on the field, which are unlikely to be considered in the laboratory.

- The effect (non-linear flow) of macrostructures and macrospores such as root openings and fissures.
- Darcy's law is valid for laminar flow of water through saturated soils, which is typical in fine-grained soil types and coarse-grained soils under low hydraulic gradients where the velocity of flow is low. Under higher hydraulic gradients the flow of water through coarse-grained soils becomes turbulent and Darcy's law is no longer valid.

For the reasons stated above, field tests are generally preferred over laboratory  $K_{sat}$ . It should also be noted that laboratory hydraulic conductivity is some magnitude lower to the field test (Herzog and Morse, 1984), and some authors conclude that the use of laboratory values in groundwater studies can lead to poor estimations of travel time (Cleary, 1990). Few authors approve permeameter derived hydraulic conductivity for coarse materials, particularly moderately to well sorted sand, but disapprove its use for fine-grained materials (Herzog, 1989, Melby, 1989; Fetter, 2001). For multi-layered lithology  $K_{sat}$  can be calculated for the separate layers, and can be summed up with average  $K_{sat}$  being determined by using Equation 5.4.

Travel times of water through the pathway largely depend on the thickness of the vadose zone. In flat alluvial regions, where only a thin vadose zone is present, travel time is generally small. On higher surface topography (slopes) where the size of the vadose zone may be much larger (assuming the water table is following topography), higher travel time is conceptually expected. In arid environments for instance, the vadose zone can be hundreds of meters thick, and infiltration fluxes very low (Dyck *et al.*, 2005). This results in the residence time of water ranging from several hundreds to thousands of years (Birdsell *et al.*, 2005).

Baumgartner and Liebscher (1996) stated the validity and reliability of Darcy's equation for assessment of regional travel time of groundwater flow in both unconsolidated and consolidated aquifers under laminar flow conditions. However, due to fractures in solid rock, karst formations and other geological formations that control turbulent groundwater flow conditions, renders using the proposed equation for these areas ineffective.

## **5.4.2 Rating of Rainfall–Travel Time Parameters**

### **5.4.2.1 Travel Time Rating**

The assumed travel time parameters (Equation 5.1) are rated in the RTt vulnerability method. The rating will be discussed in subsequent sections. In the field, hydraulic conductivity is affected by many factors which include soil type, rock type and soil texture. These factors are directly considered before assigning weight to the hydraulic conductivity and porosity values used in the travel time estimations (Figure 5.5). The extent to which these factors can affect or influence the hydraulic conductivity is still unknown (Regalado and Munoz-Carpena, 2004). Hydraulic conductivity values are therefore rated based on the soil type, rock type and textural properties.

### 5.4.3 Hydraulic Conductivity Rating

The hydraulic conductivity ( $K$ ) is the rate of flow per unit area for a unit gradient or head difference and is constant for a saturated media. Hydraulic conductivity directly affects the travel time of a fluid through a porous media. Ten to twelve orders of magnitude for saturated hydraulic conductivity for rocks were noted by Dominico and Schwartz (1990) and Freeze and Cherry (1979), respectively. The factors and  $K$ -ranges were considered before assigning weight to the hydraulic conductivity since these parameters influence and control the travel rate of fluid. Defined ranges of  $K_{sat}$  control the soil type and textural characteristics grouping. Shale and clay  $K_{sat}$  for instance have low values compared to coarse sands or gravel in alluvium. Therefore, for a given amount of clay in soil, the hydraulic conductivity increases by several orders of magnitude going from clay to silty-clay, and loam to sand.

Documented saturated hydraulic conductivities by Freeze and Cherry (1979) and Neuzil (1994) cover a wide range of soils and rocks, and serve as the background basis for the  $K_{sat}$  rating (Table 5.3). Shale and clay were assigned a weight of five, because travel time is longer and residency time of fluid increases in the vadose zone. Slower infiltration time results in smaller travel time of water or contaminants. The longer the residence time of contaminated water in clay and soil particles while in transit, the longer the possibility of biodegradation of the contaminated water. A weight of four was assigned to igneous and metamorphic rocks due to its hydraulic conductivity range (Table 5.3). Sandstones and siltstone hydraulic conductivity are similar (i.e.  $10^{-3}$ – $10^{-8}$  and  $10^{-3}$ – $10^{-7}$  cm/s, respectively) (Freeze and Cherry, 1979), and was assigned a weight of three because of its lower hydraulic conductivity compared to gravely soils. Gravel and alluvium sands were assigned the lowest weight value of one because they are highly permeable. It takes shorter residence time for contaminants to transmit in the alluvium soils, thereby increasing travel time. Table 5.3 shows the range of weight assigned to hydraulic conductivity based on rock types.

Table 5.3: Hydraulic conductivity range and weight used in calculating travel time

Hydraulic conductivity range (cm/s)*	Rock types	Weight
$10^{-8}$ – $10^{-14}$	Shale	5
$10^{-6}$ – $10^{-10}$	Clay	
$10^{-2}$ – $10^{-11}$	Weathered igneous and metamorphic rocks	4
$10^{-3}$ – $10^{-8}$	Sandstone	3
$10^{-3}$ – $10^{-7}$	Siltstone	
$1$ – $10^{-7}$	Limestone	
$10^{-1}$ – $10^{-5}$	Silty sand	2
$1$ – $10^{-4}$	Alluvium	1
$100$ – $10^{-1}$	Gravel	

\*Source: Freeze and Cherry (1979).

#### 5.4.4 Soil Rating

Infiltration rate depends on the soil types and involves two processes:

- Run-off and percolation on the soil surface.
- Infiltration rate occurring within the soil.

Other factors affecting soil infiltration include rainwater chemistry, soil chemistry, organic matter content and presence of roots and burrowing animals. On the soil surface the type of soil, its properties, and the prevailing surface slope will determine the dominant flow of water either as surface run-off or as vertical infiltration. The amount of flow is dependent on rainfall intensity and site properties. Therefore, the proportion of individual rainfall that will infiltrate the subsoil or as run-off will depend on the soil and rock type, which varies with sites. Goldscheider (2002) presented a description based on the work of Klute (2000) on the dominant flow process from hydraulic conductivity and depth of lower permeable layers within or below the soil (Figure 5.4). The dominant flow processes that are directly controlled by the soil type are infiltration, subsurface and the surface flow.

The flow process was indirectly considered in assigning weight to the soil type through hydraulic conductivity. Clay-rich soils have a high porosity, but low permeability and low infiltration tendency. Thick massive clay that restricts percolation to underground water is assigned a maximum weight of five, and a mixture of sandy and silty clay is assigned a weight of four. Flow processes from these two classes encouraged either surface run-off or subsurface flow if the clay-rich layer is within the topsoil (Goldscheider, 2002). Infiltration will be the dominant flow process when the hydraulic conductivity of the topsoil and subsequent subsoil is greater than  $10^{-4}$  m/s and the topsoil thickness is more than 100 cm. Within this range (infiltration and percolation), several soil types with different hydraulic conductivity can be identified (Freeze and Cherry, 1979). These soils include sandstone, siltstone, silty sand, alluvium and gravel.

Hydraulic conductivity (m/s)	$10^{-4}$	Saturated surface flow	Very fast Subsurface stormflow	Infiltration and subsequent percolation
			Fast Subsurface stormflow	
	$10^{-5}$	Hortonian surface flow rarely (only during storm rainfall)		
	$10^{-6}$	Hortonian surface flow frequently (also during low intensity precipitation)		
	<30 cm	30–100 cm	>100 cm	

Source: Klute (2000) and Goldscheider (2002).

Figure 5.4: Dominant flow process as a function of saturated hydraulic conductivity and depth to lower permeability lithology.

Weight was assigned according to the hydraulic conductivity properties of the above soils under infiltration flow. The pores through which water infiltrate the soil flows increases with

the particles sizes, provided there are no infilling by smaller grain size particles. A weight of three was assigned to sandstone and siltstone and a weight of two was assigned to coarse sand and silt. The pore space sizes and grain sizes accounted for the differences in the hydraulic conductivity range in sandstone and silty sand. The lowest weight value of one was assigned to gravel and alluvium (Table 5.4). Both gravely sand or alluvium sand is good soils for groundwater recharge, and transmissivity is high in aquifers within these soils. Therefore, gravel, sand and alluvium soils have the highest susceptibility rate of vulnerability.

Table 5.4: Grouping of soil type base on hydraulic conductivity

Hydraulic conductivity (cm/s)	Range*	Soil type	Weight
	$10^{-6}$ – $10^{-14}$	Massive clay	5
	$10^{-2}$ – $10^{-11}$	Sandy clay and silty clay	4
	$10^{-3}$ – $10^{-8}$	Fine sand, fine silt and limestone	3
	$10^{-1}$ – $10^{-5}$	Coarse sand and silt	2
	$100$ – $10^{-4}$	Alluvium sand and gravel sand	1

\*Source: Freeze and Cherry (1979).

#### 5.4.5 Rock Type Rating

The degree to which rock types affect groundwater vulnerability depends on the hydraulic conductivity and permeability in the rock types. Unfractured basement rock will have little or no vulnerability, while the vulnerability of fractured basement rock will depend on the distribution, range of width and frequency of fracture variation. Fractured rock vulnerability will directly depend on the hydraulic conductivity of such rocks. This gives a slightly lower weight compared to fresh unfractured rocks. Weathered basement rocks contain more pore spaces and higher vulnerability weight. For consolidated sedimentary rocks such as shale and clay stone, pore space are reduced with very low permeability.

A weight of five was assigned to fresh basement rocks and consolidated sedimentary rocks due to the expected longer travel time it will take water to infiltrate into the underground water (Table 5.5). Water percolating dense consolidated rocks is assumed to flow as surface run-off or subsurface horizontal flow, rather than as vertical infiltration flow, irrespective of the permeability of the topsoil. The unconsolidated sedimentary rocks present the highest hydraulic conductivity in all geological rocks and the hydraulic conductivity is due to the large pore spaces and higher permeability present in most of them.

Table 5.5: Rock type, hydraulic conductivity with assigned weight

Hydraulic Conductivity (cm/s)*	Rock type	Weight
$10^{-6}$ – $10^{-14}$	Consolidated dense rock, shale, igneous and metamorphic rocks	5
$10^{-2}$ – $10^{-11}$	Fractured igneous and metamorphic	4
$10^{-1}$ – $10^{-8}$	Sandstone, siltstone and limestone	3
$10^{-1}$ – $10^{-5}$	Weathered basement	2
$100$ – $10^{-1}$	Unconsolidated sediment	1

\*Source: Freeze and Cherry (1979).

#### 5.4.6 Textural Property Rating

A strong relationship exists between the hydraulic conductivity of soil and soil textural property. Soil texture is also a function of grain size and its distribution (GSD). The protective properties of subsoil material are directly related to the GSD and permeability (Daly, 2002). As clay grains are several magnitudes smaller than sand grains in a clay-sand mixture, clay particles can block the narrow channels connecting pore spaces and so effectively reduce the hydraulic conductivity. GSD can also be correlated to the attenuation capacity of soil, as used by Holting *et al.* (1995). Extensive data from standard literature on GSD and their hydraulic conductivity has been conducted and compiled by Kunothe (2000).

The degree to which the textural properties affect hydraulic conductivity is determined by the percentage of clay in soil. As clay percentages increases, soil attenuation capacity improves and the possibility of infiltration reduces. Predominant sand and silt soils have a low clay content and high infiltration rate. They were assigned a weight of one (Figure 5.5). Loamy soil textures of about 30% clay were assigned a weight of three, while a predominantly clay texture with a limited infiltration rate was assigned a weight of five. Other soil texture with their clay percentage and hydraulic conductivities is shown in Table 5.6, while the textural classification chart has been presented in Figure 4.18.

Table 5.6.: Soil textural property, hydraulic conductivity and clay percentage

Hydraulic conductivity	Soil texture	Percentage of clay	Weight
$10^{-6}$ – $10^{-14}$	Clay	>60%	5
$10^{-2}$ – $10^{-11}$	Sandy clay and silty clay	40–50%	4
$10^{-3}$ – $10^{-8}$	Silty clay loam, clay loam, sandy clay loam	30–40%	3
$10^{-1}$ – $10^{-5}$	Silt loam, sandy loam and loamy sand	10–20%	2
$100$ – $10^{-4}$	Sand and Silt	<10%	1

#### 5.4.7 Porosity

The porosity of a geological material is the ratio of the volume of pore space in a unit of material to the total volume of the material. Porosity of soil is complex and typically ranges between 0 and 1. The closer the porosity is to 1, the faster the infiltration rate of fluid in a geological material (Lyons, 1996). However, this may not apply to clay particles because of the structured nature of clay minerals; it has high porosity with very low conductivity. This means clay can hold a large volume of water per volume of bulk material but do not release the water. Soil porosity decreases as particle size increases due to presence of soil aggregate formation which increases adhesion in finer textured soils. Likewise porosity of subsurface soil is lower than in surface soil due to compaction and gravity. Sand and gravel have higher particle sizes and lower porosity as compared to clay (Table 5.7). Infiltration rate will be higher in soils and rocks with higher porosity due to increase possibility of connected

pore spaces. The rating in Table 5.7 and Table 5.8 is based on the higher the porosity the higher the infiltration rate, the higher the rating.

Table 5.7: Porosity rating based on Soil

Porosity*	Soil type	Weight
0.40–0.70	Clay	5
0.35–0.50	Silt	3
0.25–0.50	Sand	1
0.25–0.40	Gravel	1

\*Source: Freeze and Cherry (1979).

Infiltration rate will increase in higher porous rocks such as karst limestones and weathered crystalline rock as compared to shale or consolidated rock types. The weight in Figure 5.8 was assigned according to the percentage or amount of porosity of the individual rock types. Porosity is not controlled by grain size because the volume between grain spaces is related only to the method of the grain packing but controlled by rock type, pore distribution, cementation, diagenetic history and composition.

Table 5.8: Porosity rating based on rock type

Porosity*	Rock type	Weight
0.05–0.50	Karst Limestone	5
0.34–0.57	Weathered igneous rock	4
0.05–0.30	Sandstone	3
0.00–0.20	Limestone and dolomite	2
0.00–0.10	Fractured igneous and metamorphic	1
0.00–0.10	Shale	1
0.00–0.05	Dense consolidated rock	1

\*Source: Freeze and Cherry (1979).

#### 5.4.8 Depth-to-Water Rating

The overall depth-to-water is an important factor in aquifer vulnerability assessment. This is because it determines the distance infiltrating water must travel to reach the groundwater table. The depth-to-water influences the degree of interactions between the percolating contaminated water and subsurface material. The longer percolating depth-to-water table, the greater the possibility of chemical, physical and microbiological degradation of the contaminated water. Therefore, aquifer attenuation capacity increases with the increasing depth-to-water table and *vice versa*. The assigned weight decreases with increasing depth-to-water. An overall depth-to-water of between 0 and 5 m was assigned a weight of 2.5 and a depth of between 10 and 25 m was assigned a weight of 1.5, while highest overall depth of >50 m was assigned a weight of 0.5. Table 5.9 shows the overall depth and assigned weight. For regional depth estimation, the Digital Elevation Model (DEM) can be subtracted from the piezometric mean sea level values of the area, while for site-specific estimation the overall depth-to-water will then be the difference between the measured field water table and piezometric sea level.



Table 5.9: Depth-to-water range and assigned weight used in travel time calculation

Range (m)	Weight
0–5	2.5
5–10	2.0
10–25	1.5
25–50	1.0
>50	0.5

#### 5.4.9 Slope Rating

Slope is derived from the difference between the highest topographic points to the lowest topographic point of an area. Run-off, infiltration and recharge are influenced by the slope of an area. Areas with a low slope encourage ponding and retain water for a longer period, thereby increasing the possibility of percolation and infiltration and increase the potential for contaminated water migration. More run-offs occur in areas with steep slopes and low infiltration. This reduces the possibility of groundwater contamination. Flat slopes are prone to flooding and groundwater contamination because ponded surface water will readily infiltrate groundwater. This also depends on the degree of permeability of the underlying soil types and texture.

The slope is derived from the differences in contour values. Based on the slopes, weight was assigned as shown in Table 5.10. Lowest weights of 0.4 correspond to areas with the highest slopes greater than 50. These areas will encourage run-off and lower infiltration, while lowest slopes of zero correspond to areas with equal contour or water bodies, which encourage ponding, more infiltration and weight of 2.0 assigned.

Table 5.10: Slope range and assigned weight

Slopes (m)	Weight
0–2	2.0
2–5	1.6
5–25	1.2
25–50	0.8
>50	0.4

### 5.5 Rainfall–Travel Time Vulnerability Index

The final intrinsic vulnerability was computed by combining the factors of rainfall and travel time with a constant rating. This is proposed in the following formula:

$$RTt = R_R R_w + Tt_R Tt_w$$

*Equation 5.5*

Where:

$R_R$  = Rainfall rating = 10

$R_w$  = Rainfall weight

$Tt_R$  = Travel time rating = 10

$Tt_w$  = Travel time weight

The final RTt vulnerability factors were added up because each one is considered very important and impact groundwater vulnerability differently. It should be noted that travel time of water or contaminants is complicated in the field, and therefore some level of uncertainty may exist during percolation and infiltration. Rainfall carries equal weight with travel time, because the RTt method assumes precipitation as the driven force and initiator of the infiltration. If rainfall or another recharge mode is absent and there is no external release of contaminant on the land surface, travel time impact on groundwater vulnerability may be inconsequential in the RTt method. Therefore, the travel time and rainfall were assigned an equal weight. Following the recommendation of Vrba and Zaporosec (1994) and Vias (2006), The RTt vulnerability index is grouped into five classes. The classes and vulnerability value is presented in Table 5.11 and Figure 5.5.

Table 5.11: RTt vulnerability class and index

RTt index	Vulnerability class
12–29	Very low
29–47	Low
47–65	Moderate
65–83	High
83–100	Very high

The interval between the vulnerability classes are almost the same. No single factor can give a high vulnerability class, for example the highest vulnerability class rainfall can give is below 50, which is a moderate to low vulnerability class. The lowest index that can be derived from any point of vulnerability assessed will be 12, while the highest vulnerable point will be 100. The high and very high vulnerability classes correspond to areas with high hydraulic conductivity and travel time, high rainfall and a low depth-to-water table. The moderate to low classes suggest areas which has considerable protection cover, high depth-to-water table, high or steep slopes and low rainfall.

## 5.6 Rainfall–Travel-Time Vulnerability Method Limitations

Aquifer vulnerability is a relative term used to predict the protection level of a groundwater system. All aquifers are vulnerable to some degree. Therefore, the RTt vulnerability method, just like other vulnerability methods, contains some limitations, including:

- RTt does not account for human activity.
- The RTt never take into account the contaminant types.
- The RTt does not estimate groundwater flow paths and may not be used in a karst environment.
- The RTt does not model fate/ transport of chemical constituents.
- Large surface water features are not considered in the RTt method.
- Laboratory saturated hydraulic conductivity should be conducted only under steady state conditions.

- Pollution sources such as leaking underground storage tanks of fuel stations, sewer lines and pit latrines, which are a shortcut for contaminant transport, have not been considered in the method.
- Uncertainty in the assumptions of data rating such as slope and depth-to-water.

## **5.7 Conclusion**

The RTt vulnerability method is a simplified concept of the source–pathway–receptor vulnerability approach. The RTt method makes use of both the subjective and physically based vulnerability techniques. Laboratory techniques were introduced in the calculation of travel time of contaminant for the vadose zone. Laboratory saturated hydraulic conductivity is proposed to replace the infiltration rate. In the field, infiltration and percolation of rainfall is assumed as recharge under steady state conditions. Travel time is controlled by the slope, infiltration, vadose thickness and hydraulic conductivity. The vulnerability class is similar to that of other vulnerability methods and the vulnerability classes range from very low to very high vulnerability. The RTt vulnerability method parameters for evaluation are few, easy to collate and calculate, and is designed for data limited or scarce areas like the Dahomey Basin and areas with similar challenges particularly those in Africa.

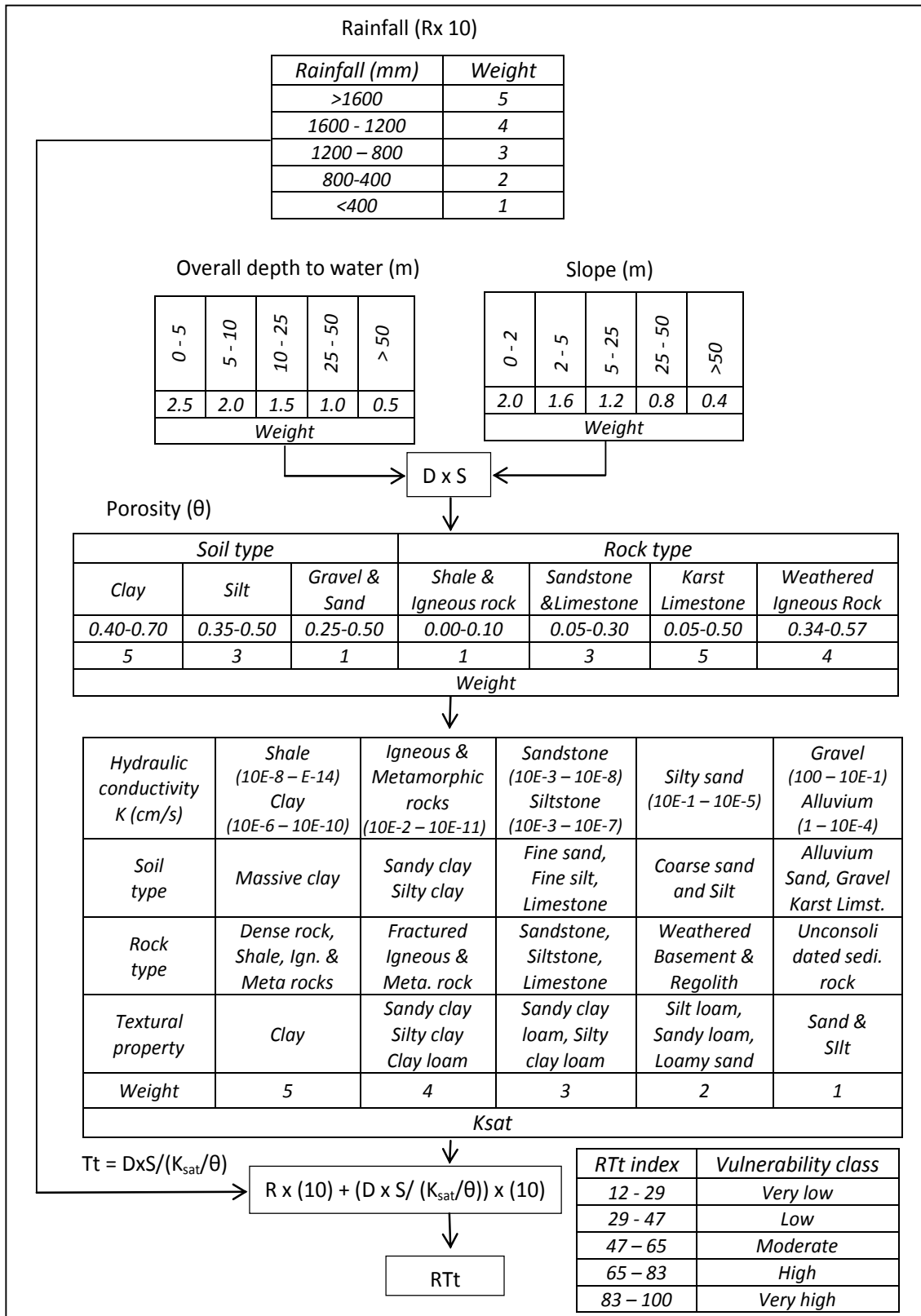


Figure 5.5: Objective and subjective criteria used in the RTt vulnerability method

## CHAPTER 6

# APPLICATION OF THE RAINFALL–TRAVEL TIME VULNERABILITY METHOD TO THE SHALLOW AQUIFERS OF THE DAHOMEY BASIN

### 6.1 Introduction

The main concept of the rainfall–travel time (RTt) groundwater vulnerability method is defined as a component of the pathway element in the context of the hazard–pathway–receptor model used in risk assessment work. The target in the Dahomey Basin is the shallow groundwater surface. Detailed characterisation of the Dahomey geology, geo–hydrology and topographical nature of the Basin was presented in Chapter 4.

### 6.2 Geology and Soils of the Dahomey Basin

RTt vulnerability assessment was done by using point data interpolation and kriging approaches. This approach was made possible due to the lateral geological and hydrogeological nature of the Dahomey Basin (Figure 6.1). Rock strata in the Dahomey Basin are in most cases composed of homogenous deposited sediments overlying each other. The nature of the rock depositions encourages groundwater accumulation, particularly in lithologies containing intercalations of sand and clay. Continuous percolations and infiltrations arising from the high amount of precipitation between 1 200 mm and 1 800 mm per year, support the groundwater accumulations in the Dahomey Basin (Oke *et al.*, 2013).

Hand-dug wells supply the majority of the Dahomey Basin's water needs. The geological nature and rainfall creates a shallow unconfined aquifer system that can be accessed with large diameter hand-dug wells over the basin (Figure 6.2 a&b). The depth of the Dahomey Basin's shallow unconfined aquifers depends on the soil properties such as soil thickness, texture, soil permeability, nearness to the river and precipitation. The amount of rainfall available for infiltration is controlled by the distance from the sea. Land surface factors such as topography and geology, along with vegetation, are the other remaining factors determining the potential recharge of Dahomey aquifers.

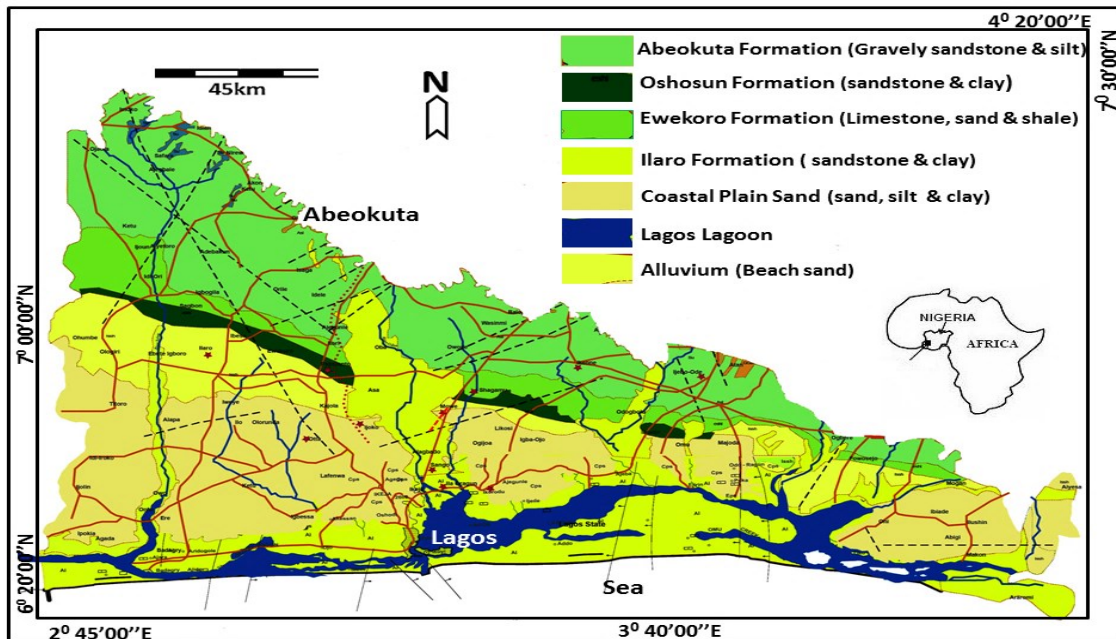


Figure 6.1: Sedimentary formation, soil and rock types in the Dahomey Basin



Figure 6.2 (a) and (b): Shallow groundwater systems at varying depths

### 6.3 Preparation of Vulnerability Maps

A Windows Interpretation System for Hydrogeologist Software (WISH), version 3.0, was used for the production of the RTt and other vulnerability maps. WISH was developed at the Institute for Groundwater Studies at the University of the Free State in Bloemfontein, South Africa. WISH is a flexible software program, with mapping facility support from GIS and other similar applications. The following steps were employed to create the vulnerability maps:

- **Shape file:** A shape file of the Dahomey Basin was created from both the geological map and topographical map of the basin. These two maps serve as the base map. The Dahomey Basin polygon was created from the base maps and saved as a raster file.
- **Coordinates:** The coordinate system input and output was set to map projection and the World Geodetic System (1984). The highest and lowest point of the Dahomey Basin coordinates were overlaid on the raster file and digitised.
- **Gridding:** A grid of 200 × 200 allowing for sufficient flexibility and speed was created. Although the borehole points did not cover all the gridding points, interpolations in each grid was performed to cover the areas without borehole data. This was done because the parameters accessed were known for each of the areas and grid. The grid was refined afterwards through means of smoothing to achieve a better resolution.
- **Search radius and method:** Three search methods are available in WISH: (i) the simple, (ii) the octant and (iii) the quadrant. The quadrant search method is sufficient in most interpolations. A quadrant search forces data to be spaced according to their coordinates during interpolation. The search radius in WISH is sufficient to include the required number of borehole points while performing interpolations.
- **Data selection:** Two possibilities of data selection for contouring are available: Firstly, (i) the values of the points selected on the map may be contoured. In this case, data were selected from selected points. Secondly, (ii) alternative data selection used in this research incorporated data from Excel and DAT files.
- **Contouring:** Contouring is done through a gridding system. Depth-to-water level, rainfall, travel time and other parameters calculated weight were contoured and overlaid on the gridded map. A good advantage of WISH is that multiple data layers from the same Excel, DAT or other compatible formats can be contoured and superimposed on the same map.
- **Smoothing:** Once data had been contoured, additional features were used by the WISH programme to smooth the map. Smoothing is done through interpolation along the boundaries between two contours.
- **Colour-coding:** Different levels of data were coloured to preferred points. Colour-coding for vulnerability maps is advisable because it allows for easy identification, understanding and interpretation.

## 6.4 Data Collection

Rainfall, slopes, hydraulic conductivity, porosity and depth-to-water table were the data used in calculating the RTt vulnerability method (Table 6.1). The Dahomey Basin rainfall data, soil hydraulic conductivity, porosity and depth-to-water table have been discussed in Chapter 4.

Table 6.1: Depth-to-water level, rainfall and topography data

SN	Longitude	Latitude	Depth-to-water (m)	Rainfall (mm)	Topography (m)
1	25463	72307	65	1 200	171
2	27344	71153	38	1 200	78
3	29024	69197	45	1 200	65
4	31306	68319	60	1 200	84
5	33062	67667	26	1 200	44
6	34592	67040	16	1 800	43
7	36549	66739	40	1 600	69
8	38053	66011	18	1 800	26
9	27337	69573	30	1 200	60
10	27391	68846	45	1 200	80
11	27996	68143	46	1 600	88
12	29626	67466	43	1 600	67
13	32686	66864	25	1 600	58
14	34141	66162	18	1 800	37
15	24635	68218	34	1 600	85
16	26014	67416	27	1 600	82
17	27444	66864	25	1 600	58
18	28096	67290	34	1 600	63
19	29049	66613	20	1 600	49
20	32184	66112	12	1 600	36
21	33739	65760	18	1 800	25
22	26391	68419	40	1 600	62
23	27770	68018	40	1 600	90
24	28472	67667	35	1 600	81
25	29576	67215	25	1 600	67
26	32611	66413	15	1 600	69
27	33739	66112	23	1 600	39
28	35746	65760	26	1 600	30
29	25387	65836	25	1 600	58
30	27469	65836	22	1 600	48
31	28748	65685	21	1 600	55
32	30429	65384	5	1 600	26
33	32360	65635	25	1 600	43
34	34191	65309	8	1 600	16
35	36599	65083	15	1 600	27
36	25162	64506	18	1 800	55
37	27043	64431	15	1 800	45
38	28447	64381	8	1 800	36
39	30519	64406	7	1 800	19
40	33363	64732	8	1 800	20
41	37150	64431	12	1 800	27



SN	Longitude	Latitude	Depth-to-water (m)	Rainfall (mm)	Topography (m)
42	40486	63729	9	1 800	21
43	41464	63930	8	1 800	23
44	42869	63303	10	1 800	37
45	30103	68018	8	1 200	44
46	30228	66689	7	1 600	36
47	31181	66488	5	1 600	30
48	31131	65485	5	1 600	27
49	31532	64481	3	1 600	6
50	29877	63027	7	1 800	10
51	33238	63077	2	1 800	2
52	35871	63603	12	1 800	12
53	42066	62375	2	1 800	4
54	39182	63102	2	1 800	4
55	24961	62817	3	1 800	5
56	27173	63318	3	1 800	7

#### 6.4.1 Rainfall Rating

Rainfall rating followed the presentation in Figure 5.5. Twenty years' rainfall spatial distribution and quantification of the Dahomey Basin have been presented in Chapter 4 (Section 4.5). The rainfall average ranges from 1 190 mm, 1 618 mm and 1 801 mm for the three meteorological stations in Abeokuta, Ijebu-Ode, and Lagos, respectively. The weight assigned to these values is presented in Table 6.2 and it follows the presentation in Figure 5.5. A maximum weight of five was assigned to rainfall values in Lagos, other coastal areas and the surrounding areas of Ijebu-Ode. Borehole points in Abeokuta and surrounding areas where the annual rainfall drops below 1 200 mm was assigned a weight of three. The spatial rainfall distribution map of the RTt method is presented in Figure 6.3.

Table 6.2: Rainfall rating and weight of the Dahomey Basin

Rainfall (mm)	Weight	Rainfall rating ×10
>1 600	5	50
800–1 200	3	30

#### 6.4.2 Travel Time Rating

Travel time calculation of the Dahomey Basin, as presented in the earlier chapters, involves addition of the overall depth-to-water, porosity and slope differences, divided by the saturated hydraulic conductivity derived in the laboratory. The slope difference in the Dahomey Basin ranges from 2-5 to 50. The northernmost section of the Dahomey Basin has a high contour value of 130 m, while the lowest point in the basin ranges between 2 and 3 m. The Dahomey slope was sourced from topographical maps and the Digital Elevation Model (DEM). Depth-to-groundwater was derived from field hydrocensus, drillers' records, and DEM (Table 6.1).

Saturated hydraulic conductivity conducted in the laboratory with the permeameter was used in the calculation of infiltration rate in the RTt method. Hydraulic conductivity is linked to soil types, rock type and textural property of the lithology. The average profile lithology of the Dahomey Basin was estimated and presented with their soil types, rock types and textural properties in Table 6.3.

Table 6.3: Saturated hydraulic conductivity range in the Dahomey Basin

Lithology	Ks (cm/s)	Soil type	Rock type	Textural	Weight
ILA	$3.5 \times 10^{-2}$	Alluvium	Unconsolidated sandstone	Sand	1
ABK	$3.2 \times 10^{-2}$	Coarse sand	Sandstone	Sand	1
EWE	$3.2 \times 10^{-3}$	Sand	Sandstone and limestone	Sand	3
OSH	$6.8 \times 10^{-3}$	Sandy clay	Sandstone	Sand-clay	3
CPS	$3.2 \times 10^{-3}$	Sand	Massive sandstone	Sand	3

Most ranges of the hydraulic conductivity values as used in the RTt method, overlaps (Figure 5.5). For proper classification and accurate weight assigned to a hydraulic conductivity value, the hydraulic conductivity value must be compared to the other rating parameters such as soil type, rock type and textural property for correlation. For example,  $3.2 \times 10^{-2}$  cm/s was derived and has the average saturated hydraulic conductivity for the ILA formation. This value could be assigned a weight of three (like the others), since it is within the range of sandstone. However, due to its alluvium soil type and unconsolidated bedrock type, it was assigned a value of one, as presented in Figure 5.5. The porosity range of the Dahomey Basin was rated based on the rock and soil types (Table 6.4). The derived laboratory porosity of the basin has been presented in Chapter Four. The porosity mostly ranges within the sandstone rating of the RTt methodology and is shown in Table 6.4.

Table 6.4: Porosity ratings of the Dahomey Basin

Lithology	Porosity	Soil type	Rock type	Weight
ILA	0.19-0.36	Alluvium	Unconsolidated sandstone	1
ABK	0.15-0.24	Coarse sand	Sandstone	3
EWE	0.31	Sand	Sandstone and limestone	3
OSH	0.20-0.25	Sandy clay	Sandstone	3
CPS	0.09-0.15	Sand	Massive sandstone	3

The description and data sources of the RTt method as used in the assessment of the Dahomey Basin unconfined aquifers are presented in Table 6.5. Travel time variations in the Dahomey Basin are primarily due to the amount of clay and hydraulic conductivity values present in the lithology and the overall depth of the vadose zone. Travel time was the shortest when the depth was low and the hydraulic conductivity was high, for example the ILA Formation. The lowest travel time in the Dahomey Basin was recorded for the EWE Formation. High overall depth-to-water and run-off possibilities as well as low hydraulic

conductivity, were responsible for the low travel time in the EWE Formation. The travel time variation map is shown is Figure 6.4

Table 6.5: Rainfall–travel time source data and description

Parameters	Description	Source
Depth-to-water	This comprises of overall thickness of the vadose zone and includes the depth from the ground surface to the water table.	Data generated by field measurement using geophysics, hydrocensus and from DEM.
Topography	Slopes difference helps identify areas with the possibility of ponding and high run-off.	Derived from topographical maps and DEM.
Recharge	Precipitation average over the study area. Rainfall mixed with pollutant at the soil surface percolate the vadose zone to the water table.	Generated from Nigeria's Metrological Agency.
Infiltration in vadose zone	Saturated hydraulic conductivity of the vadose zone determines the rate at which contaminants can travel from the land surface to groundwater surface.	Derived from the laboratory experimental set-up.

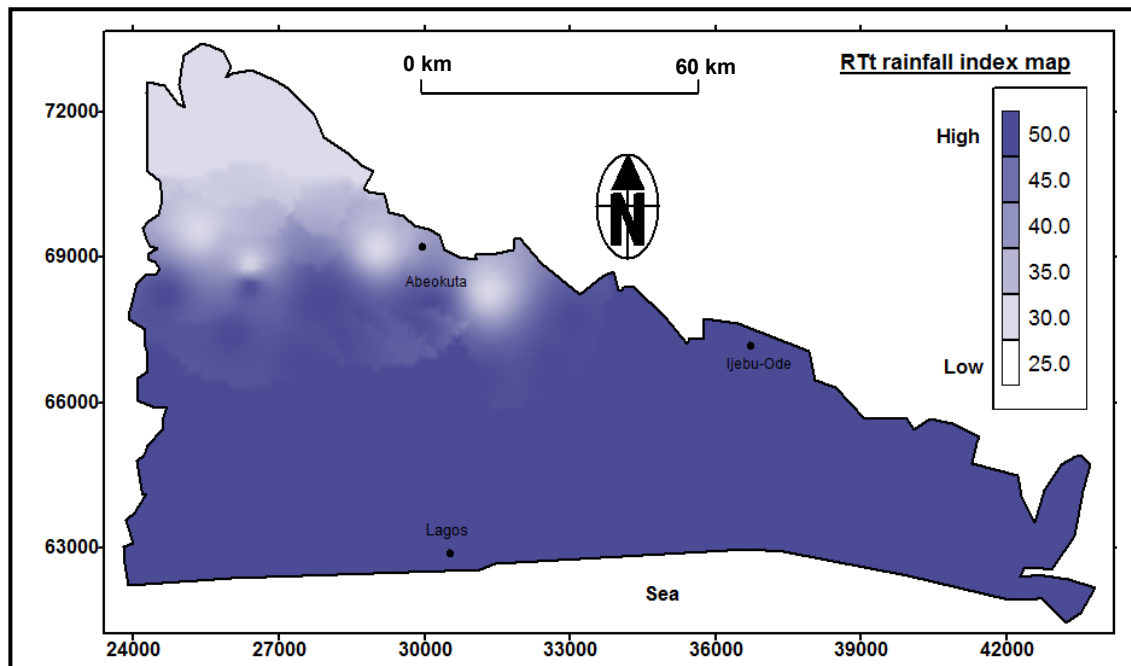


Figure 6.3: Rainfall map of the rainfall–travel time vulnerability method

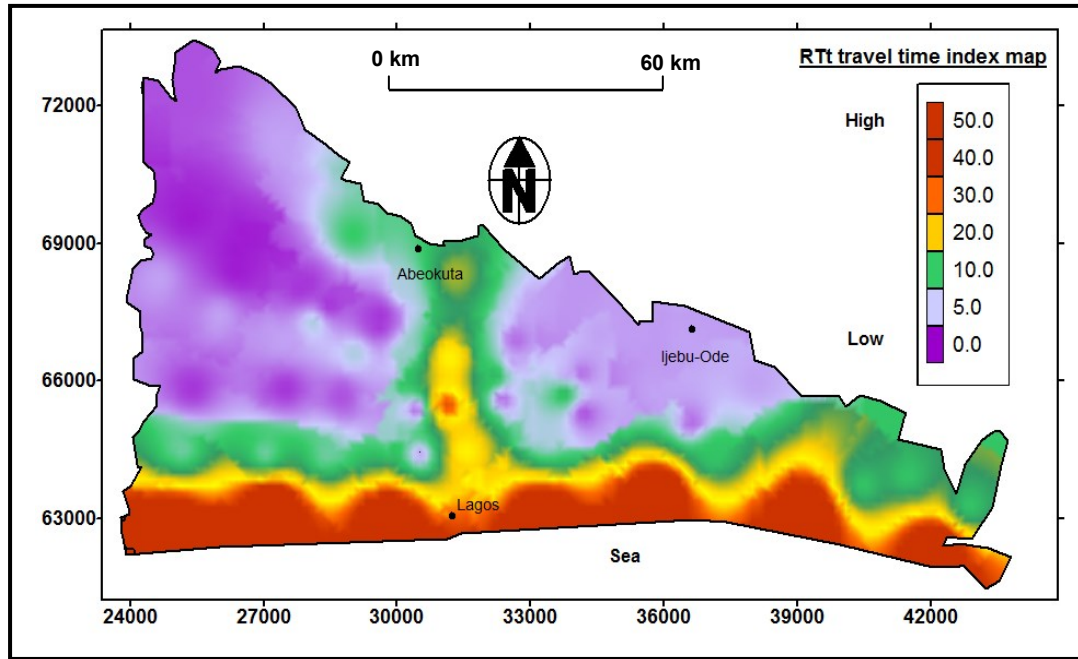


Figure 6.4: Travel time map of the rainfall–travel time vulnerability method

## 6.5 The Dahomey Basin Rainfall–Travel Time Vulnerability Map

The RTt vulnerability map is obtained by overlying the R and Tt maps, which was derived by adding the product of the rainfall weight and rating with the travel time weight and rating as shown below:

$$RTt = R_R R_w + T_t T_w$$

*Equation 6.1*

Figure 6.5 shows the RTt vulnerability map of the Dahomey Basin. The rainfall rating has more effect on the final vulnerability map, which is due to the weight value assigned and the rainfall quantity experienced in the Dahomey Basin compared to the travel time. Most areas of the Dahomey Basin have the highest rating of rainfall, except the northern part of the basin that has a slightly lower rainfall rating. Comparing this to the travel time impact on the final vulnerability map shows the highest travel time rating and greater effect for the coastal areas, and along the flood plains of the Dahomey Basin, characterised as the most vulnerable areas.

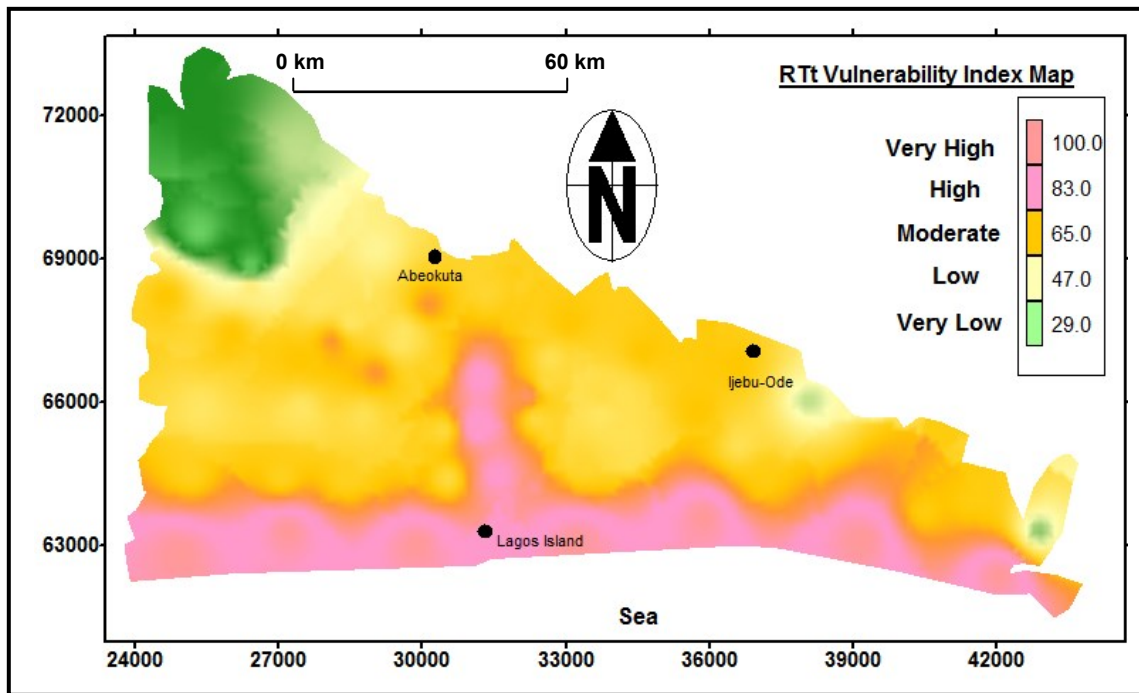


Figure 6.5: Rainfall–travel time vulnerability map of the Dahomey Basin

The Dahomey Basin vulnerability class ranges between a low to very high vulnerability class. The very high vulnerability areas range from 83 to 100 with an 18% area coverage which is characterised by poor drainage, high rainfall, very low depth-to-water level and high hydraulic conductivity. There are no thick bedrock formations before the water table in these areas. The in-situ formation contains predominantly unconsolidated alluvial sediments and deposited river sediments. The unconsolidated nature of the sediments makes permeability high and recharge fast. The high vulnerability area is also characterised by ponding after a short rain interval.

The moderate vulnerability areas cover a larger section (64%) of the Dahomey Basin. The moderate vulnerability index ranges from 47 to 65. High recharge, low slopes, massive sandstone to bedded limestone bedrock and sand to sandy clay soils characterise these areas. Within the moderate vulnerability class, areas with high overall depth-to-water level reveal lower moderate vulnerability values than areas with lower overall depth-to-water level. Groundwater depth ranges from 8 m to 45 m. Table 6.6 shows the RTt vulnerability index used in the classification of the Dahomey Basin.

Table 6.6: Rating for rainfall–travel time vulnerability index

<b>RTt Vulnerability Index</b>	
<b>RTt value</b>	<b>Implication</b>
12–29	Very low
29–47	Low
47–65	Moderate
65–83	High
83–100	Very high

Low vulnerability areas were classified from 29 to 47. The low vulnerability areas cover 11% of the basin. The major factors contributing to low vulnerability classification include high overall depth-to-water table, low recharge, bedrock of thick sandstones, high slope gradient, and high run-off possibility. The low vulnerability areas in the Dahomey Basin are limited to the northernmost end of the basin where these factors are dominant. No area of the Dahomey Basin was classified as having very low vulnerability (Table 6.7). This may be so since no aquifer is immune to contamination, and based on the concept of the RTt vulnerability that if recharge is possible, aquifer contamination is possible.

Table 6.7: Shallow aquifer formations in the Dahomey Basin and their generalised vulnerability classes

<b>Dahomey Basin Formations</b>	<b>Vulnerability Class</b>
Abeokuta Formations	Low to moderate vulnerability
Ewekoro Formations	Low to moderate vulnerability
Ilaro Formations	Moderate vulnerability
Coastal Plain Sand	Moderate vulnerability
Alluvium	Very high vulnerability

## 6.6 Conclusion

The proposed RTt vulnerability method was used to evaluate the vulnerability of groundwater in the Dahomey Basin. The vulnerability class present in the Dahomey Basin ranges from low vulnerability to very high vulnerability. Rainfall and travel time maps were generated and a final vulnerability map produced. Sources of data and their application were highlighted. The moderate vulnerability class are characterised by massive sandstones, high recharge and low slope. Generally, the RTt method's adaptability is simple and easily understandable. The generated vulnerability map is influenced by the geology, topography, precipitation and hydraulic conductivity of the overlying layers of the Dahomey Basin. Established vulnerability methods such as DRASTIC, PI and the AVI method will be applied to the shallow aquifers of the Dahomey Basin in the next chapters. This will be done in order to verify and compare the accuracy of the RTt vulnerability map.

# CHAPTER 7

## ASSESSMENT OF THE DAHOMEY BASIN VULNERABILITY WITH CONVENTIONAL METHODS

### 7.1 Introduction

In this chapter, vulnerability assessment of the Dahomey Basin will be evaluated with other established vulnerability methods such as DRASTIC, AVI and PI methods, respectively. Vulnerability maps from these methods will be compared to the RTt vulnerability methods and observe areas of similarity and differences. The selected vulnerability methods were chosen because they assess groundwater vulnerability differently. The selected vulnerability methods were established on separate intrinsic properties and parameters but they all work toward assessing the vulnerability of an aquifer to contaminations.

These methods were chosen for the following reasons:

- The PI was chosen because it includes more parameters in its vulnerability estimation than the RTt and other vulnerability methods. Although PI was designed for Karst aquifers, its application in a non-karst environment such as the Dahomey Basin is possible.
- The PI is reported to have a higher level of accuracy compared to DRASTIC or AVI when incorporating highly variable distributions and thickness of cover sediments and their protective properties (Neukum *et al.*, 2008).
- The AVI method was chosen because, like the RTt method, it uses travel time estimation.
- AVI is also effective in assessing layered rocks with varied hydraulic conductivities and regional aquifer coverage (Zwahlen, 2004).
- The DRASTIC was selected because it has been widely used, modified and criticised and is straightforward to apply (Piscopo, 2001; Lobo-Ferreira and Oliveira, 2003; Rahman, 2008).

### 7.2 Application of the DRASTIC Method

The DRASTIC index is calculated roughly analogous to the likelihood that contaminants released from the surface will reach the groundwater. Each DRASTIC parameter is assigned a rate and a weight as follows:

$$\text{DRASTIC Index} = D_R D_W + R_R R_W + A_R A_W + S_R S_W + T_R T_W + I_R I_W + C_R C_W$$

*Equation 7.1*

Where D, R, A, S, T, I and C are the seven parameters of the model, and the subscripts R and W are the corresponding ratings and weights, respectively. The source of data used in the computation of the DRASTIC method and the description of the factor considered in the

assessment is shown in Table 7.1. For the DRASTIC method, the following key assumptions are made:

- Contamination occurred at the ground surface.
- The contaminant enters the water table when rain falls on the surface and percolates into the saturated zone.
- The contaminant travels with water, at the same rate as water.
- The aquifer is unconfined.

Table 7.1: Sources of data employed in the DRASTIC computation

Factors	Description	Source
Depth-to-water	Represents the depth from the ground surface to the water table. Deeper water table implies lesser chance for pollution to occur.	Data were generated from the study area and from local drillers' directories.
Net recharge	Represents the amount of water that penetrates the vadose zone and reaches the water table. Recharge water represents the vehicle for transporting pollutants.	Generated from rainfall data from Nigeria's Metrological Agency and previous calculated evaporation and run-off.
Aquifer media	Refers to the saturated zone material properties, which controls the pollutants attenuation processes.	Field studies and interpretation of geological map of Nigeria on scale 1:50 000.
Soil media	Represents the uppermost weathered portion of the vadose zone and controls the amount of recharge that can infiltrate downwards.	Generated from field and laboratory studies.
Topography	Refers to the slope of the land surface. It indicates whether the run-off will remain on the surface to allow pollutant percolation to the saturated zone.	Digital Elevation Model (DEM) of the basin available at the Global Land Cover Facility (GLCF) of Maryland University and topography map.
Impact of vadose zone	This is defined by the vadose zone material, which controls the passage and attenuation of the contaminated material to the saturated zone. The vadose zone and aquifer media are the same materials.	Interpretation of the geological map of Nigeria from NGSA.
Hydraulic conductivity	Indicates the ability of the aquifer to transmit water, thus determining the rate of flow of the contaminants within the groundwater system.	Derived from previous literature as well as reported drillers' records.

## 7.2.1 DRASTIC Data Collection and Management

To carry out the DRASTIC vulnerability assessments, the seven thematic parameters were rated and vulnerability maps were prepared for each parameter. In consecutive steps these parameters include: depth-to-water table; net recharge; aquifer media; soil media; topography; impact of the vadose zone and hydraulic conductivity.

### 7.2.1.1 Depth-to-water table

This includes the depth from ground to water table. Depth-to-water is an important factor because it determines the thickness of the material through which infiltrating water must



travel before reaching the saturated zone. The deeper the water table, the lesser the chances of pollutants interacting with groundwater. Depth-to-water therefore suggests the possibility of physical and chemical attenuation and degradation processes between the percolating contaminant and vadose materials. In general, the aquifer potential protection increases with depth-to-water. The depth-to-water data of shallow wells were collected on the field and contoured. A weight of five was assigned to indicate the importance of the DRASTIC parameters. Depth-to-water derived from the Dahomey Basin is presented in Table 7.2 and the spatial distribution is shown in Figure 7.1.

Table 7.2: Depth-to-water range of the Dahomey Basin

Dahomey Basin depth-to-water	DRASTIC rating	Final rating × 5
1.5–4.5 m	9	45
4.5–9 m	7	35
9–15 m	5	25
15–23 m	3	15
23–31 m	2	10
>31 m	1	5

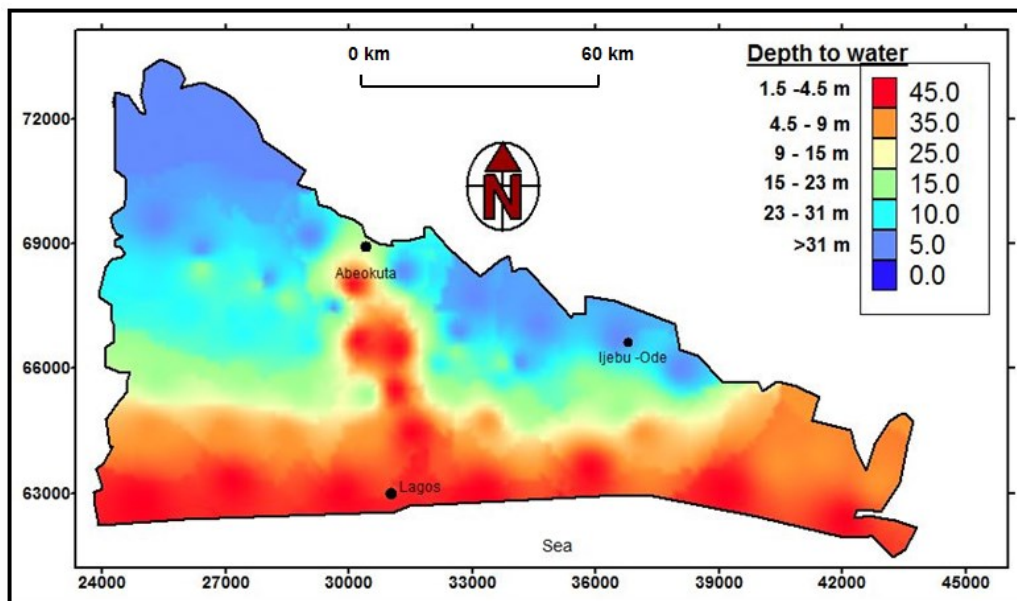


Figure 7.1: Depth-to-water map of the Dahomey Basin

### 7.2.1.2 Net Recharge

The net recharge is the amount of water from precipitation and artificial sources available to migrate down to the groundwater. Recharge water is significant in percolating and transporting contaminants within the vadose zone to the saturated zone. It carries the solid and liquid contaminants to the water table and also increases the water level. The Dahomey Basin is a coastal basin with a high population density. Rainfall serves as the basic mode of groundwater recharge (Oke *et al.*, 2013) and is influenced by the Inter-tropical Convergence

Zone (ITZC) which blows from the Atlantic Ocean to the Sahara Desert. ITZC is also responsible for the seasonality of the rainfall and the two rainfall peaks in June and September. A dry spell is usually noticed in August and is below 100 mm in Lagos (Fagbami and Shogunle, 1995) and 88.3 mm in Abeokuta (Egwuonwu *et al.*, 2012).

Groundwater level is greatly influenced by the seasonality of the rainfall. In Chapter 4, a twenty year rainfall average is presented. The rainfall pattern shows 1 200 mm/year for the northern part of the basin and 1 800 mm/year for the southern part. Most of the southern end is associated with ponding. To calculate the net recharge for the DRASTIC method evapo-transpiration (ETR) and run-off values from previous studies in the basin were used (Table 7.3). ETR in the Dahomey Basin has substantial significance on the recharge rate due to its climatic location; the tropical rainforest belts. The Blaney Morin Nigeria and Priestly Taylor methods were used to calculate the ETR and run-off for Abeokuta, Lagos and Ijebu-Ode (Fagbami and Shogunle, 1995; Egwuonwu *et al.*, 2012). Run-off within Lagos city is higher due to the built-up area, pavements and concrete, which eventually reduce infiltration and percolation and actual groundwater recharge (Adeaga, 2006). Net recharge was calculated using the following formula:

$$\text{Net recharge} = [\text{rainfall} - (\text{evapo-transpiration} + \text{run-off})] \times \text{recharge rating}$$

*Equation 7.2*

Table 7.3: Net recharges estimation from precipitation and run off

Parameters	Lagos	Ijebu-Ode	Abeokuta
Rainfall (mm)	1 800	1 600	1 200
ETR (mm)	1 367 <sup>1</sup>	1 276.0 <sup>2</sup>	1 133 <sup>2</sup>
Run-off (mm)	352 <sup>3</sup>	48.6	48.6 <sup>4</sup>
Total recharge (mm)	81	276	18.4

<sup>1</sup> Fagbami and Shogunle (1995).

<sup>2</sup> Egwuonwu *et al.* (2012).

<sup>3</sup> Adeaga (2006).

<sup>4</sup> Ufoegbune (2011).

Table 7.4 shows the net recharge and rating derived from the calculation in Table 7.3 and the net recharge map is presented in Figure 7.2.

Table 7.4: Rating of net recharge of the Dahomey Basin

Location	Dahomey recharge	DRASTIC rating	Rating × 4
Lagos	81	5	20
Ijebu-Ode	276	10	40
Abeokuta	18.4	2	8

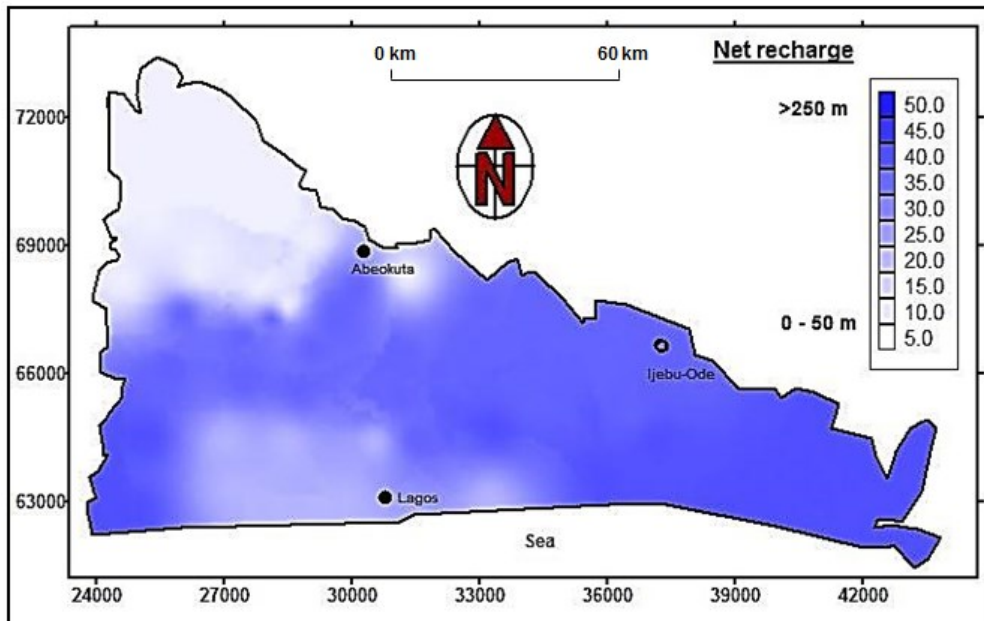


Figure 7.2: Net recharge map of the Dahomey Basin

### 7.2.1.3 Aquifer Media

Geological material that stored groundwater in the Dahomey Basin is the unconsolidated sedimentary rocks. The shallow unconfined aquifer was the target since it is the most accessible and susceptible to contamination. The shallow aquifers occur within a depth of <2–60 m to the surface. The important parameter at this point is the aquifer media characteristics. The larger the grain sizes, the higher the permeability, thus the vulnerability of the aquifer. In unconsolidated aquifers the attenuation is based on the sorting and amount of fine materials within the aquifer. The aquifer media in the Dahomey Basin includes limestone, sandstone, alluvium and sandy clay (Figure 7.3). Lithology and sediment was interpreted from geo-electric log data, field hydrocensus and well log data as presented in Chapter 4.

Often the aquifer media material is the same with the vadose material. The alluvium is composed primarily of floodplain deposits consisting of coarse to medium sand; the CPS aquifer is composed of massive sandstone. Aquifer ratings were assigned a weight of six for both fine to medium sand, and a weight of eight for coarse sand (Table 7.5). The contaminant attenuation capacity of the aquifer depends on the amount and sorting of fine grain sediments. Generally, the larger the grain sizes and porous of openings within an aquifer media, the higher the aquifer permeability and the lower the attenuation capacity of the aquifer.

Table 7.5: Rating of aquifer media of the Dahomey Basin

Aquifer media	Weight	Rating × 3
Sand and gravel	8	24
Massive sandstone	7	21
Bedded sandstone and limestone	6	18

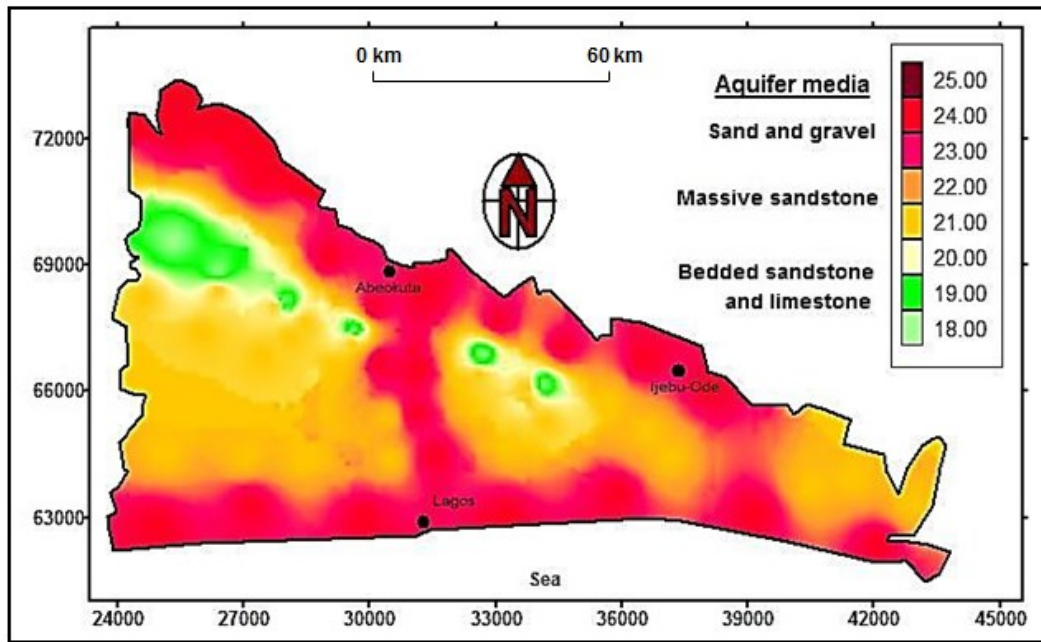


Figure 7.3: Aquifer media map of the Dahomey Basin

#### 7.2.1.4 Soil media

Soil media in the DRASTIC formulation is the upper weathered zone immediately below the soil surface. Soil has the potential to degrade any contaminant type. This will be determined by the amount of clay and silt present in the soil layer. Texture, grain size and clay type are important characteristics that influence porosity and permeability of the soil. These soil characteristics will further influence the amount of rainwater infiltrating the ground surface, the amount of potential dispersion and purifying process of contaminated water.

The presence of fine grain size materials, such as clay, peat, or silt and the percentage of organic matter within the soil cover can decrease intrinsic permeability. This can retard or prevent contaminant migration via physic-chemical processes, namely absorption, ionic exchange, oxidation and biodegradation (Rahman, 2008). The clay type investigated in the Dahomey Basin is largely kaolinite with poor swollen properties. The texture and the amount of clay, silt and sand in the Dahomey soils have been discussed in Chapter 4. The Dahomey soil media includes sandstone, alluvium, sandy loam and loam (Figure 7.4). The DRASTIC, method rate clay loam or loam lower to sandy and gravely soils types (see Figure 4.18 for the Dahomey soil classification). Coarse soil media have higher rates in comparison to fine soil media (Table 7.6).

Table 7.6: Soil media range present in the Dahomey Basin

Soil types	Weight	Rating × 2
Sandstone	9	18
Alluvium	7	14
Sandy loam	6	12
Loam	5	10

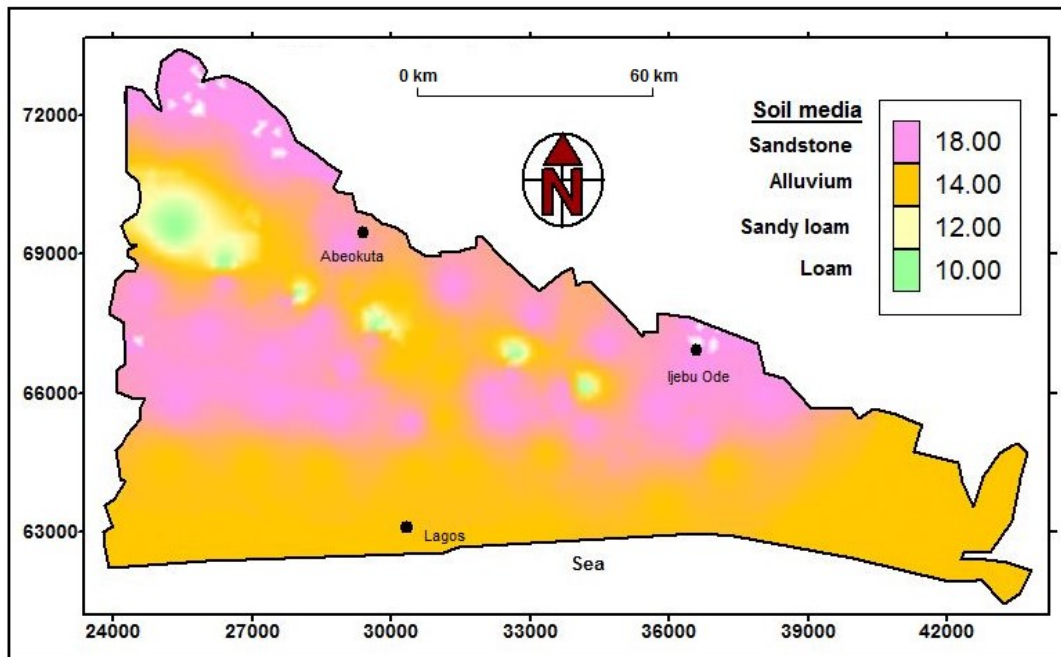


Figure 7.4: Soil map of the Dahomey Basin

### 7.2.1.5 Topography

Topography refers to the slope of the land surface. Topography controls the likelihood of contaminant infiltration in steep slopes. This is because steep slopes do not retain water or contaminated water on the surface, whilst areas with low slope tend to retain water for longer periods of time. This allows a greater infiltration and possible recharge of water and a greater potential for contaminant migration of flat terrains. Topography can give an indication of whether contaminants will remain on land surface for a longer period of time, especially when cleanup is not done or flows away. Slopes were derived from the Digital Elevation Model (DEM) and topography map.

DEM images were extracted from the National Aeronautics and Space Administration (NASA) and the United States' Geological Survey (USGS) Landsat imageries. The elevation model was reprocessed from the Global Land Survey (GLS) collection. The GLS collection contains imageries from TM, ETM+ and ALI sensors. GLS-DEM uses a 90 m resolution and covers 185 km × 185 km. This translates to one degree latitude by one degree longitude. Figure 7.5 shows DEM, adapted from the Global Land Cover Facility of the University of Maryland, USA. The slope varies from the upper end of the basin and decreases towards the sea. Water is the most significant topographical feature in the southern end of the basin, particularly in the Lagos area where water and wetlands cover over 40% of the total land area within the area. An additional 12% is also subject to seasonal flooding (Iwugo *et al.*, 2003).

The Atlantic Ocean and other major water bodies such as the Lagos Lagoon, Ogun River and the Ewekoro River impact the slope levels in the basin. Flat land, swamps and coastal areas of the Atlantic Ocean record slopes of 2–5 m. Flat areas were assigned high

vulnerability rates because their run-off rate is less, and more infiltration of contaminants to the groundwater is expected. The slope map of the Dahomey Basin is shown in Figure 7.6. The land surface in the basin generally slopes gently downwards from north to south.

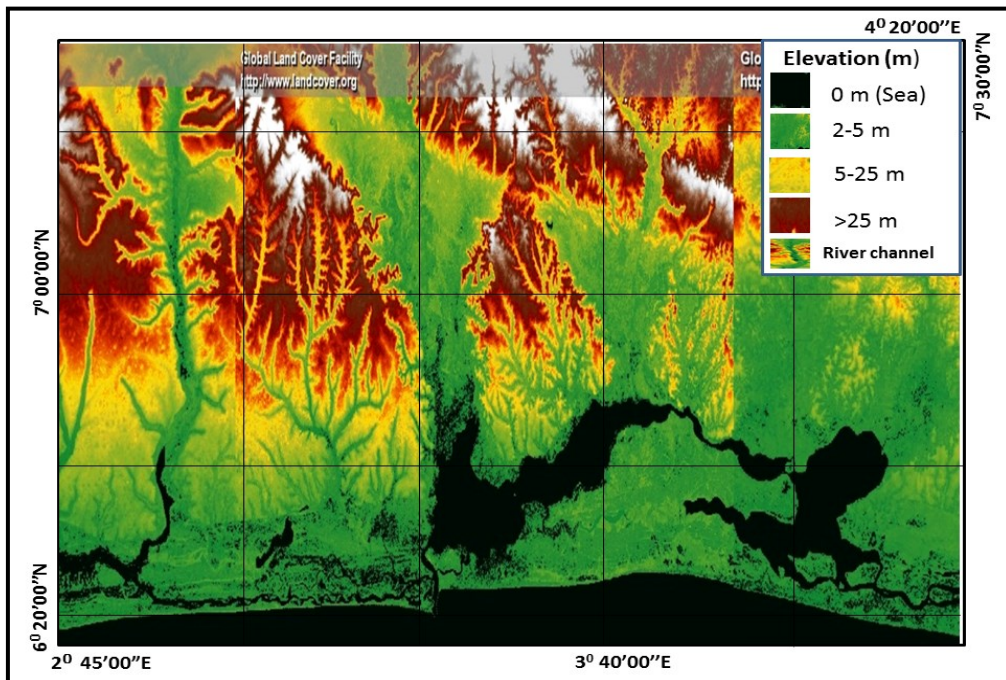


Figure 7.5: Processed topography Landsat imagery of the Dahomey Basin

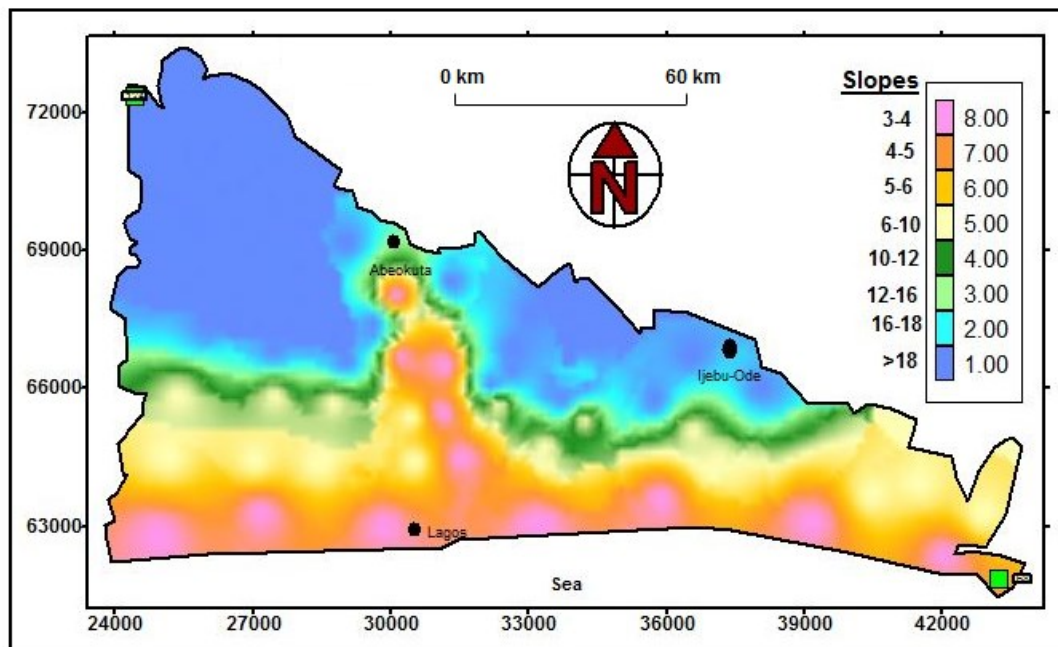


Figure 7.6: Slopes map of the Dahomey Basin

### 7.2.1.6 Impact of the vadose zone

The vadose zones influence on aquifer pollution potential is essentially similar to that of soil cover, depending on its permeability and on the attenuation characteristics of the media. The impact of the vadose zone is a complex phenomenon, combining aquifer media and vadose thickness. The impact of the vadose zone was prepared from the lithological cross-sections obtained by the geophysical data and examined borehole logs. The vadose zone has a high impact on water movement if it is composed of impermeable material. The weights and ratings of the vadose zone are shown in Table 7.7. The map of Dahomey Basin vadose zone material is shown in Figure 7.7.

Table 7.7: Vadose zone impact and rating

Dahomey vadose material	Weight	Rating × 5
Sand and gravel	8	40
Gravel sand	7	35
Limestone, gravel sand and clay	6	30
Sandysilt	5	25
Gravel and sandstone	4	20

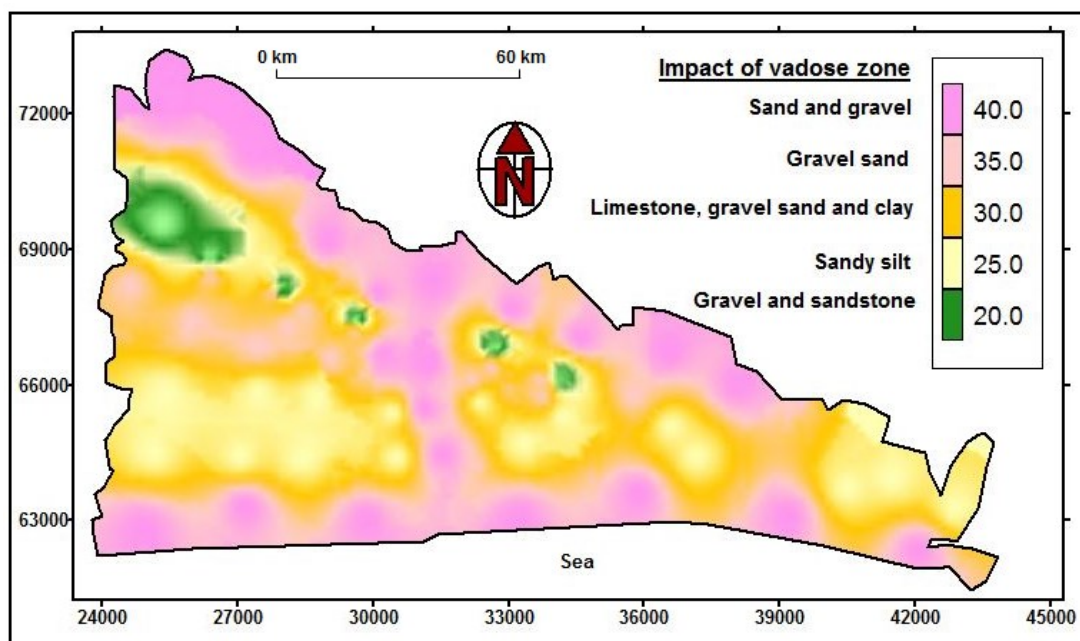


Figure 7.7: Map of the Dahomey Basin vadose zone material

### 7.2.1.7 Hydraulic conductivity

Aquifer hydraulic conductivity is the ability of the aquifer formation to transmit water. It depends on the intrinsic permeability of the material and on the degree of saturation. This is a critical factor that controls the contaminant migration and dispersion from the injection point within the saturated zone. Hydraulic conductivity values were collated from drillers' pump test data. An aquifer with high hydraulic conductivity is vulnerable to substantial

contamination as a plume of contamination can move easily through the aquifer. The Dahomey Basin hydraulic conductivity presented in Chapter 4 in  $\text{m}^3/\text{hr}$  was converted to DRASTIC  $\text{GPD}/\text{ft}^2$ . The calculated hydraulic conductivity index map in the Dahomey Basin is shown Figure 7.8.

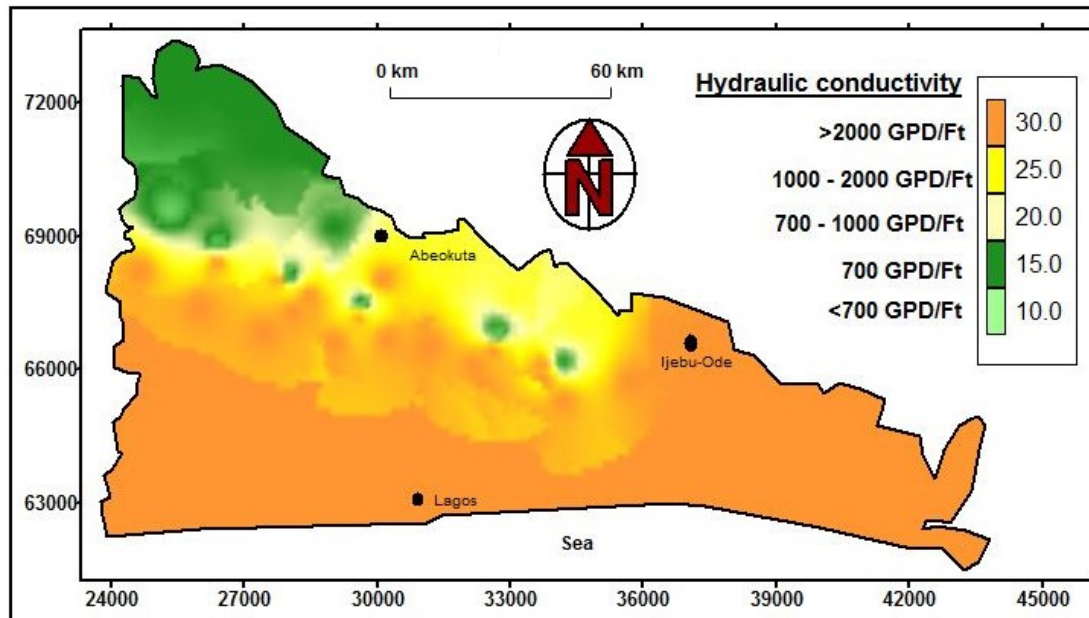


Figure 7.8: Hydraulic conductivity map of the Dahomey Basin

## 7.2.2 DRASTIC Vulnerability Map

Final DRASTIC vulnerability maps were produced by combining the seven DRASTIC ratings through interpolation (direct weighting and kriging). This was after classification through numerical rating and by creating a raster file from the numerical values. According to the DRASTIC index model, the minimum obtainable vulnerability value is 24 and the maximum is 220. This range was divided into four equal classes. These classes were:

- 24 – 71 (extremely low or no risk)
- 72 – 121 (low)
- 122 – 170 (moderate)
- 172 – 220 (high vulnerability risk)

The resulting DRASTIC vulnerability values in the basin lay between 44 and 210 (Figure 7.9). This is very low to high vulnerability. The DRASTIC vulnerability distribution of the Dahomey Basin shows high vulnerability in areas with low depth-to-water, high rainfall and flat to low topography while the low vulnerability were mapped for areas having high vadose thickness, likely run-off and lowest rainfall section of the basin.



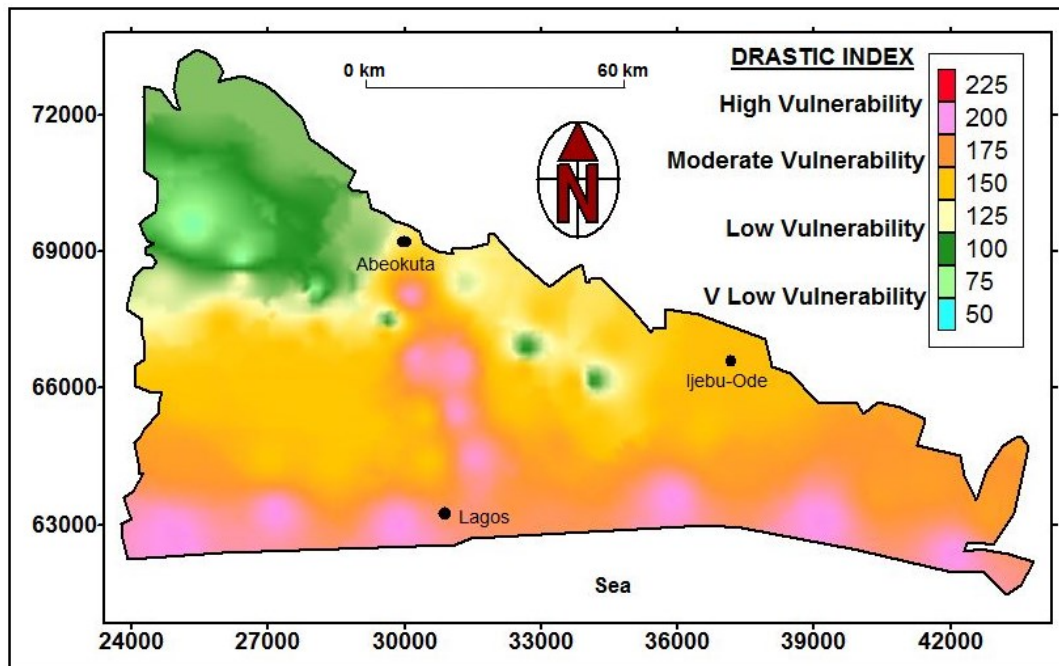


Figure 7.9: DRASTIC map of the Dahomey Basin

### 7.2.3 Comparison of Rainfall–Travel Time and DRASTIC Map

Similarities between the resultant RTt method map and the DRASTIC vulnerability method map (Figure 6.5 & Figure 7.9), respectively, is the categorisation of the same areas as high to moderate vulnerabilities. Almost the same areas were classified as having high vulnerability, except for the RTt map which assigned very high vulnerability to areas with the possibility of lowest run-off and flat terrain (Figure 6.5). In addition, the RTt is stricter in its classification with some areas classified as very high and DRASTIC as high. The differences in the higher vulnerability (as stated earlier) assumed that surface pollution has a greater potential to percolate to the water table, rather than to flow to surface water bodies common in the southern end (Figure 6.1). A great contributing factor to this is also the high rainfall. Although the areas experienced equal precipitation, the run-off effect is expected to affect the infiltration rate in the megacity of Lagos and other built-up areas which dominate the southern end of the map.

### 7.3 Application of the AVI Method

The rationale behind establishing the AVI method (Van Stempvoort *et al.*, 1993) was due to the complexity associated with the DRASTIC method. The AVI is based on the concept of travel time of water and the contaminants that move in the water (usually in a dissolved state) from the surface to an aquifer. The vulnerability is tied to the first arrival of a contaminant at the water table and/or the shallowest aquifer.

The AVI method assessed vulnerability with limited consideration for the specific attributes of the hydrogeological system or the behaviour of contaminants. The AVI methodological strength relies on vadose zone characterisation that is noted as being the most important

single parameter in aquifers vulnerability evaluation. The two key attributes considered were the depth of the water table and the hydraulic conductivity ( $K$ ) of geologic material in the unsaturated zone (or above a confined aquifer). Since the study has characterised the Dahomey Basin's vadose zone saturated hydraulic conductivity ( $K_{sat}$ ) and the overall depth of lithology above the water table as well as the thicknesses of the strata (Chapter 4), it becomes easier to evaluate the aquifer vulnerability map with this method using the formula:

$$c = \sum_{i=1}^n \frac{d_i}{K_i}$$

*Equation 7.3*

Where

$n$  = Number of sedimentary units above the aquifer

$d_i$  = Thickness of the vadose zone

$K_i$  = Hydraulic conductivity of each protective layers.  $K$  has unit of cm/s

$c$  = Travel time with dimension in seconds

It should, however, be noted that so many equally important parameters are not considered in the AVI method and assumptions made therefore include:

- Changes in hydraulic gradient are kept constant, namely groundwater flow vertically along the entire length considered for each depth of the water table.
- The role of diffusion is negligible and contaminants behave the same way as water.
- Seasonal effect, land use and other factors that may change over time are not considered.
- That contaminant is released from the land surface.

Table 7.8 shows travel time estimation of the AVI method. The  $c$  is taken as the rough vertical travel time for contaminants by advection and vertical movements through the porous vadose material of the Dahomey Basin, and contaminates the water table. The map indicating the travel time movement is shown in Figure 7.10. Estimated hydraulic resistance  $\log c$ , as computed in Table 7.8, shows the EWE Formation having the most resistance to aquifer vulnerability contamination within 48.7 days. The least amount of time for contaminants to travel to the groundwater table is the Oshosun Formation with 5.1 days. However, in strict evaluation,  $c$  cannot be travel time for water or contaminants because the formula assumes Darcy's flow at the unit hydraulic gradient. This was also because critical components such as diffusion, dispersion and sorption are not considered. The AVI vulnerability map of the Dahomey Basin is presented in Figure 7.10.

Table 7.8: Vertical travel time estimate of vadose zone material in the Dahomey Basin

Lithology	$K_p$ (cm/s)	Layer thickness (m)	$c_i = d_i/K_i$	c (sec)	c (hours)	Days	Log c
ILA A	0.0031	5	161 290.3				
ILA B	0.0029	10	344 827.6	516 117.9	143.3661	5.973587	0.776
ILA C/D	0.1	10	10 000.0				
ABK A	0.11	25	22 727.27				
ABK B	0.00262	15	572 519.1	918 197.2	255.0548	10.62728	1.03
ABK C	0.0122	15	122 950.8				
ABK D	0.005	10	200 000.0				
EWE A	0.0045	10	2 222.2				
EWE B	0.00045	10	22 222.2	4 205 685	1 168.246	48.67691	1.687
EWE C	0.00043	7	1 627 907				
EWE D	0.0075	10	133 333.3				
OSH A	0.0031	7	225 806.5				
OSH B	0.00989	8	80 889.79	444 328.2	123.4245	5.142688	0.711
OSH C	0.0068	5	73 529.41				
OSH D	0.0078	5	64 102.56				
CPS A	0.0033	4.5	136 363.6				
CPS B	0.003	5	166 666.7	660173.2	183.3814	7.640893	0.8831
CPS C	0.0035	9	257 142.9				
CPS D	0.003	3	100 000.0				

### 7.3.1 Comparison of Rainfall–Travel Time and AVI Map

The AVI map indicates the rate of hydraulic resistance to vertical flow and pollution introduced from the surface, and is shown in Figure 7.10. Log  $c$  is <0.5–1 (extremely high vulnerability), log  $c$  = 1–2 (high vulnerability), log  $c$  = 2–3 (moderate vulnerability) and log  $c$  = 3–4 (low vulnerability). The AVI method categorised major areas of the Dahomey Basin as a high to extremely high vulnerability zone with less than 10% categorised as having moderate vulnerability. This is in contrast to the RTt method which classed larger areas of the Dahomey Basin as moderate vulnerability. Areas that the AVI classed as moderate vulnerability, was classed as low vulnerability in the RTt method. According to the RTt vulnerability method, rainfall contribute the highest values to the vulnerability index ( $5 \times 10 = 50$ ), closely followed by hydraulic conductivity, overall depth and topography, respectively. Travel time in the RTt method is dependent on the relations between the parameters of lithological conditions including the slopes, while the travel time for AVI index parameters is solely based on the layer thickness and its hydraulic conductivity.

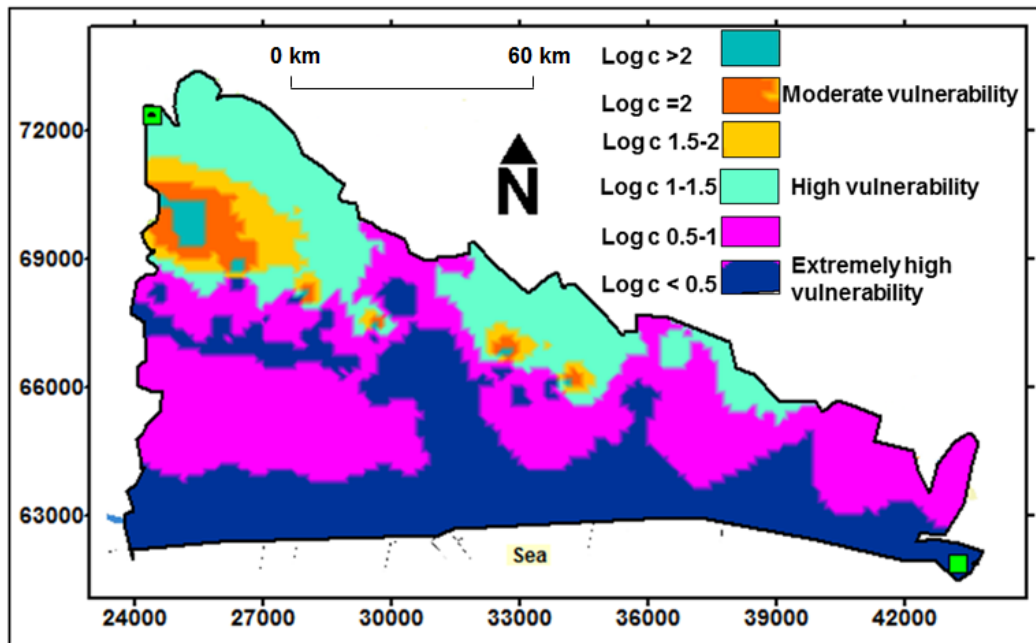


Figure 7.10: AVI travel time vulnerability map

## 7.4 Application of the PI Method

The PI method was chosen because it increased the number of parameters considered in the assessment of the vulnerability. The P-factor describes the effectiveness of the protective cover above an aquifer which can be summarily grouped two parameters: the hydraulic properties (soil, topsoil, subsoil, rock type and unsaturated zone) and the thickness. The I-factor describes the infiltration conditions which are the degree of bypass of the protective cover. The PI assessment method is derived from the product of the P-factor and I-factor.

Special note taken in developing the PI maps for the Dahomey Basin were the problems of thin, low permeability strata that can be bypassed if they are not laterally extensive, but occur in a form of lenses. As a consequence, the lateral continuity of each layer was taken into account in order to avoid overestimation of the protective function. It is extremely time-consuming to measure the permeability of each layer by field or laboratory experiments. Therefore, the recommendation of Goldscheider (2002) as to the estimation of permeability of each layer was followed. This was also done to earlier methods by assessing the thickness and type of layers on the basis of geological maps, topographical maps and field investigation, combined with the saturated laboratory conductivity performed.

*The PI method always takes the groundwater table in the uppermost aquifer as the target. Consequently, a higher aquifer is not considered to be protection for the underlying aquifer. This is in line with the selection of the uppermost-unconfined aquifer in the Dahomey Basin for assessment. Likewise, the similar parameters, excluding the karstified parameters, were employed in the assessment of the Dahomey Basin shallow aquifers.*

### 7.4.1 The P-Map

The P-map includes an assessment of the protective cover over the aquifer, which is practically assessing the vadose zone properties. The P-map parameters assessment covered a wide range of rocks. The input parameters of protective cover are as follows:

- Effective Field Capacity (eFC) of the topsoil up to 1 m in depth.
- Groundwater recharge.
- Type of subsoil.
- Type of bedrock and degree of its fracturing.
- Thickness of each layer above the groundwater level.
- Presence or lack of permanent artesian conditions.

#### 7.4.1.1 Topsoil (T)

The topsoil is represented by the eFC. The eFC is defined as the portion of field capacity which is available to plants in certain soil types. The eFC was termed available water capacity in the GLA method upon which the PI was based. Typical values of soil texture, as presented by Hennings *et al.* (2011), include 10 mm/dm for sandy loam, 10.5 mm/dm for sandy clay loam, 8.5 mm/dm for sandy clay and 7.5 mm/dm for clay. The dm is the estimated depth of soil. However, from the texture classification presented in Table 4.7, Chapter 4 shows that the topsoil are majorly sands and some layers of sandy loam. Goldscheider (2005) reported eFC on gravel and sand of Engen Test Site and reported a low to medium eFC (50–140 m). Considering that topsoils in the Dahomey Basin are alluvium, porous sand and PI method do not cater for some unconsolidated sediments, most alluvial sediments in the Dahomey Basin are devoid of topsoil. Therefore, the effect of effective water capacity up to one metre in depth is low in alluvium sediment (i.e. less than <50–90 mm), which was rated 0–50 as presented in Table 7.9.

#### 7.4.1.2 Recharge (R)

The recharge estimation in the PI method is similar to the recharge of other methods. The factor R is assessed based on the value of the groundwater recharge. Xu and Braune (2010) reported a recharge rate >500 mm/y for southern Nigeria, including that of the Dahomey Basin. PI recharge rating include <100 mm/y (1.75), 100–200 mm/y (1.50), 200–300 mm/y (1.25), 300–400 (1.0) and >400 mm/y (0.75), respectively. The Dahomey Basin's spatial recharge shows recharge values of above 400 mm/y (Table 7.9).

#### 7.4.1.3 Subsoil (S)

The subsoil in the PI method is defined as the soil interval beyond one meter from the surface. In the Dahomey Basin the soil profile is as thick as the vadose zone in most places, as indicated in several pictures in Chapter 3. The thick soil profiles were enhanced by active weathering, which resulted from the seasonality of the weather and tropical climatic belt with sunshine reaching temperatures of above 30 °C per day. The type of soil is referred to as texture class which depends on grain size distribution (GSD). A compulsory range used in the subsoil classification is presented in Figure 2.4.

The comprehensive GSD for the Dahomey Basin is presented in Table 4.7 and the particular range used in calculating the protective cover is presented in Table 7.9. The subsoil thickness of five was used in the alluvium predominant regions since most of the areas have a vadose thickness below the value. Other soil thickness' used in the PI method was the same as used in the AVI method.

#### 7.4.1.4 Lithology (L)

The geological map of Nigeria guided the lithology classification. Porous sandstone, alluvial deposits, massive sandstone and bedded sandstone and limestone are the major rock types dominating the Dahomey Basin. Table 7.9 shows the lithology and points assigned to the rock types. The lithologies used were strictly those above the water table and below the ground surface. This means that other rock types present in the basin below the water table were not considered. Fracturing was considered to be absent or with few occurrences in the Dahomey Basin and was assigned points of one. In addition, artesian pressure was not considered in this study because the unconfined aquifer was the target which had no artesian pressure.

Table 7.9: Values of the factors T, R, S, L and F

<b>eFc (mm) up to 1 m depth</b>	<b>T</b>
>250	750
200–250	500
140–200	250
90–140	125
50–90	50
< 50	0
<b>Recharge (mm/y)</b>	<b>R</b>
0–100	1.75
>100–200	1.50
>200–300	1.25
>300–400	1.00
>400	0.75
<b>Type of subsoil base on GSD</b>	<b>S</b>
Silty loam	220
Sandy silty loam, slightly sandy loam	200
Sandy loam	180
Slightly silty sand,	50
Sand	25
Sand with gravel, sandy gravel	10
<b>Lithology</b>	<b>L</b>
Marl, siltstone, claystone	20
Sandstone, quartzite, metamorphite	15
Porous sandstone, tuff	10
Limestone, conglomerate	5
<b>Fracturing</b>	<b>F</b>
Non joined	25
Slightly joined	4
Slightly karstified	1
Moderate karstic	0.5
Strongly factored or strongly karstified	0.3
Not known	1

The final protective cover vulnerability map is presented in Figure 7.11 and was derived by using the following formula:

$$P_{TS} = \left[ T + \left( \sum_{i=1}^m S_i M_i + \sum_{i=1}^n B_i M_i \right) \right] R + A$$

Equation 7.4

Where  $T$  refers to topsoil (up to 1 m);  $S$  = subsoil;  $B$  = bedrock;  $M$  is the thickness of each layer in metre;  $R$  is the recharge factor;  $A$  is the artesian pressure factor;  $m$  is number of subsoil layers; and  $n$  is the bedrock layers. The factor  $B$  presents the product of  $B = LF$ , where  $L$  depends on the type of bedrock and  $F$  on the degree of its fracturing or karstification. The  $P$ -map ranged from moderate to high class. This means that the protective cover of the Dahomey Basin is highly effective.

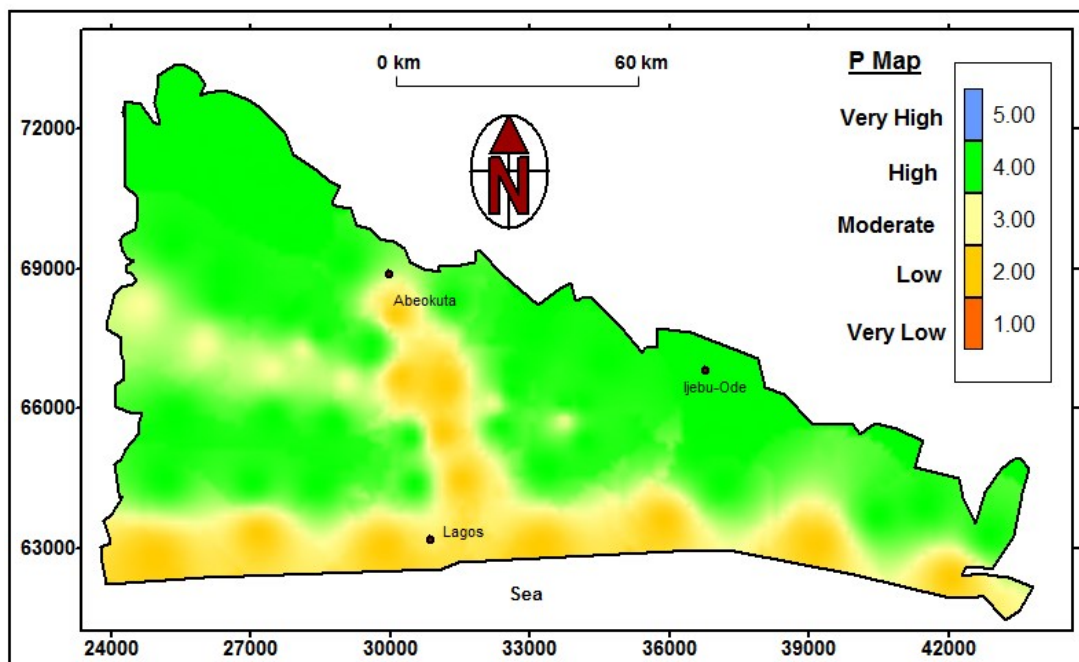


Figure 7.11: Protective cover map of the Dahomey Basin

### 7.4.2 The I-Map

The  $I$  factor shows the degree to which the protective cover is bypassed by lateral surface and subsurface flow, and subsequent concentrated recharge. The following three steps, as stated by Goldscheider (2002), were observed in order to determine the  $I$  factor and construct the  $I$  map, respectively:

- Saturated hydraulic conductivity of topsoil.
- Infiltration processes.
- Lateral surface and subsurface flow.

The topsoil properties decide on the dominant flow process. Infiltration flow predominates on high permeability soils ( $K > 10^{-4}$  m/s) with type A, as was the case in the basin. Infiltration flow and subsequent percolation takes place in permeable topsoils overlying layers with absent low permeability layers. Infiltration processes and run-off generation are also influenced by the slope gradient and vegetation. Gentle slopes and forests (natural forests and plantations) favour infiltration and percolation. Steep slopes and agricultural land use favour run-off. Northern areas of the Dahomey Basin contain steep slopes, thick vegetation and were assigned a point of 0.8. The southern end is relatively flat and has swampy vegetation, and was assigned a point of one. The third condition of the surface catchment map depends on the two earlier conditions.

Consequently, the I Map (showing the degree to which the protective cover is bypassed) is obtained by intersecting the I Map (showing the occurrence and intensity of lateral flow) with the so-called surface catchment map (Landsat imagery). The I Map is shown in Figure 7.12.

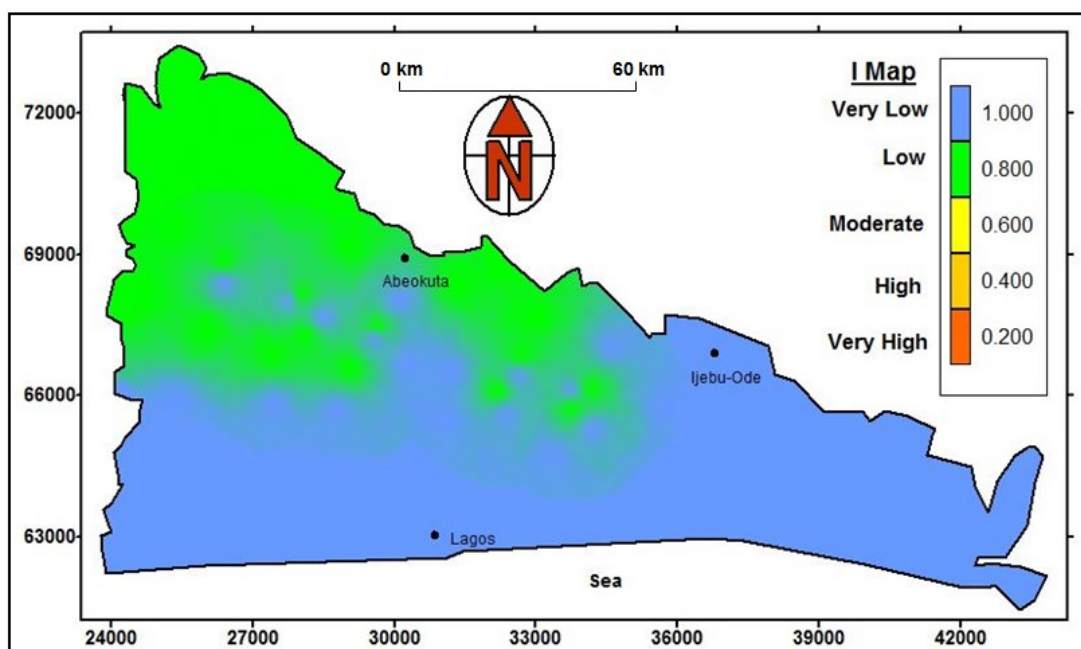


Figure 7.12: The I-Map of the Dahomey Basin

### 7.4.3 PI-Map

The final vulnerability map is the product of the P Map and I Map, and is presented in Figure 7.13. As can be seen in the PI vulnerability map, the vulnerability class of the Dahomey Basin range from moderate to very low vulnerability. The PI method rated its classes with specified colours, namely very high vulnerability (red), high (orange), moderate vulnerability (yellow), low vulnerability (green) and very low vulnerability (blue). Areas showing moderate vulnerability is characterised by low subsoil, high rainfall and a very low water table and low lithology thickness resulting from unconsolidated sediment. The lithology is alluvium and porous sandstone that is highly permeable.



Low vulnerability areas result from lithology containing sandstone and sandy loam texture. Slopes are high, saturated hydraulic conductivity of the topsoil supports infiltration and the water table is relatively high. Very low vulnerability areas represented by the blue colour are massive sandstone with infiltration topsoils. The lithology thickness and overall depth to the water table is high. However, the low vulnerability areas contain flat topography that supports high infiltration, but due to the rating of other factors, it shows little significance in the overall vulnerability map.

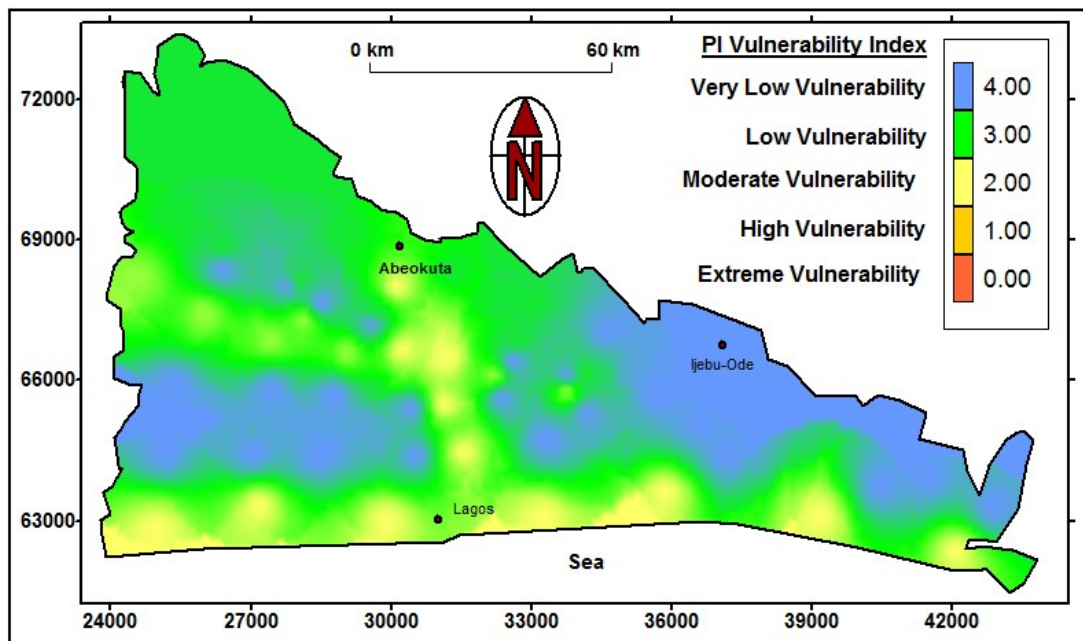


Figure 7.13: PI vulnerability map of the Dahomey Basin

## 7.5 Conclusion

In this chapter, three groundwater vulnerability methods were compared and used to characterise the shallow unconfined aquifer of the Dahomey Basin. The vulnerability index classes ranged from moderate to very high vulnerability in the study area. All the methods show similar vulnerability classes, especially in the northwestern section and southern most section of the Dahomey Basin. Nevertheless, it is important to remember that the vulnerability assessment carried out were for the intrinsic evaluation of protective cover above the aquifer. These intrinsic properties were shown in the vulnerability maps of the three methods considered. The validation and comparison of the three vulnerability methods considered in this chapter with the RTt method will be presented in the next chapter.

# CHAPTER 8

## VALIDATION OF THE RAINFALL–TRAVEL TIME METHOD

Validation of vulnerability is a process by which the calculated vulnerability indices are compared to a measured physical or chemical parameter. This is important to evaluate the ability of the RTt method to calculate vulnerability values that are a close reflection of the physical system. Validation is an exact method used differently from most vulnerability methods. Validation analysis can stand on its own in vulnerability studies or can be used for verification of an existing methodology. The common validation analyses carried out in groundwater vulnerability studies, as stated by Daly *et al.* (2002), include:

- Hydrograph of chemical properties.
- Bacteriology.
- Tracer techniques.
- Water balance.
- Calibrated numerical simulations.
- Analogy studies.

### 8.1 Validation Techniques of the Rainfall–Travel Time Method

Validation analysis presented in this section includes the use of a conservative tracer, bacteriology and a dissolved oxygen analysis. Bacteria and chemical parameters are used because it is in-situ, easily available to map and simple to analyse. It is also the best when comparing the intrinsic vulnerability maps of resources. Resources such as drinking water assessment are both quantitative and qualitative. The concentrations of dissolved elements in groundwater are useful when planning (protection) and for treatment. However, in relation to travel time of possible contaminants from the surface to aquifer, elemental concentrations may be important in detecting surface input in the groundwater.

#### 8.1.1 Validation with Chloride

One of the indicators used as tracer validation is chloride. Chloride validation involves the use of known mechanisms of chloride in the evaluation of groundwater vulnerability. Chloride is a conservative mineral and is assumed to originate from the sea. If there are no other sources, the amount of chloride in a groundwater system should be the amount of chloride deposited by precipitation. The precipitation effect on the chloride concentration deposited into a groundwater system depends on the quantity of chloride present in the aquifer and vadose zone, and the distance from the sea. The choice of chloride as the measure of vulnerability validation was based on some important observations in the Dahomey Basin and the chloride properties, which include:

- Chloride is a conservative element and is not removed by evaporation or plant transpiration. Chloride is non-volatile and therefore stable, and concentration is relatively assured not to leave the system.

- Below the root zone chloride concentrations should remain constant if recharge rates have not varied over time (Scanlon *et al.*, 2003).
- Chloride in the vadose zone was low or absent. This was confirmed with the absence of halite as a major mineral in the XRD results in Chapter 4. The dominant clay types were kaolinite and anatase. The chloride investigated was absent, which means the available chloride from rainfall might have been washed down (infiltrated) into the groundwater. This is a measure of water movement through the vadose zone.
- Chloride concentrations in the groundwater vary and it is spatially distributed which give a regional possibility for usage.
- Groundwater geochemical modelling results reveal rainfall as the main source of groundwater chloride, particularly in the wet season. This was concluded after results of geochemical models show under-saturation of halite and gypsum, and other evaporite minerals as the other sources of chloride in the Dahomey Basin. The under-saturation means chloride present in the groundwater cannot precipitate as salt. However, geochemical modelling cannot be precise on the origin of chloride in water because under-saturation of chloride does not necessarily mean there is an absence of other forms of chloride sources such as evaporite minerals. They are just not yet in equilibrium to precipitate as salt.

A west to east cross-sectional line A–AA was created on the RTt vulnerability map and the chloride concentration map of the Dahomey Basin (Figure 8.1a&b) respectively. The cross-section cut through the various vulnerability indexes (low to high vulnerability). Plot of RTt vulnerability values against chloride along the cross-section are presented in Figure 8.1c. High vulnerability areas on the RTt map correspond to low chloride values. The low vulnerability areas also record high chloride values. Although, some authors infer that vulnerability assessment validation with the chloride method is based on the principle that the more chloride in the water, the more susceptible the groundwater will be to contamination (Ramos-Leah and Rodriguez-Castillo, 2003; Saidi *et al.*, 2011).

This is inversely related as the chloride concentrations in groundwater are related to recharge rate, which are related to groundwater susceptibility (Scanlon *et al.*, 2003). Low chloride concentrations in groundwater indicate high recharge rates since chloride is flushed out of the system, whereas high chloride concentrations indicate low recharge rates since chloride accumulates as a result of evapotranspiration (Scanlon *et al.*, 2003). A high recharge rate means high vulnerability and a low recharge rate means low vulnerability. Therefore, low chloride concentration indicates high vulnerability and high concentration indicates low vulnerability.

The correlation plot (Figure 8.2) shows that the chloride decreases with RTt vulnerability index rise with 57%. High chloride concentration with low RTt index means high residence time of water in the vadose zone and low aquifer vulnerability. Subsequently, a low chloride concentration means low residence time of chloride in the vadose zone and high vulnerability. This principle is obtain only in a perfect system, and one major challenge of vulnerability validation with chemical parameter data is the perfect compatibility of the results

with the groundwater dynamic system. Spatial variability may generally be expected for coastal areas with the wet and dry chloride deposition method (Keywood *et al.*, 1997; Kayaalp, 2001). The variability is attributed to these two reasons:

- Distance away from the coast.
- Seasonal variability.

In a study by Moysey *et al.* (2003), which is a follow-up to an earlier study done by Knies *et al.* (1994) at Indiana, USA, they showed that atmospheric chloride deposition decreased exponentially with distance from the coast. These result in coastal regions to have a high chloride deposition rate compared to inner-continental locations. Higher chloride concentrations at coastal locations are interpreted to reflect the influence of marine aerosols, and lower values inland reflect progressive rainout of chloride (Eriksson, 1960; Johnston and McDermott, 2008). Wet and dry depositions are the two mechanisms controlling the removal of chloride from the atmosphere to the land surface. Wet chloride deposition mechanisms control rainy season chloride concentration. During the rainy season, chloride-bearing aerosols are washed out from falling raindrops or rained out from the clouds (Guan *et al.*, 2010). Wet chloride deposition is dependent on precipitation characteristics which decline during rainstorms (Hainsworth *et al.*, 1994; Guan *et al.*, 2010) and rain-out has been correlated with the precipitation rate (Knies *et al.*, 1994).

The use of chloride as an RTt validation technique is to some degree a reflection of the travel time of surface contaminants to infiltrate and percolate into the shallow groundwater. This is assuming chloride concentration in groundwater has only rainfall as a source. However, chloride background concentration of an aquifer should be determined before using it as a validation criterion, which is due to the presence of chloride in some minerals such as evaporate or halite before using it as a groundwater vulnerability validation tool. A combination of other validation techniques such as bacteriology with some chemical parameters must be employed, as was done by Nguyet and Goldscheider (2006) as a further validation check.

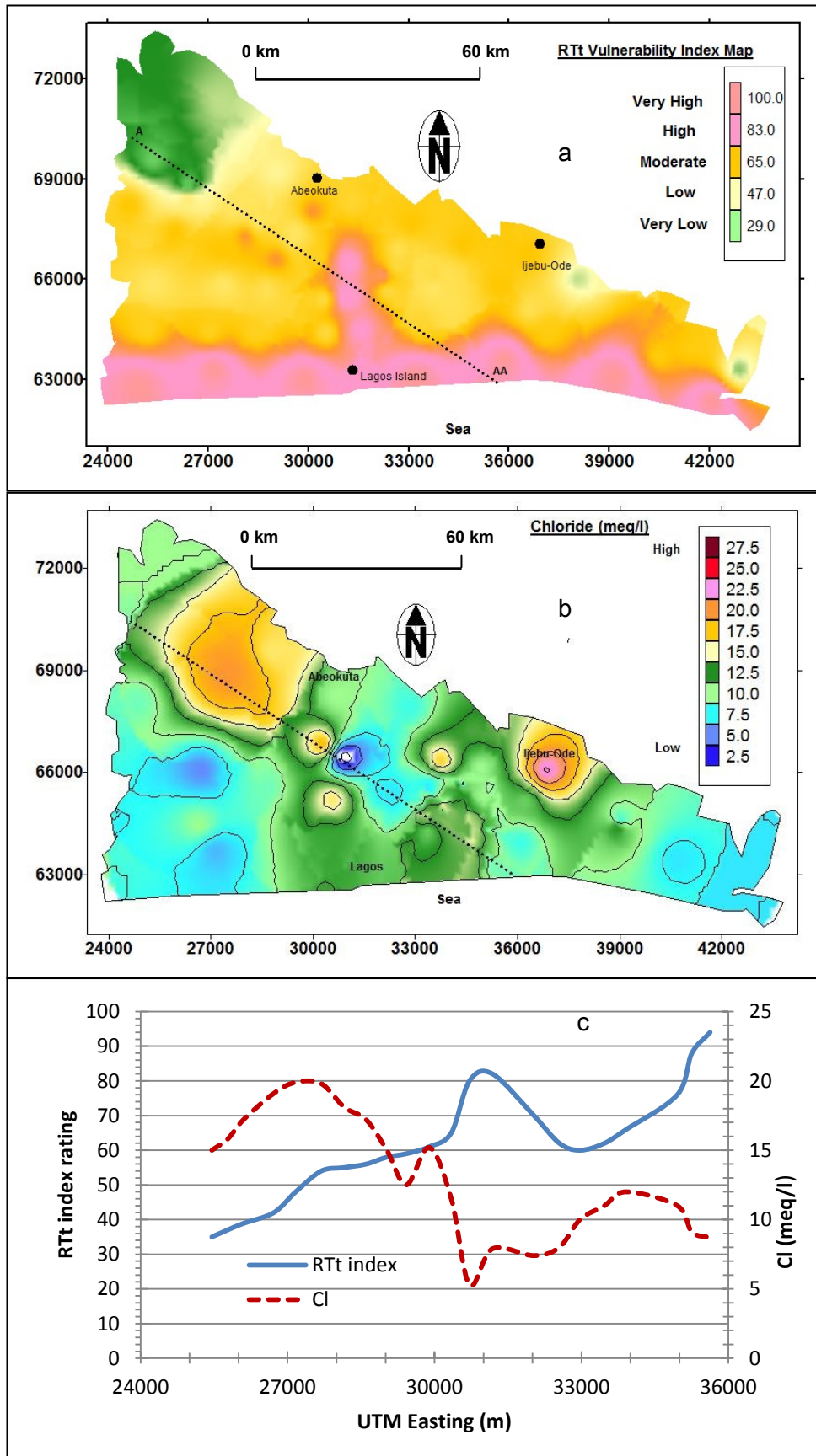


Figure 8.1: (a) RTt vulnerability map cross-section; (b) Cross-section over chloride concentration map, (c) Plot of RTt index and Cl along the cross-section

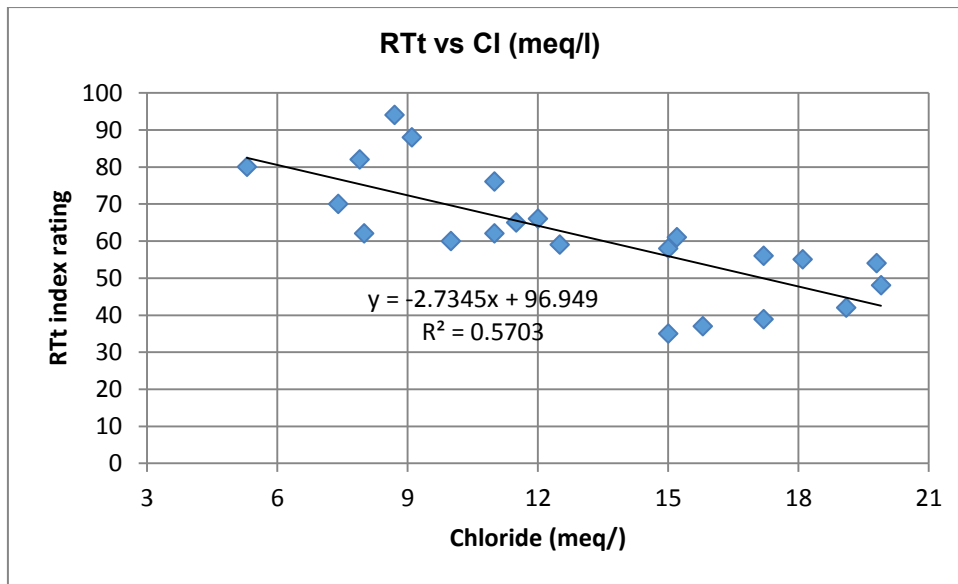


Figure 8.2: Chloride plots against the rainfall–travel time index

### 8.1.2 Validation with Dissolved Oxygen

Studies have shown that specific chemistry can serve as useful tracers to fingerprint the hydrogeological history of groundwater (Kalinsky *et al.*, 1994; McLay *et al.*, 2001). This is because concentrations of a particular chemical in groundwater are influenced by the following factors; recharge source, reactivity of aquifer sediments, oxidation–reduction (Redox) chemistry, residence time and land-use activities. Redox conditions can be a useful vulnerability validation tool. Dissolved oxygen is a good indicator of Redox conditions in groundwater. Low dissolved oxygen concentrations in groundwater indicate a reduced condition (although depending on background concentrations), and high concentrations indicate an oxidising condition. This is because the atmosphere is the source of DO in most groundwater (Rose and Long, 1988). This means aquifers under frequent recharge, particularly from rainfall as RTt vulnerability assumes, will have increasing oxidation and shorter travel time of water, thereby suggesting more vulnerability to contamination and vice versa (Starr and Gillham, 1993; Chapelle, 2000; Datry *et al.*, 2004).

The Dahomey Basin shallow aquifers vulnerability to contamination decreases northwards (Figure 8.3a). The RTt method correlation plot (RTt *versus* DO) suggests an increase in vulnerability by 55% from north to south along the cross section A–AA (Figure 8.4a). This also means recharge is more likely to increase along the same trend since the mechanism supporting groundwater vulnerability to contamination favours recharge (Scanlon *et al.*, 2003). However, groundwater recharge is a complex mechanism, which considers so many factors that are outside the scope of this research. Therefore, actual recharge into the Dahomey aquifer is not directly calculated.

The dissolved oxygen increases in the direction of increased vulnerability. This corresponds to the prediction of the RTt vulnerability method, which increases from lower DO in the low vulnerability areas, to higher DO in highly vulnerable areas (Figure 8.3c).

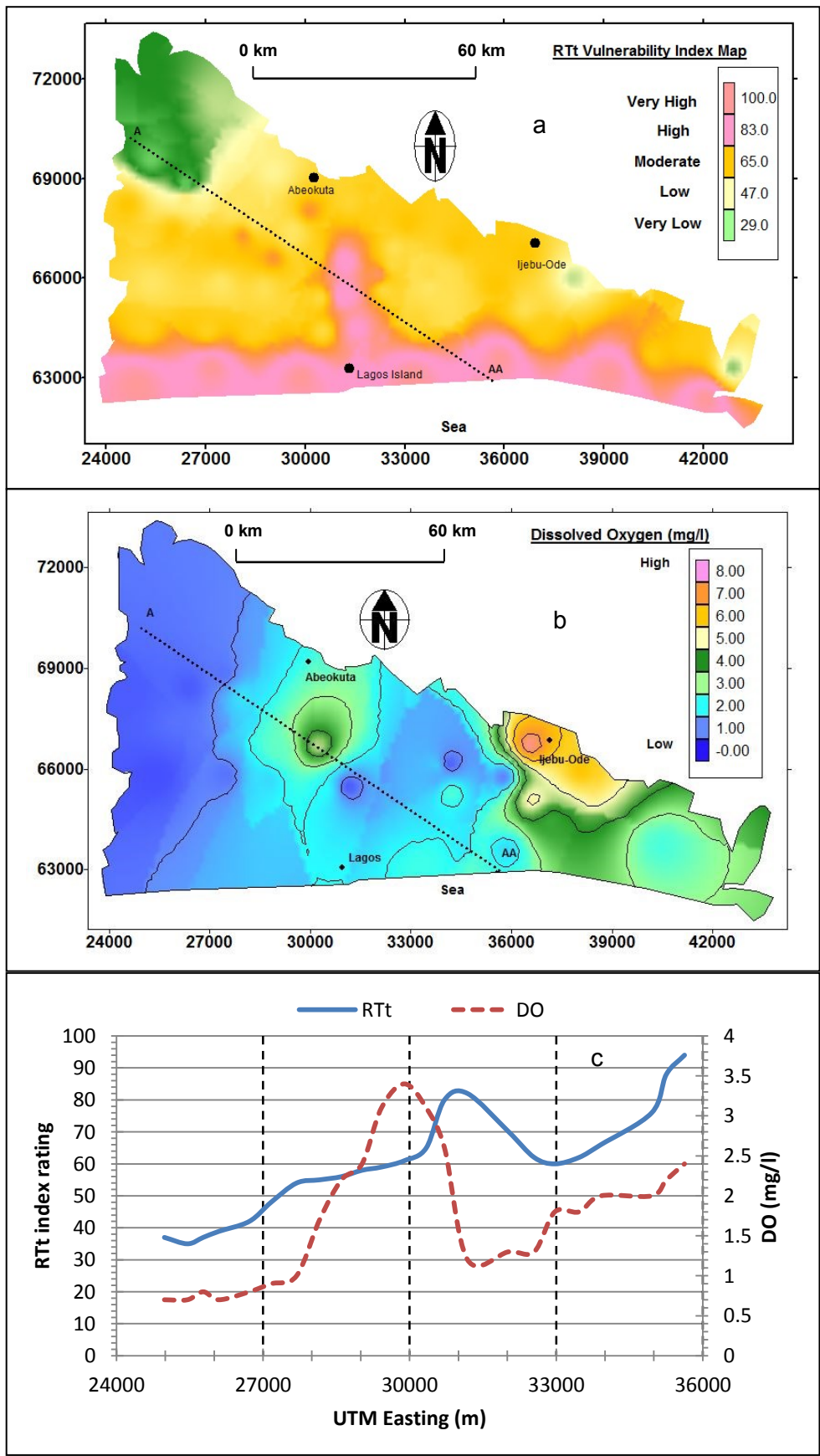


Figure 8.3: (a) Section A–AA plots of RTt vulnerability index; (b) Cross-section plot A–AA on DO contour map; (c) Plot of cross-section of RT index with DO

Although the correlation value of the DO and RTt index along the A–AA on the UTM Easting is imperfect, it gives a direction along the vulnerability index trend. DO is the amount of oxygen that will dissolve in the water at a stable temperature and pressure. Aquifers having short travel times from the surface are frequently recharged compared to aquifers showing longer travel times to reach. Therefore, DO increases along high vulnerability areas and decreases in low vulnerability areas (Figure 8.3c & Figure 8.4a). A relationship depicting this concept is established and shown in Figure 8.4b.

Dissolved oxygen is reported to control the fate of dissolved organic contaminants from land surface by controlling the types and numbers of micro-organisms present within an aquifer. It is suggested to be considered in any investigation of groundwater contamination (Rose and Long, 1988) or as aquifer vulnerability validation (as done in this study).

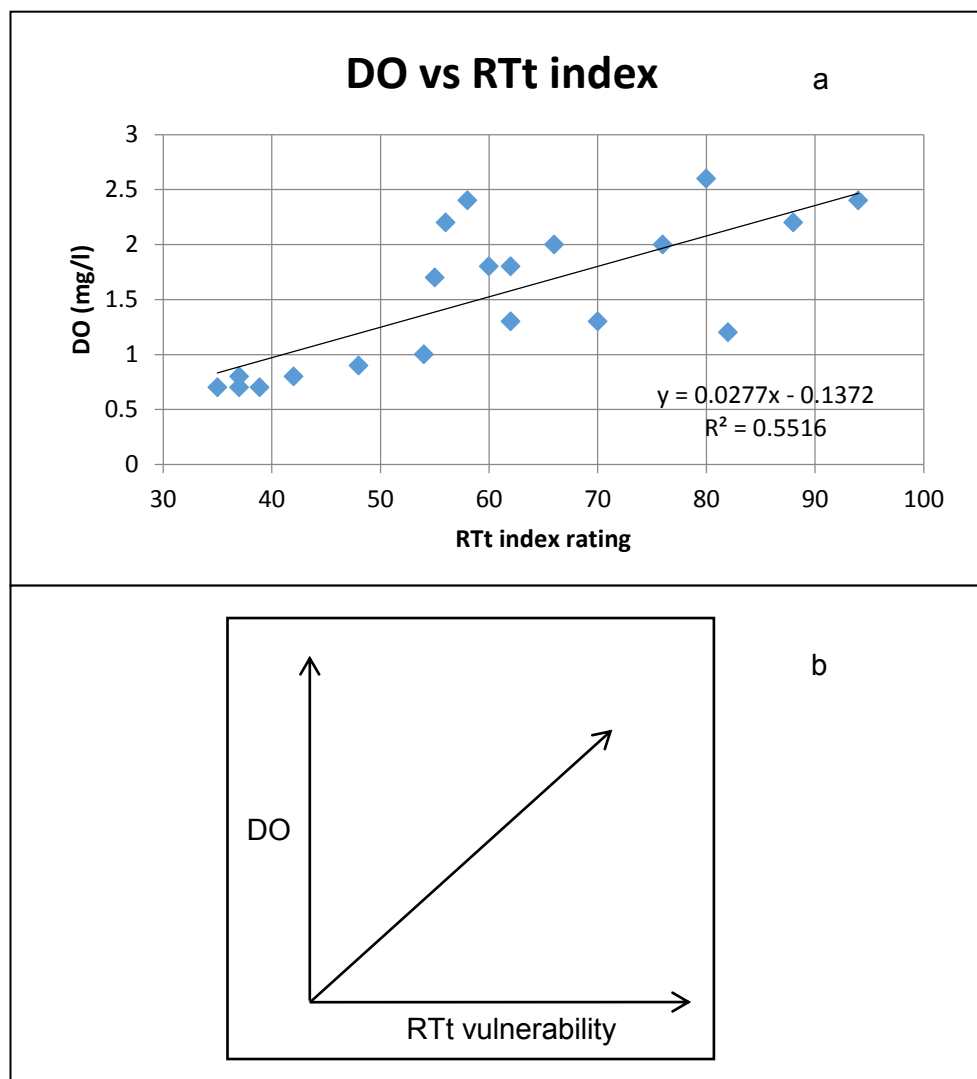


Figure 8.4: (a) Cross plot of DO and RTt index vulnerability; (b) DO correlation plots with RTt vulnerability



### 8.1.3 Validation with Bacteriological Counts

The validation of vulnerability maps with microbial contaminations is unique in the sense that microorganisms directly affect water quality. Although many vulnerability validation methods have been established, very few of them considered the use of microorganisms (Butscher *et al.*, 2011). RTt, like other vulnerability methods, assess the intrinsic properties of an area to pollution, which is estimated without considering the types of the polluting materials. Pollution of groundwater may take many forms, including microbial migration to the water bodies. The likelihood of bacterial contamination to groundwater bodies is dependent on recharge conditions, filtration and degradation (organic matter and contaminant) and time. Therefore, in order to use microorganisms as vulnerability validation tools, important factors contributing to microbial generation and survival in groundwater systems such as oxygen, organic carbon and residence time of water must be considered (Payment, 1999).

Total heterotrophic bacteria counts (THBC) were considered a good tool for groundwater vulnerability validation because they are everywhere in natural environments and stable over time in groundwater (Griebler and Lueders, 2009; Foulquier *et al.*, 2011). THBC were reported to range between 1.0 and more than 10 000 CFU/mL in groundwater (Payment 1999, Pepper *et al.*, 2004; Stine *et al.*, 2005). Analysis of THBC followed the standard of APHA, AWWA and WEF (2005). THBC analysis does not specify the type or source of bacteria. Heterotrophic bacteria use organic compounds as a source of energy and multiplication. They can be linked to the residence time of water and the amount of oxygen present in an aquifer. For vulnerability validation purposes, THBC will multiply in longer residence groundwater by depleting available oxygen (Winograd and Robertson, 1982). Therefore, groundwater with a lower DO and higher THBC implies fewer recharges, high residence time and therefore low groundwater vulnerability.

In the Dahomey Basin shallow aquifers, the DO and groundwater vulnerability increases southward with the RTt method (Figure 8.3c), the THBC decreases southward in the opposing manner with 58% correlation (Figure 8.6a). The RTt method assumes areas with low vulnerability experience, lower recharge and higher residence time of water. Therefore, a relationship where THBC increases with decreasing oxygen and low vulnerability can be established (Figure 8.6a&b). In addition, the THBC *versus* RTt index plots along the cross section A–AA on the UTM Easting, showing a good correlation for low vulnerability and high THBC as well as high vulnerability with high THBC (Figure 8.5c). This is possible due to the availability of oxygen at high vulnerability and high recharge. Moderate vulnerability areas show THBC varying between a low and high number. Towards the coast, which is a high vulnerability zone, THBC display a sharp decline. This could be attributed to many reasons including temperature, seasonality and unfavourable environmental conditions (salinity). Similar results of heterotrophic bacteria correlation with dynamic vulnerability index can be found in the work of Butscher *et al.* (2011).

For drinking water consumption, heterotrophic bacteria are generally reported to be of no severe health concern (WHO, 2002; Bartram *et al.*, 2004), except for those with a compromised immune system (Rusin *et al.*, 1997; Pavlon *et al.*, 2004).

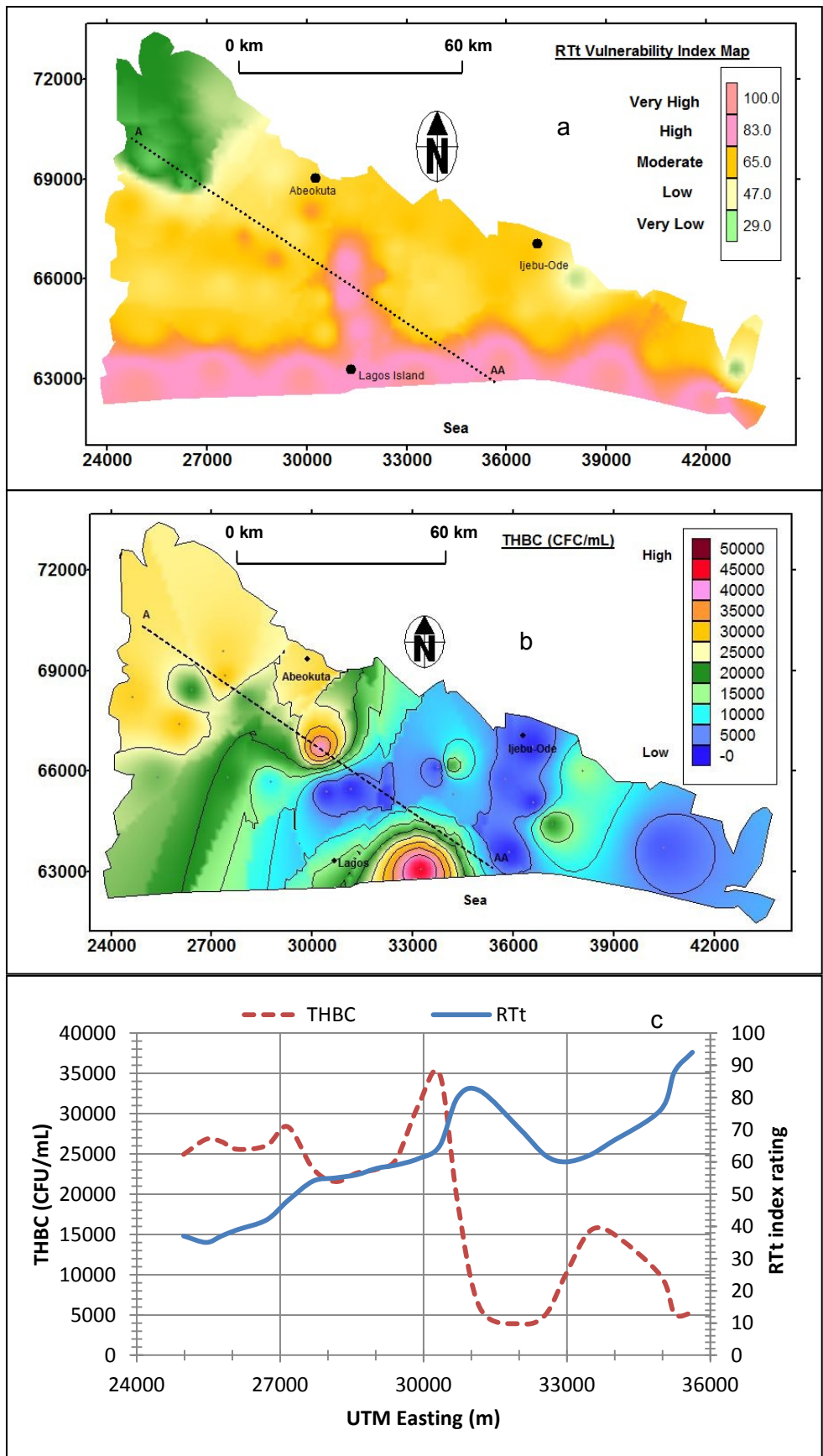


Figure 8.5: (a) Cross-section plot of A–AA on the RTt index map; (b) THBC cross–section map; (c) Correlation plot between THBC and RTt index

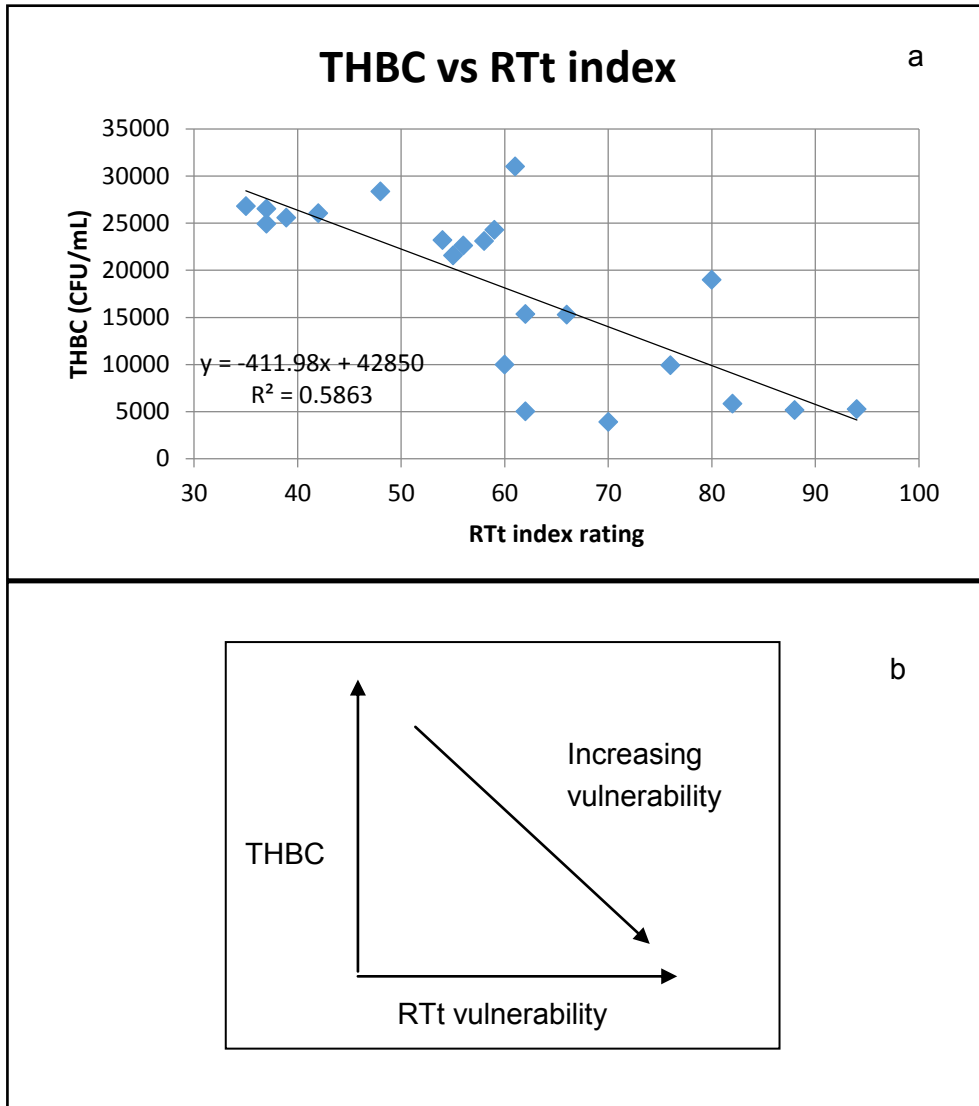


Figure 8.6: (a) Bacteriology plots against the RTt index rating; (b) relationship between THBC and RTt groundwater vulnerability

## 8.2 Comparison between the Rainfall–Travel Time and Common Existing Methods

The vulnerability map developed from the RTt method shows zones from low to moderate and high vulnerability degrees. To check the reliability of the RTt vulnerability method, further assessments were conducted with other vulnerability methods as presented in Chapter 7. These methods are the PI, AVI and DRASTIC methods. The criteria for selecting these methods, as used in this study, were the following:

- Number of parameters considered in the assessment of the methods, PI>DRASTIC>AVI (Table 8.1).
- The level of the professed accuracy of the methods (PI>DRASTIC>AVI), respectively.
- The extent of acceptability of the methods (DRASTIC>PI>AVI), respectively.
- The adaptability to regional evaluation (AVI>DRASTIC>PI) and their physically based approach (PI>AVI>DRASTIC), respectively.

These criteria influenced the outcome of the vulnerability maps.

Figure 8.7 shows the discrepancy plot of the RTt method against the other methods. This was done to ascertain the degree of inconsistency or accuracy between the established vulnerability methods and the RTt method. The higher the discrepancies between any two vulnerability indexes, the lower the accuracy between the two vulnerability methods. The discrepancy diagrams were plotted on a rescaled chart. The Dahomey Basin normalised RTt vulnerability index used in drawing the vulnerability maps were rescaled with the respective DRASTIC, AVI and PI normalised vulnerability values.

The lowest discrepancy and inconsistency was noted between the RTt and the AVI methods. An almost perfect overlap was recorded from borehole points 44 to 56 (Figure 8.7a). This means higher accuracy between the two methods as compared to other methods, despite the vulnerability index class differences (Figure 8.7). This suggests the applicability of the RTt method to the suitability of regional vulnerability estimation, as the AVI method had been tested for (Zwahlen, 2004).

The highest discrepancy for the three charts in the Dahomey Basin was noted between the RTt vulnerability index and the DRASTIC vulnerability index. For example, from borehole point 45 to 50 where the DRASTIC index was almost flat, the RTt index was undulating (Figure 8.7c). However, this does not mean that there was no accuracy between the two methods. In fact, the RTt method and the DRASTIC method show the best correlation in Figure 8.9 and Figure 8.10. Analysis from this discrepancy diagram, as applied to the aquifers of the Dahomey Basin, has suggested that despite the differences in class of vulnerability (as shown on the vulnerability map and which are sometimes due to the vulnerability index calculations), it does not translate to incorrect vulnerability maps.

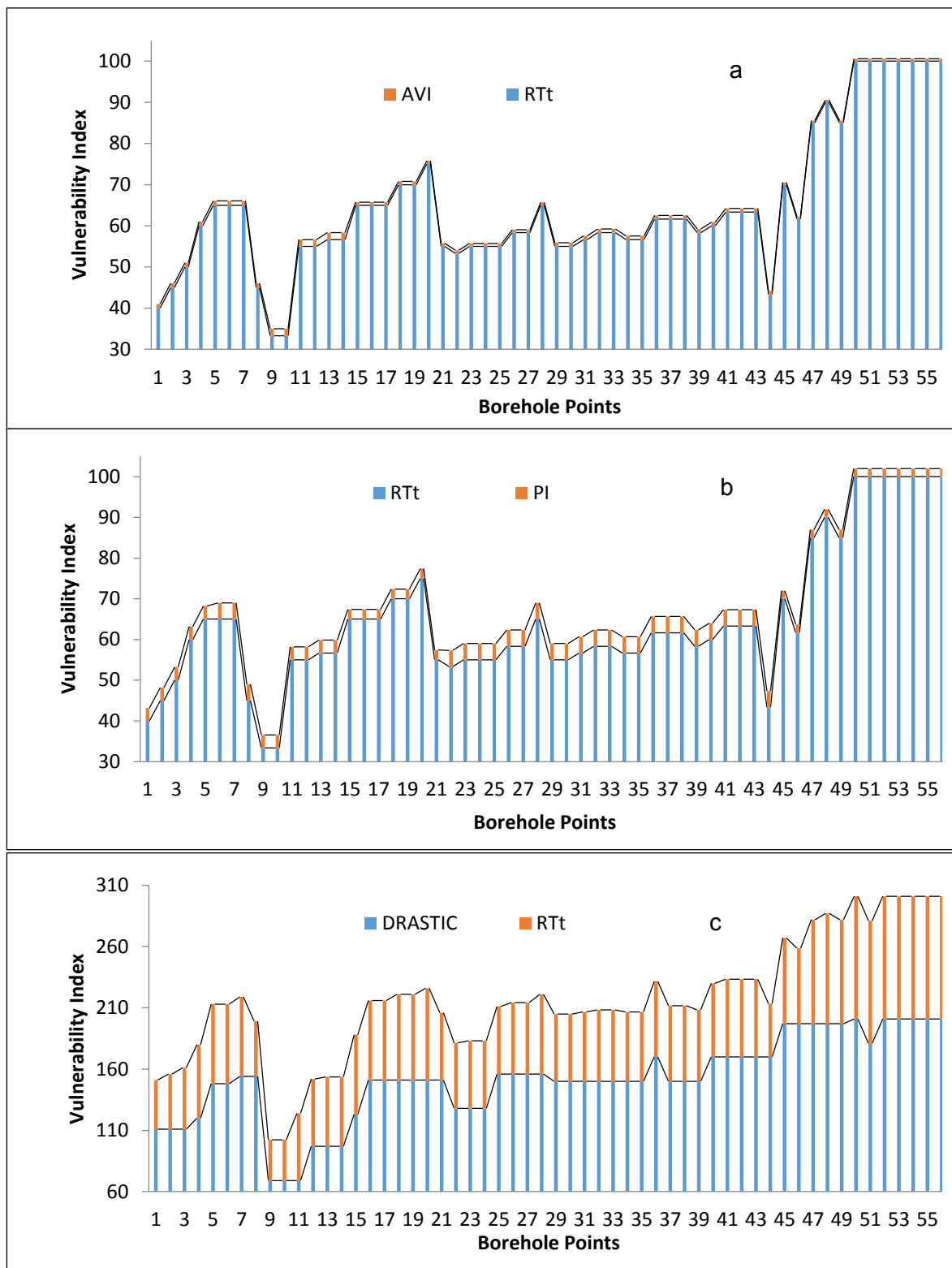


Figure 8.7: Discrepancy plot of RTt with other vulnerability methods

### 8.3 Comparison of the Vulnerability Methods and Maps

The four vulnerability maps show some similarities as well as differences. Comparisons of the parameters considered in the RTt vulnerability methods, with other methods considered in this research, is presented in Table 8.1.

Table 8.1: Parameters considered under the four vulnerability methods in this research

Parameters	RTt	DRASTI C	PI	AVI
Top soil thickness	+	+	+	-
Top soil texture	+	-	+	-
Top soil structure	-	-	+	-
Subsoil permeability	+	+	+	+
Subsoil thickness	+	+	+	+
Depth of the unsaturated zone	+	+	+	+
Fracturing	+	-	+	-
Epikarst development/ geomorphological features	-	-	+	-
Travel time estimation	+	-	-	+
Confined condition	-	+	+	-
Concentration of flows	-	-	+	-
Slope gradient	+	+	+	-
Land use/vegetation cover	-	-	+	-
Recharge	+	+	+	-
Hydraulic characteristics of aquifer	-	+	-	-
Resources vulnerability	+	+	+	+
Source vulnerability	-	-	-	-

The AVI method has the least considered parameters, while the PI method has the most. Only the RTt and AVI considered the travel time. None of the methods were developed for source vulnerability. The depth of the unsaturated zone, subsoil thickness and soil permeability were considered by all the methods. The PI, RTt, and DRASTIC methods considered possible recharge and slope.

The AVI shows larger areas (75%) classified as very high vulnerability. The very high vulnerability is due to the porous soil types of alluvium and sandstone, while 25% was assigned to the rest of the areas as high vulnerability. No area passed as very low or low to moderate vulnerability. The AVI vulnerability evaluation of the Dahomey Basin is strict in comparison to all the other methods. Pertaining to the DRASTIC evaluation of the Dahomey Basin vulnerability, low vulnerability areas covered 18% of the areas. The areas with low vulnerability include high slope and depth-to-water, compacted soils and rock type. The majority of the areas in the basin were classified as moderate vulnerability with a value of 61%. However, in the other methods, the coast lines of the Atlantic Ocean and wetlands along the Ogun River covers about 21% high vulnerability class. The DRASTIC does not have a classification for very high or extreme vulnerability (Table 8.2).

Table 8.2: Vulnerability classification and range

Methods	Very low Vulnerability	Low Vulnerability	Moderate Vulnerability	High Vulnerability	Very High Vulnerability
RTt	12–29	29–47	47–65	65–83	83–100
DRASTIC	24–71	72–121	122–170	171–220	–
AVI	Log c >4	log c = 3–4	log c = 2–3	log c = 1–2	Log c <1
PI	>4–5	>3–4	>2–3	>1–2	>0–1

According to the PI map and method, 66% of the areas are covered by very low to low vulnerability. These areas have some measures of protective cover which ranged from 7 m to 60 m. Shallow groundwater is easily accessible by hand-dug wells, but the soil cover and thick vegetation in most cases may reduce infiltration. About 34% of the catchment of the basin falls under moderate vulnerability zones. These areas are characterised by very shallow or no soil covers. Soil permeability is high under the moderate class areas. The aquifers in the PI moderate class is classified as high to extremely high by the RTt and AVI methods, and high by the DRASTIC method. Based on this, the PI method is the mildest of all the vulnerability methods applied in the evaluation of the Dahomey Basin.

The AVI vulnerability method is the strictest of all the methods used in this study. This could be assumed as an overestimation of the groundwater vulnerability when compared to other methods. A normalised plot of the vulnerability method values of the borehole points is shown in Figure 8.8. The diagram shows the correlation of vulnerability degrees and the methods of RTt with DRASTIC, PI and AVI, respectively. The differences in the diagram are the vulnerability class ranges used in the evaluation. RTt and DRASTIC were ranged up as vulnerability increases from low to high, while the AVI and PI methods were ranged down as the vulnerability increases from low to high (Table 8.2). The comparison chart in Figure 8.8 is different from the reliability diagram of Figure 8.7, because the vulnerability index was rescaled and plotted in reference to the RTt method for comparison of its accuracy in Figure 8.7.

Further analysis between the RTt method and other established methods were shown with correlation plots based on their normalised calculated vulnerability values. The highest correlation of 62% was noticed between the RTt method and the DRASTIC method (Figure 8.10). This was followed by a 61% correlation between the RTt method and the PI method. The lowest correlation of 57% is between the RTt method and AVI method. The good correlation values of the RTt method with the established methods confirms the accuracy and usefulness of the RTt method in the assessment of aquifer vulnerability in data limited areas, which is the focus of this research.

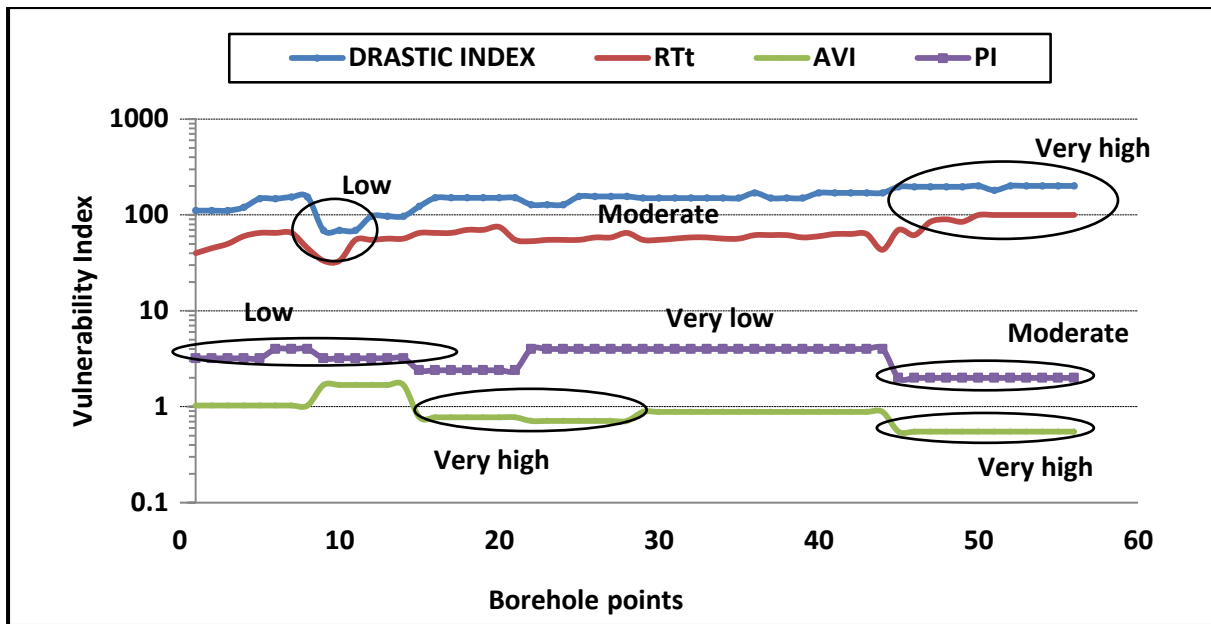


Figure 8.8: Normalised plot of the Dahomey Basin vulnerability index

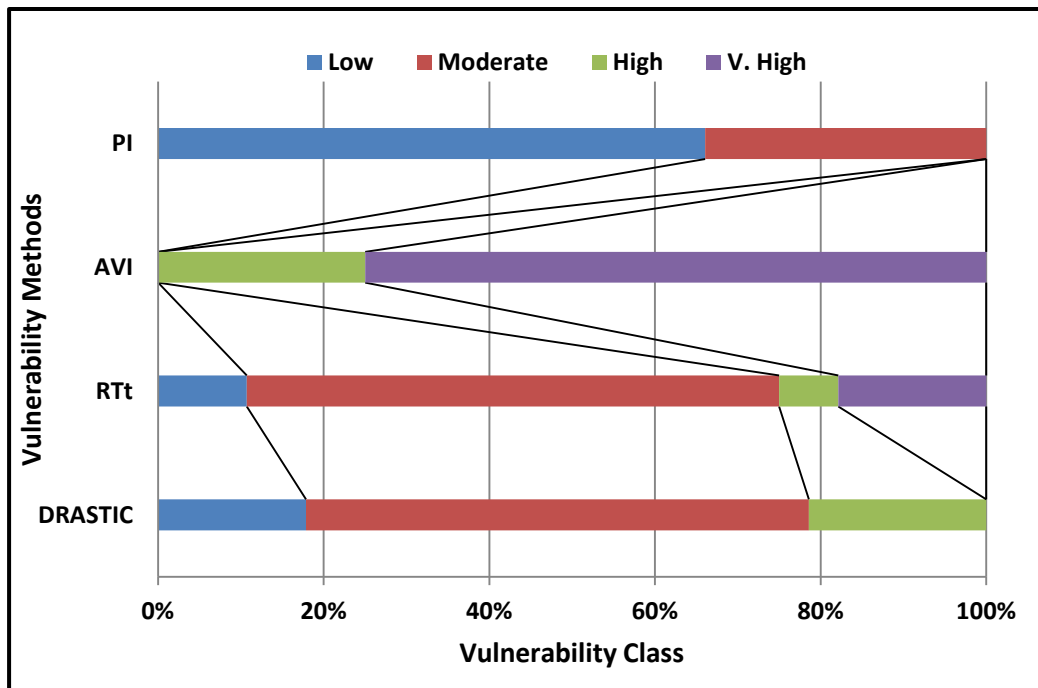


Figure 8.9: Comparison of percentages of vulnerability classes obtained by the application of the four different methods on the Dahomey Basin aquifers



## 8.4 Significance of the Rainfall–Travel Time and other Vulnerability Methods on the Dahomey Basin Evaluations

The RTt vulnerability method that was developed used the Point Count System Model (PCSM). This model followed other parametric methods of the groundwater vulnerability estimation. Vulnerability classes of RTt were divided into five classes. According to the rating calculation, the highest RTt range is 100 and the lowest 12. The classes are 12–29 (very low), 29–46 (low risk), 46–65 (moderate), 65–83 (high) and 83–100 (very high). The highest range, as presented in the Dahomey vulnerability calculations, is 100 and the lowest was 32 (Figure 6.5). This means a low to a very high risk.

The RTt formulation followed the framework of the Cost Action 620 (Zwahlen, 2003) approach to vulnerability of groundwater, particularly the physically based estimation. The physical estimation method is based on the simulation of the physical processes that takes place in hydrogeological systems. The RTt method maps of the Dahomey Basin shows the highest vulnerability in regions with high rainfall and low run-off. The majority of these areas also consist of porous unconsolidated sediments that permit gradual infiltrations of water from the surface and covers 7–10% of the basin.

The moderate vulnerability areas in the RTt model are the north western section of the map. At this region, the depth-to-water level is high and the thickest vadose sediment is recorded. This permits longer infiltration time. The low net precipitation, high run-off arising from high topography and low rainfall experienced in the region further contributes to the regions moderate vulnerability class. The moderate vulnerability covers 64% of the total area of the Dahomey Basin.

High to extremely high vulnerability similar to the RTt method is the AVI and DRASTIC methods, and moderate vulnerability in the PI method were the coast lines of the Atlantic Ocean and the wetlands of the Ogun River. Ojuri and Bankole (2013) classified the coastal areas as high vulnerability. Other areas with high vulnerabilities include Badagry, Ikoyi, Apapa, Lagos Island, Igammu, Central Lagos, Ijebu watersides, wetlands in the Ofada-Mowe-Ibafo axis, Ikorodu, Ijebu-Ode and Ojodu Berger.

The majority of these areas' high vulnerability index results from their physical factors such as gentle to flat slopes, high water tables as low as 2 m from the ground surface, porous soils, unconsolidated alluvium rock types and high yearly rainfall. Presently, most groundwater from these areas is not suitable for drinking and other domestic purposes. Proper enlightenment needs to be done to prevent further deterioration of the aquifer system in the areas.

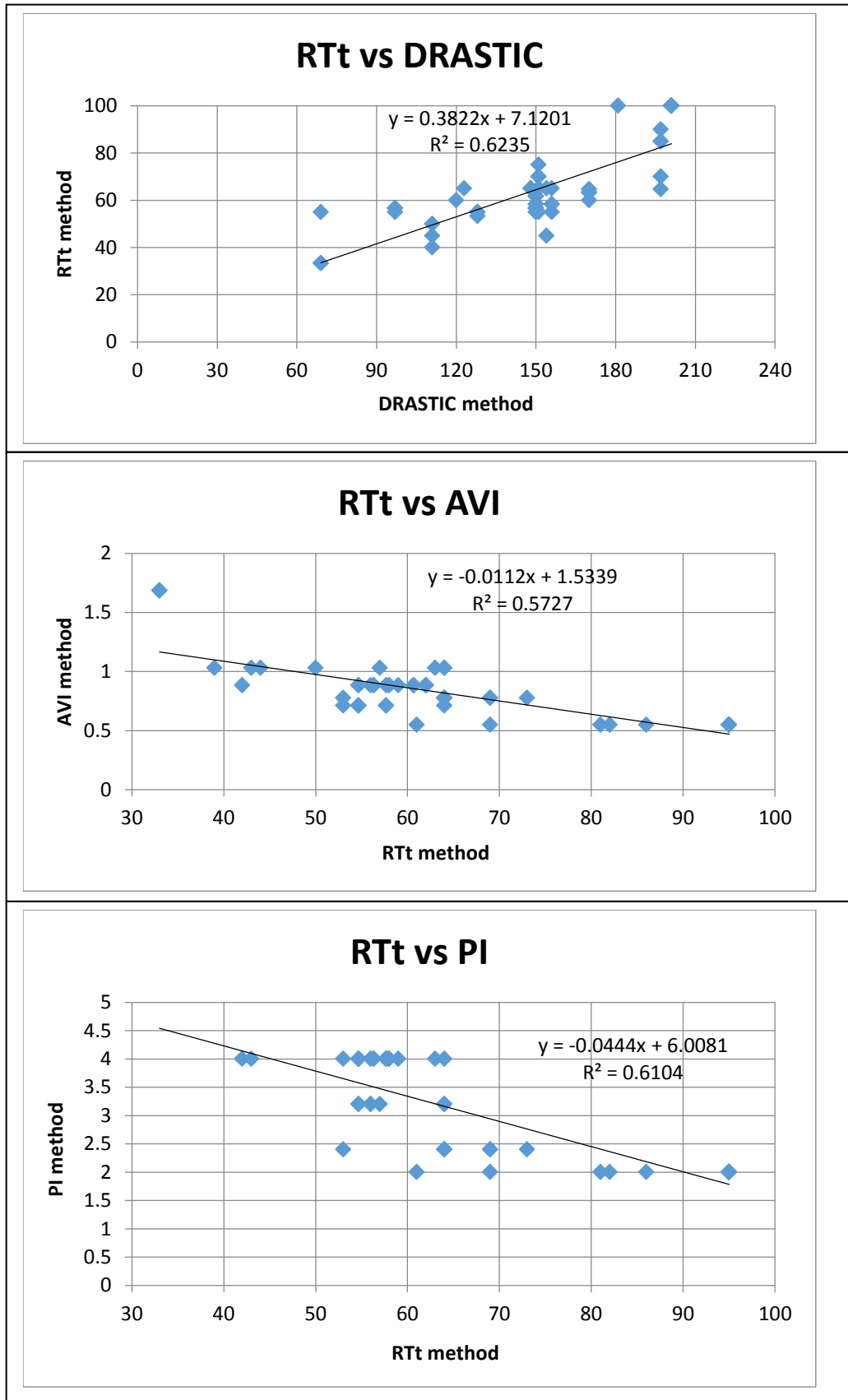


Figure 8.10: Correlation plots of the RTt vulnerability method with other methods

Low vulnerability areas for all the methods include Aiyetoro, Igbogilla, and Ibeshe, but exclude PI vulnerability method. The factors contributing to these areas classifications as low vulnerability were a very low water table, sometimes as high as 65 m below the ground surface, lower annual precipitation, steep slopes that encourage run-off and the thick consolidated rocks. These areas contain a thick overlying cover that serve as natural protection to the aquifer body and do not need extensive protection. It could be targeted for siting of waste plants, landfills and other activities that can pollute groundwater in future.

Areas classified as a moderate vulnerability index by the RTt and DRASTIC, but high in AVI method, include a major part of central Lagos, Ilaro, Otta, Ijoko, Odelemo, Igbesa, Shagamu and Ijebu-Ode. These areas are not totally devoid of pollution. This is due to the anthropogenic impact caused by high population densities, poor urban planning and indiscriminate waste disposal systems. These areas need more regulation and constant monitoring to prevent possible pollution.

## **8.5 Strengths and Weaknesses of the Rainfall–Travel Time Vulnerability Method**

Vulnerability maps are simplifications of natural conditions over an aquifer; therefore, the maps are influenced by diverse heterogeneity conditions of most aquifers. The RTt vulnerability method was developed with a set of objectives among which are to address the challenges of undertaking vulnerability studies in limited data areas. Therefore, the RTt method does have flaws and strengths. It includes:

- RTt is flexible and allows for ranges for its soil hydraulic conductivity consideration, unlike PI which gives a specific soil value.
- RTt method cannot be used for the evaluation of karst environments because epikarst and swallow holes were not considered in the method.
- The RTt method is best applied to areas where there is constant surface rainfall. This is because of RTt rating of water that is readily available to infiltrate and recharge the aquifer. This is also why equal rating was given to rainfall with the travel time. It also assumes saturated vadose front in the movement of surface water/ contamination movement.
- RTt is only effective when assessing resources vulnerability. This means it cannot be used for source evaluations such as a drinking well, river sources and springs.
- RTt assess groundwater vulnerability by physical assumptions, compared to DRASTIC and other vulnerability methods which are strictly subjective-based.
- RTt vulnerability methods combined the objective and subjective methods in its classification index. This is not common in most vulnerability assessment methods.
- Land use and other human features were not considered into the RTt calculation. Therefore, it cannot be used to map features of human influence.
- Some features can be updated if more or better data of some parameters are available in future (e.g. hydraulic properties or unlisted rock, soil and precipitation data). This allows for the vulnerability maps update.

## 8.6 The Significance of Groundwater Assessment

An underlying theme of this research is that all groundwater is to some degree vulnerable. As such, the terms high aquifer vulnerability and moderate to low aquifer vulnerability on the reference map are relative characterisations of the state of the vulnerability, with reference to the method used in assessing them. This concept clearly distinguishes vulnerability from pollution risk. Pollution risk depends not only on vulnerability, but also on the existence of significant pollutants entering the subsurface environment. If there is no significant pollutant loading, it is possible to have high aquifer vulnerability, but no risk of pollution, and to have high pollution risk in spite of low vulnerability, if the pollutant loading is exceptional. It is important to highlight the distinction between vulnerability and risk.

It is well-known and agreeable that a highly vulnerable groundwater body needs more protection (stricter land-use restrictions) than a lowly vulnerable one. However, vulnerability by itself is not a sufficient criterion for the required groundwater protection. The importance or value (economic, ecological and social) of the groundwater body should be taken into account as an additional criterion for a complete groundwater vulnerability evaluation (Drew and Hotzl, 1999). For example, the coastal areas of the Dahomey Basin show high vulnerability zones with the RTt and other methods used, but it also has a high economic and social importance because high urban residential areas and Nigeria's commercial concentration are within this zone. This is different to other high vulnerability areas south of Abeokuta in the northern end of the map and along the wetland zone of the Ogun River that is not inhabited or used for commercial farming.

According to the Irish groundwater protection scheme (Daly and Drew, 1999), aquifers of regional importance are considered to be more valuable than less productive, poor aquifers. The required protection and the resulting land-use restrictions depend on both the vulnerability and the importance of the groundwater body. The highest protection and the strictest land-use restrictions are required on extremely vulnerable zones within a regionally important aquifer (or within the inner source protection area of a spring or well, respectively). Extremely vulnerable zones within a generally unproductive aquifer require less protection (Geological Survey of Ireland [GSI], 1999).

## 8.7 Rainfall–Travel Time Vulnerability Method and Future Evaluation

It is confirmed that the definition of aquifer vulnerability is ambiguous and even if the term vulnerability is not defined in a physically precise way, it is possible to base the concept on sensible and applicable physical assumptions. Therefore, aquifer vulnerability should be assessed on more physical evaluations than it has always been. The Rainfall–Travel time (RTt), just like other methods such as the PI, COP and AVI methods, are based on the assumptions that intrinsic vulnerability depends on three attributes: the travel time of water (and contaminants), the relative quantity of water (and contaminants) that can reach the target and the physical attenuation process in the vadose zone by filtration and dispersion (Goldscheider *et al.*, 2000; Daly *et al.*, 2002).

These three assumptions take place within the vadose zone and is hereby summarised as pathway processes under the concept of the RTt groundwater vulnerability method (Figure 8.11). The pathway is part of the component of the hazard–pathway–receptor model commonly used in risk assessment work, as suggested by the Cost Action 620 (Goldscheider *et al.*, 2000; Zwahlen, 2003).

Contaminant sources comprise of land-use activities, including waste disposal, unregulated urban development, farming and mining that pose a threat to groundwater. The RTt method contaminating source is generally characterised by the amount of rainfall through infiltration processes on the land surface. Rainfall is assumed as the main driving force controlling the infiltration extent of pollutant release on the surface. The higher the amount and intensity of rain, the higher the rating and the faster the possibility of contaminants reaching the water table.

Pathways represent all the processes between the contaminating sources and the receptor. The pathway is also the vadose zone. It starts from the point of release of contaminants at the surface to the uppermost main water table. The pathway has been summarised together into the concept of travel time. It is simple, easy to calculate and considers the Tt of each lithological property.

A receptor in this research is the unconfined groundwater table. It is assumed that the vertical flow of contaminants at the surface reaches the water table directly beneath it without the possibility of dispersion within the pathway (vadose zone). Water chemistry is the major source of verifying contaminated groundwater sources and it has been used in this study as a validation tool. Once contaminated, groundwater can be extremely difficult to clean; its abstraction will be useless because of its poor quality. The receptor evaluation is the only measure for ascertaining the contaminant concentrations that reaches the groundwater bodies.

RTt parameters are few and easy to collate and calculate. This addresses the challenges faced by areas with limited data, unlike the DRASTIC, PI and other methods which involved a wide range of parameters that are difficult to collate in data limited areas. This especially includes developing countries where geological and geohydrological data are scarce. The choice/ source of data used to assess vulnerability need to be more simplified and standardised than what is presently available. Vulnerability approaches from high and low end methodology could be an option. Although new vulnerability methods that need few parameters to assess are now being proposed, there are gaps still needed to be filled by the vulnerability assessor for planners and policy-makers to make an informed decision.

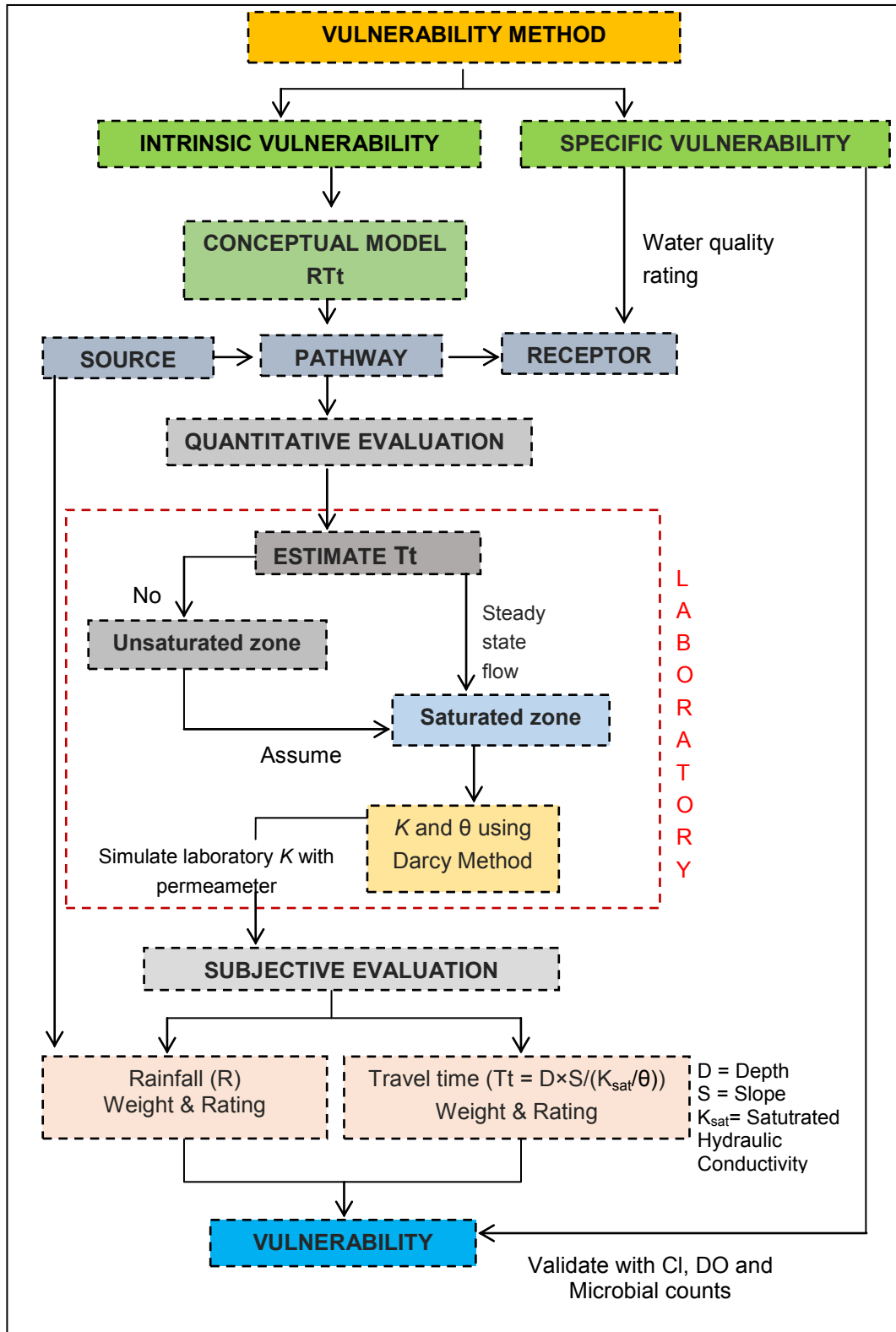


Figure 8.11: Conceptual tree for the study of the RTt groundwater vulnerability method

# CHAPTER 9

## CONCLUSIONS AND RECOMMENDATIONS

### 9.1 Conclusions

This research thesis was mainly aimed at evaluating the vulnerability of selected aquifer systems in Eastern Dahomey Basin South Western, Nigeria. This aim and the set objective have been achieved. To achieve this aim, the thesis was divided into sub-aims with objectives. The conclusions are therefore presented under the sub-aims as follows:

#### 9.1.1 Geological and Geohydrological Site Characterisations of the Dahomey Basin.

- Depth to water table ranges and sediment types from porous sandstone to clay to gravely sand were identified using resistivity. Lithology thickness was derived from the inverted resistivity curves. The use of geophysics in vadose zone estimation was to give an overview of the depth of the vadose zones and lithology correlation across the basin. The major challenges was the number of resistivity carried out which were limited due to constraint of funding for this research.
- The research thesis' findings highlighted the relationship between groundwater vulnerability and vadose sediment properties. Geological formations with appreciable amount of clay sizes and even distribution of particle sizes possess better attenuation capacity and low vulnerability than the formations with sand and uneven distribution of particle sizes. The order of soil attenuation capacity for soil of the Dahomey Basin is sandy clay loam > sandy loam > loamy sand > sand. This was in addition to the sorption property of Kaolinite noted as the dominant clay in the basin.
- Different magnitude of hydraulic conductivities was derived for the formations of the Dahomey Basin. These include 2.42-0.001 cm/s for ILA Formations, 5.21-0.0035 cm/s for EWE Formations, 12.9-0.0061 cm/s for ABK Formations, 9.03-0.00046 cm/s for OSH Formations and 2.79-0.00042 cm/s for CPS Formations. The permeameter hydraulic conductivity values were applied to the vulnerability assessment of the basin.
- Four groundwater aquifers were reported for Lagos and the general populace taps from two of these formations for uses. Advective flow movement through rainfall was the principal recharge mode and the amount of precipitation varies across the basin. The rainfall quantity decreases from the coast in Lagos from a yearly average of 1 800 mm to 1 200 mm in Abeokuta areas.
- The major water types were of calcium-magnesium-chloride and sodium-potassium-chloride water types. The water types suggest water rock interactions and sea influence on the shallow groundwater chemistry of the Dahomey Basin.

- Microbial investigations show high number of bacterial populations for the groundwater of the Dahomey Basin. Population of THBC, TSSS and TECC as contained in the groundwater could result in water-borne diseases and severe health hazard. The heterotrophic bacteria were used as a validation tool for the vulnerability assessment of the Dahomey Basin.
- It is observed from literature that no work has done a comprehensive characterisation on the Dahomey Basin as this thesis as presented by using geophysical, geochemical, hydrological and hydrochemical evaluation of the basin. The thesis has therefore; provide more information on one of the transboundary aquifers in Africa. Likewise, the vadose zone properties of the different lithologies and formations discussed in this thesis will be a reference point for future research working on the Basin.

### **9.1.2 Development of Groundwater Vulnerability Maps for the Dahomey Basin Using Selected Existing Methods.**

- Another contributing point of this research is that the groundwater vulnerability of the different formations and areas of the Dahomey Basin have been evaluated. This is an important contribution to groundwater management in the Dahomey Basin in particular and Nigeria in general. This is because the thesis is the first attempt to comprehensively evaluate the Dahomey Basin groundwater management most especially from the vulnerability point.
- The AVI method classified 25% of the Dahomey Basin as high vulnerability areas and 75% as very high vulnerability areas. The DRASTIC classified 11% as low vulnerability areas, 64% as moderate vulnerability areas, 7% as high vulnerability areas and 18% as very high vulnerability areas. The PI method classified 66% and 34% as low vulnerability and moderate vulnerability areas respectively. The major significance of using these methods is the delineation of areas with likelihood of severe impact in the occurrence of surface pollution.
- Intrinsic vulnerability properties present in the basin identified with the methods were the basis upon which the land use activities were recommended. The PI method in specific has shown that the protective cover of major areas of the Dahomey Basin is very effective.

### **9.1.3 Development of a New Simplified Vulnerability Assessment Method and Test its Application in the Dahomey Basin.**

- RTt vulnerability method was a solution to the challenges encountered in the vulnerability assessment of data scarce areas using existing methods. RTt method is designed to use few important intrinsic parameters to assess groundwater vulnerability. The governing principle of the RTt method followed the concept of the hazard–pathway–target model commonly use in vulnerability assessment and it uses the subjective and physically based vulnerability approach.



- The RTt method was tested in the Dahomey Basin and it highlights the most and least vulnerable areas for protection in the Dahomey Basin. The RTt method classified 11% areas of the basin as low vulnerability, 64% as moderate vulnerability, 7% as high vulnerability and 18% as very high vulnerability. The RTt method classified none of the areas of the Dahomey Basin as a very low vulnerability zone. This is because no aquifer is totally immune to contamination in as much as recharges occur.
- The RTt vulnerability results are presented in vulnerability maps showing areas with different colours symbolising different degrees of vulnerability. Colour was used because it is easily interpreted. An Excel spreadsheet was developed with the RTt concept to calculate aquifer vulnerability. This was done in order to simplify the way vulnerability is measured.
- The RTt method was validated with chloride concentrations in groundwater, measured concentration of dissolve oxygen and the amount of microbial pathogens presence in the groundwater of the Dahomey Basin. The research has shown that chloride decreases with increasing vulnerability and it increases with decreasing vulnerability. This has been mis-interpreted before in other studies.
- Validation with dissolved oxygen show a decrease in dissolved concentration of groundwater of the Dahomey Basin with a decreasing vulnerability and an increase in dissolved oxygen concentration with an increasing vulnerability. Cross plot along the RTt vulnerability map and the dissolved oxygen concentration map show a correlation of 55%.
- A relation between the degree of groundwater vulnerability and the population of heterotrophic bacteria and dissolved oxygen was identified in the thesis. THBC decreases with increasing groundwater vulnerability and a decreasing dissolved oxygen. This relationship was further verified with a cross plots value of 58% between THBC and the RTt index. Validation with bacteriological pupulation in groundwater is recently being research in vulnerability studies.
- Comparisons between the RTt vulnerability method and the established vulnerability methods show the highest correlation between the RTt vulnerability method and the DRASTIC method with 62%. 61% correlation value between the RTt method and the PI method and 57% between the RTt method and the AVI method.

A fundamental challenge in geohydrology is the complexity of the geohydrological environment and the processes that govern flow of water and the transport of contaminants through geological media. Groundwater supplies more than half of the Dahomey Basin's water needs. In the quest for African countries to establish a framework for water policy development and protection, the groundwater vulnerability investigation must be an important component. In this research thesis, the protection of the shallow groundwater resource in the Dahomey Basin, using the subjective and physical based vulnerability methods, has been attempted. The research has evaluated the vulnerability of the Dahomey Basin and formulated better ways to investigate and determine the difficulties encountered in vulnerability studies in a typical African setting.

## 9.2 Recommendations

The vulnerability map of the Dahomey Basin presents an alarming picture of the risk that is taken if groundwater in the basin remains unprotected. Restrictions are needed for potential pollution sources such as industrial activities, petroleum storage facilities of potentially harmful substances, wastewater treatment plants and unsafe onsite sanitation and disposal. Therefore, recommendations and measures in the research thesis are based on the findings and challenges encountered during the research of this thesis for the protection of the Dahomey Basin aquifers. These recommendations are under two categories which are:

### 9.2.1 Recommendations on Further Studies

- Future evaluation of the Dahomey Basin should involve extensive tracers testing for the revalidation of the vulnerability maps developed in this thesis.
- Further characterisations of the Dahomey Basin for vulnerability investigations with geophysics methods should include electro-magnetic and other methods. This is because larger areas can be covered within short period of time with some methods but a comparison with the geoelectrical method is recommended.
- Further improvement on the RTt vulnerability method should include sorption, porosity and land use activities in the formula.
- Karst landforms can be added to the RTt method for its adaptability in karst regions.
- This research adopted a modified core drilling method in the vadose zone sampling due to several limitations. However, future characterisation of the basin should include whole core sampling of the lithologies from the surface to the water table. This will give a more precise representation of the vadose materials.
- New vulnerability concept considering the unsaturated zone of the Dahomey Basin should be developed. This is because the RTt vulnerability concept assumes only saturated condition for the advective flow of contaminant in the Dahomey vadose zone.
- Field test is recommended for further evaluation of the hydraulic conductivity of the Dahomey Basin and a comparison with the laboratory hydraulic conductivity. This is due to the field conditions absent in laboratory as stated in the thesis.
- The research explores more on the usability of laboratory techniques in vulnerability studies and is recommending further applications of laboratory studies in groundwater vulnerability assessment.
- Pore water velocity is another option by which the travel time formula for calculating contaminant can be modified in the future.
- The RTt vulnerability methodological evaluation is a practical and applicable tool for land-use planning and risk assessment. The method can be used to investigate aquifer vulnerability in a similar basin with limited data.

### **9.2.2 Recommendations to Governments, Communities and the General Populace of the Dahomey Basin**

- A major contributing factor to groundwater vulnerability in the Dahomey Basin is the improper land-use patterns across the basin. Indiscriminate waste dumps, poor drainage, an absence of sewer in the most densely populated town, low environmental sanitation awareness and the rapid urbanisation further reinforce groundwater risk in the Dahomey Basin. Therefore, continuous monitoring and education is necessary to safeguard the vulnerable groundwater resources of the Dahomey Basin.
- Lowering of groundwater level due to over extraction should be prevented with appropriate laws by the government.
- There should be an improvement on public water distribution. This will reduce the stress on groundwater dependency.
- Government should formulate proper land-use management act particularly for vulnerable aquifer areas identified in this research. It is more cost-effective to use natural contaminant attenuation than to apply universal controls over land use and effluent discharge.
- Strict borehole regulations, particularly in vulnerable aquifers in over congested areas in the Dahomey Basin, should be formulated and enforced. This is because there is a misplaced priority in Nigeria over protection of groundwater resources (aquifers as a whole) and specific sources (borehole, springs and wells).
- Low vulnerability areas identified in this research could be targeted for siting waste plants and effluent discharges.
- Solid waste dumps should be professionally designed on the basis of the hydrogeological information to protect groundwater resources of the Dahomey Basin.
- The indiscriminate siting of waste dumps around most vulnerable aquifers should be discouraged. Solid and liquid waste should be sorted before dumping, and liquid waste should not be dumped around vulnerable aquifers.
- Sanctions and reward systems should be put in place to discourage indiscriminate dumping.
- Shallow hand-dug wells should be lined inside with prefabricated concrete rings to prevent seepage of contaminated water and growth of microbial plants.
- About one metre concrete protector rims should be constructed around the low lying hand-dug wells to prevent surface run-off into the aquifer.
- Groundwater vulnerability zoning, based on the methods used in this research, needs to be established with matrices that indicate what activities are possible where and at what acceptable risk to groundwater.
- The government should pass effective regulations for the protection of abandoned wells. For example, the Decree 101 on water related regulations are solely based on

socio-economic factors and not on scientific research such as groundwater vulnerability and aquifer sensitivity.

- Capacity building and training of regulatory agencies at federal, state and local level on the activities leading to aquifer contamination is important. Although, sub-Saharan Africa countries and Nigeria lack the funding and good number of expert hydrogeologist, but the help of philanthropic groups identified by Kreamer and Usher (2010) such as the Hydrogeologist Without Borders could be of help.
- Further vulnerability studies on the western section of the Dahomey Basin covering from Ghana to Togo to Benin should be undertaken.
- Trans-boundary aquifer protection working groups should be set up among the countries sharing the Dahomey Basin aquifers.
- Unlike South Africa who has instituted aquifer vulnerability assessments in many areas, Nigeria does have neither ground water map nor aquifer vulnerability map. This research therefore supports Adelman *et al's*. (2008) recommendation for aquifer vulnerability assessment on a national scale with local and municipal governments embarking on similar projects based on the resources available to them.
- The vulnerability maps produce in this thesis is recommended for use by groundwater managers and decision-makers in the realisation of groundwater overall assessments that are related to the implementation of programmes or measures aimed at the protection of groundwater resources.

## REFERENCES

- Adams, B and Foster, SSD. 1991. National groundwater protection policy: Hydrogeological criteria for division of the land surface area. *National Rivers Authority, R&D Note 6*.
- Adeaga, O. 2006. Climate variability and change – Hydrological Impact, *IAHS Publication*, pp. 308.
- Adegoke, OS. 1969. Eocene stratigraphy of Southern Nigeria. *Bur. Rech. Geol. Min., Mem. No. 69*, pp. 23–47.
- Adegoke, OS. 1977. Stratigraphy and Paleontology of the Ewekoro Formation (Paleocene) of Southern Nigeria, *Bull. Am. Paleont.*, No. 71, pp 1–1250.
- Adegoke, OS, Adeleye, DR, Ejeagba, DM, Odebode, MO and Petters, SW. 1980. Geological guide to some Nigerian Cretaceous–Recent localities Shagamu quarry and bituminous sands of Ondo and Ogun States, *Nig. Min. Geo Soc. Pub.*, pp 1–44.
- Adegoke, OS, Dessauvagie, TF, Kogbe, CA and Ogbe, FGA. 1970. The type section, Ewekoro Formation (Paleocene) of Southwestern Nigeria, *Biostratigraphy and microfacies proceeding*, 14<sup>th</sup> African Micropal. Colloquim, Abidjan, 1970, pp. 27–39.
- Adekeye, OA, Akande, SO, Bale, RB and Erdtmann, BD. 2005. Carbon and oxygen isotopic compositions and diagenesis of the Ewekoro Formation in the eastern Dahomey Basin, southwestern Nigeria, *J. Min. Geol.*, pp. 87-95.
- Adelana, SMA, Bale, RB & Wu, M. 2003. Quality assessment and pollution vulnerability of groundwater in Lagos metropolis, SW Nigeria. In: Proceedings of the Aquifer Vulnerability Risk Conference AVR03, Salamanca, Mexico, 2:1–17.
- Adelana, SMA, Bale, RB & Wu, M. 2004. Water quality in a growing urban centre along the coast of southwestern Nigeria. In: Seiler, KP, Wu, C & Xi, R (Eds.) Research Basins and Hydrological Planning. Balkema, The Netherlands, pp. 83–92.
- Adelana, SMA, Bale, RB, Olasehinde, PI & Wu, M. 2005. The impact of anthropogenic activities over groundwater quality of a coastal aquifer in southwestern Nigeria. In: Proceedings of Aquifer Vulnerability & Risk, 2nd International Workshop & 4th Congress on the Protection and Management of Groundwater, 21–23 September 2005, Reggio di Colorno – Parma.
- Adelana, SMA and MacDonald, AM. 2008. Applied Groundwater Studies in Africa, *IAH Special Publications in Hydrogeology*, Vol 13, Leiden: CRC Press/Balkema.
- Adelana, SMA, Olasehinde, PI, Bale, RB, Vrba, P, Edet, AE and Goni, IB. 2008. *An overview of the geology and hydrogeology of Nigeria*, In: Adelana, SMA & MacDonald AM (Eds.) Applied Groundwater Studies in Africa, IAH Special Publications in Hydrogeology, Vol 13. Leiden: CRC Press/Balkema, pp. 171–197.
- Adelana, SMA, Tamiru, A, Nkhuwa, DCW, Tindimugaya, C and Oga, MS. 2008. *Urban groundwater management and protection in sub-Saharan Africa*, In: Adelana, SMA & MacDonald AM (Eds.) Applied Groundwater Studies in Africa, IAH Special Publications in Hydrogeology Vol. 13, Leiden: CRC Press/Balkema, pp. 231–259.
- Adeleye, DR. 1975. Nigerian late Cretaceous stratigraphy and paleogeography, *AAPG Bull* Vol. 59/12, pp. 2302–2313.
- Agagu, OK. 1985. *A geological guide to bituminous sediments in southwestern Nigeria*. M.Phil dissertation (unpublished), Dept. Geol. Univ. Ibadan, pp. 212.

- Ahianba, JE, Dimuna, KO and Okogun, GRA. 2008. Built environment decay and urban health in Nigeria. *Journal of Human Ecology*, 23(3): pp. 259-265.
- Akhavan, S, Mousavi, SF, Abedi-Koupai, J and Abbaspour, KC. 2011. Conditioning DRASTIC model to simulate nitrate pollution case study: Hamadan–Bahar plain, *Environ Earth Sci*, 63, pp. 1155–1167.
- Ako, BD, Adegoke, OS and Petters, SW. 1981. Stratigraphy of the Oshosun Formation in southwestern Nigeria, *J. Min. Geol.*, 17(1), pp. 97–106.
- Ako, BD. 2002. *Applied geophysics*. Obafemi Awolowo University Press limited, Ile-Ife, Nigeria, pp. 25.
- Al-Adamat, RAN, Foster, IDL, Baban, SMJ. 2003. Groundwater vulnerability and risk mapping for the basaltic aquifer of the Azraq Basin of Jordan using GIS, remote sensing and DRASTIC, *Appl Geogr* 23, pp. 3–324.
- Albinet, M and Margat, J. 1970. Cartographie de la vulnérabilité à la pollution des nappes deau souterraine Orleans, France. *Bull BRGM 2ème série*, 4:13–22.
- Al-Hanbali, A and Kondoh, A. 2008. Groundwater vulnerability assessment and evaluation of human activity impact (HAI) within the Dead Sea groundwater basin, Jordan, *Hydrogeology Journal*, 16:499-510.
- Aller, L, Bennett, T, Lehr, J, Petty, R, and Hackett, G. 1987. DRASTIC: A standardised system for evaluating ground water pollution potential using hydrogeologic settings, *National Water Well Association, Dublin, Ohio and Environmental Protection Agency, Ada, OK*. EPA-600/2-87-035.
- Al-Ruwaih, FM. 1995. Chemistry of groundwater in the Damman aquifer, Kuwait, *Hydrogeol. J.* 3, pp. 42-55.
- Andersen, LJ and Gosk, E. 1987. Applicability of vulnerability maps, In: Duijvenbooden W van, Waegeningh HG van (Eds.) TNO Committee on Hydrological Research, The Hague. *Vulnerability of soil and groundwater to pollutants, Proceedings and Information*, 38: pp. 321–332.
- Andreo, B, Goldscheider, N, Vadillo, I, Vias, JM, Neukum, C, Sinreich, M, Jimenez, P, Brechenmacher, J, Carrasco, F, Hotzl, H, Perles, MJ and Zwahlen, F. 2006. Karst groundwater protection: First application of a Pan-European Approach to vulnerability, hazard and risk mapping in the Sierra de Libar (Southern Spain), *Science of the Total Environment*, 357(1-3):54-73.
- Andreo, B, Ravbar, N and Vias, JM. 2009. Source vulnerability mapping in carbonate (karst) aquifers by extension of the COP method: Application to pilot sites, *Hydrogeology Journal*, Vol. 17, no. 3, pp. 749–758, doi:10.1007/s10040-008-0391-1.
- Annor, AE. 1986. Thermo-tectonic evolution of the Basement Complex around Okene, Nigeria with special reference to deformation mechanism, *Pre Cambrian Research Journal of Mining and Geology*, 28:269–281.
- Antolini, P. 1968. Eocene phosphate in the Dahomey Basin *J. Min. Geol.*, 3:17–23.
- APHA, AWWA and WEF. 2005. Standard methods for the examination of water and wastewater. 21st edition. American Public Health Association, American Water Works Association, and Water Environment Federation. Government Printing Office, Washington, DC.
- Appelo, CAJ and Postma, D. 2005. *Geochemistry, groundwater and pollution*, (2nd ed). Balkema, Rotterdam.

- Archies, GW. 1942. The electrical resistivity log as an aid in determining some reservoir characteristics, *Trans. Am. Inst. Min. Met. Eng.*, 146: 54–62.
- Asiwaju-Bello, YA and Oladeji, OS. 2001. Numerical modelling of groundwater flow patterns within Lagos metropolis, Nigeria, *Nigeria Journal of Mining and Geology*, 37, pp. 185-194.
- Auken, A and Christiansen, AV. 2004. Layered and laterally constrained 2D inversion of resistivity data, *Geophysics*, 69 (3), pp. 752–761.
- Bachmat, Y and Collin, M. 1987. Mapping to assess groundwater vulnerability to pollution, In: Duijvenbooden, W van, Waegeningh, HG van (eds) TNO Committee on Hydrological Research, The Hague, *Vulnerability of soil and groundwater to pollutants, Proceedings and Information*, 38, pp. 297–307.
- Babiker, IS, Mohammed, MAA, Hiyama, T and Kato, K. 2005. A GIS-based DRATIC model for assessing aquifer vulnerability in Kakamigahara Heights, Gifu Prefecture, central Japan, *Science of the Total Environment*, 345, pp. 127–140.
- Barber, C, Bates, LE, Barron, R and Allison, H. 1993. Assessment of the relative vulnerability of groundwater to pollution: A review and background paper for the conference workshop on vulnerability assessment, *J. Austr. Geol. Geophys.* 14(2/3), pp. 1147–1154.
- Bartram, J., Fricker, C., Exner, M., Cotruvo, J. and Glasmacher, A. 2004. Heterotrophic plate count measurement in drinking water safety management: Report of an Expert Meeting, Geneva, 24–25 April 2002. *Int. J. Food Microbiol.*, 92: 241–247.
- Basu, NB, Jindal, P, Schilling, KE, Wolter, CF and Takle, ES. 2012. Evaluation of analytical and numerical approaches for the estimation of groundwater travel time distribution, *Journal of Hydrology*, 475, pp. 65-73.
- Baumgartner, A and Liebscher, HJ. 1996. Lehrbuch der Hydrologie: Band 1: *Allgemeine Hydrologie*. 2, Gebruder Borntrager, Berlin Stuttgart, pp. 694.
- Bear, J .1979. *Hydraulics of groundwater*, McGraw-Hill, New York, pp. 567.
- Belkhir, L & Mouni, L. 2013. Geochemical modelling of groundwater in the El Eulma area, Algeria, *Desalination and Water treatment* 51, pp. 1468-1476.
- Beyer, W. 1964. Zur Bestimmung der Wasserdurchlässigkeit von Sanden und Kiesen, aus der Kornverteilungskurve, *Z Wasserwirt-Wassertech* 14: pp. 165–168.
- Billman, HG. 1976. Offshore stratigraphy and palaeontology of the Dahomey Embayment, *Proc. 7<sup>th</sup> Micropaleontology Colloquim*, Ile-Ife, Nigeria, pp. 21 – 46.
- Billman, HG. 1992. Offshore stratigraphy and paleontology of the Dahomey (Benin) Embayment, West Africa, *1st. NAPE Bull. No. 2, Vol. 7*, pp. 121 – 130.
- Binley, A and Kemna, A. 2005. DC resistivity and induced polarization methods. In Yuram R, Hubbard SS (eds.): *Hydrogeophysics. Water and Science Technology Library* 50, pp. 129–156. Springer, New York.
- Birdsell, KH, Newman, BD, Broxton, DE, Robinson, BA. 2005. Conceptual models of vadose zone flow and transport beneath the Pajarito Plateau, Los Alamos, New Mexico, *Vadose Zone J.* 4(3), pp. 620–636.
- Bischoff, WD, Mackenzie, FT and Bishop FC. 1987. Stabilities of synthetic magnesian calcites in aqueous solution; Comparison with biogenic materials. *Geochem. Cosmochim. Acta*, 51, pp. 1413-1424.

Bobachev, C. 2003. *IPI2Win A Windows software for an automatic interpretation of resistivity sounding data*, PhD Dissertation Moscow State University, Russia. <http://geophys.geol.msu.ru/ipi2win.htm>

BRGM (The French Geological Survey). 1979. *Maps of ground water vulnerability to contamination, 31 sheets, 1:50 000* (in French). BRGM, Orléans, France.

Bricker, OP. 1971. *Carbonate cements*, Johns Hopkins University studies Geology No. 19, pp. 376.

Brosig, K, Geyer, T, Subah, A and Sauter, M. 2008. Travel time based approach for the assessment of vulnerability of karst groundwater: The Transit Time Method, *Environ Geol.* 54, pp. 905–911.

Brouyère, S, Jeannin, P.J, Dassargues, A, Goldscheider, N, Popescu, I.C, Sauter, M, Vadillo, I and Zwahlen, F. 2001. Evaluation and validation of vulnerability concepts using a physical based approach, *7th Conference on Limestone Hydrology and Fissured Media, Besançon, Sci. Tech. Envir. Mèm. H. S.*, 13: 67-72.

Burke, KCB, Dessauvagie, TJF and Whiteman, AJ. 1971. The opening Gulf of Guinea and the geological history of the Benue Depression and Niger Delta, *Nature: Physical Science*, 233 (38), pp. 51 – 55.

Butscher, C, Auckenthaler, A, Scheidler, S and Huggenberger, P. 2011. Validation of a Numerical Indicator of Microbial Contamination for Karst Springs, *Groundwater*, Vol. 49, No. 1: 66-76.

Campbell, MD, Starrett, MS, Fowler, JD and Klein, JJ. 1990. Slug test and hydraulic conductivity, *Proceedings of Petroleum Hydrocarbons and Organic Chemicals in Groundwater: Prevention, Detection, and Restoration*, 31 Oct. 1990 Texas. *Ground Water Management* 4: 85-99.

Carman, PC. 1956. *Flow of gases through porous media*, Academic Press New York, 189.

Carter, AD, Palmer, RC, Monkhouse, RA. 1987. Mapping the vulnerability of groundwater to pollution from agricultural practice, particularly with respect to nitrate, In: Duijvenbooden W van, Waegeningh HG van (eds) *Vulnerability of soil and groundwater to pollutants*, TNO Committee on Hydrological Research, The Hague. *Proceedings and Information*. 38: pp. 333–342.

Casas, A, Himi, M, Diaz, Y, Pinto, V, Font, x and Tapias, JC. 2008. Assessing aquifer vulnerability to pollutants by electrical resistivity tomography (ERT) at a nitrate vulnerable zone in NE Spain. *Environmental Geology* 54, pp. 515–520.

Chapelle, FH. 2000. *Groundwater Microbiology and Geochemistry*, New York: John Willey & Sons, p. 468.

Chattopadhyay, PB and Singh, VS. 2013. Hydro-chemical evidences: Vulnerability of atoll aquifers in western Indian Ocean to climate change, *Global and Planetary Change* (106) pp. 123-140.

Chen, W and Kao, J. 1997. Fuzzy DRASTIC for landfill siting, *In Proceedings of the 13th international conference on solid waste technology and management*, Vol. 1, Widener University.

Civita, M. 1994. Le carte della vulnerabilità degli acquiferi all'inquinamento, *Teoria and practica (Aquifer vulnerability maps to pollution)*, Pitagora, Bologna.

Civita, M and De Regibus, C. 1995. Sperimentazione di alcune metodologie per la valutazione della vulnerabilità degli acquiferi, *Q Geol. Appl. Pitagora, Bologna* 3: pp. 63–71.



- Civita, M and De Maio, M. 2000. SINTACS R5 a new parametric system for the assessment and automatic mapping of groundwater vulnerability to contamination, *Publ. NO. 2200 del GNDCI-CNR Pitagora Editrice*, Bologna, pp. 240.
- Collins, AG. 1975, *Geochemistry of oilfield waters*, Amsterdam, Elsevier, pp. 496.
- Connell, LD and Daele, GVD. 2003. A quantitative approach to aquifer vulnerability mapping, *J Hydrol.*, 276 (1–4), pp. 71–88.
- Custodio, E. 1997. Seawater intrusion in coastal aquifers, guidelines for study, monitoring and control, *Water Report No. 11. Food and Agriculture Organization of the United Nations*, Rome, Italy.
- Dahlin, T and Zhou, B. 2004. A numerical comparison of 2D resistivity imaging with 10 electrode arrays. *Geophysical Prospecting* 52, pp. 379– 398.
- Daly, D and Drew, D. 1999. Irish methodologies for karst aquifer protection, In: Beck B (ed) *Hydrogeology and engineering geology of sinkholes and karst*, Balkema, Rotterdam, pp. 267–272
- Daly, D, Drew, D, Goldscheider, N and Hotzl, H. 2000. Suggested Outline of a European Approach to Mapping Groundwater Vulnerability, *Recommendations to Working Group 1 of COST 620, Results of the Task Group Meeting, European Approach*“, Karlsruhe, (unpubl.), pp. 6.
- Daly, D, Dassargues, A, Drew, D, Dunne, S, Goldscheider, N, Neale, S, Popescu, C and Zwhalen, F. 2002. Main concepts of the “European Approach” for (karst) groundwater vulnerability assessment and mapping, *Hydrogeology Journal* 10(2) pp. 340–345.
- Dane, JH and Topp, GC. 2002. Methods of Soil Analysis, Part 4, *Physical Methods, Soil Science Society of America Book Series No. 5*, Madison, pp. 1692.
- Datry, T, Malard, F and Gilbert, J. 2004. Dynamics of solutes and dissolved oxygen in shallow urban groundwater below a stormwater infiltration basin, *Science of the Total Environment* 329: 215-229.
- Davis, SN and De Wiest, RJM. 1966. *Hydrology*. Wiley, New York, pp. 234.
- Dirksen, C. 1999b. Direct conductivity measurements for evaluating approximate and indirect determinations. In *Proceedings of the International Workshop on Characterization and Measurement of the Hydraulic Properties of Unsaturated Porous Media*, van Genuchten M.Th., et al. (Eds.), University of California, Riverside, pp. 271 – 278
- Dixon, B. 2001. *Application on neuro-fuzzy techniques to predict groundwater vulnerability in Northwest Arkansas*, Ph.D. thesis, Fayetteville, Arkansas: University of Arkansas.
- Dixon, B. 2004. Prediction of groundwater vulnerability using integrated GIS-based neuro-fuzzy techniques, *Journal of Spatial Hydrology* (St. Petersburg), 4(2).
- Dixon, B. 2005. Applicability of neuro–fuzzy techniques in predicting groundwater vulnerability: a GIS–based sensitivity analyses, *J Hydrol*, 309, pp. 17–38.
- Dixon, B. 2005a. Groundwater vulnerability mapping: A GIS and fuzzy rule based integrated tool *Applied Geography*, 25(4), pp. 327–347.
- Dixon, B, Scott, HD, Dixon, JC and Steele, KF. 2002. Prediction of aquifer vulnerability to pesticides using fuzzy rule–based models at the regional scale, *Phys Geogr*, 23, pp.130–153.

Dodds, AR and Ivic, D. 1988. Integrated Geophysical Methods Used for Groundwater Studies in the Murray Basin, South Australia. In: *Geotechnical and Environmental Studies. Geophysics, Vol. II*. Soc. Explor Geophys. Tulsa, OK pp. 303-310.

Doerfliger, N. 1994. Réflexion sur la variabilité des fonctions de transfert obtenues par traçage en milieu karstique (jura tabulaire et alpes du domaine helvétique), *Bulletin d'Hydrogéologie*, Vol. 13, pp. 69-86.

Doerfliger, N, Jeannin, P.Y and Zwahlen, F. 1999. Water vulnerability assessment in karst environments: A new method of defining protection areas using a multi-attribute approach and GIS tools (EPIK method), *Environmental Geology*, v. 39, no. 2, pp. 165-176.

Dorfliger, N, Plagnes, V and Kavouri, K. 2010. PaPRIKa a multi-criteria vulnerability method as a tool for sustainable management of karst aquifers. Example of application on a test site in SW France, *Sustainability Of The Karst Environment*, pp. 49.

Domenico, PA and Schwartz, FW. 1990. *Physical and Chemical Hydrogeology*, John Wiley & Sons, New York, pp. 824.

Drever, JI. 2002. *The geochemistry of natural waters: Surface and groundwater environments*. (3rd ed.), Prentice Hall, Upper saddle River, New Jersey, pp. 60.

Drew, D and Hotzl, H. 1999. Karst hydrogeology and human activities Impacts, consequences and implications, *Int Contrib Hydrogeol* 20, pp. 322.

Dreybrodt, W. 1988. Processes in karst systems, *Physics, chemistry and geology*, Springer, Berlin, pp. 288.

Durfor, CN and Becker, E. 1964. Public water supplies of the 100 largest cities in the United States, *U.S. Geological Survey Water-Supply Paper 1812*, pp. 364.

Dyck, S and Peschke, G. 1995. *Grundlagen der Hydrologie* Berlin, (Verlag für Bauwesen), pp. 536.

Dyck, MF, Kachanoski, RG and de Jong, E. 2005. Spatial variability of long-term chloride transport under semiarid conditions: Pedon scale, *Vadose Zone J.* 4(4), pp. 915–923.

Eberts, SM, Böhlke, JK, Kauffman, LJ and Jurgens BC. 2012. Comparison of particle tracking and lumped-parameter age-distribution models for evaluating vulnerability of production wells to contamination, *Hydrogeology Journal* 20: pp. 263–282.

Edmunds, WM and Smedley, PL. 2005. Fluoride in natural waters, *Essentials of Medical Geology, BJ Alloway and O Selinus (eds.)*, London: Elsevier, pp. 301–29.

Egwuonwu, CC, Okafor, VC, Ezeanya, NC, Nzediegwu, C and Okorafor OO. 2012. A comparison of the reliability of six evapotranspiration computing models for Abeokuta in SW Nigeria, *Greener Journal of Physical Sciences, Vol. 2 (4)*, pp. 064-069.

El-Waheidi, MM, Merlanti, F and Pavan, M. 1992. Geoelectrical resistivity survey of the central part of Azraq basin (Jordan) for identifying saltwater/ freshwater interface. *Journal of Applied Geophysics* 29, pp. 125–133.

Ekweozor, CM. 1990. Geochemistry of oil sands of southwestern Nigeria, In: *Occurrence, utilisation and economics of Nigeria tar sands, Nig. Min. Geo. Soc. Publication on tar sands workshop, Ako BD & Enu, EI (eds.)*, Ago–Iwoye, pp. 50–62.

Enu, EI. 1990. Nature and occurrence of tar sands in Nigeria In *Occurrence, utilisation and economics of tar sands, Nigeria Mining and Geosciences Society publication on tar sands workshop, Ako, BD & Enu, EI. (eds)*. Olabisi Onabanjo University, Ago-Iwoye, pp. 11–16.

- Eriksson, E. 1960. The yearly circulation of chloride and sulphur in nature; meteorological, geochemical and pedological implications, part II, *Tellus*, 12, pp. 63-109.
- Ernstson, K and Kirsch, R. 2006. Geo-electrical methods basic principles, In Kirsch R (ed): *Groundwater Geophysics: A Tool for Hydrology*, Springer. Pp. 85–108.
- European Commission COST Action 620. 2003. *Vulnerability and risk mapping for the protection of carbonate (karst) aquifers: Scopes-goals-results*. Zwahlen, F. (Ed.). Luxembourg: European Commission, Directorate-General: Science, Research and Development, pp. 1-42.
- Fagbami, AA, and Shogunle, EAA. 1995. Nigeria: Reference soils of the coastal swamps near Ikorodu (Lagos State), *Soil Brief Nigeria 2. University of Ibadan, Ibadan and International Soil Reference and Information Centre, Wageningen*. pp. 17.
- Fair, GM and Hatch, LP. 1933. Fundamental factors governing the streamline flow of water through sand, *J. Amer. Water Works Assoc.* 25, pp. 1151-1565.
- Fenton, O, Schulte, R.P.O, Jordan, P, Lalor, S.T.J and Richards, K.G. 2011. Time-lag: A methodology for the estimation of vertical and horizontal travel and flushing timescales to nitrate threshold concentrations in Irish aquifers, *Environmental Science & Policy* 14, no. 4: pp. 419–431.
- Fetter, CW. 2001. *Applied Hydrogeology*, 4th ed. Upper Saddle River, NJ: Prentice Hall, Inc, pp. 598.
- Fies, JC, Louvigny, ND and Chanzy, A. 2002. The role of stones in soil water retention *European Journal of Soil Science* 53, pp. 95–104.
- Fitts, CR. 2002. *Groundwater Science*, Academic Press, Elsevier UK, pp. 65.
- Focazio, MJ, Reilly, TE, Rupert, MG and Helsel, DR. 2001. Assessing groundwater vulnerability to contamination: providing scientifically defensible information for decision makers, *U.S. Geological Survey Circular 1224*.
- FOS (Federal Office of Statistics). 2001. *Annual Report 2000*. FOS, Abuja, Nigeria.
- Foster, SSD. 1987. Fundamental concepts in aquifer vulnerability, pollution risk and protection strategy, In: van Duijvenboden, W, van Waegeningh, H.G. (Ed.), *Vulnerability of Soil and Groundwater to Pollutants, TNO Comm. on Hydro. Research Hague, Proceeding and Information*, 38: pp. 69–86.
- Foulquier, A, Mermillod-Blondin, F, Malard, F and Gilbert, J. (2011). Response of sediment biofilm to increased dissolved organic carbon supply in groundwater artificially recharged with stormwater. *J. Soils Sediments* 11:382–393.
- Freeze, RA and Cherry, JA. 1979. *Groundwater*. Englewood Cliffs, NJ, Prentice-Hall, pp. 604.
- Fried, JJ. 1987. Groundwater resources in the European Community, *2nd phase, Vulnerability-Quality* (Synthetical Report) (unpublished).
- Frind, EO, Molson, JW and Rudolph, DL. 2006. Well Vulnerability: A quantitative approach for source water protection. *Ground water* 44, No.5: pp. 732-742.
- Fritch, TG, McKnight, CL, Yelderman JC and Arnold JG. 2000. Aquifer vulnerability assessment of the paluxy aquifer, Central Texas, USA, using GIS and a modified DRASTIC approach, *Environ Manage* 25, pp. 337–345.

- Frohlich, RK, Barosh, PJ, and Boving, T. 2008. Investigating changes of electrical characteristics of the saturated zone affected by hazardous organic waste, *Journal of Applied Geophysics* 64, pp. 25–36.
- Frohlich, RK, Fisher, JJ and Summerly, E. 1996. Electrical hydraulic conduction correlation in fractured crystalline bedrock: Central Landfill, Rhode Island, USA, *Journal of Applied Geophysics* 35, no. 4: pp. 249–259
- Frohlich, RK and Kelly, WE. 1987. Estimates of specific yield with the geo-electric resistivity method in glacial aquifers. *Journal of Hydrology* 97: 33–44.
- Frohlich, RK and Parke, CD. 1989. The electrical resistivity of the vadose zone-Field survey, *Groundwater Vol. 27*. No. 4.
- Gargini, A and Pranzini, G. 1994. Map of protection against pollution of the Middle Valdarno plain aquifers, *Memorie della Società Geologica Italiana, Vol. XLVIII*, pp. 923-928.
- Gemitzi, A, Petalas, C, Tsihrintzi, VA and Pisinaras, V. 2006. Assessment of groundwater vulnerability to pollution: A combination of GIS, fuzzy logic and decision making techniques, *Environ Geol*, 49: pp. 653–673
- Genesis Project. 2013. Critical review of methods for assessment of vulnerability of groundwater systems, *Groundwater and Dependent Ecosystems: New Scientific and Technological Basis for Assessing Climate Change and Land-use Impacts on Groundwater*, pp.1-115, www.thegenesisproject.eu.
- Gibbs, RJ. 1970. Mechanisms controlling world water chemistry *Science, Vol. 170*, pp. 795–840.
- Giordano, M. 2009. Global groundwater Issues and solutions, *Annu. Rev. Environ. Resour.* 34. pp. 153–78.
- Glover, ET, Akiti, TT and Osaе, S. 2012. Major ion chemistry and identification of hydrogeochemical processes of groundwater in the Accra Plain, *Elixir Geoscience (50)*, pp. 10279-10288.
- Goel, PK. 2006. *Water pollution causes, effect and control*. (2nd ed). New Age Publications, pp. 221-236.
- Gogu, R.C and Dassargues, A. 2000a. Current trends and future challenges in groundwater vulnerability assessment using overlay and index methods, *Environ. Geol.* 39(6), pp. 549–559.
- Gogu, RC and Dassargues, A. 2000b, Sensitivity analysis for the EPIK method of vulnerability assessment in a small karstic aquifer, southern Belgium, *Hydrogeol. J.*, 8, 3, pp. 337-345.
- Gogu, R.C, Hallet, V and Dassargues, A. 2003. Comparison of aquifer vulnerability assessment techniques; Application to the Néblon river basin Belgium, *Environ Geol* 44, pp. 881–892.
- Goldich, S. 1938. A study in rock weathering, *J Geol* 46: pp. 17–58.
- Goldscheider, N. 2002. *Hydrogeology and vulnerability of karst systems, examples from the Northern Alps and Swabian Alb, PhD thesis*, University of Karlsruhe, pp. 1-259.
- Goldscheider, N. 2005. Karst groundwater vulnerability mapping: Application of a new method in the Swabian Alb, Germany, *Hydrogeology Journal*, v. 13, no. 4, pp. 555-564.

- Goldscheider, N, Hötzl, H, Fries, W and Jordan, P. 2001. Validation of a vulnerability map (EPIK) with tracer tests. In: Mudry J, Zwahlen F (eds) *7th Conference on Limestone Hydrology and Fissured Media, Besançon, France, University de Franche-Comté, Besançon*, pp. 167–170.
- Goldscheider, N, Klute, M, Sturm, S and Hötzl, H. 2000. The PI method: A GIS-based approach to mapping groundwater vulnerability with special consideration of karst aquifers. *Z Angew Geol* 46 (3) pp. 157–166.
- Goossens, M and Van Damme, M. 1987. Vulnerability mapping in Flanders, Belgium, Proceedings at Vulnerability of soil and groundwater to pollutant, In: Duijvenbooden W van, Waegeningh GH (Eds) TNO Committee on Hydrological Research, the Hague, Proceedings and Information 38, pp. 355–360.
- Grant, NK. 1970. Geochemistry of Precambrian Basement rocks from Ibadan, southwestern Nigeria, *Earth planet. Sci. Lett.*, 10, pp. 29 – 38.
- Griebler, C and Lueders, T. 2009. Microbial biodiversity in groundwater ecosystems. *Freshwater Biol.* 54: 649–677.
- Geological Survey of Ireland (GSI). 1999. *Groundwater protection schemes guidelines document*, Department of the Environment and Local Government, Environmental Protection Agency Geological Survey of Ireland, Dublin, pp. 24.
- Guan, H, Love, AJ, Simmons, CT, Makhnin and Kayaalp, AS. 2010. Factors influencing chloride deposition in a coastal hilly area and application to chloride deposition mapping, *Hydrol. Earth Syst. Sci.*, 14, pp. 801-813.
- Gvirtzman, H, Ronen, D and Magaritz, M. 1986. Anion exclusion during transport through the unsaturated zone, *Journal Hydrol.*, 87, no.314: pp. 267-284.
- Hainsworth, LJ, Mignerey, AC, Helz, GR, Sharma, P and Kubik, PW. 1994. Modern Cl-36 deposition in southern Maryland, USA. *Nucl. Instrum. Methods Phys. Res., B Beam Interact. Mater. Atoms* 92, pp. 345-349.
- Haith, DA and Laden, EM. 1986. Screening of groundwater contamination by travel time distributions, *Journal of Environmental Engineering, ASCE Vol. 115*, 3: pp. 497-512.
- Hallenbach, F. 1953. Geoelectrical problems of the hydrology of West Germany areas. *Geophysical Prospecting* 1(4): pp. 241–249.
- Hanusa, TP. 2014. Ca chemical element, *Encyclopedia Britannica*. [www.global.britannica.com](http://www.global.britannica.com). Accessed on 10 October 2014.
- Harleman, DRF, Mehlhorn, PF and Rumer, RR Jr. 1963. Dispersion-Permeability Correlation in Porous Media, *Journal of Hydraulics Division, American Society of Civil Engineers, Vol. 89*, no. 2.
- Hazen, A. 1911. Discussion: Dams on sand foundations. *Transaction* . American Society of Civil Engineers, 73, pp. 199.
- Heigold, PC, Gilkeson, RH, Cartwright, K and Reed, PC. 1979. Aquifer transmissivity from surficial electrical methods, *Ground Water* 17, no. 4, pp. 338–345.
- Helstrup T, Jorgensen, NO and Banoeng-Yakubo, B. 2007. Investigation of hydrochemical characteristics of groundwater from the Cretaceous–Eocene limestone in southern Ghana and southern Togo using hierarchical cluster analysis, *Hydrogeology* 15, pp. 977–989.
- Hem, JD. 1989. Study and interpretation of chemical characteristics of natural water *US Geological Survey Water- Supply paper 2254* (3rd ed.), pp. 40.

- Hem, JD. 1992. Study and interpretation of the chemical characteristics of natural water United State, *Geol. Surv. Water Supply Paper*, 2254, pp. 263.
- Hennings, V. 2011. Regionalisation of Soil Physical Parameters and Estimation of Mean Annual Percolation Rates in the Lusaka Area, *Technical Report No. 5, Department of Water Affairs, Zambia and Federal Institute for Geosciences and Natural Resources*, Germany, Lusaka (unpublished work).
- Herbst, M, Hardelauf, H, Harms, R, Vanderborght, J and Vereecken, H. 2005. Pesticide fate at regional scale: Development of an integrated model approach and application, *Physics and Chemistry of the Earth 30(8–10)*, pp. 542–549.
- Herlinger, RJr and Viero, AP. 2006. Evaluation of contaminants retention in soils from Viamao District, Rio Grande do Sul State, Brazil, *Environ Geol* 50: pp. 47–54.
- Herrmann, F, Berthold, G, Fritsche, JG, Kunkel, R, Voigt, HJ and Wendland, F. 2012. Development of a conceptual hydrogeological model for the evaluation of residence times of water in soil and groundwater: The state of Hesse case study Germany, *Environ Earth Sci.* 67, pp. 2239–2250 DOI 10.1007/s12665-012-1665-4.
- Herzog, BL. 1989. Investigation of failure mechanisms and migration of organic chemicals at Wilsonville, Illinois, *Groundwater*, Vol. 9, No. 2,, pp. 82-89.
- Herzog, BL and Morse, WJ. 1984. A comparison of laboratory and field determined values of hydraulic conductivity at a waste disposal site, *Proceedings of the 7<sup>th</sup> Annual Madison Waste Conference, Department of Engineering and Applied Science, University of Wisconsin*, pp. 30-52
- Hillel, D. 1998. *Environmental Soil Physics*, Academic Press, New York, USA, pp. 771.
- Hojberg, AL, Kjær, J and Nolan, BT. 2006. Characteristics of European groundwater vulnerability scenarios *Report DL10 of the FP6 EU-funded FOOTPRINT project*, www.eufootprint.org, pp. 38, Accessed on 1 April 2013.
- Holting, B.1996. *Hydrogeologie*. Enke, Stuttgart.
- Holting, B, Haertle, T, Hohberger, KH, Nachtigall, KH, Villinger, E, Weinzierl, W and Wrobel, JP. 1995. Konzept zur Ermittlung der Schutzfunktion der Grundwasserüberdeckung [Concept to assess the protective function of the layers above the groundwater surface], *Geol Jahrb, Hannover, C 63*, pp. 5–24.
- Hounslow, AW. 1995. *Water Quality Data – Analysis and interpretation*, CRC Press LLC, pp. 85.
- Hsu, KJ. 1967. Chemistry of dolomite formation, In GV, Chilingar, HJ, Bassel, & RW, Fairbridge Eds., *Carbonate Rocks, Amsterdam, Nertherlands: Elsevier*. pp. 169-191.
- Hubert, MK. 1956. Darcy's Law and the field equations of flow for underground fluids. *Transactions of the American Institute of Mining and Metallurgical Engineers*, 207, pp. 222-239.
- Iwugo, KO, Arcy, BA and Andoh, R. 2003. Aspect of land based pollution of an African coastal megacity of Lagos, *Diffuse Pollution Conference, Dublin, (14)* pp. 122-124.
- Jeannin, PY, Cornaton, F, Zwahlen, F and Perrochet, P. 2001. VULK: A tool for intrinsic vulnerability assessment and validation. In: Mudry J, Zwahlen F (eds) *7th Conference on Limestone Hydrology and Fissured Media, Besançon, France, University de Franche-Comté, Besançon*, pp. 185–190.

- Johnston, VE and McDermott, F. 2008. The distribution of meteoric Cl-36 in precipitation across Europe in spring 2007. *Earth and Planetary Science Letters* (275), pp. 154-164.
- Jones, HA and Hockey, RD. 1964. The geology of parts of southwestern Nigeria, *Geol. Surv. of Nigeria Bull.* 31, pp. 87.
- Jones, BF, Vengosh, A, Rosenthal, E and Yechieli, Y. 1999. Geochemical investigations. In seawater intrusion in coastal aquifers – concepts, methods and practices, In J Bear, AHD Cheng, S Sorek, D Ouazar & I Herrera (Eds). Kluwer Academic, Dordrecht, The Netherlands, pp. 51-72.
- Kalinski, RJ, Kelly, WE, Bogardi, I, and Pesti, G. 1993. Electrical resistivity measurements to estimate travel times through unsaturated ground water protective layers *Journal of Applied Geophysics* 30, pp. 161–173.
- Kalinski, RJ, Kelly, WE, Bogardi, I, Ehrman, RL and Yamamoto, PD. 1994. Correlation between DRASTIC vulnerabilities and Incidents of VOC contamination of municipal wells in Nebraska, *Ground Water Journal* 32 (1), pp. 31–34.
- Kasenow, M. 2002. Determination of hydraulic conductivity from grain sizes analysis, *Water Resources Publication, LLC*, pp. 71.
- Kayaalp, AS. 2001. Application of rainfall chemistry and isotope data to hydrometeorological modeling, PhD Thesis, Flinders University, Adelaide, Australia, 273.
- Kelly, WE and Frohlich, RK. 1985. Relations between aquifer electrical and hydraulic properties, *Ground Water* 23, pp. 182-189.
- Keywood, MD, Chivas, AR, Fifield, LK, Cresswell, RG and Ayers, GP. 1997. The accession of chloride to the western half of the Australian continent, *Australian J. Soil Res.* 35(5), pp. 1177-1189.
- Kim, KY, Park, YS, Kim, GP and Park, KH. 2009. Dynamic freshwater–saline water interaction in the coastal zone of Jeju Island, South Korea, *Hydrogeology Journal* 17, pp. 617 629.
- Kingston, DR, Dishroon, CP and Williams, PA. 1983. Global Basin Classification System, *AAPG. Bull.*, Vol. 67, pp. 2175-2193.
- Kirsch, R 2006. Aquifers structures-pores aquifers. In *Groundwater Geophysics a Tool for Hydrogeology. Springer*, pp. 361.
- Kirsch, R and Hinsby, K. 2006. Aquifer vulnerability. In *Groundwater resources in buried valleys; a challenge for geosciences, Hannover*, pp. 149-156.
- Kleczkowski, AS. 1990. *The map of the Critical Protection Areas (CPA) of the Major Groundwater Basins (MGWB) in Poland, 1:500,000*. Central Research Program – Environmental Management and Protection, AGH – Univ. of Science and Technology, Krakow pp. 44.
- Klute, M. 2000. *GIS-gestützte Anwendung und Entwicklung von Methoden zur Vulnerabilitätskartierung unter besonderer Berücksichtigung der Infiltrationsbedingungen am Beispiel eines Karstgebietes bei Engen (Hegau, Baden- Württemberg)*, Master thesis Univ. Karlsruhe (unpubl.), pp. 130.
- Klute, A and Dirksen, C. 1986. Hydraulic conductivity and diffusivity: Laboratory methods. In *Methods of Soil Analysis, Physical and Mineralogical Methods*, Klute A. (Ed.), American Society of Agronomy, Soil Science Society of America: Madison, pp. 687–734.

- Knies, DL, Elmore, D, Sharma, P, Vogt, S, Li, R, Lipschutz, ME, Petty, G, Farrell, J, Monaghan, MC, Fritz, S and Agee, E. 1994. Be-7, Be-10, and Cl-36 in precipitation, *Nucl. Instrum. Methods Phys. Res., B Beam Interact. Mater. Atoms* 92, pp. 340-344.
- Koefoed, O. 1979. Geo-sounding principle; Resistivity sounding measurements, tome 1. *Methods in Geochemistry and Geophysics 14A*, pp. 277.
- Kogbe, CA. 1976. *Geology of Nigeria*, Rock View (Nigeria) Limited, Jos pp.1–538.
- Kosinski, WK and Kelly, WE. 1981. Geo-electric soundings for predicting aquifer properties. *Ground Water* 19, no. 2: pp.163–181.
- Kreamer, DK and Usher, B. 2010. Sub-Saharan African Ground Water Protection-Building on International Experience. *Ground Water* 48, no. 2: pp. 257–268.
- Krogulec, E. 2004. Groundwater vulnerability to contamination in the central part of Vistula River valley, Kampinoski National Park, Poland, In Witkowski, A.J, Kowalczyk, A and Vrba, J 2004 eds., *Selected papers from the Groundwater Vulnerability Assessment and Mapping-Ustron, Poland*, pp. 124-132.
- Kunkel, R and Wendland, F. 1997. WEKU—a GIS-supported stochastic model of groundwater residence times in upper aquifers for the supra-regional groundwater management, *Environ Geol.* 30(1–2), pp. 1–9.
- Kunoth, K. 2000. *GIS-gestützte Vulnerabilitätskartierung als Beitrag zur Entwicklung der Europäischen Methode unter besonderer Berücksichtigung der Schutzfunktion der Grundwasserüberdeckung am Beispiel des alpinen Karstgebietes Gottesacker-Hochifen (Vorarlberg, Bayern)*, Master thesis Univ. Karlsruhe, Karlsruhe (unpubl.) pp. 94.
- Langmuir, D. 1997a, *Aqueous environmental chemistry*, Upper Saddle River, NJ: Prentice-Hall, pp. 600.
- Lashkarripur, GR. 2003. An investigation of Groundwater Condition by Geo-electrical Resistivity Method: A Case study in Kori Aquifer, Southeast, Iran, *Journal of Spacial Hydrology* 3(1), pp. 1-5.
- Lashkaripur, G R and Nakhaei, M. 2005. Geo-electrical investigation for the assessment of groundwater conditions: A case study *Ann. Geophys.* 48 pp. 937–44.
- Lasserre, F, Razack, M and Banton, O. 1999. A GIS-linked model for the assessment of nitrate contamination in groundwater, *J. Hydrol.* 224(3–4), pp. 81–90.
- Lebron, I and Robinson, DA. 2003. Particle size segregation during hand packing of coarse granular materials and impacts on local pore-scale structure. *Vadose Zone Journal*, vol. 2, pp. 330–337.
- Leyland, RC. 2008. *Vulnerability mapping in Karst terrains, exemplified in the wider Cradle of Human World Heritage Site*, Dept. of Geology, University of Pretoria, pp. 1-114.
- Liggett, JE and Talwar, S. 2009. Groundwater vulnerability assessments and integrated water resource management. *Streamline Watershed Management Bulletin Vol. 13 (1)*, pp. 19.
- Linde, N, Chen, J, Micheal, B, Kowalsky and Hubbard, S. 2006. Hydrogeophysical parameter estimation approaches for field scale characterisation, *In Applied hydrogeophysics*, Verecken, H I (eds) Springer, pp. 9-44.
- Lobo-Ferreira, JP and Oliveira, MM. 1997. DRASTIC groundwater vulnerability mapping of Portugal, groundwater: An endangered resource, In *Proceedings of the 27th congress of the international association for hydraulic research*, San Francisco, USA, pp. 132–137.



- Longe, EO, Malomo, S and Olorunniwo, MA. 1987. Hydrogeology of Lagos metropolis, *Journal of African Earth Sciences*, 6, pp.163-174.
- Lowe, M, Wallace J, Burk, N, Johnson, J, Johnson, A and Riding, R. 2005. Groundwater sensitivity and vulnerability to pesticides, Salt Lake Valle, *Miscellaneous Publication 05-7*, Utah geological Survey, pp. 1-25.
- Lyons, WC. 1996. *Standard handbook of petroleum and natural gas engineering*, Gulf Publishing Company, pp. 159.
- Ma, DH and Shao, MA. 2008. Simulating infiltration into stony soils with a dual-porosity model, *European Journal of Soil Science* 59, pp. 950–959.
- MacDonald, AM, Bonsor, HC, Dochartaigh, BEO and Taylor, RG. 2012. Quantitative maps of groundwater resources in Africa, *Environ. Res. Lett.* 7, 024009 pp. 1-7.
- MacDonald, A, Davies, J, Calow, R and Chilton, J. 2005. *Developing Groundwater. A guide for Rural Water Supply*, ITDG Publishing.
- Macioszczyk, T. 1992. Parametry hydrogeologiczne. In: *W sluzbie polskiej hydrogeologii, Wyd. AGH, Krakow*, pp. 191-196.
- Magiera, P. 2000. Methoden zur Abschätzung der Verschmutzungsempfindlichkeit des Grundwassers, *Grundwasser* 3/2000, pp. 103-114.
- Mahe, G, Girard, S, New, N, Paturel JE, Cres A, Dezetter, A, Dieulin, C, Boyer, JF, Rouche, N and Servat, E. 2008. Comparing available rainfall gridded datasets for West Africa and the impact on rainfall-run-off modelling results, the case of Burkina-Faso, *Water SA* Vol. 34, No. 5: 529-536.
- Margat, J. 1968. Vulnerabilite des nappes deau souterraine a la pollution: Bases de la cartographie: Orle'ans, France, *Bureau de Recherches Geologiques et Minieres, Document 68 SGL 198 HYD*.
- Marin, AI, Andreo, B, Jimenez-Sanchez, M, Dominguez-Cuesta, MJ and Melendez-Asensio, M. 2012. Delineating protection areas for caves using contamination vulnerability mapping techniques: the case of Herrerias Cave, Asturias, Spain, *Journal of Cave and Karst Studies*, Vol. 74, no. 1, pp. 103–115. DOI: 10.4311/2011jcks0197.
- Matias, MJS. 2002. Squary array anisotropy measurements and resistivity sounding interpretation, *Journal of Applied Geophysics* 49, pp. 185–194.
- Matthess, K and Ubell, G 2003. *Allgemeine Hydrogeologie – Grundwasserhaushalt* Borntraeger, Berlin, Stuttgart.
- Matthew, J, Lenahan, Bristow, A, KL and De Caritat, P. 2011. Detecting induced correlations in hydrochemistry, *Chemical Geology* 284, pp. 182–192.
- Maya, AL and Loucks, MD. 1995. Solute and isotopic geochemistry and groundwater flow in the Central Wasatch Range, Utah, *J. Hydrol.* 172, pp. 31–59.
- McLaughlin, D and Townley, LR. 1996. A reassessment of the groundwater inverse problem, *Water Resource Res.*, 32 (5), pp. 1131–1161.
- McLay, CDA, Dragden, R, Sparling, G and Selvarajah, N. 2001. Predicting groundwater nitrate concentrations in a region of mixed agricultural land use a comparison of three approaches, *Environmental Pollution*, vol. 115, pp.191–204
- Mehta, S, Fryar, AE, Brady, RM and Morin, RH. 2000B. Modelling regional salinisation of Ogallala aquifer, southern high plain Texas *Appl. Geochem.* 15, pp. 849-864.

Mehuys, GR, Stolzy, LH, Letey, J and Weeks, LV. 1975. Effect of stones on the hydraulic conductivity of relatively dry desert soils, *Soil Science Society of America Journal*, vol. 39, pp. 37–42.

Meinardi, CR, Beusen, AHW, Bollen, MJS, Klepper, O and Willems, WJ. 1982. Vulnerability to diffuse pollution and average nitrate contamination of European soils and groundwater, *Water Science and Technology* 31, 8, pp. 159-165.

Melby, JT. 1989. *A comparative study of hydraulic conductivity determinations for a fine grained alluvium*, Masters Thesis, Oklahoma State University, pp. 172.

Mende, A, Astorga, A and Neumann, D. 2007. Strategy for groundwater management in developing countries: A case study in northern Costa Rica, *J Hydrol*, 334 (1–2): 109–24.

Mercado, A. 1985. The use of hydrogeochemical patterns in carbonate sand and sandstone aquifers to identify intrusion and flushing of saline water, *Ground Water* 23, pp. 635–645.

Merchant, JW. 1994. GIS-based groundwater pollution hazard assessment: A critical review of the DRASTIC model, *Photogramm Eng. Remote Sensing* 60(9), pp. 1117–1127.

Merkel, BJ and Planer-Friedrich, B. 2003. Integrierte Datenauswertung Hydrogeologie., *TU Bergakademie Freiberg*, Germany.

Merz, B. 1996. Modellierung des Niederschlags-Abfluß-Vorgangs in kleinen Einzugsgebieten unter Berücksichtigung der natürlichen Variabilität, *Ph.D. thesis, Mitt. des Instituts für Hydrologie und Wasserwirtschaft (IHW)*, 56: pp. 215.

Mhamdi, A, Gouasmia, M, Gasmi, M, Bouri, S and Dhia, H. 2006. Evaluation de la qualité de leau par application de la méthode géoélectrique: exemple de la plaine d'El Mida—Gabes nord (Sudtunisien). *Comptes Rendus Geosciences* 338(16): 1228–1239.

Milsom, J. 2003. *Field Geophysics* (3<sup>rd</sup> ed.), John Wiley and Sons, pp. 88.

Moore, and John, S. 1990. "SEEPAGE: A system for early evaluation of the pollution potential of agricultural groundwater environments," USDA. SCS, Northeast Technical Center, Geology Technical Note 5.

Moysey, S, Davis, SN, Zreda, M and Cecil, LD. 2003. The distribution of meteoric Cl-36/Cl in the United States: A comparison of models, *Hydrogeol. J.* 11, pp. 615-627.

Munoz-Carpena, R, Regalado. CM, Alvarez-Benedi, J and Bartoli, F. 2002. Field evaluation of the new philip-dunne permeameter for measuring saturated hydraulic conductivity, *Soil Science*, 167(1), pp. 9–24.

Murat, V, Rivera, A, Pouliot, J, Miranda-Salas, M and Savard, MM. 2004. Aquifer vulnerability mapping and GIS: A proposal to monitor uncertainty associated with spatial data processing, *Geofi Int* 43(4), pp. 551–565.

Napolitano, P and Fabbri, AG. 1996. Single-parameter sensitivity analysis for aquifer vulnerability assessment using DRASTIC and SINTACS, In: K. Kovar & H.P. Nachtnebel, eds. *Application of Geographic Information Systems in Hydrology and Water Resources Management*, Wallingford, IAHS Press, pp. 559–566.

National Agency for Food and Drug Administration and Control (NAFDAC). 2004. *Guidelines for Production and Registration of Packaged Water*, New guidelines and regulations. NAFDAC, Abuja Nigeria, pp. 1-10.

National Population Commission (NPC) [Nigeria] and ICF International. 2014. *Nigeria Demographic and Health Survey 2013*, Abuja, Nigeria, and Rockville, Maryland, USA: NPC and ICF International.

National Research Council (NRC). 1993. *Groundwater vulnerability assessment, contamination potential under conditions of uncertainty*, National Academy Press, Washington DC. Natural Resources Canada, 2005.

Natural Environment Research Council (NERC). 2015. Quantitative Groundwater maps of Africa. British Geological Survey. [www.bgs.ac.uk/research/groundwater/international/african/Groundwater/maps](http://www.bgs.ac.uk/research/groundwater/international/african/Groundwater/maps). Accessed January, 2015.

Neukum, C and Azzam, R. 2009. Quantitative assessment of intrinsic groundwater vulnerability to contamination using numerical simulations, *Science of the Total Environment*, 408(2): 245-254.

Neukum, C, Hötzl, H and Himmelsbach, T. 2008. Validation of vulnerability mapping methods by field investigations and numerical modeling, *Hydrogeology Journal*, 16(4), pp. 641–658.

Nigeria Hydrological Service Agency (NIHSA). 2011. *Groundwater Monitoring Network*, Federal Ministry of Water Resources, Utako District, Abuja.

Nguyet, VTM and Goldscheider, N. 2006. Tracer tests, hydrochemical and microbiological investigations as a basis for groundwater protection in a remote tropical mountainous karst area, Vietnam, *Hydrogeology Journal* 14: 1147–1159.

Nguyet, VTM and Goldscheider, N. 2007. A simplified methodology for mapping groundwater vulnerability and contamination risk, and its first application in a tropical karst area, Vietnam *Hydrogeology Journal* 14: 1666–1675.

Nton, ME. 2001. *Sedimentological and geochemical studies of rock units in the eastern Dahomey Basin, southwestern Nigeria*, unpublished Ph.D thesis, University of Ibadan, pp. 315.

Ocheri, MI, Odoma, LA and Umar, ND. 2014. Groundwater quality in Nigeria urban areas: A review, *Global Journal of Science Frontier Research: H Environment & Earth Science*, Vol. 14, Issue 3: 35-45.

Odeyemi, IB. 1976. Preliminary report on the field relationships of Basement Complex rocks and Igarra, mid-western Nigeria, In *Geology of Nigeria*, Kogbe, CA (Ed.), Elizabethan Publishing Company Lagos, pp. 58–63.

Offodile, ME. 2014. *Hydrogeology: Groundwater Study and Development in Nigeria*, 3<sup>rd</sup> edn, Mecon Geology & Engineering Services Ltd, pp. 485-514.

Ogbe, FGA. 1970. Stratigraphy of strata exposed in the Ewekoro quarry, western Nigeria. In *African Geology* TFJ Dessauvagie & Whiteman eds, University Press, Nigeria, pp. 305–322.

Ojuri, O and Bankole, O. 2013. Groundwater vulnerability assessment and validation for a fast growing city in Africa: A case study of Lagos, Nigeria, *Journal of Environmental Protection*, 4, pp. 454-465.

Oke, MO, Martins, O, Idowu, O. and Aiyelokun, O. 2013. Comparative analysis of empirical formulae used in groundwater recharge in Ogun-Oshun river basins, *Journal of Scientific Research and Reports* 2(2), pp. 692-710.

Okosun, EA. 1998. Review of the early Tertiary stratigraphy of southwestern Nigeria, *Jour. Min. and Geol. Vol. 34*, no 1, pp. 27–35.

Olorunfemi, MO and Enikanselu, PK. 1999a. Direct current resistivity sounding for groundwater potential in Basement Complex area of NC-Nigeria, *J. of Applied Sci, Vol.2, No 1*, pp. 31-34.

- Olorunfemi, MO, Ojo, JS and Akintunde, OM. 1999b. Hydrogeophysical evaluation of the groundwater potentials of the Akure metropolis, southwestern Nigeria, *Journal of Mining and Geology*, 35(2), pp. 201-228.
- Omatsola, ME and Adegoke, OS. 1981. Tectonic evolution of the Cretaceous stratigraphy of the Dahomey Basin, *Journal of Mining and Geology* 15 (2), pp. 78 – 83.
- Onuoha, KM and Mbazi, FCC. 1988. Aquifer Transmissivity from Electrical Sounding Data: The Case of the Ajali Sandstone Aquifers South-West Enugu, Nigeria, In: C. O. Ofoegbu, (Ed.), *Groundwater and Mineral Resources of Nigeria*, F. Vieweg, Braunschweig/Wiesbaden, pp. 17-30.
- Onwuka, MO. 1990. Groundwater Resources of Lagos State, *M.Sc thesis (Unpub), Dept. of Geology, University of Ibadan, Nigeria*. pp.144.
- Orehova, TV, Gerginov, PN and Karimova, OA. 2009. *Geologica Balcanica*, 38, Nos 1–3, pp. 59–67.
- Oyawoye, MO. 1964. The Geology of Nigeria Basement Complex, *Jour. Nig. Min. Geol.* Vol. 1, pp. 87–103.
- Panagopoulos, GP, Antonakos, AK and Lambrakis, NJ. 2006. Optimization of the DRASTIC method for groundwater vulnerability assessment via the use of simple statistical methods and GIS, *Hydrogeology Journal*, 14, pp. 894–911.
- Pavlov, D, de Wet, CME, Grabow, WOK and Ehlers, MM. 2004. Potentially pathogenic features of heterotrophic plate count bacteria isolated from treated and untreated drinking water. *Int. J. Food Microbiol.*, 92: 275–287.
- Payment, P. 1999. Heterotrophic bacteria. In: AWWA manual of water supply practices. AWWA M48. Waterborne pathogens. American Water Works Association, Denver, Colorado, pp. 83–87.
- Pepper, IL, Rusin, P, Quintanar, DR, Haney, C, Josephson, KL and Gerba, CP. 2004. Tracking the concentration of heterotrophic plate count bacteria from the source to the consumer tap. *Int. J. Food Microbiol.*, 92: 289–295.
- Perrin, J, Pochon, A, Jeannin P.Y and Zwahlen, F. 2004. Vulnerability assessment in karstic areas: Validation by field experiment, *Environmental Geology* 46, 2: 237-245.
- Peschke, G, Etzenberg, C, Muller, G, Topfer, J and Zimmermann, S. 1999. Das wissensbasierte System FLAB, ein Instrument zur rechnergestützten Bestimmung von Landschaftseinheiten gleicher Abflußbildung, *IHI-Schriften*, 10, pp. 122.
- Piscopo, G. 2001. *Groundwater vulnerability map explanatory notes - Castlereagh Catchment*. Australia NSW Department of Land and Water Conservation, Parramatta.
- Plummer, LN and Mackenzie, FT 1974. Predicting mineral solubility from rate data: Application to the dissolution in magnesian calcites. *Am. J. Sci.*, 274, pp. 61-83.
- Popescu IC, Gardin N, Brouyère S and Dassargues A. 2008. Groundwater vulnerability assessment using physically based modelling: From challenges to pragmatic solutions In: *Model CARE 2007. Proceedings, calibration and reliability in groundwater modelling*. JC Refsgaard, K Kovar, E Haarder and E Nygaard (Ed.), Denmark, IAHS Publication No. 320.
- Province of Ontario. 2006. *Assessment report: Draft guidance module 3, Groundwater vulnerability analysis*, Ministry of the Environment, Toronto: Queens printer.
- Rahman, MA. 1988. Recent advances in the study of the Basement Complex of Nigeria, Precambrian geology of Nigeria, *Publ. Of the Geol. Survey of Nigeria, Kaduna* pp. 11 – 41.

- Rahman, A. 2008. A GIS based DRASTIC model for assessing groundwater vulnerability in shallow aquifer in Aligarh, India. *Appl Geogr*, 28(1) pp. 32–53.
- Rajmohan, N and Elango, L. 2004. Identification and evolution of hydrogeochemical processes in an area of the Palar and Cheyyar River Basin, Southern India. *Environmental Geol.* pp. 47-61.
- Ramos-Leal JA, Rodri'guez-Castillo R. 2003. Aquifer vulnerability mapping in the Turbio River Valley, Mexico, a validation study, *Geofi' Int* 42: 141–15.
- Rao, SN. 2008. Factors controlling the salinity in groundwater in parts of Guntur district, Andhra Pradesh, India, *Environ Monit Assess* 138, pp. 327–341. DOI 10.1007/s10661-007-9801-4.
- Rao, P, Hornsby, A and Jessup, R. 1985. Indices for ranking the potential for pesticide contamination of groundwater, *Proceedings of Soil Crop Science Soc, Florida*, 44, pp. 1-8.
- Ravbar, N. 2007. *Vulnerability and risk mapping for the protection of karst waters in Slovenia: Application to the catchment of the Podstenjšek springs*, PhD Thesis, University of Nova Gorica, Slovenia.
- Ravbar, N and Goldscheider, N. 2007. Proposed methodology of vulnerability and contamination risk mapping for the protection of karst aquifers in Slovenia, *Acta Carsol* 36(3), pp. 397-411.
- Ravbar, N and Goldscheider N. 2009. Comparative application of four methods of groundwater vulnerability mapping in Slovene karst catchment, *Hydrogeology Journal* 17, Issues 3, pp. 725-733.
- Regalado, CM and Munoz-Carpena, R. 2004. Estimating the saturated hydraulic conductivity in a spatially variable soil with different permeameters: A stochastic Kozeny–Carman relation, *Soil and Tillage Research* 77, pp. 189-202.
- Reyment, RA. 1965. *Aspects of the Geology of Nigeria*, Ibadan University Press, pp.1–65.
- Reynolds, WD, Bowman, BT, Brunke, RR, Drury, CF and Tan, CS. 2000. Comparison of tension infiltrometer, pressure infiltrometer, and soil core estimates of saturated hydraulic conductivity, *Soil Sci. Soc. Am. J.* 64, pp. 478–484. doi:10.2136/sssaj2000.642478x.
- Risser, DW, Gburek, WJ and Folmar, GJ. 2005. *Comparison of methods for estimating ground-water recharge and base flow at a small watershed underlain by fractured bedrock in the eastern United States*, U.S. Geological Survey Scientific Investigations Report 2005-5038, pp. 31.
- Robins, NS. 1998. Recharge the key to groundwater pollution and aquifer vulnerability, In: *groundwater pollution, aquifer recharge and vulnerability*. Robins, NS (ed.) Geological Society, London Special Publications.
- Robins, NS, Chilton, PJ and Cobbing, JE. 2007. Adapting existing experience with aquifer vulnerability and ground- water protection for Africa, *Journal of African Earth Sciences*, Vol. 47, No. 1, pp. 30-38. doi:10.1016/j.jafrearsci.2006.10.003.
- Rose, S and Long, A. 1988. Monitoring Dissolved Oxygen in Ground Water: Some Basic Considerations, Winter 1988 GWMR, pp. 93-97.
- Rosenthal, E, Jones, BF and Weinberger, G. 1998. The chemical evolution of Kurnob Group paleowater.
- Ross, M, Richard, M, Lefebvre, R, Parent, and Savard, M. 2004. Assessing rock aquifer vulnerability using downward advective time from a 3D model of surficial geology; Case

studies from the St. Lawrence Lowlands Canada, *Geofisica International*, vol. 43. Num. 4, pp. 591-602.

Rusin, PA, Rose, JB, Haas, CN and Gerba, CP. 1997. Risk assessment of opportunistic bacterial pathogens in drinking water. *Rev. Environ. Contam. Toxicol.*, 152: 57–83.

Russ, W. 1924. The geology of part of Niger, Zaria and Sokoto provinces with special reference to the occurrence of gold, *Nigeria Geol. Surv. Bull. No 27*, pp. 42.

Saayman, IC, Beekman, HE, Adams, S, Campbell, RB, Conrad, J, Fey, MV, Jovanovic, N, Thomas, A and Usher, BH. 2007. *Assessment of Aquifer Vulnerability in South Africa*, WRC Report No. 1432/1/07, pp. 1-111.

Saidi, S, Bouri, S, Ben Dhia, H and Anselme, B. 2011. Assessment of groundwater risk using intrinsic vulnerability and hazard mapping: application to Souassi aquifer, *Tunisian Sahel, Agric Water Manag.*, 98(10), pp. 1671–82.

Saidi, S, Bouri, S and Ben Dhia, H. 2011. Sensitivity analysis in groundwater vulnerability in the Mahdia-Ksour Essaf aquifer, *Hydrological Science Journal*, 56: 2, 288-304.

Salama, RB. 1993. The chemical evolution of groundwater in a first order catchment and the process of salt accumulation in the soil profile, *J. Hydrol.* 143, pp. 233-258.

Sarma, WJ, Krishnaiah, N. 1976. Quality of Groundwater in the Coastal Aquifer near Visakhapatnam, India. *Groundwater*, 14 (15): 290-295.

Satpathy, CC, Mathur, PK and Nair, KVK. 1987. Contribution of Edayur-sadras estuarine system to the hydrographic characteristics of Kalpakkam coastal waters, *Journal of the Marine Biological Association* 29 (1–2), pp. 344–350.

Savannah River Company. 2007. Vadose Zone Contaminant Migration Model - Multi-Layered Software (VZCOMML) Calculation Note and Documentation, *United States Department of Energy*, pp. 1-44.

<http://www.srs.gov/general/programs/soil/gen/VZCOMML/Calc/documentation>.

Scanlon, BR, Reedy, RC and Keese, KE. 2003. *Estimation of Groundwater Recharge in Texas Related to Aquifer Vulnerability to Contamination*, Texas Bureau of Economic Geology, Jackson School of Geosciences, The University of Texas at Austin, Austin, Texas, pp. 19.

Schluster, T. 2005. *Geological Atlas of Africa*. Springer Berlin Heidelberg New York pp. 25.

Schoeller, H. 1955. *Geochemie des eaux souterraines Revue de L'Institute Francais du Petrole*, Vol. 10, pp. 230-244.

Schlumberger (Nigeria) Ltd. 1985. *Geology of Nigeria, Conference on Well Evaluation*, Lagos, pp. 15-47.

Schwarz, SD. 1988. Application of Geophysical Methods to Groundwater exploration in the Tolt River Basin, Washington State, In: *Geotechnical and Environmental Studies. Geophysics, Vol. II*. Soc. Explor Geophys.: Tulsa, OK, pp. 213-217.

Seelheim, F. 1880. Methoden zur bestimmung der durchlässigkeit des bodens, *Z Analy. Chem.* 19, pp. 387-402.

Shahid, S. 2000. A study of groundwater pollution vulnerability using DRASTIC/GIS, west Bengal, India, Sacramento, USA, *Journal of Environmental Hydrology*, 8, pp. 124.

Sharma, S1996. *Applied Multivariate Techniques*, John Wiley and Sons, New York.

- Shirazi, SM, Imran HM, Akib, S, Zulkifli, Y and Harun, ZB. 2013. Groundwater vulnerability assessment in the Melaka State of Malaysia using DRASTIC and GIS techniques, *Environ Earth Sci*. Springer-Verlag Berlin Heidelberg, DOI 10.1007/s12665-013-2360-9.
- Sililo, OTN, Saayman, IC and Fey, MV. 2001. *Groundwater vulnerability to pollution in urban catchment*. WRC Project No 1008/1/01.
- Sinreich, M, Cornaton, F and Zwahlen, F, 2007. Evaluation of reactive transport parameters to assess specific vulnerability in karst systems, In: Witkowski, AJ, Kowalczyk, A, Vrba, J, *Groundwater Vulnerability Assessment and Mapping, Selected Papers on Hydrogeology 11*, pp. 21-32.
- Slansky, M, 1962. Contributional etude Geological du Basin sedimentative corfell all Dahomey at du too Bearaeu du Kuchercher, *Geologue at Mounever memoir*, pp. 11-12.
- Smedley, PL, 1996. Arsenic in rural groundwater in Ghana, *J. Afr. Earth Sci.* 22, pp. 459–70.
- Sørensen, KI, Auken, E, Christensen, NB and Pellerin, L, 2005. An Integrated Approach for Hydrogeophysical Investigations: New Technologies and a Case History In Butler DK (Ed.) *Near-Surface Geophysics 2, Investigations in Geophysics 13*: Society of Exploration Geophysics, pp. 585–603.
- Sorichetta, A, 2010. *Groundwater vulnerability assessment using statistical methods*, PhD Thesis, Scuola di Dottorato in Terra, Ambiente e Biodiversita. Universita degli Studi di Milano.
- Sousa, MR, Jones, JP, Frind, EO and Rudolph, DL, 2013. A simple method to assess unsaturated zone time-lag in the travel time from ground surface to receptor *Journal of Contaminant Hydrology, Volume 144, Issue 1*, January 2013, pp. 138-151.
- Starr, RC and Gillham, RW, 1993. Denitrification and organic carbon availability in two aquifers, *Ground Water*, 31: 934-947.
- Stigter, TY, Ribeiro, L and Dill, AMMC, 2006. Evaluation of an intrinsic and a specific vulnerability assessment method in comparison with groundwater salinisation and nitrate contamination levels in two agricultural regions in the south of Portugal, *Hydrogeol J.* 14: pp. 79–99.
- Stine, S.W., Pepper, I.L. and Gerba, C.P 2005. Contribution of drinking water to the weekly intake of heterotrophic bacteria from diet in the United States. *Water Res.*, 39: 257–263.
- Taylor, RG, Barrett, MH and Tindimugaya, C, 2005. *Urban Areas of sub-Saharan Africa: weathered crystalline aquifer systems*, In Lerner, D 2005 (Ed.) *Urban Groundwater Pollution: IAH International Contribution to Hydrogeology 24*, CRC Press, pp. 155–179.
- Telford WM, Geldart, LP and Sheriff, RE. 1995. *Applied geophysics*, Second Edition, Cambridge University Press, pp. 751.
- Teso, R, Poe, M, Younglove, T and Mccool, P. 1996. Use of logistic regression and GIS modelling to predict groundwater vulnerability to pesticides, *J. Environ. Qual.*, 25: 425-432.
- Tijani, MN, 1994. Hydrogeochemical assessment of groundwater in Moro area, Kwara State, Nigeria, *Environ. Geol.*, 24. pp. 194-202.
- Tijani, MN, Olatunji, AS, Sangolade, OO and Chukwurah, BN. 2005. Hydrochemical evaluation of seawater influence on water quality in metropolitan Lagos, Nigeria, *African Geoscience Review, Vol. 12, No. 3*, pp. 225-240.
- Thirumalaivasan, D, Karmegam, M and Venugopal, K. 2003. AHPDRASTIC: Software for specific aquifer vulnerability assessment using DRASTIC model and GIS, *Environ Model Software* 18, pp. 645–656.

- Ufoegbune, GC, Yussuf, HO, Eruola AO and Awomeso, JA. 2011. Estimation of water balance of Oyan lake in northwestern region of Abeokuta, Nigeria, *British Journal of Environment & Climate Change* 1(1): 13-27.
- UN Millenium Project Task Force on Water and Sanitation. 2005. Health Dignity and Development: What Will It Take, Millenium Project, Stockholm International Water Institute.
- United Nations. 2013. World Population Prospect. The 2012 Revision, Highlights and Advance Tables, Department of Economic and Social Affairs, Population Division, United Nations, pp. 5.
- Urish, DW. 1981. Electrical resistivity-hydraulic conductivity relationships in glacial outwash aquifers, *Water Resources Research* 17, no. 5, pp. 1401–1408.
- United States Environmental Protection Agency (USEPA). 1988. *Superfund Exposure Assessment Manual*, EPA/540/1-88/001. Washington D.C.
- Van Genuchten, MTh. 1980. A closed form equation for predicting the hydraulic conductivity of unsaturated soils. *Soil Science Society of America Journal*, vol. 44, pp. 892–898.
- Van Stempvoort, D, Ewert, L and Wassenaar, L. 1993. Aquifer vulnerability index: A GIS compatible method for groundwater vulnerability mapping, *Canadian Water Resources Journal* 18, pp. 25–37.
- Vengosh, A. 2003. Salinization and saline environments. *Treatise on geochemistry*, Vol. 9, Elsevier, pp. 333-365.
- Vengosh, A. 2013. Salinization and Saline Environments, *Earth System and Environmental Sciences* Vol. 11, pp. 325-378. [10.1016/B978-0-08-095975-7.00909-8.
- Vengosh, A, Gill, J, Davisson, ML and Hudson, GB. 2002. A multi-isotope (B, Sr, O, H and C) and age dating study of groundwater from Salinas Valley, California: hydrochemistry, dynamics, and contamination process *Water Resources Research*, 38 (1), pp. 1–17.
- Vereecken, H, Binley, A, Cassiani, G and Titov, K. 2006. Applied Hydrogeophysics. *Earth and Environmental Sciences Springer*, Vol. 71.
- Vias, JM, Andreo, B, Perles, MJ and Carrasco, F. 2005. A comparative study of four schemes for groundwater vulnerability mapping in a diffuse flow carbonate aquifer under Mediterranean climatic conditions, *Environ Geol* 47(4): 586–595.
- Vías, JM, Andreo, B, Perles, JM, Carrasco, F and Vadillo, I. 2006. Proposed method for groundwater vulnerability mapping in carbonate (karstic) aquifers: the COP method Application in two pilot sites in Southern Spain, *Hydrogeology Journal*, 14 (6), pp. 912-925.
- Vienken, T and Dietrich, P. 2011. Field evaluation of methods for determining hydraulic conductivity from grain size data, *Journal of Hydrology*, (400), pp. 58-71.
- Vierhuff, H, Wagner, W and AUST, H. 1981. Die Grundwasservorkommen in der Bundesrepublik Deutschland, *Geol. Jb.*, C30: 3-110.
- Vogel, HJ and Roth, K 2001. Quantitative morphology and network representation of soil pore structure. *Advances in Water Resources*, vol. 24, pp. 233–242.
- Voigt, H. J, Heinkele, T, Jahnke, C and Wolter, R. 2004. Characterisation of groundwater vulnerability to fulfil requirements of the water framework directive of the European Union, *Geofísica Internacional*, 43, pp. 567-574.
- Von Hoyer, M and Sofner, B. 1998. Groundwater vulnerability mapping in carbonate (karst) areas of Germany, *Federal institute for geosciences and natural resources*, Archive no 117854, Hanover, Germany.



- Vrba, J and Zaporozec, A. 1994. Guidebook on mapping groundwater vulnerability. *IAH, HeiseVerlag, Hannover, International Contributions to Hydrogeology* No. 16.
- Wang, QJ, Horton, R and Shao, MA. 2002. Horizontal infiltration method for determining Brooks-Corey model parameters. *Soil Science Society of America Journal* 66, pp.1733–1739.
- Water Framework Directive (WFD). 2000. Directive 2000/60/EC of the European Parliament and of the Council establishing a framework for community action in the field of water policy, *Official Journal of the European Communities*, L, 327/1.
- Wei, W, Kastner, M and Spivak, A. 2008. Chlorine stable isotopes and halogen concentrations in convergent margins with implications for the Cl isotopes cycle in the ocean. *Earth and Planetary Science Letters* 266, pp. 90–104.
- Westbrook, SJ, Rayner, JL, Davis, GB, Clement, TP, Bjerg, PL and Fisher, SJ. 2005. Interaction between shallow groundwater, saline surface water and contaminant discharge at a seasonally and tidally forced estuarine boundary, *Journal of Hydrology* 302 (1–4), pp. 255–269.
- Whiteman, A. 1982. *Nigeria: Its Petroleum Geology resources and potential*, Graham and Trotman Ltd, 1, pp. 166.
- World Health Organization (WHO). 2002. Heterotrophic plate count measurement in drinking water safety management. Report of an Expert Meeting, Geneva, 24–25 April 2002. Department of Protection of the Human Environment, Water, Sanitation and Health, World Health Organization, Geneva, Switzerland. Available at: [www.who.int/water\\_sanitation\\_health/dwq/wsh0210/en](http://www.who.int/water_sanitation_health/dwq/wsh0210/en)
- World Health Organization (WHO). 2011. *Guidelines for drinking water quality*, Final Task Group Meeting, Geneva.
- Wilson, S, Chanut, P, Rissmann C and Ledgard, G. 2014. Estimating Time Lags for Nitrate Response in Shallow Southland Groundwater, Environment Southland, Publication No 2014-03: 1-47.
- Winograd, I and Robertson, F. 1982. Deep oxygenated groundwater: Anomaly or common occurrence, *Science*, Vol. 216: 12227-12229.
- Witczak, S. 2011. *Groundwater Vulnerability Map of Poland*, Ministerstwo Środowiska, Warszawa.
- Witczak, S, Duda, R. and Zurek, A. 2007. The Polish concept of groundwater vulnerability mapping. In: *Groundwater vulnerability assessment and mapping, selected papers on hydrogeology11*, Witkowski AJ, Kowalczyk A, Vrba J (Eds.), pp. 45-59.
- Witczak, S, Szczepański, A Mikołajków, J and Skrzypczyk, L. 2010. Protection of groundwater quality and quantity of strategic groundwater resources of the Major Groundwater Basins, *Przegląd Geol.*, 58(9/1): 754–761.
- Witczak, S and Zurek, A. 2002. Wykorzystanie map glebowo-rolniczych w ocenie ochronnej roli gleb dla wód podziemnych, In: *Metodyczne podstawy ochrony wód podziemnych*, Kleczkowski, AS (Ed.). Projekt badawczy KBN. Wyd. AGH, Krakow.
- Witczak, S and Zurek, A. 2002. Vulnerability assessment in fissured aquifers, In: *Groundwater quality and vulnerability*, Silesian University. Sosnowiec, pp. 241-254.
- Witkowski, AJ and Kowalczyk, A. 2004. A simplified method of regional groundwater vulnerability assessment, *Proceedings of Groundwater Vulnerability Assessment and Mapping- Ustron, Poland -2004*.

- Wosten, JH, Bannink, JJ, De Gruijter, J and Bouma, J. 1986. A procedure of identifying different groups of hydraulic conductivity and moisture retention curves for soils horizons, *Journal of Hydrology*, Vol. 86, pp. 133-145.
- Xu, Y and Braune, E. 2010. *Sustainable Groundwater Resources in Africa; water supply and sanitation environment*, CRC Press, Taylor and Francis Group, pp. 23.
- Xu, Y and Usher, B. 2006. Issues of groundwater pollution in Africa, In Xu, Y and Usher, B eds, *Groundwater Pollution in Africa*. Taylor & Francis/Balkema, pp. 3-9.
- Yu, Ch, Yao, Y, Hayes, G, Zhang, B and Zheng, Ch. 2010. Quantitative assessment of groundwater vulnerability using index system and transport simulation, Huangshuihe catchment, China, *Science of the Total Environment* 408, pp. 6108–6116.
- Zhang, S, Howard, K, Otto, C, Ritchie, V, Sililo, OTN and Appleyard, S. 2004. Sources, Types, Characteristics and Investigation of Urban Groundwater Pollutants In D.N. Lerner, *Urban Groundwater Pollution*, IAH Publications, Taylor and Francis London, pp. 53-107.
- Zohdy, AAR, Eaton, GP and Mabey, DR. 1974. Application of Surface Geophysics to Ground-Water Investigation *Techniques of Water Resources Investigation US Geological Survey*, pp. 116.
- Zwahlen, F. 2003. *Vulnerability and risk mapping for the protection of carbonate (karst) aquifers – Final report*, European Cooperation in Science and Technology (COST), Action 620. Brussels: EU Publications Office, pp. 1-42.
- Zwahlen, F. 2004. *Vulnerability and risk mapping for the protection of carbonate (karst) aquifers, final report COST action 620*: European Commission, Brussels.

## APPENDIX A

- Excel spreadsheet for calculating RTt vulnerability

## SUMMARY

This study aimed to evaluate the vulnerability of the shallow aquifer systems of the Dahomey Basin and formulate a simple vulnerability method with which data limited areas (which include the shallow unconfined aquifers in the Dahomey Basin) can be predicted. The Dahomey Basin is a transboundary aquifer which extends from Ghana to the western parts of Nigeria. The study covered the eastern section of the basin. The methodological approach involved a source–pathway–receptor vulnerability model. The Dahomey Basin was characterised through the geophysical, hydrological, litho-geochemical and hydrogeochemical approaches. The geology of the basin includes sedimentary rock types of sandstone, shale, limestone, alluvium conglomerate and the formations which are composed of sand, silt, clay, laterite and gravel.

The geophysical study, which mainly aimed to estimate the depth-to-water table, identification of strata and vadose zone thickness, revealed topsoil, sandy clay, dry porous sandstone, conglomeratic sandstone, limestone and alluvium as the major lithological units in the basin. Geo-electrical curve types revealed an overlying multilayered rock. The vadose zone characterisation, which is the pathway through which contaminants infiltrate, aimed to determine the lithological properties which dictate the travel time of water. This was achieved by determining the hydraulic conductivity of the vadose lithology in the laboratory. Other important parameters such as grain size, porosity, shapes, textural classification and clay types were examined for their attenuation capacity.

The hydrogeochemical investigation involving the collection and analysis of water samples from the hand-dug wells and shallow boreholes during the rainy and dry season was aimed at monitoring the groundwater quality of the basin. Ca-Mg-Cl water types and Na-K-Cl water types were delineated. Bacteriological examination of the shallow water reveals the presence of E.Coli, Heterotrophic bacteria and Salmonella/ Shigella. Precipitation which is a component of groundwater recharge ranged between 1 200–1 800 mm from the northern end to the southern end of the basin, respectively. Groundwater level were measured, monitored and average water level were delineated for the formations of the Dahomey Basin.

The proposed RTt vulnerability method was applied to evaluate the groundwater vulnerability of the Dahomey Basin. The RTt method is an intrinsic physically based vulnerability method based on the concept of groundwater recharge from rainfall and travel time within the covering lithology over the aquifer. Travel time is the infiltration derived from multiplication of the slope and thickness of the vadose zone divided by fluid velocity. The fluid velocity is derived from the division of hydraulic conductivity by porosity. RTt method application results for the Dahomey Basin were presented on the RTt vulnerability map. The RTt vulnerability map was classified from very low vulnerability (12) to very high vulnerability (100). The RTt vulnerability results for the Dahomey Basin showed 18% of the areas classified as very high vulnerability, 7% of the areas classified as high vulnerability, 64% of the areas classified as moderate vulnerability and 10% of the areas classified as low vulnerability.

The compared vulnerability maps of the RTt method and those of the DRASTIC, PI and AVI methods, showed similarities between the RTt method and the AVI and DRASTIC method, respectively. Areas classified as high vulnerability by these methods showed very shallow protective covers, high precipitation and porous aquifer materials, while areas classified as low vulnerability areas include thick protective cover, reduced rainfall, higher slope and higher depth-to-water. The RTt vulnerability map was validated with the hydrochemical tracer using chloride, DO and microbial loads as vulnerability indicators.

This study has formulated an RTt method that can be used to predict the vulnerability of shallow unconfined aquifer systems, a key component in groundwater management. The major advantage of the RTt method is the use of less number of parameter to assess groundwater vulnerability. The method has been applied to investigate the regional aquifer of the Dahomey Basin and can be used to predict the aquifer vulnerability of similar basins across Africa with limited data.

Keywords: Dahomey Basin, aquifer vulnerability, validation, groundwater, RTt method.